Growth and differentiation factor 15 causes skeletal muscle wasting in pulmonary arterial hypertension through actions on transforming growth factor β activated kinase 1

Dr. Benjamin Edward Garfield

Imperial College London

National Heart and Lung Institute

Submitted for the degree of PhD

June 2017

Re-submitted with corrections

April 2018

Declaration of originality

I declare that the work presented below in this thesis is my own or is appropriately referenced. Work carried out by, or in collaboration with others and materials purchased or attained from other sources are also explained in the narrative**.**

Copyright Declaration

Acknowledgments

I would like to take this opportunity to thank the people that have helped with this thesis. These include members of the muscle, molecular medicine and vascular biology labs as well as the clinical team in the pulmonary hypertension department at the Royal Brompton Hospital particularly: Amy Lewis, Jen Lee, Martin Connolly, Roser Farre Garros, Susannah Bloch, Mehul Patel, Ghulam Haji, Katrina Curtis, Richard Paul, Margherita Ciano, Dongmin Shao, Sharon Mumby, Louit Thakuria, David Salman, Carl Harries and Lisa Parfitt. I would also like to thank the team at the University of Cambridge particularly Professor Nick Morrel, Alexi Crosby and Brian Peng for all their help with the animal work contained in this thesis. I would like to make special mention of my supervisors Professor Michael Polkey, Dr Paul Kemp and Dr John Wort for their help support and advice on both professional and personal matters throughout my PhD. It would not have been possible to complete this work without the time and dedication of the patients with pulmonary hypertension who agreed to be studied.

Finally I would like to thank my family Alex, Josh, Harry, Eddie, Andrew, Mum and Dad for all your help, support I will always be grateful for your patience and understanding.

Abstract

Muscle wasting is an important complication of a wide range chronic diseases. Pulmonary arterial hypertension (PAH) is no different. Novel targets and treatments are required to help improve outcomes in patients with PAH complicated by muscle wasting. GDF-15 is prognostic marker in PAH and has been shown to cause muscle wasting *in vitro* and *in vivo.* The pathway through which GDF-15 acts in muscle cells is not established.

I used a human study, animal models of PAH; the monocrotaline (MCT) rat; and Sugen/hypoxia mouse, as well as C2C12 muscle cells to determine whether GDF-15 and its downstream signals may be important in the development of muscle wasting and low physical activity in PAH.

Muscle wasting and low physical activity were associated with poor outcomes in a population of patients with PAH. Circulating GDF-15 levels were associated with markers of muscle strength and size in 2 animal models and in patients with PAH. In the MCT rat the pulmonary vasculature was an important site of production of GDF-15. GDF-15 acted by increasing the expression of ubiquitin ligases, which are involved in muscle wasting. GDF-15 decreased the activity of SMAD 1, 5 whilst increasing transforming growth factor β activated kinase 1 (TAK1) phosphorylation in muscle cells. Antagonising TAK1 with 5(Z)-7-oxozeaenol partially prevented muscle loss and rises in ubiquitin ligase expression in muscle cells and prevented weight loss in some MCT rats treated for 9 days with the drug.

Muscle wasting and low physical activity are potentially modifiable risk factors for poor prognosis in PAH. GDF-15 may be a useful biomarker of muscle loss in PAH. Antagonising GDF-15 through its downstream mediator TAK1 requires further evaluation in animal models and patients with PAH to establish its usefulness in clinical practice.

Table of contents

Title Page 1

Declaration of originality 2

Copyright Declaration 2

Acknowledgements 3

Abstract 4

Table of contents 5

Chapter 1 Introduction 23

1.1 Pulmonary hypertension (PH) 23

1.1.1 Clinical information 23

1.1.2 PAH 25

1.1.2.1 Definition 25

1.1.2.2 Epidemiology and prognosis in PAH 25

1.1.2.3 Pathophysiology of PAH 25

1.1.2.4 Clinical features of PAH 26

1.1.2.5 PAH treatments and its effects on outcomes 26

1.2 Skeletal muscle wasting in chronic cardio-respiratory disease 27

1.2.1 Muscle loss in the vicious cycle of disease progression 27

1.2.2 Clinical Studies of muscle loss in COPD and heart failure 28

1.2.3 Muscle fibres in health COPD and heart failure 28

1.2.4 Molecular pathways leading to muscle loss in chronic disease 29

1.2.5 The drivers of muscle loss in chronic disease 32

1.2.5.1 Physical inactivity 32

1.2.5.2 Malnutrition 32

1.2.5.3 Inflammation 33

1.2.5.4 Hypoxia 33

1.2.6 Treatments aimed at improving muscle function in chronic disease 34

1.2.6.1 Rehabilitation 34

1.2.6.2 Nutritional supplementation 34

1.2.6.3 Anabolic agents 35

1.3 Muscle wasting in PH and PAH 36

1.3.1 Muscle wasting in animal models of PAH 36

1.3.2 Muscle wasting and physical activity in PAH clinical observations 39

1.4 TGFβ signalling 42

1.4.1 TGFβ signalling pathway 42

1.4.2 TGFβ signalling in PAH 46

1.4.3 TGFβ signalling in skeletal muscle atrophy 47

1.5 GDF-15 49

1.5.1 GDF-15 in health and disease 49

1.5.2 GDF-15 in muscle wasting 51

1.5.3 GDF-15 and food intake 53

1.5.4 GDF-15 and physical activity 54

1.5.5 GDF-15 and PH 54

1.5.6 GDF-15 and downstream signalling 56

1.6 TAK1 59

1.6.1 TAK1 signalling 59

1.6.2 TAK1 as a target for therapeutic intervention 61

1.6.3 TAK1 in PH 62

1.6.4 TAK1 in muscle wasting 62

1.7 Summary, aims and hypotheses 63

1.7.1 Summary 63

1.7.2 Hypothesis 64

1.7.3 Aims 64

Chapter 2 Methods 66

2.1 Clinical methods 66

2.1.1 Ethical approval 66

2.1.2 Inclusion and exclusion criteria 66

2.1.3 Demographics 66

2.1.4. Measurement of muscle mass, size and strength 67

2.1.4.1 Fat free mass index 67

2.1.4.2 Rectus femoris cross sectional area 67

2.1.4.3 Quadriceps maximal volitional capacity 69

2.1.5 Physical activity measurements 71

2.1.6 Quality of life questionnaires 73

2.1.6.1 The St. George's respiratory questionnaire 73

2.1.6.2 The Cambridge pulmonary hypertension outcome review 73

2.1.6.3 The emPHasis 10 questionnaire 74

2.1.7 Echocardiogram 74

2.1.8 Six minute walk test distance 75

2.1.9 Blood tests 75

2.1.10 Muscle biopsies and protein extraction 75

2.2 Animal models 76

2.2.1 The monocrotaline rat 77

2.2.1.1 Observational study 77

2.2.1.2 TAK1 inhibitor study 77

2.2.2 The Sugen/hypoxia mouse 77

2.2.3 MRI imaging 78

2.2.4 Right heart catheter 78

2.2.5 Dissection and tissue removal 78

2.2.7 Right ventricular / left ventricular plus septal weight 79

2.2.8 Assessment of muscle mass 80

2.2.9 Tissue processing 80

2.3 Cell culture 81

2.3.1 C2C12 mouse myoblasts cells 81

2.3.2 C2C12 treatment 82

2.3.2 Harvesting mRNA and protein from cell culture 83

2.4 Plasmids, restriction digests cloning and transfection 84

2.4.1 Plasmids, restriction digests and transformation of super-competent bacteria 84

2.4.2 Cloning the truncated TGFBR2 (TTGFBR2) 86

2.4.3 Cloning a BMP responsive element luciferase and removing a BRE from pRL-TK 90

2.4.4 Transfection of DNA for luciferase, immunofluorescence and fibre diameter 92

2.5 Molecular techniques 93

2.5.1 Luciferase assay 93

2.5.2 cDNA synthesis and quantitative PCR for mRNA 94

2.5.3 Western blotting 98

2.5.4 Enzyme-linked immunosorbent assay 100

2.5.5 Muscle fibre and myotube diameter 100

2.5.6 Immunohistochemistry 102

2.5.7 Immunofluorescent staining for nuclear localisation of NFκB and over-expression of TGFβ receptors 104

2.6 Data handling and statistical analysis 105

Chapter 3 Clinical outcomes pertaining to muscle wasting and physical activity in PAH 108

3.1 Background 108

3.2 Aims 109

3.3 Hypotheses 110

3.4 Methods 110

3.4.1 Participants 110

3.4.2 Baseline measurements 110

3.4.3 Physical activity outcomes 111

3.4.4 Follow up period and measurements 111

3.4.5 Data analysis 112

3.5 Results 112

3.5.1 Demographics and compliance 112

3.5.2 Muscle mass, strength and size and physical activity across WHO functional groups in patients with PAH 114

3.5.3 Correlations of muscle strength and size and physical activity in patients with PAH 116

3.5.4 Association of muscle size, strength and cardiovascular markers with physical activity in PAH 121

3.5.5 Muscle bulk and physical activity predict mortality in patients with PAH 121

3.5.6 Muscle bulk and strength identify those patients with PAH at risk of hospital admission 122

3.5.7 Muscle strength and physical activity are correlated with future levels of quality of life in patients with PAH 123

3.5.8 Activity scores from QOL questionnaires can predict those patients with low physical activity in the context of PAH 124

3.6 Discussion 130

3.7 Limitations 135

3.8 Conclusions 136

Chapter 4 TGFβ signalling in muscle wasting in pulmonary hypertension 138

4.1 Background 138

4.2 Aims 138

4.3 Hypotheses 139

4.4 Methods 139

4.4.1 Animal models 139

4.4.2 Tissue processing and analysis 140

4.4.3 Clinical study 140

4.4.4 Statistics 140

4.5 Results 141

4.5.1 The MCT rat is a model of PH and muscle loss 141

4.5.2 TGFβ super-family member expression in the muscle and blood in the MCT rat 145

4.5.3 The pulmonary vasculature is a source of circulating GDF-15 in the MCT rat 147

4.5.4 Sugen/hypoxia mice develop PAH and associated muscle loss 149

4.5.5 The circulating and muscle levels of GDF-15 and other TGFβ superfamily ligands in the Sugen/hypoxia mouse 150

4.5.7 The Sugen/hypoxia mouse also over-expresses GDF-15 in the lung 152

4.5.8 Circulating GDF-15 is negatively correlated with physical activity, muscle strength and size in patients with PAH 153

4.6 Discussion 156

4.7 Limitations 159

4.8 Conclusions 159

Chapter 5 GDF-15 causes muscle atrophy *in vitro* through actions on TAK1 160

5.1 Background 160

5.2 Aims 162

5.3 Hypotheses 162

5.4 Methods 162

5.4.1 C2C12 cells 162

5.4.2 Animal experiments 163

5.4.3 Human samples 163

5.4.4 Cloning 163

5.4.4.1 Truncated TGFBR2 163

5.4.4.2 BMP responsive element 163

5.4.4.3 pRL-TK without BRE 164

5.4.5 Luciferase experiments 164

5.4.5.1 Transfection 164

5.4.5.2 Luciferase Activity 164

5.4.6 Myotube Diameter 164

5.4.7 Western blotting 165

5.4.8 Quantitative PCR 165

5.4.9 Immunofluorescence 165

5.4.10 Statistics 166

5.5 Results 166

5.5.1 In myoblasts GDF-15 does not stimulate SMAD 2, 3 and decreases SMAD 1, 5 response 166

5.5.2 GDF-15 causes a significant increase in significant increase in SMAD 2, 3 dependent response in TGFBR2 over-expressing cells 168

5.5.3 In myoblasts longer term treatment with GDF-15 increased SMAD dependent luciferase activity but failed to alter TGFβ1 or BMP-4 dose responses 176

5.5.4 A truncated TGFBR2 (TTGBFR2) failed to prevent GDF-15 mediated atrophy in myotubes 178

5.5.5 GDF-15 may act through non-canonical TGFβ pathways, which is best studied in myotubes 181

5.5.6 GDF-15 activated TAK1 and NFκB p65 at high and low dose in C2C12 myotubes 185

5.5.7 GDF-15 mediated myotube atrophy can be antagonised by the TAK1 inhibitor 5(Z)-7-oxozeaenol 188

5.5.8 Downstream mediators of GDF-15 are up-regulated in the muscle of the MCT rat 193

5.6 Discussion 198

5.7 Conclusions 202

Chapter 6 The effect of 5(Z)-7-oxozeaenol on muscle wasting in the MCT rat 203

6.1 Background 203

6.2 Aim 205

6.3 Hypothesis 205

6.4 Methods 205

6.4.1 Animal experiments 205

6.4.2 Tissue processing and analysis 206

6.4.4 Statistics 207

6.5 Results 207

6.5.1 TAK1 inhibition prevents weight loss in the MCT rat model of PAH 207

6.5.2 TAK1 inhibition may partially prevent loss of TA fibre diameter and prevents MCT induced increases in activated NFκB and atrogin-1 expression 209

6.5.3 TAK1 inhibition did not significantly change pulmonary pressure, right ventricular remodelling or GDF-15 levels in the MCT rat 212

6.5.4 Circulating GDF-15 levels were associated with markers of muscle loss as well as continued growth in MCT rats treated with 5(Z)-7-oxozeaenol 214

6.6 Discussion 215

6.7 Limitations 219

6.8 Conclusions 220

Chapter 7 Discussion 221

7.1 Summary 221

7.2 My findings in context 221

7.3 Limitations 230

7.3.1 Sample size 230

7.3.2 Missing data 231

7.3.3 Validity of equipment 231

7.3.4 Animal licensing and assessment 231

7.3.5 The primary deficit causing muscle loss, GDF-15 production and its actions 232

7.4 Conclusions 232

7.5 Future work 234

Chapter 8 References 238

Tables

Table 1.1 Clinical Classification of PH 24

Table 2.1 WHO/NYHA functional class in PH 67

Table 2.2 Number of cells seeded per well in different plates 82

Table 2.3 Plasmids 85

Table 2.4 Primers 96

Table 2.5 Antibodies for western blot 99

Table 2.6 Antibodies for immunofluorescence 105

Table 3.1 Demographics 113

Table 3.2 Muscle bulk, physical activity, and quality of life 114

Table 3.3 Follow up data 114

Table 4.1 Demographics 154

Figures

Figure 1.1 The vicious cycle disease progression 27

Figure 1.2 Pathways of muscle loss in chronic disease 31

Figure 1.3 TGFβ super-family signalling 44

Figure 1.4 TGFβ super-family members and their potential receptors 45

Figure 1.5 The interaction of TGFβ and TAK1 signalling 60

Figure 2.1 Ultrasound image of RF_{CSA} 68

Figure 2.2 Chair used to measure QMVC 70

Figure 2.3 Sensewear armband position 72

Figure 2.4 Sketch of muscles in rat mouse hind limb 79

Figure 2.5 PCR product of the truncated TGFBR2 receptor 87

Figure 2.6 PCR screening for TTGFBR2 insert in pCDNA3 89

Figure 2.7 pCNDA3 hum TTGFBR2 plasmid cut with PST-1 showing directionality 90

Figure 2.8 BRE luciferase cut with Nhe 1 to show the presence of the insert 91

Figure 2.9 Renilla activity in BMP-4 treated cells transfected with pRL-TK with and without BRE 92

Figure 2.10 Example of melt curve generated by qPCR 97

Figure 2.11 Immunofluorescent image of p-CAGGs-EGFP over-expressing myotube co-stained with DAPI 102

Figure 3.1 Muscle measurements across functional class 115

Figure 3.2 Physical activity across functional class 116

Figure 3.3 Correlations of 6MWD 118

Figure 3.4 Correlations of SGRQ quality of life 119

Figure 3.5 Correlations of CAMPHOR quality of life 120

Figure 3.6 Correlations of physical activity and muscle parameters 121

Figure 3.7 Survival in PAH by muscle bulk and activity 122

Figure 3.8 Muscle parameters predict hospitalisation in PAH 123

Figure 3. 9 Correlates of future quality of life in PAH 124

Figure 3.10 SGRQ and CAMPHOR activity scores correlate with objectively measured physical activity 126

Figure 3.11 ROC curves of activity scores from the SGRQ, CAMPHOR and 6MWD in predicting low step count 127

Figure 3.12 ROC curves of activity scores from the SGRQ, CAMPHOR and 6MWD in predicting low PAL 128

Figure 3.13 ROC curves of activity scores from the SGRQ, CAMPHOR and 6MWD in predicting active individuals 129

Figure 3.14 Kaplan-Meier and ROC curve predicting survival in patients based on SGRQ activity scores 130

Figure 4.1 The MCT rat is a model of PH 142

Figure 4.2 Growth, body weight, muscle weight and food intake in the MCT rat 143

Figure 4.3 MRI imaging of the hind limb of the MCT rat 144

Figure 4.4 Tibialis fibre diameter in the MCT rat 145

Figure 4.5 TGFβ super-family member mRNA expression in the muscle of the MCT rat 146

Figure 4.6 Circulating GDF-15 and muscle loss in the MCT rat 147

Figure 4.7 GDF-15 mRNA and protein in the lung of the MCT rat 148

Figure 4.8 GDF-15 in the pulmonary vasculature of the MCT rat 149

Figure 4.9 Tibialis anterior (TA) weight and fibre diameter in Normoxic, Hypoxic and Sugen/hypoxia mouse 150

Figure 4.10 Circulating GDF-15 and muscle loss in the Sugen/hypoxia mouse 151

Figure 4.11 TGFβ super-family member mRNA expression in the muscle of the Sugen/hypoxia mouse 152

Figure 4.12 GDF-15 mRNA expression in the lung of the Sugen/hypoxia mouse 153

Figure 4.13 Circulating GDF-15, muscle wasting and physical activity in patients with PAH 155

Figure 5.1 SMAD 2, 3 dependent luciferase activity in C2C12 myoblasts treated with GDF-15 167

Figure 5.2 SMAD 1, 5 dependent luciferase activity in C2C12 myoblasts treated with GDF-15 168

Figure 5.3 Western blot showing over-expression of receptors in C2C12 cells 169

Figure 5.4 Immunofluorescence showing over-expression of receptors in C2C12 cells 170

Figure 5.5 Effect of receptor over-expression on SMAD 2, 3 and SMAD 1, 5 dependent luciferase activity in C2C12 cells. 171

Figure 5.6 SMAD 2, 3 dependent luciferase activity in C2C12 myoblasts over-expressing pCDNA3, TGFBR2, or ACVR2B treated with vehicle control or GDF-15 at 50 ng/ml for 6 hours 173

Figure 5.7 SMAD 2, 3 dependent luciferase activity in C2C12 myoblasts over-expressing pCDNA3 or TGFBR2 with vehicle control or GDF-15 at 5 ng/ml for 6 hours 174

Figure 5.8 SMAD 1, 5 dependent luciferase activity in C2C12 myoblasts over-expressing pCDNA3, TGFBR2, ACVR2B or BMPR2 treated with vehicle control or GDF-15 at 50 ng/ml for 24 hours 175

Figure 5.9 SMAD 2, 3 and SMAD 1, 5 dependent luciferase activity in cells co-treated with GDF-15 and TGFβ1 / BMP-4 177

Figure 5.10 SMAD 2, 3 dependent luciferase responses in TTGFBR2 over-expressing cells 179

Figure 5.11 Myotube diameter in TTGFBR2 over-expressing GDF-15 treated myotubes 180

Figure 5.12 Nuclear localisation of NFκB p65 in response to GDF-15 treatment 182

Figure 5.13 mRNA expression of NFκB p65 in response to GDF-15 and TAK inhibition 183

Figure 5.14 Non-canonical GDF-15 signalling in myoblasts versus myotubes 184

Figure 5.15 Western blots of day 10 myotubes treated for 0, 10, 30, 60 and 120 minutes with 50 ng/ml of GDF-15 186

Figure 5.16 Western blot of day 10 myotubes treated for 60 minutes with 0, 1, 5 or 10 ng/ml of GDF-15 187

Figure 5.17 Myotube diameter in high dose GDF-15 / 5(Z)-7-oxozeaenol treated cells 189

Figure 5.18 Ubiquitin ligase expression high dose GDF-15 / 5(Z)-7-oxozeaenol treated cells 190

Figure 5.19 Myotube diameter in low dose GDF-15 / 5(Z)-7-oxozeaenol treated cells 191

Figure 5.20 Ubiquitin ligase expression low dose GDF-15 / 5(Z)-7-oxozeaenol treated cells 192

Figure 5.21 Atrogin-1 mRNA expression in high dose GDF-15/ ALK5 inhibitor treated cells 193

Figure 5.22 Ubiquitin ligase mRNA expression in the TA of the MCT rat 194

Figure 5.23 Ubiquitin ligase mRNA expression in the TA of the Sugen/hypoxia mouse 195

Figure 5.24 mRNA expression of TAK1, NFκB p65 and p38 MAPK in the TA of the MCT rat 196

Figure 5.25 Phospho-TAK1 in the TA of the MCT rat and in the rectus femoris of patients with PAH 197

Figure 6.1 Weight in the MCT rat treated with 5(Z)-7-oxozeaenol 208

Figure 6.2 Growth in the MCT rat treated with 5(Z)-7-oxozeaenol 209

Figure 6.3 Muscle wasting in the MCT rat treated with 5(Z)-7-oxozeaenol 210

Figure 6.4 TA Fibre diameter in the MCT rat treated with 5(Z)-7-oxozeaenol 210

Figure 6.5 Phospho-NFκB p65 in the TA of the MCT rat treated with 5(Z)-7-oxozeaenol 211

Figure 6.6 Ubiquitin ligase mRNA expression in the TA of the MCT rat treated with 5(Z)-7-oxozeaenol 212

Figure 6.7 Pulmonary hypertension in the MCT rat treated with 5(Z)-7-oxozeaenol 213

Figure 6.8 GDF-15 in the MCT rat treated with 5(Z)-7-oxozeaenol 213

Figure 6.9 Correlations of circulating GDF-15 levels in MCT rats treated with 5(Z)-7-oxozeaenol 214

Figure 6.10 GDF-15 as a biomarker of continued growth in MCT rats treated with 5(Z)-7-oxozeaenol 215

Figure 7.1 Diagram showing potential mechanism through which GDF-15 may cause direct muscle atrophy in patients with PAH. 234

Appendices

Appendix 2.1 265

Appendix 2.2 267

Appendix 2.3 269

Appendix 2.4 270

Appendix 4.1 272

Appendix 5.1 273

Appendix 5.2 274

Appendix 5.3 275

Chapter 1. Introduction

1.1 Pulmonary hypertension (PH)

1.1.1 Clinical information

PH describes a situation where there is raised pressure in the vessels taking blood from the heart to the lungs to pick up oxygen. The blood vessels are thicker and less elastic meaning the heart has to pump harder to meet the needs of the body, especially during exercise (1). 'Pulmonary vascular sclerosis', a pathological description of PH, was first noted in an autopsy specimen by Ernst von Romberg in 1891 (2, 3). PH can only be confirmed by readings taken at right heart catheter (RHC) and is defined as a mean pulmonary artery pressure of greater than 25mmHg. PH is caused by a wide range of conditions (4). The current clinical classification of PH is based on the 5th World Symposium on PH, which was held in Nice in 2013 (5), which was the most recent update of the classification first outlined in Evian in 1998 (6). This classification system split PH into 5 groups based on the cause, pathophysiology and response to treatment (6). The current classification system is outlined in Table 1. There are 5 clinical groups: Group 1, pulmonary arterial hypertension (PAH); Group 2, PH due to left heart disease; Group 3, PH due to lung disease and / or hypoxia; Group 4, chronic thromboembolic PH; and Group 5 PH with unclear, multifactorial mechanisms (5). The only group of patients that responds to treatment targeted at the pulmonary vasculature are those with Group 1 disease (PAH). Current guidelines suggest that treatment of the other groups of PH should focus on optimisation of the underlying disease and identification of disproportionate PH that may respond to targeted therapy (7).

Group	Description
1	Pulmonary arterial hypertension
1.1	Idiopathic
1.2	Heritable
1.2.1	BMPR2
1.2.2	ALK-1, ENG, SMAD 9, CAV1, KCNK3
1.2.3	Unknown
1.3	Drug and toxin induced
1.4	Associated with
1.4.1	Connective tissue disease
1.4.2	HIV infection
1.4.3	Portal hypertension
1.4.4	Congenital heart disease
1.4.5	Schistosomiasis
1'	Pulmonary veno-occlusive disease and /or pulmonary capillary haemangiomatosis
1''	Persistent pulmonary hypertension of the new-born
2	Pulmonary hypertension due to left heart disease
2.1	Left ventricular systolic dysfunction
2.2	Left ventricular diastolic dysfunction
2.3	Valvular disease
2.4	Congenital / acquired left heart inflow / outflow tract obstruction and congenital cardiomyopathies
3	Pulmonary hypertension due to lung disease and / or hypoxia
3.1	Chronic obstructive pulmonary disease
3.2	Interstitial lung disease
3.3	Other lung diseases with mixed restrictive and obstructive pattern
3.4	Sleep-disordered breathing
3.5	Alveolar hypoventilation disorder
3.6	Chronic exposure to high altitude
3.7	Developmental lung diseases
4	Chronic thromboembolic pulmonary hypertension (CTEPH)
5	Pulmonary hypertension with unclear multifactorial mechanisms
5.1	Haematologic disorders: chronic haemolytic anaemia, myeloproliferative disorders, splenectomy
5.2	Systemic disorders: sarcoidosis, pulmonary, histiocytosis, lymphangiolieiomyomatosis
5.3	Metabolic disorders: glycogen storage disease, Gaucher disease, thyroid disorders
5.4	Others: tumoural obstruction, fibrosing mediastinitis, chronic renal failure, segmental PH

Table 1. Clinical Classification of Pulmonary hypertension. Updated clinical classification of Pulmonary Hypertension during the 5th World Symposium in NICE 2013. BMPR = bone morphogenetic protein receptor type II; CAV1 = caveolin-1; ENG = endoglin; HIV = human immunodeficiency virus (5).

1.1.2 PAH

1.1.2.1 Definition

As well as a mean pulmonary artery pressure of > 25 mmHg, PAH / Group 1 disease is further characterised by pre-capillary haemodynamics: (a wedge pressure of ≤ to 15 mmHg) and raised pulmonary vascular resistance (PVR), (> 3 Wood units), with no evidence of significant left heart disease, lung disease or chronic thromboembolic PH (5). PAH, and the associated increased PVR ultimately leads to right heart failure and death (8). The sub-categories of PAH are outlined in Table 1 (5). Once again, they have been grouped together as they exhibit similar patho-physiological changes. These include typical vascular remodelling in the resistance arterioles of the pulmonary bed (<500 μm in diameter) and responses to disease targeted therapy (9).

1.1.2.2 Epidemiology and prognosis of PAH

PAH is a rare condition with a prevalence of 15 – 60 per million people (10-12). PAH in the modern era tends to be diagnosed in patients aged between 50 and 65 years old and has a female preponderance of between 60 and 83% in current registries (11). Historically 3 year survival was quoted at 50%, however with the emergence of novel therapies the prognosis of patients with PAH has improved, with current 3 year mortality being between 10 and 30% (13, 14), and 5 year mortality being 35 - 40% (15). The prognosis depends both on the cause of the PAH and the functional status of the patient. Patients with systemic sclerosis and portal hypertension associated PAH have the worse prognosis with 5 year survival of only approximately 40%, whilst those with congenital heart disease and toxin induced PAH had 5 year survival of 70-75%, with the other causes being somewhere in the middle (15).

1.1.2.3 Pathophysiology of PAH

On a biological level PAH is caused by endothelial cell dysfunction, vasoconstriction, endothelial and smooth muscle cell proliferation and in-situ thrombosis in the small and medium sized pulmonary

arteries. All of these factors contribute to narrowing of these vessels resulting in raised resistance, pressures and eventually lead to progressive heart failure (14). The pathogenesis underlying this vascular remodelling is incompletely understood. A number of factors have been shown to be important, including an increase in growth factors, inflammation, aberrations in calcium and bone morphogenetic protein (BMP) signalling cascades, a change in extra-cellular matrix structure and function and an imbalance between factors promoting vasoconstriction and vasodilation (16). Reversing the imbalance between vasoconstrictors and vasodilators is the basis for current targeted therapy in PAH (14).

1.1.2.4 Clinical features of PAH

The symptoms of PAH include dyspnoea, initially on exertion and then at rest, swelling of the ankles, palpitations and syncope (14). Prognostic indicators from the Reveal registry predicting poorer survival in PAH included: male gender; age over 60 years; portal hypertension; connective tissue disease; familial disease; functional WHO class III or IV; a PVR of greater than 32 Wood units; a right atrial pressure of more than 20mmHg; the presence of a pericardial effusion; a brain natriuretic peptide (BNP) of greater than 180 pg/ml; renal dysfunction; a transfer factor of carbon monoxide (DLCO) percent predicted of less than 32%; and a six minute walk distance (6MWD) of less than 165m. Predictors of good prognosis included: a BNP of less than 50 pg/ml; a 6MWD of greater than 440m; a DLCO percent predicted of more than 80%; and being in WHO functional class I (17).

1.1.2.5 PAH treatment and its effects on outcomes

PAH treatment has advanced significantly over the past 20 years. Current established treatments include anticoagulation, diuretics, management of anaemia, calcium channel blockers in those who have positive vaso-reactivity tests, phosphodiesterase inhibitors, endothelin antagonists and intravenous prostacyclin (7). As discussed earlier this modern combination of therapies has significantly improved outcomes in PAH (13-15).

Despite these treatments patients still suffer with excess morbidity and a reduction in quality of life (QOL), which is at least in part related to a poor exercise tolerance and an inability to engage in activities of daily living (18). The 6MWD has repeatedly been identified as predictor of prognosis and one of the primary outcomes by which interventions in PAH are evaluated (19). 6MWD is determined not only by a patients' cardiorespiratory reserve but also by neuromuscular function (20). Loss of muscle function and size seems to be a ubiquitous outcome of chronic disease and PAH is no exception (21). Current guidelines have recognised this fact and now recommend increase in physical activity as well as supervised exercise programmes as general measures to improve both well-being and exercise tolerance in PAH (22).

1.2 Skeletal muscle wasting in chronic cardio-respiratory disease

1.2.1 Muscle loss in the vicious cycle of disease progression

Muscle loss has been implicated as an important complication in individuals with a number of chronic diseases affecting both the heart and the lung. In these conditions muscle loss contributes to a downward spiral of breathlessness, fatigue, exercise intolerance, lack of physical activity, metabolic syndrome, and disease progression (Figure 1.1) (23).

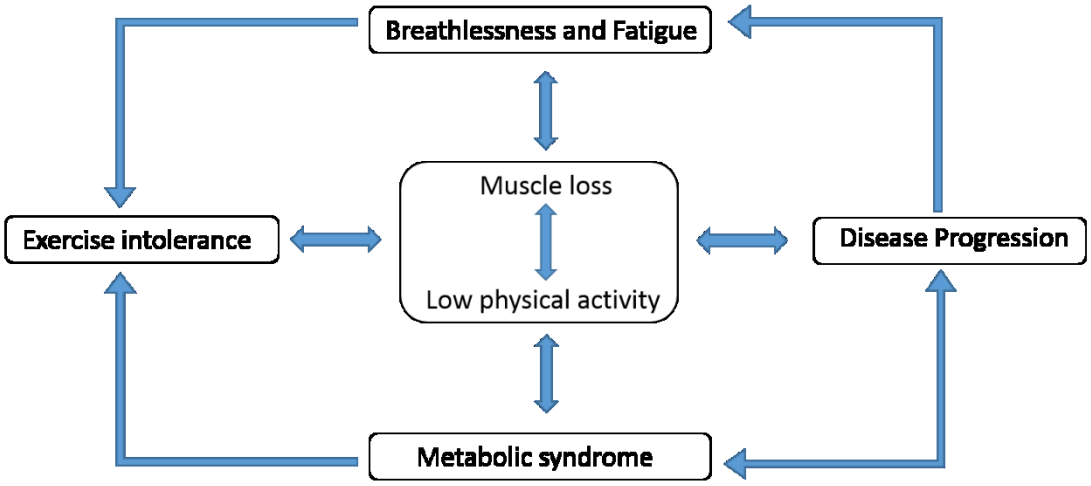

Figure 1.1. The vicious cycle disease progression. Muscle weakness and low physical as a focus of the spiral of breathless, fatigue, exercise intolerance, metabolic syndrome and disease progression in chronic cardio-respiratory disease.

1.2.2 Clinical studies of muscle loss in chronic obstructive pulmonary disease (COPD) and heart failure

Unlike in PAH, muscle loss in COPD and heart failure have been widely studied. In COPD up to 36% of patients experience a reduction in quadriceps strength (24) which may be present in early disease and is only weakly associated with lung function (25-27). Studies using both ultrasound (28) and computerised tomography (29) have shown that this loss of strength is accompanied by a proportionate loss in quadriceps size (30). In COPD loss of quadriceps muscle function has been shown to be associated with a reduction in exercise tolerance (31), QOL (32) and an increase in healthcare utilisation (33) and mortality (34).

In heart failure, in one study, approximately 20% of patients were found to have skeletal muscle wasting (35). Quadriceps cross sectional area was lower in patients than controls as was strength, however unlike in COPD, researchers have reported that even when muscle size was corrected for, strength remained impaired (36). Again, as opposed to COPD, where little relationship existed between muscle function and lung function (37), muscle loss was more strongly linked to left ventricular ejection fraction and with maximal oxygen uptake (VO_2 max), independent of other variables, in heart failure (35). A reduction in quadriceps strength in heart failure has been associated with both a reduction in QOL (38) and an increase in mortality (39). One author has even implicated skeletal muscle wasting as the predominant cause of exercise intolerance in patients with heart failure (40).

1.2.3 Muscle fibres in health, COPD and heart failure

In normal human skeletal muscle there are 3 different types of muscle fibre, which depend on which type of myosin heavy chain the fibre produces. Type 1 fibres are oxidative and fatigue resistant. Type 2x fibres are glycolytic and type 2a fibres have a mixed phenotype. Because of the disparate metabolic pathways that these fibres rely on to function the proportion of each fibre within a given muscle can

help define its metabolic efficiency, with type 1 fibres conferring greater endurance to a muscle. Fibre shift is a change in proportion of these fibres within a muscle (41, 42).

In the quadriceps of patients with COPD, there is a reduction in type 1 fibres and an increase in type 2x fibres (43), which is associated with exercise intolerance, lower DLCO but interestingly not with forced expiratory volume in 1 second (FEV1) or physical activity (44). Concurrently there is a type 2x fibre specific atrophy (45), with a predictable reduction in oxidative enzymes, without any change in glycolytic enzymes (46). The quadriceps of patients with heart failure exhibit similar changes to those seen in COPD, with a shift towards a type 2 fibre predominance (47) and a reduction in oxidative enzymes (48). In the diaphragm of these patients the fibre shift is reversed with an increase in type 1 fibres and a decrease in type 2 fibres, suggesting an increase in fatigue resistance and improved performance (49, 50).

1.2.4 Molecular pathways leading to muscle loss in chronic disease

Loss and gain of muscle depends on the interplay between protein synthesis and breakdown (51). In chronic diseases loss of muscle function and size is thought to be due to a relative up-regulation of atrophic and down-regulation of hypertrophic pathways, loss of muscle satellite stem cell function, upregulation of autophagy and apoptosis, and shift in fibre type (51-53). The signalling pathways involved in muscle wasting are vast and complex but some of the major pathways that are retained across the spectrum of chronic diseases are shown in figure 1.2.

In muscle it has been suggested that the ubiquitin-proteasomal system is important in stimulating the breakdown of protein, a cause of muscle atrophy. The most well studied ubiquitin ligases that have been shown to be involved in this pathway are atrogin-1 and muscle ring finger 1 (MuRF1) (51, 53, 54). A number of studies have shown that the ubiquitin ligases atrogin-1 and MuRF-1 are variably up-regulated in the quadriceps of patients with COPD (52, 55-58), heart failure (59) and in an animal model of cardio-respiratory disease (60). This increase in ubiquitin ligase expression is, however, not a universal finding. Members of my group found no difference in MuRF-1 and a decrease in atrogin-1

expression in the quadriceps of patients with COPD when compared to controls. The authors argued that this lack of association between muscle mass and ubiquitin ligase expression did not exclude a role for these proteins in the muscle wasting process, as their levels may vary with time (61). This conclusion is supported by data from animal studies of denervation muscle injury, which shows that ubiquitin ligase levels peak at day 4 and return to baseline by 2 weeks (54).

Hypertrophy in muscle is driven by a number of factors. One of the most important mediators of muscle hypertrophy is insulin like growth factor 1 (IGF-1). IGF-1 binds to its receptor and stimulates protein kinase B (AKT) phosphorylation which in turn activates mechanistic target of rapamycin (mTOR), leading to upregulation of pro-hypertrophic transcription factors. IGF-1 also inhibits forkhead box protein O1 (FOX-O1) activity, which is a major stimulus for muscle breakdown (51, 53). IGF-1 has been shown to be both up and downregulated in the quadriceps of patients with chronic disease. For example, in 2 studies, in patients with COPD quadriceps mRNA levels of IGF-1 were upregulated, (62, 63), whilst in another study in a study in early heart failure they were downregulated (64).

Another important mediator of muscle loss and gain is myostatin (Growth and Differentiation Factor 8 (GDF-8)). GDF-8 is a transforming growth factor beta (TGFβ) super-family member which acts as a potent negative regulator of muscle growth (65). It acts through SMADs (66) and non-SMAD pathways (67) to alter transcription of a number of mediators of muscle strength and size. It interacts with both ubiquitin proteasome and IGF-1 pathways (51, 53). GDF-8 has been shown to be upregulated in the muscle of both COPD (68) and heart failure (69) patients.

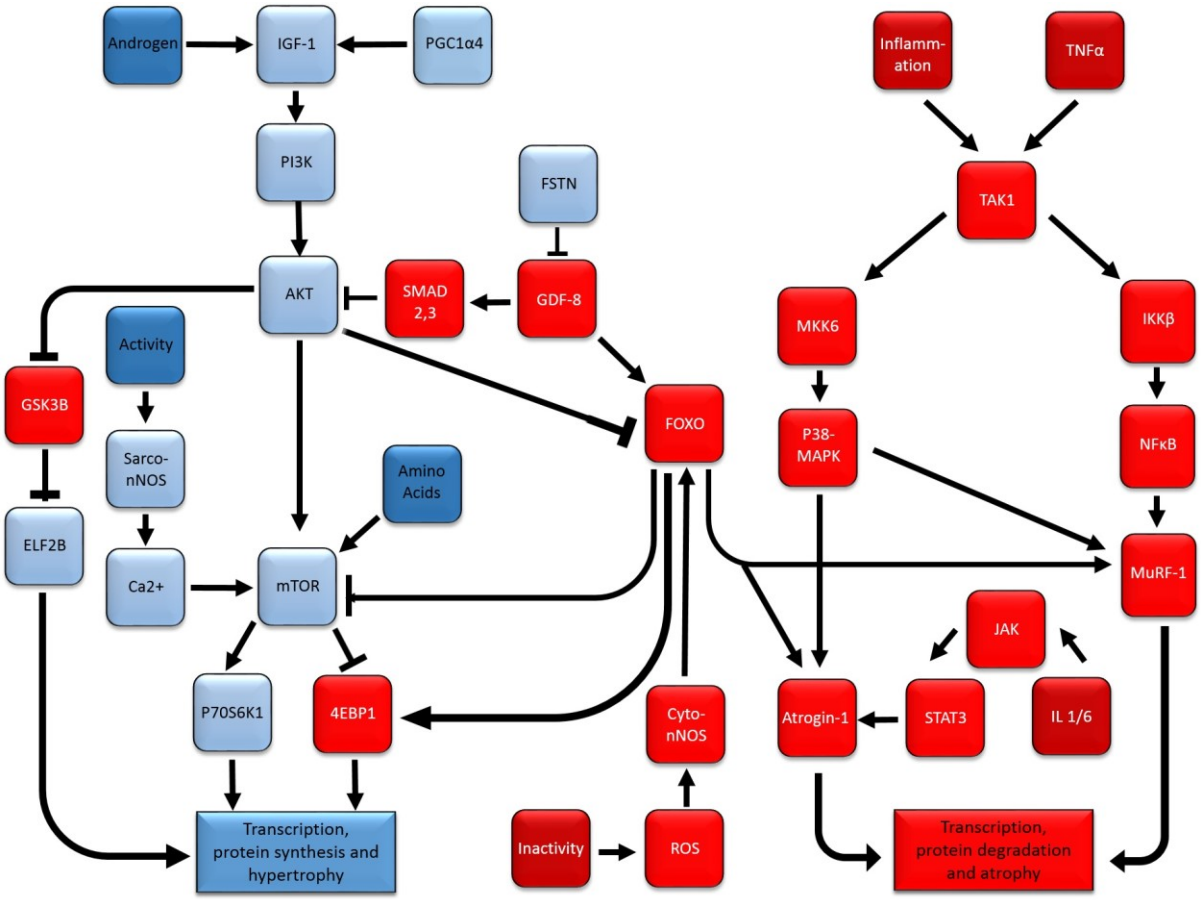

Figure 1.2. Pathways of muscle loss in chronic disease. Some of the major pathways involved in the development of muscle hypertrophy and atrophy. Blue boxes contain stimuli of hypertrophic responses whilst red boxes represent atrophic signalling molecules. Insulin like growth factor 1 (IGF-1), phosphoinositide 3-kinase (PI3K), protein kinase B (AKT), mammalian target of rapamycin (mTOR), calcium ($Ca2^{+}$), sarcoplasmic neuronal nitric oxide synthase (sarco-n NOS), P70S6 kinase (P70S6K), eukaryotic translation initiation factor 4E binding protein 1 (4EBP1), glycogen synthase kinase 3 beta (GSK3B), eukaryotic initiation factor 2B (ELF2B), reactive oxygen species (ROS), cytoplasmic neuronal nitric oxide synthase (cyto-nNOS), myostatin (GDF-8), follistatin (FSTN), peroxisome proliferator-activated receptor gamma coactivator 1-alpha (PGC1α4), tumour necrosis factor α (TNFα), forkhead box protein (FOXO), TGFβ activated kinase 1 (TAK1), mitogen-activated protein kinase 6 (MKK6), p38-mitogen-activated protein kinase (p38-MPAK), inhibitor of nuclear factor kappa-B kinase subunit β (IKKβ), nuclear factor kappa B (NFKB), Muscle RING finger protein 1 (MuRF-1), Interleukin 1/6 (IL1/6), janus kinase (JAK), signal transducer and activator of transcription (STAT)(based on references(51-53, 70-73)).

The molecular pathways activated by chronic disease leading to muscle loss are thought to be driven by a number of factors including disuse, malnutrition, inflammation, hypoxia, oxidative stress, acidosis and medication, some of which will be outlined below (51-53).

1.2.5 The drivers of muscle loss in chronic disease

1.2.5.1 Physical inactivity

As well as being implicated in the development of both heart failure (74) and COPD (75) physical inactivity is also a common consequence of chronic cardio-respiratory disease which may interact with inflammation, metabolic abnormalities and oxidative stress to increase transcription of various genes involved in the muscle wasting process (76). Disuse has been shown to promote atrophy through increases in oxidative stress and inflammation, particularly through the upregulation of nuclear factor kappa B (NFκB), as well as by reducing pro-hypertrophic neuronal nitric oxide synthase. This process may be further enhanced by physical inactivity effects on insulin resistance, apoptosis and a reduction in antioxidants (77, 78). Taken together this data suggests a central role for physical inactivity in propagating muscle loss in patients suffering with chronic diseases of the heart and lung.

1.2.5.2 Malnutrition

Malnutrition makes a significant contribution to skeletal muscle wasting in COPD (79) and heart failure (80). Increased amino acid availability has been shown to activate a number of pathways involved in protein synthesis including the mTOR pathway (51). In an elderly population sensitivity to essential amino acids particularly leucine is significantly reduced, meaning supra-normal supplementation in these individuals may be required to stimulate muscle growth (81); this may be similar in COPD and heart failure where some authors argue that the disease process causes an accelerated ageing phenotype (82, 83).

1.2.5.3 Inflammation

Systemic Inflammation is found in some patients suffering with both COPD and heart failure (84, 85). Inflammatory cytokines, particularly NFκB and tumour necrosis factor alpha (TNFα), have been shown *ex-vivo* to be important mediators of muscle atrophy through up-regulation of ubiquitin ligases. Other inflammatory mediators including interleukin 6 and 1, signal transducer and activator of transcription 3, Janus kinase and TNF receptor associated factor 6 (TRAF6) have also all been shown to mediate muscle loss. As well as up-regulating ubiquitin ligases and promoting atrophy these pro-inflammatory ligands inhibit hypertrophy through down-regulation of IGF-1 / AKT signals (51). It is not clear however whether systemic inflammation plays a significant role in the development of muscle wasting in all chronic disease. In COPD there is some evidence that systemic but not local inflammation may be associated with loss of muscle (86).

1.2.5.4 Hypoxia

Tissue hypoxia is an important consequence of COPD (86) and heart failure (87), which has been associated with a decrease in overall muscle mass (88) and muscle fibre cross sectional area (89). Hypoxia causes an increase in hypoxia inducible factor (HIF) which in turn inhibits mTOR activity and increases mitogen activated protein kinase (MAPK) activity resulting in decreased protein synthesis and increased protein atrophy. Other proteins implicated in hypoxia induced muscle wasting include peroxisome proliferator-activated receptor (PPAR), peroxisome proliferator-activated receptor gamma coactivator 1-alpha (PGC1α), NFκB, and GDF-8 (90). Reactive oxygen species (ROS) are generated in mitochondria exposed to hypoxic conditions. Excess ROS, which are found in both COPD (91) and heart failure (92), lead to muscle tissue damage, apoptosis, a decrease in mTOR activity and a reduction in protein synthesis (93) resulting in wasting.

1.2.6 Treatments aimed at improving muscle function in chronic disease

1.2.6.1 Rehabilitation

In patients with COPD, pulmonary rehabilitation has been shown to increase exercise capacity and QOL (94), whilst reducing anxiety and depression (95). Although a survival benefit has not been demonstrated (96), rehabilitation has also been shown to and reduce exacerbation and admission rates in COPD patients (30, 37, 97, 98).

Cardiac rehabilitation programs have been shown to have similar effects in ischaemic heart disease and heart failure to those seen with pulmonary rehabilitation in COPD. Rehabilitation results in a reduction in hospital admissions and an improvement in QOL (99) and exercise tolerance (100) in cardiac patients. There is also a demonstrable mortality benefit in cardiac patients undergoing rehabilitation, that was not seen in patients with COPD, possibly due to the smaller numbers of patients enrolled in these studies (101).

Rehabilitation, which includes resistance training, has been shown to increase muscle strength in both patients with COPD and heart disease (102-106). A study in COPD has examined the effects of strength training on the expression of various proteins known to be involved in the balance between muscle hypertrophy and atrophy. They showed that there was no change in ubiquitin ligase or GDF-8 expression, but there was a significant upregulation of MyoD, a transcription factor involved in myogenesis (107).

1.2.6.2 Nutritional Supplementation

COPD patients, who were treated with nutritional supplements gained weight, improved their QOL, increased their exercise tolerance and, overall, improved their muscle strength in some studies (108-110), although the latter finding was not universal (111). In patients with heart failure nutritional supplementation, in some studies also caused patients to gain weight and improve their exercise tolerance without altering muscle size, strength or QOL (112). The exact nature of the ideal

supplement to the diet in COPD and heart failure is yet to be established with some advocating a high fat, low carbohydrate diet (113) whilst others have recommended the supplementation of essential amino acids (114). The biological basis for supplementing amino acids such as leucine in patients with cardio-respiratory disease has been investigated. Leucine can activate the IGF-1 pathway including AKT and mTOR in skeletal muscle, potentially stimulating hypertrophy signalling (115).

1.2.6.3 Anabolic agents

Anabolic agents have been shown to cause an increase in weight and muscle size in COPD and heart failure. The clinical use of these supplements has been limited by off target adverse side effects, which limit their potential clinical benefits (116, 117).

Growth hormone has been used effectively in patients with human immunodeficiency virus (HIV) related cachexia (118). In those with COPD growth hormone caused a gain in lean weight but failed to increase peripheral muscle strength (119, 120). In an unselected group of heart failure patients growth hormone had no positive effects on functional outcomes (121), whereas in those patients identified as growth hormone deficient replacement did improve exercise duration, QOL and ejection fraction, suggesting that its primary effect in these patients was in cardiac rather than skeletal muscle (122).

Testosterone, as an anabolic agent, has been trialled alone and alongside resistance training in COPD. In one trial testosterone increased lean body mass and muscle strength in patients with COPD, an effect that was amplified by the combination of injection of testosterone with resistance exercise training (123). In a recent meta-analysis it was concluded that testosterone was able to increase muscle strength but had no effect on exercise performance or on QOL in COPD (124).

Inhibition of angiotensin converting enzyme (ACE) with ACE inhibitors theoretically might be used to improve muscle strength in COPD and in heart disease, through actions on both the IGF-1 and ubiquitin proteasomal pathways (125). However in a trial of ACE inhibition versus placebo in a cohort of COPD

patients undergoing pulmonary rehabilitation the placebo group gained more muscle mass than the intervention arm suggesting that ACE inhibition is not effective in improving muscle strength in these patients and in fact may be detrimental (126).

Alternative drugs under development include selective androgen modulators (SARMS) which theoretically have fewer off target effects than testosterone (127), GDF-8 antagonists (128), ghrelin analogues (129) and anti-catabolic / pro-anabolic agents like MT-102 (130).

1.3 Muscle wasting in PH and PAH

Muscle wasting has been studied much less frequently in PAH than in COPD or in heart failure. The monocrotaline (MCT) rat has, however, been widely used for many years as a model of cardiac cachexia and PH. The available literature on this model and other animal models of PH is therefore summarised below.

1.3.1 Muscle wasting in animal models of PAH

The most widely studied animal model of PAH related muscle loss is the MCT rat model. MCT is a pyrrolizidine alkaloid which is the main toxic component of the Crotalaria spectabilis species of plants. It is known to induce pulmonary hypertension and either compensatory right ventricular hypertrophy or right heart failure (131). It is well established that after 4-6 weeks treatment with MCT, rats who develop heart failure also exhibit significant weight loss despite increases in water retention (132-137).

MCT treated rats have previously been shown to have lower hind-limb muscle dry weights and fibre cross sectional area when compared to control animals, although this is not a universal finding. Studies have shown loss of muscle mass in the soleus, tibialis anterior (TA) and extensor digitorum longus (EDL) muscles (132-141). In small animals, such as rodents there is an additional fibre type which, is not present in man, is faster than the type 2x fibres and has been termed 2b (142). It is in these type 2b fibres that the fibre specific atrophy occurs in the EDL of MCT, much like the fibre specific atrophy

seen in the 2x fibres in humans (60). The contractile properties of these same muscle in the MCT rat are also impaired, suggesting the decline in muscle mass observed is accompanied by a decline in the functional properties of that muscle (143).

After MCT treatment, rats that developed heart failure showed a significant reduction in skeletal muscle oxidative enzymes, a reduction in antioxidants and an increase in lipid hydroperoxide, suggesting a significant decrease in potential for aerobic metabolism and an increase oxidative stress (132, 144). EDL (fast twitch) and TA (mixed fast and slow twitch) muscles also exhibited significant myosin heavy chain shift from 2a to 2b fibres, whilst the soleus (slow twitch) showed significant change from myosin heavy chain 1 to 2a fibres. This was associated with a significant decrease in skeletal muscle blood flow (134, 135, 138, 140, 145-147).

The loss of muscle mass in the MCT rat is driven at least in part by increases in apoptosis. In the EDL of the MCT rat there is an increase in proportion of apoptotic nuclei in both myofibres and interstitial cells, which has been associated with a decrease in the anti-apoptotic bcl-2 and an increase in the pro-apoptotic caspase-3 (138, 145, 146, 148). The number of apoptotic nuclei in the muscle of these animals is significantly correlated with plasma BNP levels, right ventricular hypertrophy (138) and circulating levels of TNFα and its secondary messenger sphingosine (145), suggesting that both severity of heart failure and levels of systemic inflammation may be involved in propagating muscle loss in this model of PAH.

Loss of muscle mass in the MCT rat is driven by a decrease in capacity for regeneration and an increase in atrophy. MCT rat EDL and soleus muscles exhibit a decrease in factors regulating muscle differentiation, development and regeneration including myoD, myogenic factor 6 (Mrf4) and myogenic (136, 141). It has also been shown that MCT treatment causes a significant reduction in soleus myoD^{+} and pax 7^{+} positive satellite cells (147), which have the potential to both differentiate and form new muscle. Taken together, this data suggests that there is a reduction in capacity for skeletal muscle regeneration in the MCT model of PAH. As mentioned before, 2 key drivers of muscle

atrophy are the ubiquitin ligases atrogin-1 (60, 136) and MuRF-1 (60), both of which have been found to be over-expressed in the hind limb muscles of the MCT rat. In fact, higher atrogin-1 levels were associated with lower EDL muscle mass in this model (136).

Mitochondrial dysfunction has been shown to be another factor involved in muscle loss in the MCT rat. Mitochondrial enzymes and markers of mitochondrial function *PGC*-1α, cytochrome c and calcineurin are all reduced in the muscle of the MCT rat (135). It has been demonstrated that there is a reduction in mRNA expression of mitochondrial proteins sirtuin 1 (SIRT1), PGC-1α and mitochondrial transcription factor A (TFAM) in the gastrocnemius of the MCT rat 2 weeks prior to these changes being seen in the right ventricle suggesting that mitochondrial dysfunction occurs in the skeletal muscle before the cardiac muscle in these animals (149).

Other factors which may contribute to the muscle wasting process in the MCT rat include upregulation of expression and activity of the pro-inflammatory matrix metalloproteinase 9 (MMP9) (150) and a decrease phosphorylation of the pro-hypertrophic AKT and FOX0-3. There is also an increase in the E2 activating ligases, e214k and ubiquitin-conjugating enzyme E2 (UBC7), which help ubiquitin ligases like atrogin-1 contribute to muscle wasting (136).

Anorexia may also contribute to some of the changes in body weight, muscle weight and atrogene expression in the MCT rat (136). This anorexia was reversed by the soluble TNFα receptor but not by pentoxyfylline, a known inhibitor of TNFα function, and was associated with a reduction but not a normalisation of atrogene expression in the rodent's EDLs (136). Interestingly in a MCT mouse model, where mice were injected weekly with 60 mg/kg of MCT for 6 - 8 weeks, there was no difference in the food intake between animals with PAH and controls (137).

A number of interventions have been shown to be effective in reversing at least some of the changes seen in the skeletal muscle of rats with pulmonary hypertension and heart failure. This includes irbesartan, thalidomide, high dose growth hormone, L-carnitine and nebivolol which were able to partly restored normal MHC expression pattern (134, 140, 146, 151, 152). High dose growth hormone was able to partially reverse the atrophy seen in the TA (134) but not significantly in the soleus (135)

of treated animals as evidenced by a relative increase in fibre cross sectional area. This treatment was associated with decreased apoptosis, TNFα, and sphingosine blood levels (134) as well as normalization of PGC1α, cytochrome c and calcineurin expression (135). Carvedilol treatment of the MCT rat was shown to reduce the oxidation of muscle proteins and restored normal contractile properties to muscle (143). Nebivolol was also able to restore total animal and TA weight as well as fibre cross sectional area to normal. It also reduced oxidation of proteins in the soleus, reduced apoptosis as measured by the presence of TUNEL positive nuclei and improved muscle twitch performance (140). Both a soluble TNFα receptor and pentoxyfylline, a TNFα antagonist, were able to reverse changes seen in ubiquitin ligase expression in MCT rat muscle in a food intake dependant and independent mechanism respectively (136). The subcutaneous injection of human stem cells into the MCT rat was also associated with a significant increase in soleus weight and soleus fibre cross sectional area, as well as a reduction in apoptosis and an increase in pax-7^{+} and $MyoD^{+}$ expressing satellite cell numbers back to near normal levels, as well as a significant shift in MHCs back to a normal distribution (147).

Studies focussing on the role of TGFβ super-family ligands in the development of PAH associated muscle loss in animal models is limited to a single study examining circulating GDF-8 levels in the MCT rat (153).

1.3.2 Muscle wasting and physical activity in PAH clinical observations

Muscle dysfunction was first identified in the respiratory muscles of patients with PAH by Meyer *et al*. They showed that patients had reduced maximal inspiratory and expiratory pressures compared to controls indicating significant respiratory muscle weakness in this cohort (154). They also found that unlike patients with congestive cardiac failure (155, 156) and similar to patients with COPD (157), patients with IPAH suffered from an equal decrease in maximal inspiratory and expiratory pressures (154, 158). These findings were confirmed by Kabitz *et al.* using non-volitional techniques to stimulate the respiratory muscles. His group was also able to demonstrate that maximum inspiratory pressures

and sniff nasal inspiratory trans-diaphragmatic pressures correlated significantly with exercise tolerance as measured by 6MWD in the group studied (159).

Peripheral skeletal muscle dysfunction in PAH was first shown in 2007 when Bauer *et al*. demonstrated that maximal isometric forearm strength was significantly lower in patients with PAH than in healthy controls. They also demonstrated a significant correlation between 6MWD distance and hand grip, inspiratory and expiratory muscle strength. Interestingly there was no significant relationship between measured pulmonary artery pressure and handgrip strength (160). Mainguy *et al.* demonstrated that quadriceps maximal volitional capacity and quadriceps twitch strength was significantly lower in patients with PAH than in age matched controls. They confirmed the close correlation between exercise capacity and muscle strength and again demonstrated that there was no significant relationship between muscle strength and pulmonary haemodynamics. They also showed that strength correlated with maximal oxygen uptake on CPET (161).

Whilst not all researchers have found a change in peripheral skeletal muscle in PAH (162) Batt *et al*. have recently added significantly to the breadth of our knowledge in this area. They demonstrated that in 12 patients with IPAH computerized tomography assessed quadriceps cross sectional area was significantly reduced compared to controls (163). They also showed that muscle biopsies from patients with PAH showed a lower proportion of type 1 muscle fibres and increase in type 2 fibres (163) confirming earlier work by Mainguy *et al.* (161). Type 1 fibres also had lower cross sectional area than controls (163) and there was an increase in phosphofructokinase: 3-hydroxyacyl–Co-A-dehydrogenase ratio suggesting an increase potential for anaerobic metabolic work (163, 164). Further elucidation of the metabolic pathways involved in the muscle wasting in PAH has shown that AKT, p70S6Kinase and FOX-O3 phosphorylation was decreased whilst both atrogin-1 and MuRF-1 were over-expressed in the quadriceps of patients (163).

Some authors have understandably compared muscle weakness seen in PAH to that seen in congestive cardiac failure. It is thought that some of the exercise intolerance associated with heart failure is due

to a phenomenon known as the ergoreflex, where abnormalities in skeletal muscle metabolism in chronic heart failure results in a significant increase in ventilatory demand of exercise (165).The driver to this process is felt to be a reduction in skeletal muscle blood flow during exercise. Interestingly it has been noted that all 3 major classes of drugs prostaglandins (166), sildenafil (167) and endothelin receptor antagonists (168) used to treat PAH have the capability of vasodilating the skeletal muscle circulation as well as increasing patients' exercise capacity, potentially through a reduction in this ergoreflex. Although this theory has not been formally tested in PAH, is it possible that the increases in exercise tolerance seen with these drugs may be in part due to a blunting of this ergoreflex (169) .

Further data suggesting a link between right heart failure and muscle dysfunction come from an investigation into patients with congestive cardiac failure which suggested that maximal inspiratory pressure, which is an independent and important predictor of prognosis, is significantly and inversely correlated with mean pulmonary artery pressure, PVR, and pulmonary capillary wedge pressure suggesting a potential relationship between the pulmonary vasculature and muscle dysfunction in other cardio-respiratory conditions (170).

Indirect evidence of the importance of a peripheral myopathy in PAH comes from studies looking at the effects of pulmonary rehabilitation on the condition. Mereles *et al.* showed that contrary to previous thinking, rehabilitation was safe and effective in patients with PAH. At 15 weeks, an exercise program was able to improve 6MWT distance by an average of 111m as well as improving QOL, WHO functional status, BORG score, peak oxygen consumption, oxygen consumption at the anaerobic threshold, and achieved workload, without altering haemodynamic parameters (171). De Man *et al.* showed that a 12 week supervised exercise training program involving cycling, muscle strength and endurance exercises was able to increase the patients anaerobic threshold, and exercise endurance time by 89% without changing distance achieved on 6MWD. Quadriceps strength increased by 13%, leg circumference remained unchanged and fibre type distribution was not altered. There was however, a significant increase in the number of capillaries per myocyte and increase oxidative

capacity measured by succinate dehydrogenase levels in type I fibres (172). Mainguy *et al.* has demonstrated that a 12 week rehabilitation program involving 5 patients exposed to cycling, walking and weight training resulted in a nearly 60m increase in 6MWD and significant decrease in the proportion of type 2x muscle fibres in quadriceps biopsy (164).

As mentioned above physical activity is one unifying cause of muscle loss across a wide spectrum of diseases. Physical activity has been infrequently measured in PAH but is emerging as both a target for intervention and an outcome measure in this group of patients. The latest ESC/ERS guidelines have suggested that patients with PAH should be encouraged to remain as active as possible within symptom limits and that supervised rehabilitation is beneficial in terms of both exercise capacity and QOL (7, 22). A small number of studies have shown that physical activity is reduced in patients with PAH when compared to healthy controls (173-176). Physical activity has been correlated with 6MWD (173), WHO functional class (174) and with QOL (175). Measuring and improving physical activity in PAH is a goal of treatment that requires further attention. The optimal method of assessing physical activity is not yet known with activity monitors and questionnaire having their own advantages and disadvantages (177).

One molecular pathway that may play a critical role in muscle wasting but has, so far, not received much attention in muscle wasting in PAH is the TGFβ super-family of proteins.

1.4 TGFβ signalling

1.4.1 TGFβ signalling pathway

The TGFβ super-family, is a group of proteins which are involved in developmental, physiological, homeostatic and pathological processes. They have a preserved structural homology with a 6-12 residue cysteine knot and can be broadly divided into the TGFβ / activin group and the BMPs. GDFs are a divergent group with some members having more BMP- like properties, whilst others are more like TGFβ (178-180).

TGFβ super-family proteins act primarily in an autocrine and paracrine manner (178, 181), but recent evidence suggests that circulating levels can effect organs well away from their site of expression, suggesting they can also have endocrine actions (182). Generally TGFβ super-family proteins are secreted and stored in the extracellular matrix as inactive pro-peptides which are cleaved by proteases and activated to become dimeric proteins which then bind to their target receptors (183). The receptors are classed as type 1 and 2 (184). The ligand binds to its receptor which forms a heterotetrameric complex consisting of 2 type 1 and 2 type 2 receptors (185). The type 2 receptor is a constitutively active serine threonine kinase which is able to phosphorylate the type 1 receptor (184). This in turn phosphorylates intracellular SMAD molecules (186). The TGFβ / activin ligands tend to activate SMAD 2 and 3 whilst BMPs activate SMAD 1,5,8 but there is significant overlap within the system (187). These SMADs combine with the co-SMAD SMAD4 and the complex translocates to the nucleus to stimulate gene transcription (188). All SMADs recognise the binding site CAGAC whilst SMADs 1 and 5 have higher affinity for GC rich areas of DNA (179). Meanwhile SMAD 6 and 7, known as the inhibitory SMADs, regulate the cellular signalling by enhancing degradation of receptors and inhibiting receptor/receptor-SMAD/co-SMAD interactions (189). The TGFβ super-family are also regulated by proteins which bind to them directly preventing them from interacting with their receptor, e.g. follistatin (187) (Figure 1.3).

Despite nearly 40 TGFβ ligands being identified there are only 5 type 2 receptors and 7 type 1 receptors meaning that most ligands can bind to different combinations of receptors with different affinities, altering the consequences for downstream signalling (178). The combination of receptors able bind different TGFβ ligands are outlined in Figure 1.4.

As well as classical SMAD signalling it has been established that TGFβ superfamily members can interact directly and indirectly with a number of other pathways. Particularly important pathways include the TGFβ activated kinase 1 (TAK1) pathway, inhibitor of nuclear factor kappa-B kinase subunit beta *(*Ικκβ), NFκB axis (190) p38 MAPK (191), extracellular signal regulated kinase 1 and 2 (ERK 1 / 2)

(192), c-Jun N terminal kinase (JNK) (193) and phosphoinositide 3 (PI3) kinase–AKT (194) pathways. These non-canonical pathways are often involved in antagonising or augmenting the effects of SMAD signalling. Taken together this data suggests that by activation of a number of competing and cooperating pathways the TGFβ super-family can fine tune its effects in a cell, time and environment dependent manner (178, 179) (Figure 1.3).

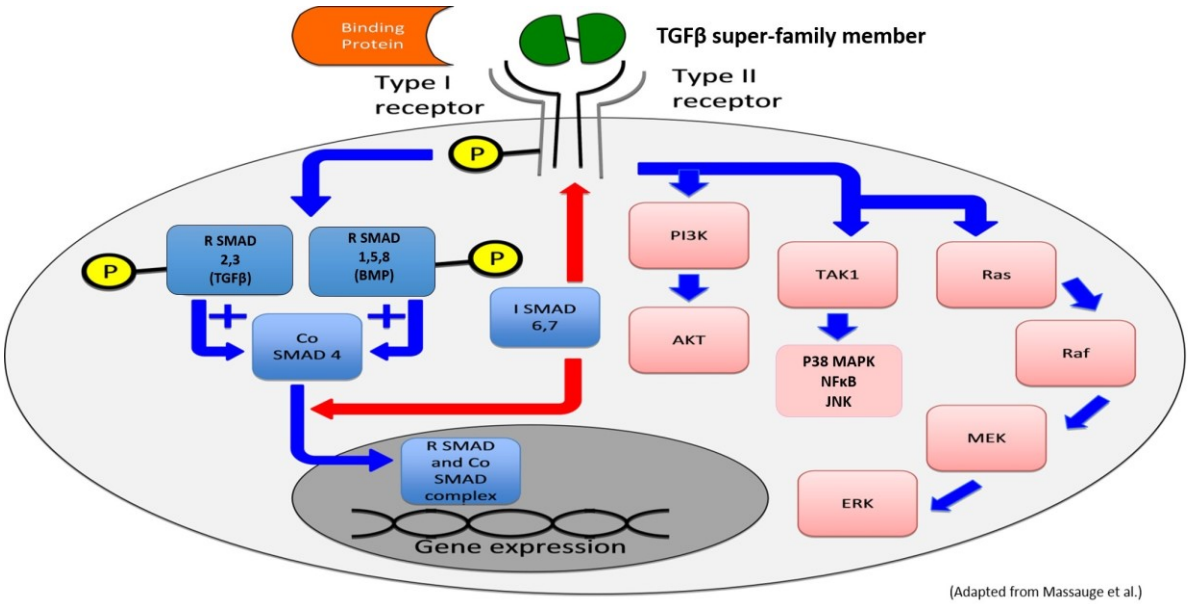

Figure 1.3 Transforming growth factor β (TGFβ) super-family signalling. Blue boxes represent classical SMAD signalling, whilst red boxes represent non-canonical signalling. Blue arrows represent stimulatory signals, whilst red arrows represent inhibitory signals. Abbreviations used include receptor SMAD (R SMAD), inhibitory SMAD (I SMAD), phosphoinositide 3-kinase (PI3K), protein kinase B (AKT), TGFβ activated kinase 1 (TAK1), p38-mitogen-activated protein kinase (p38 MAPK), nuclear factor kappa B (NFκB), c-Jun N-terminal kinase (JNK) and extracellular signal-regulated kinase (ERK) (179).

Figure 1.4 TGFβ super-family members and their potential receptors. TGFβ super-family members (blue) and their potential type 1 (red) type 2 (green) and non-specific (orange) receptors. Bone morphogenetic proteins (BMPs), growth and differentiation factor (GDF), antimullerian hormone (AMH), inhibins (inh), activin receptor like kinase 3 / BMP receptor 1A (ALK3) activin receptor like kinase 6 / BMPreceptor 1B (ALK6) activin receptor like kinase 2 / activin receptor type 1 (ALK2), activin receptor like kinase 4 / activing receptor 1B (ALK4), activin receptor like kinase 1 / TGFß-super-family receptor (ALK1), activin like kinase 5 / TGFβ receptor type 1 (ALK5), BMP receptor 2 (BMPR2), activin receptor 2A/B (ACVR2A/B), TGFβ receptor 2 (TGFBR2), Glial cell line-derived neurotrophic factor (GDNF) receptor a (GRFa), Other (GDNF, neurturin, artemin , persephin) (adapted from Mueller *et al.*)(178).

The complex interplay between the relatively few constitutive components that make up the TGFβ system with an almost limitless potential for interaction thus allows the TGFβ signalling pathway to control the wide range of biological functions it contributes to. The outcome of the signal is dependent on: the amount of signal transduction apparatus present both inside and outside the cell, including the amount, ratio and type of TGFβ ligand; the receptor expression properties of the cell, the amount of downstream material available for activation; the other nuclear signals that are present at the time

of stimulation; the presence of co-factors required to propagate the signalling pathways; and the availability of the target genetic material which may be altered by processes such as methylation (195).

1.4.2 TGFβ signalling in PAH

Abnormalities in TGFβ signalling have been shown to be instrumental in the development of PAH. Eighty percent of those with familial and up to 25% of those with IPAH have a mutation in the bone morphogenetic proteins type 2 receptor (BMPR2) (196). BMPR2 dysfunction is not limited to those with genetic disorders as lower levels of expression of the receptor have been found in patients with IPAH without mutations (197). Furthermore mutations in the activin like kinase (ALK) 1 receptor account for the majority of cases of hereditary haemorrhagic telangiectasia (HHT) associated PAH with a smaller subset being caused by other mutations, for example those that code for endoglin, a TGFβ receptors (198) or SMAD 4 (199).

In pulmonary artery smooth muscle cells (PASMCs) BMPR2 mutations result in an absence or reduction in SMAD 1, 5 signalling in response to BMPs whilst SMAD 2, 3 responses are up-regulated due to compensatory effects of the activin type 2 receptors (200). BMPs 2, 4 and 7 activate both anti-proliferative SMAD and pro-proliferative p38 MAPK signalling in PASMCs. Normally these ligands have predominant anti-proliferative effects in proximal vessels and pro-proliferative effects in the distal vasculature. In cells lacking BMPR2 the anti-proliferative actions of the BMPs are lost resulting in unchecked smooth muscle hyperplasia (201). In endothelial cells BMP 4 and 6 cause cell proliferation and migration as well as protecting from apoptosis. Lack of BMP signalling in these cells results in loss of the endothelial cell layer exposing the PASMCs, and contributing to a lack in their ability to respond normally to hypertrophic signalling by growth factors. This causes uncontrolled PASMC proliferation, whilst an apoptotic resistant pool of endothelial cells is selected out allowing them to proliferate forming plexiform lesions (202).

Abnormalities in the BMPR2 and ALK1 pathways are not the only aberrations in TGFβ signalling seen in PAH. In MCT rats pulmonary vascular TGFβ1 and SMAD 2 were up-regulated and were associated with disease progression and increased apoptosis. Furthermore pulmonary haemodynamics and vascular remodelling were improved by an ALK-5 inhibitor (203). TGFβ1 which is normally anti-proliferative in PASMCs has been shown to cause proliferation in PASMCs from patients with IPAH (204). This has led some to suggest that aberration in BMPR2 function is able to switch the effect of TGFB1 from anti to pro-proliferative in smooth muscle cells. However this is not a universally accepted hypothesis as other groups have shown a reduction in TGFβ1 and SMAD signalling in response to treatment with MCT (205).

Other TGFβ super-family members have been found in increased levels in patients with PAH. Activin A and its natural antagonist follistatin have been linked to prognosis in PAH and activin A has been shown to cause PASMC proliferation *in vitro*, suggesting it may be an important mediator in the development of PAH (206).

GDF-15 is a molecule of interest that has been associated with prognosis in PAH (207) and will be discussed later in the introduction.

1.4.3 TGFβ signalling in skeletal muscle atrophy

As mentioned GDF-8, is a TGFβ super-family member and potent negative regulator of muscle mass. GDF-8 has been shown to be elevated in the muscle of the elderly, the inactive and those with chronic diseases including COPD, HIV, heart failure, renal failure and cancer (70). GDF-8 null mice exhibit an increase in muscle mass compared to controls (208). Transgenic expression of follistatin, GDF-8's trapping protein, resulted in a further increase in mass above GDF-8 inhibition alone, suggesting other TGFβ super family proteins that are bound by follistatin protein can also influence muscle mass. Candidate proteins include the activins (209). GDF-8 acts via the activin receptor 2B (ACVR2B) and ALK 4/5 and SMAD 2/3 (51). It has multiple effects inhibiting both hypertrophic and hyperplastic signalling

pathways (53). GDF-8 also down-regulates phosphorylation of the AKT pathway (210) whilst follistatin is able to induce a significant increase in AKT phosphorylation and is associated with hypertrophy (211). GDF-8 can cause muscle atrophy through an increase in the ubiquitin ligase atrogin-1, but not MuRF1. Interestingly this is dependent on FOX-O activation but independent of SMADs and AKT (71). GDF-8 can also act via TAK1 to stimulate NFκB, P38 MAPK, ERK1/2 and JNK all of which are involved in inhibiting hypertrophy and promoting atrophy (72). In muscle cells GDF-8 has been shown to cause a reduction in levels of the regenerative transcription factors MyoD, MRF5 and myogenin (73). This process may keep satellite cells in a quiescent state (71). It has recently been shown that in an animal model of heart failure systemic levels of GDF-8, influenced primarily by up-regulation of GDF-8 expression from the heart, can have a significant impact on peripheral muscle mass suggesting that this and other TGFβ super-family proteins can function in an endocrine manner (212). This observation is supported by evidence suggesting that over-expression of GDF-8 in one leg muscle of a mouse cause leak of the protein into the circulation resulting in a generalised wasting of other hind limb muscles. It therefore seems possible that circulating levels of TGFβ super-family members may make an important contribution to muscle mass in chronic disease by influencing the availability of active local stores of the ligand (182).

Other TGFβ super-family members have been implicated in the development of muscle atrophy and hypertrophy. TGFβ1 has been associated with fibrosis, inflammation, SMAD 2, 3 activation and muscle dysfunction through impairing hypertrophy and stimulating atrophy (213, 214). BMPs, particularly BMP 7, 13 and 14 have been associated with hypertrophy in adult skeletal muscle probably dependent on SMAD 1, 5 phosphorylation, and may be related to up-regulation of mTOR, inhibition of FOXO, down-regulation of ubiquitin ligases and maintenance of a pool of replicating satellite cells (215, 216).

TGFβ super-family members, such as the activins and BMPs can bind to the ACVR2B and influence downstream signalling (73). Antagonising the ACVR2B has proved more successful than blocking the effects of GDF-8 alone, with soluble ACVR2B treatments resulting in a 60% increase in muscle size

(209) and causing an improvement in cardiac function, metabolic handling of glucose and an increase in longevity in a mouse cancer cachexia model (217). Further evidence that we should be looking beyond GDF-8 in muscle comes from my group. Bloch *et al.* showed that in patients on intensive care (ICU) blood GDF-8 levels were not different in those who did and did not develop quadriceps atrophy following aortic surgery. GDF-8 levels actually declined in patients immediately after surgery. Conversely, another TGFβ super-family member, GDF-15 was elevated in the blood of patients following surgery and remained significantly elevated in the patients who lost more than 10% of the area of their rectus femoris muscle but not in those that lost less than 10% (218).

1.5 GDF-15

1.5.1 GDF-15 in health and disease

One TGFβ super-family protein of interest that has a potential role in the development of both muscle wasting and PAH and is a potential target for future drug development is GDF-15.

Initially called macrophage inhibitory cytokine 1 (219), placental bone morphogenetic protein (220), prostate derived factor (221), placental TGFβ (222), non-steroidal anti-inflammatory associated gene (223), GDF-15 was discovered almost simultaneously in a number of tissues including macrophages (219), the placenta (220, 222), the prostate (221) and in colorectal cancer cells (223). It was also found in low levels in other tissues (220) particularly the epithelial tissue of the intestine, lung, submandibular gland, kidney, liver, spleen, lactating mammary glands (224, 225), skin and cartilage (221) the choroid plexus in the brain (224) and the CSF (226).

GDF-15 is a 62-kDa intra-cellular protein which is secreted as a 25kDa protein after cleavage by a furin like protease (219). It was noted to be similar in structure to other members of the TGFβ super-family of cytokines (219-221), which have 7 cysteine residues arranged in a knot (219-221) but, due to its lack of structural homology to pre-existing subgroups, it has been hypothesised that GDF-15 was the first member of a new sub-family (178, 219, 220).

GDF-15 has generally low expression levels during periods without cellular stress, but on stimulation by hypoxia, inflammation, short wavelength light exposure, tissue injury and cancer progression, levels can substantially increase. Some of the stimulants to GDF-15 expression include TNF α, interleukin-1B (IL-1B), IL6, granulocyte monocyte colony stimulating factor, androgens, non-steroidal anti-inflammatory drugs, PPAR γ ligands, retinoids, resevratol, etopiside, doxorubicin, cyclophosphamide and epirubicin, tissue plasminogen activator, early growth response protein 1, NFκB, hypoxia inducible factor 1α, hydrogen peroxide, TGFβ1, AKT, α dihydrotestosterone, MAPK, microphtlamia-associated transcription, p53 tumour suppressor and $p21^{WAF1}$ (227).

The physiological role of GDF-15 remains to be fully elucidated. GDF-15 levels are raised in pregnancy (228). GDF-15 is produced in large quantities by the placenta (220) and low levels in pregnancy are associated with increased risk of pre-eclampsia and miscarriage (229, 230). GDF-15 also seems to be anti-inflammatory, as it prevents activation of macrophages (219). One of the physiological roles of GDF-15 may be in preventing maternal inflammatory proteins from affecting the developing foetus and modulating the immune system allowing the mother to develop immune-tolerance to the foetus (220, 229, 230). Further evidence of the importance of GDF-15 in human reproduction comes from data showing that GDF-15 has anti-inflammatory effects in seminal fluid, where it is found at high levels (231).

Even though GDF-15 null mice are viable and female mice are fertile (232) there is some evidence that GDF-15 plays an important role in health and disease. GDF-15 may have a physiological role in the regeneration of neurones (233). For example, GDF-15 knockout mice lose sensory and motor neurones at a faster rate than wild type mice (234). There is also some evidence that GDF-15 is a cardio-protective TGFβ super-family member. GDF-15, both locally produced and exogenously administered, may have role in limiting the cardiac hypertrophic response to pressure overload (235). GDF-15 knockout mice exhibit increased extent of ischaemia reperfusion injury after coronary artery ligation (236) and due to an increase in inflammatory cell infiltrate suffered with fatal myocardial rupture more often than wild type mice (237). GDF-15 also has also been reported to have some negative effects on

the heart. In one study GDF-15 increased protein synthesis and caused hypertrophy of cardiomyocytes as well as protecting against apoptosis (238), in contrast to findings discussed above. Others have shown that GDF-15 deficient mice or mice with GDF-15 deficient macrophages are resistant to the formation of unstable, occlusive atherosclerotic plaques, resulting in a reduction in ischaemic heart disease (239, 240). Overall it seems that GDF-15 may be involved in disease progression but is also intrinsic in limiting the damage done by the disease process.

Like in cardiovascular disease, GDF-15 has been shown to have a number of opposing effects in cancer. It is generally felt that early on in the disease that GDF-15 is pro-apoptotic and anti-proliferative (227). This anti-tumorigenic effect was first seen in vitro in breast cancer cells and in vivo in athymic mice xenografted with colorectal cancer cells (223, 241). GDF-15 seems to have the opposite role in later stages of cancer progression, where in general it has been shown to enhance invasiveness and be pro-metastatic. GDF-15 has been shown to enhance malignant behaviour in melanoma (242), gastric (243, 244), breast (244, 245), oral squamous cell (246) and prostate cancer (247). GDF-15 has also been shown to confer chemotherapeutic resistance to cancer cells. This was first shown in breast cancer where excess GDF-15 conferred tamoxifem resistance (248) and may be particularly relevant in prostate cancer resistant to docetaxel and mitoxantrone (249, 250).

Perhaps most importantly high circulating GDF-15 levels are a strong independent predictor of outcomes in a wide range of conditions (207, 251-255) and in the general population higher levels have been linked to all-cause mortality (256-258). Muscle loss another ubiquitous outcome of chronic disease and a marker of poor prognosis in almost every condition that it has been measured (21) has consistently been associated with raised circulating GDF-15 levels.

1.5.2. GDF-15 in muscle wasting

GDF-15 deficient mice weigh more (234, 259) whilst GDF-15 over-expressing mice weight less than their normal counterparts, interestingly this is independent of whether GDF-15 had a tumour enhancing or inhibiting effect in the animal model studied (259, 260).

GDF-15 levels have been associated with the development of weight loss and muscle wasting in a number of cancers. In mice injected with GDF-15 secreting prostate cancer cells those who developed raised circulating GDF-15 levels had lower body weight than those with normal levels. The weight loss involved a decrease in muscle mass of between 25 and 30% and was reversed by a GDF-15 antibody. The authors noted significant hypophagia in these animals which they felt completely explained the weight loss. The associations of circulating GDF-15 with weight loss was confirmed in patients with prostate cancer and those with renal failure (260).

Members of my group have shown that, as well as an effect on appetite, GDF-15 has a direct effect on muscle. Circulating GDF-15 levels are associated with muscle atrophy in patients with ICU acquired weakness, with patients who exhibited quadriceps wasting after cardiopulmonary bypass having persistently raised serum levels of GDF-15. *In vitro* they also showed for the first time that adding GDF-15 to myotubes was able to cause atrophy (218). Other groups have shown that GDF-15 has a role in the development of mitochondrial skeletal myopathies (261), that circulating GDF-15 levels are associated with muscle loss in both patients with cancer (262) and in healthy elderly women (263). Furthermore, one group commented that GDF-15 was one of the only proteins that could potentially cause cancer cachexia, where circulating levels were also correlated with BMI (264). More recently my group has shown that GDF-15 can up-regulate atrogin-1 and MuRF-1 ubiquitin ligase mRNA expression *in vitro*. GDF-15 was raised in the serum and in the muscle of patients with ICUAW and was associated with markers of muscle wasting. They also showed that systemic GDF-15 levels were negatively associated with a number of pro-hypertrophic microRNAs (265). Other results from my group confirm the association of circulating GDF-15 with muscle mass in a stable cohort of COPD patients. We also showed that when GDF-15 was over-expressed in mouse muscle their fibre diameter was lower than in muscle over-expressing control vectors (266).

One exception to this association is the case of obese patients with diabetes where GDF-15 levels were associated positively with BMI (267). Another study in gastric cancer showed no correlation between GDF-15 with weight loss nor with BMI (268).

Finally in cancer cachexia GDF-15 was shown to be an important mediator of both fat and muscle loss. In this study treatment with a GDF-15 antibody was able to prevent weight loss in a number of models of cancer cachexia, and when given in conjunction with tumour suppressing chemotherapy it was able to prolong survival (269).

1.5.3 GDF-15 and food intake

GDF-15's effect on muscle mass has been shown to be at least partially dependant on reduced food intake. Johnen *et al.* suggested that this was the predominant reason for muscle loss in GDF-15 over-expressing states. Xenografted GDF-15 over-expressing tumours resulted in a significant reduction in food intake, which was prevented by administration of a GDF-15 antibody. GDF-15 was also able to induce weight loss through appetite suppression in obese mice, whilst GDF-15's effects on weight loss was completely obviated by pair feeding animals. Furthermore direct injection of GDF-15 into the hypothalamus upregulated the anorexigen pro-opiomelanocortin and downregulated the appetite stimulus neuro-peptide Y (260). Macia *et al.* also suggested that GDF-15 transgenic mice lost more fat mass than lean mass, primarily as a result of decrease food intake (270). Further evidence for an anorexigenic effect of GDF-15 comes from data showing knockout mice ate less than wild type counterparts, a process that was rescued by GDF-15 infusion (271). The same group showed that injection of GDF-15 into the CNS resulted in reduced weight and a reduction of food intake that was dependent on an intact brainstem axis (272).

GDF-15 levels have not universally been associated with poor oral intake. Although GDF-15 levels were associated with prognosis in patients with gastric cancer they were only weakly correlated with nutritional intake in these patients (268). A GDF-15 over-expressing mouse model lost weight but ate more than control animals (273). Finally although GDF-15 levels changed diurnally and were inversely related to BMI in a twin cohort, they did not change post-prandially making the authors of one study suggest that it was unlikely to be a satiety factor (274). These findings suggest that GDF-15 may not

just act via appetite suppression and that alternative mechanisms by which GDF-15 can cause muscle loss are worth investigating.

1.5.4 GDF-15 and physical activity

Muscle loss is both a cause and effect of physical inactivity (75). GDF-15 has been infrequently measured at the same time as physical activity and energy expenditure. GDF-15 over-expressing mice have been shown to have both a reduction (260, 270) and an increase in energy expenditure and metabolic rate (273). Furthermore, female but not male GDF-15 knockout mice had a lower physical activity level than wild type counterparts (271). Taken together this suggests that GDF-15's effects on physical activity and energy expenditure are dependent on a complex interplay of factors in individual experiments and animals, or a result of type 1 errors.

In health, in ultra-marathon athletes, circulating GDF-15 levels transiently increased to an average of above twice the upper limit of normal, falling back to baseline at days 2 post race. This rise was postulated to be due to the endothelial dysfunction associated with endurance sport (275) and is supported by data showing similar findings in professional footballers and rugby players (276, 277).

In cardiac disease where GDF-15 levels were compared pre- and post- coronary intervention and then pre and post 6 months rehabilitation there was a transient rise in GDF-15 levels around the time of stent insertion which fell back to baseline. Furthermore there was no change in GDF-15 level after the exercise program, suggesting GDF-15 levels are not responsive to the amount of exercise performed during the rehabilitation program (257).

1.5.5 GDF-15 and PH

In patients with IPAH, GDF-15 is an independent marker of prognosis. GDF-15 levels above 2097pg/ml predicted those with an increase in mortality. Patients with higher GDF-15 levels were older, were more likely to be male, were in a higher functional class and had higher creatinine levels. GDF-15 levels correlated significantly with 6MWD, BNP and right atrial pressure. Interestingly there was no

association with cardiac output, pulmonary vascular resistance or pulmonary arterial pressure. Furthermore, in follow up, GDF-15 levels responded to changes in PAH treatment in line with changes in BNP levels (207). In adult congenital heart disease GDF-15 has been shown to be associated with BNP, elevated pulmonary artery pressure, exercise tolerance and NYHA functional class (278). In systemic sclerosis GDF-15 could be used to define those with and without evidence of PAH. In this cohort GDF-15 levels correlated with right ventricular systolic pressure and BNP and inversely with DLCO percent predicted (279). GDF-15 levels have also been shown to be raised in the serum of patients with CTEPH (280), sickle cell disease (281) and β-thalassaemia (282) when associated with pulmonary hypertension.

In the lung tissue of patients with IPAH and Eisenmenger's syndrome, GDF-15 messenger ribonucleic acid (mRNA) expression was shown to be significantly increased compared to controls. GDF-15 was localised in endothelial cells and plexiform lesions confirmed by immunohistochemistry and laser capture micro-dissection (283). GDF-15 has also been shown to be up-regulated in the lungs of patients with systemic sclerosis with PAH and IPAH but not in those with systemic sclerosis without PAH. The source of this GDF-15 in this study was felt to be macrophages (279). Mechanistic studies on the role GDF-15 might play in the development of PAH has been limited to one study investigating its effect on human microvascular endothelial cells. In these cells exposure to hypoxia and sheer stress increased GDF-15 expression. In endothelial cells, GDF-15 at low levels (5ng/ml) was shown to be pro-proliferative, whilst at high levels (50ng/ml) it was anti-proliferative. However both high and low concentrations were able to prevent hypoxia associated apoptosis and induce AKT phosphorylation (283).

In human vascular endothelial cells (HUVECs) GDF-15 treatment of hypoxic cells stimulated angiogenesis through an increase in VEGF, an increase in HIF 1 α and a reduction in p53 (284). Circulating GDF-15 has been associated with a number of vascular endothelial markers, including tissue inhibitor of metalloproteinases metallopeptidase inhibitor 1, D-dimer and von Willebrand

factor, suggesting that GDF-15 is involved in cellular inflammation in the endothelium promoting endothelial dysfunction (285).

Few investigations into the physiological role of GDF-15 in vascular tissue have been performed. GDF-15 knockout mice exhibit an increase in platelet aggregation after induction of pulmonary embolism which was associated with an increased risk of early death. Furthermore GDF-15 treatment of wild type mice improved outcomes after PE suggesting that GDF-15 has an antithrombotic role in acute pulmonary embolism.(286). A further role for GDF-15 in vascular tissue is suggested by a study which showed that GDF-15 interferes with nitric oxide mediated changes in vascular tone in mice aortic tissue (287).

1.5.6 GDF-15 and downstream signalling

The signalling cascades activated by GDF-15 are wide, varied and cell, environment and dose dependant. The pathways that GDF-15 activates have not been examined in detail in skeletal muscle cells, but have been characterised in other cells lines.

The receptor through which GDF-15 acts is unclear (227). In cells expressing mutant TGFBR2, mutant ALK-5 or those cells lacking SMAD 4, GDF-15 had no growth inhibitory effect on cancer cells, indicating that GDF-15 requires an intact TGFβ receptor complex and canonical pathway in order to function in some cells (288). Johnen *et al.* added support to the argument that GDF-15 acts via the TGFBR2 by injecting a cohort of mice directly into to one half of their hypothalamus, a known site of action of GDF-15, with a TGFBR2 blocking antibody. They then injected the mice with GDF-15 and showed that these blocking antibodies prevented GDF-15 mediated c-fos activation only in the side with the blocking antibody. (260). In vascular cells GDF-15 has been shown to interact with TGFBR2, ALK-5 and SMAD 3 but that blockade of the type 1 receptor had the opposite effect to blockade of the type 2 receptor suggesting a complicated receptor ligand interaction (239). Other studies have shown that the TGFBR2 but not ALK-5 is necessary for GDF-15 to have its clinical effect on potassium channels in rat granular cerebellar neurones (289). In fact in colorectal cells, GDF-15 induced phosphorylation of

SMAD 2 and 3, which was dependant on the intact ALK-4, 6 or 7 (290), whilst in airway epithelial cells GDF-15 was able to inhibit cigarette smoke induced senescence through ALK1 receptor and SMAD1 activation, suggesting that GDF-15 can act via a number of type 1 receptors (291). The requirement for an intact TGFβ1 receptor complex has not been a universal finding, with GDF-15's effects on urokinase receptor upregulation being TGFβ1 receptor independent (243).

More recently 3 groups have identified with some certainty the receptor through which GDF-15 acts in the hindbrain to control appetite (292-294). The glial cell line-derived neurotrophic factor family receptor-alpha-like (GFRAL) was first described in 2005 and is located solely in the membrane of cells in the area prostrema of the brain (295). GDF-15 has been shown to bind directly to the GFRAL (292-294) to activate ERK, and AKT (294). Knockout of the GFRAL has been shown to prevent GDF-15 mediated weight loss in obese (294) and normal weight animals (296). This process is mediated through prevention of the anorexigenic effects of GDF-15 on neural pathways (292-294). Interestingly the GFRAL has not been found in skeletal muscle (295) and its knockout seems to have a greater relative effect on fat compared to lean body mass (293).

A number of groups have investigated the effects of GDF-15 on SMADs. GDF-15 has been shown to activate (235, 297), inhibit (298) and have no effect (238, 260, 299, 300) on SMAD 2, 3. It has also been shown to activate (235, 238, 300) and have no effect (260, 299) on SMAD 1, 5. This is dependent on the dose used and the cell type investigated.

With an increase in constituent parts the effects of GDF-15 on the non-canonical pathway is even more complicated and varied. Some of the most widely studied pathways are AKT and ERK 1 and 2. In cardiac myocytes GDF-15 activated AKT (235, 236, 238) and ERK (235, 238). This was also true in breast, gastric, epithelial oesophageal and colon cancer cells, all of which showed that GDF-15 can activate ERK and AKT concurrently with some of the cancer progression seen in these models dependant on PI3Kinase and mTOR activity (243-245, 301-305). GDF-15 has also been shown to induce AKT phosphorylation in HUVEC cells (283), Huh7.5.1 cells (306), in human epithelial lung NCI-H292 cells

(307, 308), in glioblastoma (297) and in tracheobronchial epithelial cells (308), whilst in fibroblasts and in the hypothalamus of mice, GDF-15 resulted in ERK phosphorylation (260, 309). The up-regulation of both AKT and ERK activity in the presence of GDF-15 is not a universal finding. In cerebellar granular neurones GDF-15 caused an increase in phosphorylation of AKT and was shown to act through upregulating PI3 kinase but down-regulated ERK activity (310). Furthermore, in gastric cancer HCT116 cells inhibiting GDF-15 expression, through siRNA, increased phosphorylation of both AKT and ERK1/2, suggesting that GDF-15 might actually inhibit their activity in this cell line (311). *In vivo* in GDF-15 over-expressing mice there was no increase in lung AKT or JNK phosphorylation (312). This finding was mimicked in RAW 267.4 cells, where GDF-15 had no effect on AKT or JNK (300). Finally in neonatal rat cardiomyocytes GDF-15 inhibited activation of AKT and ERK (313), suggesting that there is a significant difference in the pathways activated by GDF-15 in mature and developing cells.

Another potential downstream target of GDF-15 examined in the literature is p38 MAPK. GDF-15 has been shown to upregulate p38 MAPK activity in RAW267.4 cells (300), in SK-BR-3 and HER2 breast cancer cells (303, 314), in HUVECs (315) and in ovarian cancer cells (304). In contrast, in both normal lung tissue and in lung tumours in GDF-15 over-expressing mice there was a reduction in phospho-p38 MAPK. Furthermore in A549 cells, GDF-15 was able to inhibit increases in p38 MAPK induced by cigarette smoke (312), suggesting a potential role for GDF-15 and p38 MAPK inhibition in the propagation of lung cancer progression. In cardiac myocytes GDF-15 did not seem to have any effect on p38 MAPK activity (235)

GDF-15's effect on the NFκB pathway have also been examined in a number of cell lines with varying results. In HUVECs GDF-15 knockout seemed to have an enhancing effect on glucose mediated NFκB activation (316), whilst in RAW 267.4 cells GDF-15 delayed the induction of IKKB and thereby inhibited activation of NFκB, measured by luciferase (300). In contrast Hinoi *et al.* showed that GDF-15 induced phosphorylation of NFκB p65 in these same cells in the presence of receptor activator of nuclear NFκB ligand (317). Some of the most convincing evidence of GDF-15's downstream pathway comes from E-

Coli infected intestinal cancer cells, where GDF-15 siRNA prevented TAK1 and NFκB p65 activation. Furthermore, GDF-15 induced TAK1 phosphorylation peaking at 240 minutes and TAK1 inhibition with 5(Z)-7-oxozeaenol prevented enteropathic E-Coli mediated increases in phosphorylation of NFκB p65 (318). The same pathway was shown to be involved in Ras homolog gene family, member A guanosine triphosphatase (RhoA GTPase) cell survival pathway in the same cell line (319). This suggests that GDF-15 may propagate its signal, in at least some cells, through actions on TAK1.

1.6 TAK1

1.6.1 TAK1 signalling

TAK1 was discovered in 1995. It is a mitogen activated protein kinase kinase kinase that was stimulated by both TGFβ and BMPs (320). It is found bound to accessory proteins TAB1 (321), and TAB2 (322) or 3 (323). The potential mechanism through which TGFβ1 activates TAK1 has been investigated. In one study TGFβ 1 was shown to bind to TGFBR2 which combines with the type 1 receptor ALK-5 resulting in its phosphorylation. The TGFBR2 was found bound directly to TAK1. As well as stimulating SMAD signalling ALK-5 was shown to be able to bind to X-linked inhibitor of apoptosis. This, in turn, bound to TAB1, combining TAK1 with both the type 1 and type 2 receptor, allowing it to phosphorylate downstream kinases (324) (Figure 1.5 A). Another group has shown that under unstimulated conditions TAK1 is bound via TAB2 and TRAF 6 to the ALK-5 receptor. Stimulation of the TGFBR2 by TGFβ1 resulted in the recruitment of ALK-5 causing a polyubiquination of TRAF6 and TAK1 at Lysine 158, allowing the release of TAK1 from the receptor complex, leaving it free to combine with TAB1 stimulating auto-phosphorylation (325, 326) (Figure 1.5 B). TGFβ1 is not the only TGFβ superfamily member that can activate TAK1. Studies have shown that GDF-8 which acts through the ACVR2B receptor can also stimulate TAK1 activity (327).

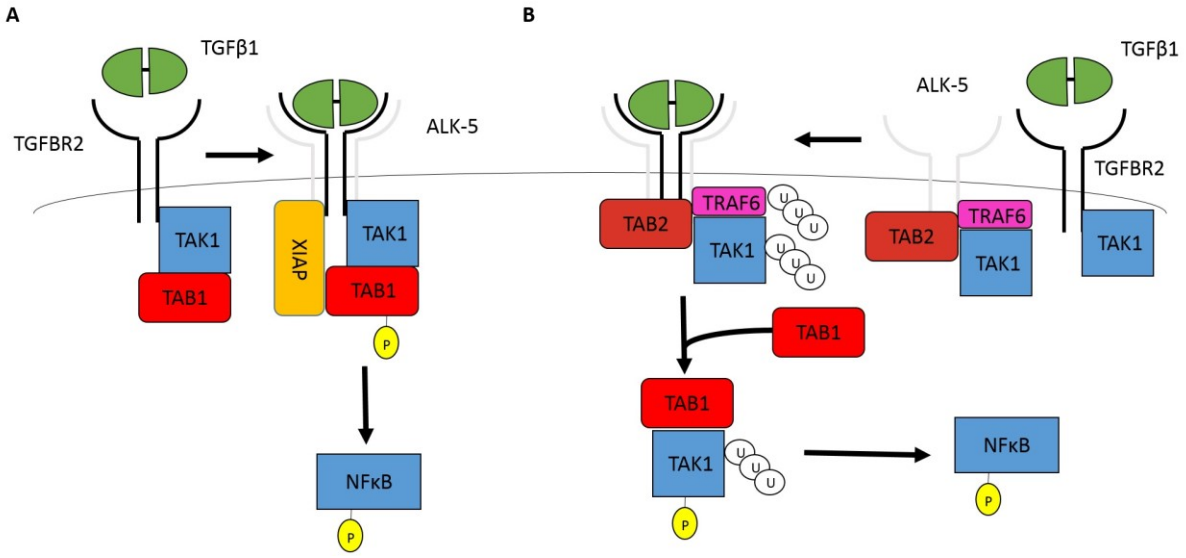

Figure 1.5 A and B. The interaction of TGFβ and TAK1 signalling. Schematic representations of potential mechanisms by which TGFβ1 might stimulate TAK1 activity. X-linked inhibitor of apoptosis protein (XIAP), phosphorylation (P), ubiquination (U) (324-326).

As well as TGF β there are a number of other factors that have been shown to stimulate TAK1 including interleukin-1 (328), interleukin 18 (329), TNFα (330) and lipopolysaccharide (331).

TAK1 activation has been shown dependant on phosphorylation at a number of sites including Serine 192 (332) Threonine 184 and 187 (333, 334) and Serine 412 (335). Recent data has suggested that Serine 412 phosphorylation is required for full activation of TAK1 (335). Downstream TAK1 activates NFκB (336), p38 MAPK (337) and JNK (338). TAK1 also interacts with a number of other important pathways including (339), PPAR (340) and the canonical TGFβ SMADs (341). Importantly SMAD 6 and 7 can inhibit TAK1 mediated p38 MAPK activation (341) and SMAD 7 can inhibit TNFα mediated TAK1 activation (342). Furthermore TAK1 can interact with the linker region of SMAD 2 and is essential for its phosphorylation (343).

1.6.2 TAK1 as a target for therapeutic intervention

TAK1 is essential for embryonic development, innate and adaptive immunity and homeostasis of essential organ function (344-346). TAK1 is also involved in a number of disease processes. TAK1 activity has been associated with inflammatory conditions, cancers (347), cardiovascular disease (348), and fibrosis (349, 350). TAK1 has become an exciting potential therapeutic target in a wide range of conditions and a number of compounds, aimed at antagonising its actions, are in development. These include: covalent cysteine binders such as 5(Z)-7-oxozeaenol and hypothemycin, which act on the cysteine residue in the Asp-Phe-Gly / DFG region; type I molecules which interact with the hinge region of the kinase, e.g. AZ-TAK1; and type II DFG out-binders, like PF-04358168, which change the confirmation of the active region of the protein rendering it inactive (351). All the mechanisms by which it might be possible to inhibit TAK1 have advantages and disadvantages with some compounds being potent but having off-target effects whilst others may be more specific but less effective (351).

5(Z)-7-oxozeaenol was the first TAK1 inhibitor characterised (352) and has been the most widely used to inhibit TAK1 *in vitro* and *in vivo*. It is a resorcyclic lactone naturally produced by a fungus (352). It acts as an irreversible kinase inhibitor by forming a covalent bond between the cis-enone group of 5(Z)-7-oxozeaenol and the functional thiol group of the cysteine residue of TAK1 resulting in alkylation of the protein and preventing the binding of TAK1 and ATP at its DFG site (353). *In vivo* 5(Z)-7-oxozeaenol has been shown to: enhance the chemotherapeutic effect of doxorubicin on neuroblastoma tumours in mice (354); prevent diabetes in a mouse model of the disease (355); reduce the severity of nephropathy in diabetic mice (356); increase neuronal survival and decrease seizure duration in epileptic rats (357); reduce the size of infarct after stroke (358); and prevent neo-intimal formation in wire induced vascular injury (359). Its effects on muscle wasting have not been investigated. 5(Z)-7-oxozeaenol has been used intra-peritoneally at doses of between 0.5 – 5 mg/kg/day (356, 358, 359).

1.6.3 TAK1 in PH

Only one paper has examined the role of TAK1 in pulmonary hypertension. In mutant BMPR2 knockout mouse primary pulmonary artery smooth muscle cells TAK1 inhibition with 5(Z)-7-oxozeaenol prevented proliferation both at baseline and in response to TGFβ1 stimulation. 5(Z)-7-oxozeaenol also increased apoptosis in both wild type and BMPR2 knockout cells. The researchers found increased activity of TAK1 in the lung tissue of both MCT and hypoxic rats. It was also established that TAK1 inhibited BMP induced SMAD1 signalling which was rescued by 5(Z)-7-oxozeaenol. Taken together the authors argued that TAK1 could be a target for therapeutic intervention in PH (360).

1.6.4 TAK1 in muscle wasting

A detailed study of TAK1 in skeletal muscle showed that phsopho-TAK1 and TAK1 levels are high in cells at day 1 and in young mice and fall as cells differentiate and mice grow. This group also found that regenerating muscle had higher mRNA expression of TAK1 and that TAK1 was required for proliferation but not survival of myoblasts. They confirmed that TAK1 was involved in differentiation through a number of normally competing pathways including p38 MAPK, AKT, IGF-1 and myoD (361). The p38 MAPK and AKT pathways were also activated *in vitro* and *in vivo* in response to TAK1 phosphorylation by TRAF 6, which is stimulated in differentiating and regenerating cells (362). In keeping with these results TAK1 seems to be a vital component of satellite stem cell function in regenerating muscle or in muscle development in immature animals (363, 364).

In contrast to its role in regeneration and development TAK1 activity can be stimulated by nutrient withdrawal as well as inflammation. As we have discussed above, both of these may be propagated by an increase in GDF-15 (365). The direct effects and influence of TAK1 activation in skeletal muscle has been rarely studied. GDF-8, a known TGFβ super-family member, and negative regulator of muscle mass, requires TAK1 to propagate its growth inhibitory signal in muscle cells (67, 366). TAK1 has also been shown to be vital in the over-expression of matrix metalloproteinase 9 in C2C12 muscle cells treated with TNFα, suggesting a role for TAK1 in the development of muscle wasting (367).

Adiponectin is a negative mediator of muscle mass in chronic heart failure (368), APPL1 is an adaptor protein for adiponectin and is vital for its signalling. TAK1 seems to be integral in allowing APPL1 to stimulate p38 MAPK phosphorylation and thereby allow adiponectin to propagate its downstream signal. These researchers also found no interactions between p38 MAPK activated by TNFα and that activated by APPL1 /adiponectin, suggesting that the TAK1 axis has a complicated role in determining skeletal muscle mass (369). The effect of inhibition of TAK1 with a small molecule inhibitor has not as yet been studied *in vivo*.

1.7 Summary, aims and hypotheses

1.7.1 Summary

Muscle wasting is a ubiquitous outcome of chronic disease. Rehabilitation is now a mainstay of treatment for many conditions. There are currently no established pharmacological interventions or biomarkers for muscle wasting in chronic cardio-respiratory disease. Novel targets for intervention and biomarkers are needed to improve outcomes in diseases complicated by muscle loss including PAH.

From the data presented above I described the reasons that muscle wasting is likely to be important in influencing outcomes in PAH, but unlike in COPD and heart failure, there is very little established evidence that physical activity or muscle wasting in these patients directly affects mortality, admissions to hospital or QOL.

I have described the animal models used to study muscle wasting in PAH. I have presented the evidence that GDF-15, a member of the TGFβ super-family, is raised in the circulation of patients with PAH. I have also shown that GDF-15 can influence muscle mass in vitro and in vivo, both directly and through actions on appetite suppression. The role of GDF-15 in the development of muscle wasting in PAH is unclear. It is also not established whether local or systemic levels of GDF-15 are important in the development of muscle wasting *in vivo* and in man.

Previous work has shown that GDF-15 may act through the TGFBR2 and ALK-5 to stimulate both SMAD and non-SMAD pathways, including TAK1 and NFκB. The specific pathway through which GDF-15 acts in muscle has not been determined, although there is some evidence that it can cause muscle wasting through up-regulation of ubiquitin ligases atrogin-1 and MuRF-1.

Targeting GDF-15 and its downstream signalling may be a viable method to prevent and treat muscle wasting in PAH.

1.7.3 Hypotheses

Circulating GDF-15 levels released from the pulmonary vasculature and not locally are associated with muscle loss in patients and in animal models of PH. GDF-15 causes muscle loss directly, through a non-canonical pathway and up-regulation of atrophic signalling, a process that may be reversed by blocking GDF-15 signalling via its receptor or downstream mediators. This may have clinical value as muscle loss and low physical activity in PAH is associated with poor outcomes.

1.7.2 Aims

To measure the associations of muscle strength and size and physical activity in a well characterised group of patients with PAH.

To determine the effects of muscle strength and size and physical activity on outcomes such as hospitalisation and mortality in patients with PAH

To investigate the association of physical activity outcome measures from QOL questionnaires with objectively measured physical activity in patients with PAH to determine the best way of measuring physical activity in PAH.

To define the association of GDF-15 with muscle function and size in animal models and in patients with PAH.

To identify the source of GDF-15 in animal models of PAH

To define the pathway through which GDF-15 might cause muscle wasting *in vitro* with a view to antagonising its effects.

To determine whether inhibition of the pathway identified as being downstream of GDF-15 prevented muscle loss in the MCT rat model of PAH

Chapter 2 Methods

2.1 Clinical methods

2.1.1 Ethical approval

The clinical study performed as part of this thesis was undertaken with ethical approval given by the National Research Ethics Committee under study number 13/LO/0481. The study was approved by the Royal Brompton Hospital (RBH) research and development team and was undertaken with the support of the RBH National Institute for Health Research (NIHR) Respiratory Biomedical Research Unit. Two control muscle biopsy samples were kindly donated by Professor Polkey and Ghulam Haji under REC approval 12/LO/0088. All patients gave written informed consent.

2.1.2 Inclusion and exclusion criteria

Patients aged 16 and over with PAH with World Health Organisation (WHO) stage I - III disease were eligible for recruitment. Interested healthy age-matched volunteers were also enrolled. Exclusion criteria included: those patients with co-morbidities including other significant cardio-respiratory disease, metabolic abnormalities including diabetes, eating disorders or untreated thyroid disease. Potential participants were excluded if they could not safely exercise or if they were wheelchair bound. Patients with other, pre-existing, known causes of muscle weakness or wasting, including, but not limited to, debilitating stroke, neuromuscular disease or active malignancy were also excluded. Patients with platelet counts of less than 80 were excluded from the muscle biopsy portion of the study. Finally those unable to give informed consent and those who were pregnant were also excluded.

2.1.3 Demographics

Age, sex, and date of birth were documented along with diagnosis, date of diagnosis, co-morbidities and treatment. WHO functional status for pulmonary hypertension was also defined. The different functional classes are listed in Table 2.1.

Functional Class	Symptomatic Profile
I	No limitation on physical activity. Ordinary activity does not cause symptoms
II	Slight limitation of physical activity. Comfortable at rest. Ordinary activity can cause symptoms
III	Marked limitation of physical activity. Comfortable at rest. Less than ordinary activity can cause symptoms
IV	Inability to carry out physical activity without symptoms. Signs of right heart failure. Discomfort increased by physical activity.

Table 2.1 WHO / NYHA functional class in pulmonary hypertension (22).

2.1.4 Measurement of muscle mass, size and strength.

2.1.4.1 Fat free mass index

Fat free mass is a measure of lean body weight and can define those patients with sarcopaenia (370). In our study fat free mass index (FFMI) was measured by bioelectrical impedance using the Bodystat 1500 (Bodystat, Isle of Man, UK). Electrodes were placed over the right foot (one behind the second toe and one between the malleoli) and on the right hand (one on the knuckle of the middle finger and one on the wrist adjacent to the ulnar head). Alligator clips were attached to the electrodes. The red clips were attached distally and the black clips were attached proximally. The machine was then turned on and individual patient data entered. The machine went through a number of prompts after which measurements were taken and the results were displayed and documented. Cut offs for FFMI of low, normal and high FFMI were < 14, 14-19 and > 19 kg/m^2 respectively.

2.1.4.2 Rectus femoris cross sectional area

Cross sectional area of the rectus femoris muscle was assessed using ultrasound (US RFcsa). This was undertaken with an 8MHz 5.cm linear transducer array in B-mode (PLM805, Toshiba Medical Systems, Crawley, UK) or a 10MHz 12L-RS probe (Logiq E, GE Healthcare, UK). The subject was asked to lie down with the dominant leg held straight and relaxed. A point 3/5 of the way between the anterior superior iliac spine (ASIS) and the upper border of the patella was marked. The cross sectional ultrasound image was taken at this point. Contact gel and minimal pressure was used to reduce image distortion. The

smallest cross sectional area of the rectus femoris was identified by small movements of the probe to avoid oblique sampling. The femur was visualised in all images as a reference point. The septa which defined the edges of the muscle were identified. This process was aided by asking the patients to perform voluntary contractions of the leg. Three images of the rectus femoris were frozen and the inner echogenic line of the muscle was delineated. The area of the rectus femoris was measured using a planimetric technique (Nemio, Toshiba Medical Systems). The average of the 3 $USRF_{CSA}$ measurements that were within 10% of each other was taken and documented. The technique is that described by Seymour *et al* (28) and used in a number of other studies (371-373). An example image of the US RF_{CSA} is shown in Figure 2.1.

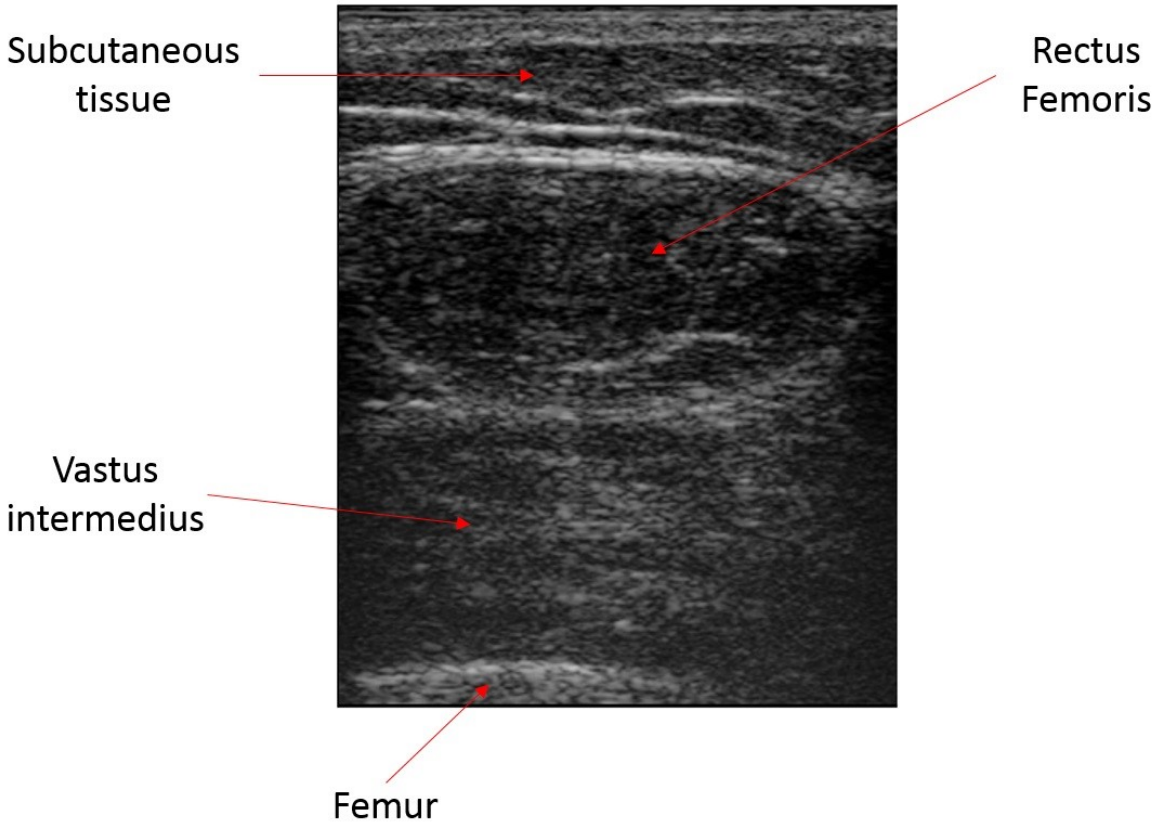

Figure 2.1 Ultrasound image of rectus femoris cross sectional area ($USRF_{CSA}$). Representative cross sectional ultrasound image of the thigh used to measured rectus femoris cross sectional area.

2.1.4.3 Quadriceps maximal volitional capacity (QMVC)

Quadriceps maximal voluntary contraction (QMVC) is the gold standard for assessment of quadriceps strength. This is best assessed using the method first described by Edwards *et al*. (374). A specially designed chair (figure 2.2) was calibrated daily with a 29kg weight. Measurements were made using Labchart version 7 (ADI instruments, Oxford, UK). The patient was placed in a sitting position. A strap attached to a strain gauge was looped around the participants' dominant leg. The participant was asked to make an isometric voluntary contraction of the quadriceps muscles. The procedure was repeated until the maximum contraction was determined. This was normally the 3rd or 4th attempt. There were no adverse events in the patients with PAH performing this task (374). For analysis quadriceps QMVC was normalised to body mass index to allow comparison across different individuals, with variable height and weight. This method has been used in studies by Swallow *et al.* (34) and Canavan *et al.* (375). Cut off values of a QMVC/BMI of > 1.5 were chosen to represent those patients with preserved muscle strength.

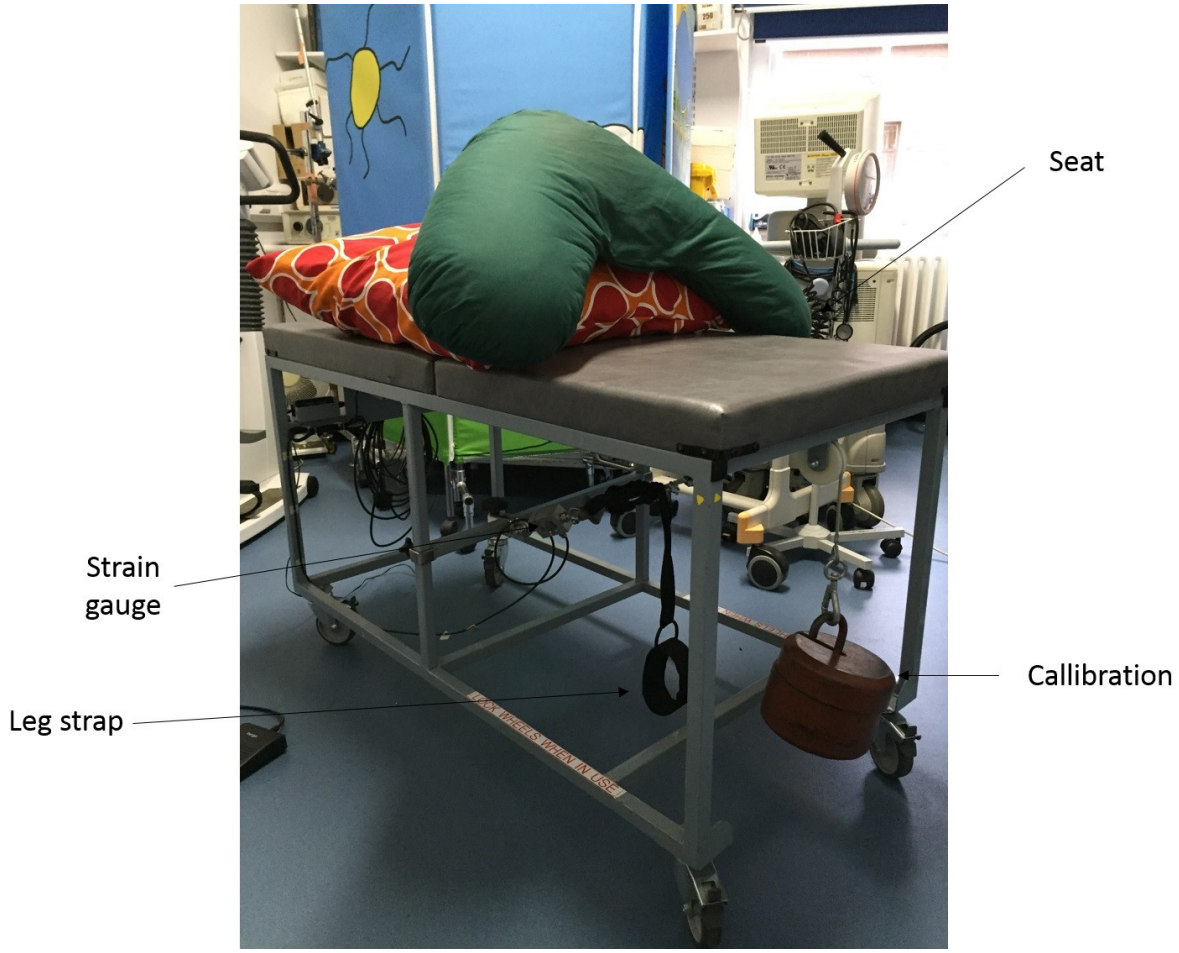

Figure 2.2 Chair used to measure quadriceps maximal volitional capacity (QMVC). Picture of specially designed chair for measurement of QMVC.

2.1.5 Physical activity measurements

The Sensewear armband (SWA) (SenseWear Pro armband; BodyMedia Inc., Pittsburgh, PA, USA) is a physical activity monitor that is worn over the triceps in the position shown in Figure 2.3. It is a biaxial accelerometer, with other sensors including those for galvanic skin response, heat flux, skin temperature, and near-body ambient temperature. It has been validated in healthy individuals (376) and in some patients with chronic disease such as COPD (377). It has also been used to evaluate activity in patents with PAH (173). Participants were given the monitor to wear for seven days at all times except when bathing or swimming to avoid the armband getting wet. The SWA data output includes steps per day, total energy expenditure and time spent in moderate physical activity (above 3.0 metabolic equivalents) (378). The physical activity level (PAL: total energy expenditure per day divided by basal metabolic rate) was calculated using minute to minute data generated by the SWA Pro software version 6.1.0 (BodyMedia Inc., Pittsburgh, PA, USA) (379). PAL, total energy expenditure and time spent in moderate physical activity data was excluded from analysis if the SWA was worn for less than an average of 22.5 hours per day for 5 days including at least one weekend day as described by Watz *et al.* (378). Steps per day were excluded if the patient wore the armband for fewer than 8 hours for 4 days as described by Demeyer *et al.* (380). In analysis of the data basal, and therefore very low activity, was defined as: <2500 steps per day based on recommendations by Tudor-Locke *et al.* (381) or a PAL < 1.4 which has previously used to define extremely inactive individuals (382, 383). Highly active individuals were defined as those achieving 30 minutes of at least moderate activity (> 3.0 metabolic equivalents (METs)) as per current recommendations (384).

Figure 2.3 Sensewear armband (SWA) position. Picture showing the positioning of the SWA over the triceps of a control subject.

2.1.6 Quality of life questionnaires

2.1.6.1 The St. George's respiratory questionnaire (SGRQ)

The SGRQ is a QOL questionnaire, which consists of 7 sections and 50 questions, which are weighted to allow the user to define the participants QOL (385). A copy of the SGRQ is available in appendix 2.1. Permission to use the questionnaire for this study was granted by the copyright holder and is also contained in appendix 2.1. All participants were asked to fill in the questionnaire and answer all the questions according to instructions in the SGRQ manual (386). Completed questionnaires were scored by entering data generated into a specifically designed excel spreadsheet which weights answers and produces scores in a number of domains (386). The questionnaire was developed for use specifically in obstructive lung diseases asthma and COPD in which it has been validated (385). However, it has also been used to measure QOL in a number of other diseases including PAH (387). The outputs of the SGRQ include scores related to symptoms, activity, impact and total or overall QOL. All of these have a minimum score of 0 and a maximum score of 100, with lower scores representing better outcomes (388).

2.1.6.2 The Cambridge pulmonary hypertension outcome review (CAMPHOR)

The CAMPHOR QOL questionnaire was specifically designed for use in pulmonary hypertension (389). It has been related to outcomes in the condition(390). It consists of 3 sections: symptoms, which has 25 questions; activities, which has 15 questions; and QOL, which has 25 questions. It is scored according to the manual with each section generating its own maximum score of 25, 30 and 25 points respectively. A total overall score with a maximum of 80 is also generated as a sum of all the sub-sections (389). The CAMPHOR was used with permission of the copyright holder Galen research after signing a material transfer agreement and paying a nominal fee. A copy of the license for the questionnaire is included in appendix 2.2.

2.1.6.3 The emPHasis 10 questionnaire

As part of normal clinical practice, patients in PH clinic at the Royal Brompton Hospital have their QOL measured and followed up with the emPHasis 10 questionnaire. This questionnaire is specifically developed for use in PH and uses only 10 questions. The maximum score is 50 with higher scores indicating worse QOL. Higher scores are associated with worsening functional status and exercise tolerance (391). The emPHasis 10 questionnaire provides only one outcome unlike the other questionnaires employed in the study. It was therefore used primarily to track changes in QOL over time in the population studied, and the relation of baseline characteristics to this change.

2.1.7 Echocardiogram

Echocardiography was carried out according to European association of echocardiography guidelines by a trained echocardiographer as part of the patient's routine clinical assessment in clinic. Right ventricular function was assessed with tricuspid annular plane systolic excursion (TAPSE). The difference in distance between the position of the tricuspid lateral annulus in systole and diastole is measured. A TAPSE of ≥ 16mm is considered normal. Although it officially only measures longitudinal function, it is closely correlated with overall right ventricular function in a number of studies. Measurement of tricuspid regurgitant velocity (TR vel) and right atrial pressure (RAP) allows estimation of right ventricular systolic pressure (RVSP), where RVSP is (peak TR vel) ^{4} + RAP. RAP can be accurately estimated by IVC collapse during respiration. Normal values of TRvel are < 2.8 -2.9 m/s, which corresponds to a RVSP of 35 or 36 mmHg if the RAP is 3-5. (392, 393) Pulmonary artery acceleration time (PAcT) is the time between the onset of systolic pulmonary artery flow and the peak velocity of this flow. It has been shown to correlate with invasively measured mean pulmonary artery pressure and can be measured in those without tricuspid regurgitation. It also correlated closely with pulmonary vascular resistance (394).

2.1.8 The six minute walk test distance (6MWD)

The 6MWD is one of the best markers of prognosis in patients with PAH (395). It is an accepted end point in the testing of novel therapies in clinical trials (396). Six minute walk tests were carried out according to ATS guidelines (397) adapted to suit the environment in the clinic. Briefly patients walked as far as they could on a 20 m track over 6 minutes. The instructions were given as per the guidelines (397).

2.1.9 Blood tests

Participants had blood drawn at the time of enrolment into the study. Blood was taken in ethylenediamineteracetic acid (EDTA) and serum separator tubes (SST) tubes. Within 30 minutes EDTA tubes were spun down in a cold centrifuge at 4^{o}C at 14000 revolutions per minute (rpm) for 10 minutes. Plasma was extracted with a Pasteur pipette and stored for later use at -80 ^{0}C. BNP is a prognostic marker in PAH (398). It was measured in the patients by ELISA by the hospital laboratory as part of the routine assessment of patients in clinic. A cut off of BNP of 100 pmol/L was used to define high and low values. Growth and differentiation factor 15 plasma levels were measured by ELISA (R&D systems, Abingdon, UK) according to manufacturer's instructions.

Samples in the SST tubes were left for at least 30 minutes to allow for coagulation. Samples were then spun in a cold centrifuge at 10000 rpm at 18^{o}C. Serum was removed and an assay was carried out for C-reactive protein (CRP) in the hospital laboratory according to local protocols and as part of the patients' standard care. A CRP of > 10 mg/L was used as a cut off of high and low values.

2.1.10 Muscle biopsies and protein extraction

In this study 3 patients and 1 healthy volunteer consented and underwent muscle biopsy as described by Bergstrom *et al.* (399). Other biopsies from healthy adults were kindly donated by Dr. Ghulam Haji; those patients' biopsies were covered by a separate REC permission (12/LO/0088) which included sharing of material to further the understanding of muscle disease in patients with cardiorespiratory

disease. Patients had anticoagulation stopped for an appropriate length of time (depending on the medicine used to achieve anticoagulation) prior to the biopsy taking place. Bergstrom needles (Stille, Stockholm, Sweden) were used with a modified suction port as described by Tarnopolsky *et al.* (400). The patient's right vastus lateralis muscle was biopsied, just anterior to the lateral fascia and at approximately 50% of the distance from the greater trochanter to the knee. The area was cleaned with chlorhexidine and then infiltrated with up to 10 mls of 1% lidocaine first with a 26 gauge needle and then a 22 gauge needle ensuring the fascia is not affected. Next an incision was made in the skin just into the fascia with a scalpel and the needle was advanced into the incision. The biopsy needle was advanced into the muscle with a twisting motion to at least 1 cm beyond the fascia. The trochar was removed by at least a centimetre to expose the muscle to the cutting surface of the needle. An assistant attached a sterile 60 ml syringe to the end of the needle and suction was applied. The needle was rotated and the trochar advanced up and down to take the sample. The needle was removed and the sample was placed on saline soaked filter paper prior to processing. Pressure was applied to the area for 10-15 minutes to avoid bleeding. The wound was closed with steri-strips and patients were provided with paracetamol pain relief. The biopsy sample was frozen in liquid nitrogen for analysis or mounted on cork using TissueTech optimal cutting temperature compound (OCT) (VWR, Leicester, UK) and frozen in isopentane (Fisher Scientific, Loughborough, UK) cooled in liquid nitrogen. Samples were then stored at -80^{O}C for later analysis.

2.2 Animal models

All animal model experiments were performed in conjunction with Dr. Alexi Crosby, Mr. Pieran Yang, Mr. Stephen Moore, Mr. Cai Reed, Dr. Stephen Sawiak, Mr. Martin Rice, Dr. Mark Ormiston and Professor Nicholas Morrel at the University of Cambridge under Home office license number 80/2460.

2.2.1 The Monocrotaline rat model

2.2.1.1 Observational study

Male Sprague-Dawley rats (Charles River Laboratories, Harlow, UK), (6 to 7 weeks old) received a single subcutaneous injection of MCT (Sigma-Aldrich, St-Louis, MO, USA) (40 mg/kg) or Phosphate buffered saline (PBS) control (Sigma-Aldrich, St-Louis, MO, USA) (401). 120mg of MCT was dissolved in 1.2ml of 0.5N hydrochloric acid (ThermoFisher Scientific, MA, USA) to which 0.72ml of 0.5N sodium hydroxide was added. The pH was adjusted to between 7 and 7.5 and the solution was made up to 4mls with water for injection to give a working concentration of 30mg/ml. Food intake was monitored throughout the experiment on a per cage basis with 2-4 similarly treated rats per cage. To characterise the muscle loss associated with PAH animals were humanely killed, by exsanguination, after 4 weeks, after weighing and haemodynamic assessment (402).

2.2.1.2 Transforming growth factor β activated kinase 1 (TAK1) inhibitor study

In the TAK1 inhibitor (TAK1i) study rats were treated with MCT or with control injections as above. After 2 weeks half the animals in the MCT group were treated with 5(Z)-7-oxozeaenol (Merck Millipore, MA, USA) 0.5mg/kg/day (dissolved in 10% Dimethyl sulfoxide(DMSO) (Sigma-Aldrich, St-Louis, MO, USA) / 90% PBS (Sigma-Aldrich, St-Louis, MO, USA)) intra-peritoneally for 9 days as previously described (358). 1 mg of 5(Z)-7-oxozeaenol was dissolved in 800µl of DMSO and made up to 8ml with PBS to give a working concentration of 0.125mg/ml. Control treated and the other MCT animals were treated with 10% DMSO/90% PBS for the same length of time. One animal in the MCT TAK1i group failed to reach the endpoint of the experiment and was therefore excluded from further analysis. Rats were humanely killed, by exsanguination, after assessment as above. Rats were weighed regularly throughout the experiment.

2.2.2 The Sugen/hypoxia mouse

Male C57BL/6J mice (Charles River Laboratories, Harlow, UK), (11 weeks old) were injected subcutaneously with SU5416 (Sugen) (Sigma-Aldrich, St-Louis, MO) (20 mg/kg) or vehicle control

on a weekly basis by Stephen Moore. Mice were exposed to either room air or chronic normobaric hypoxia inside a ventilated plexiglass chamber as previously described (403). To characterise the muscle loss associated with PAH animals were humanely killed, by exsanguination, after 3 weeks, immediately after haemodynamic assessment.

2.2.3 MRI Imaging

Hind limb MRI was carried out by Stephen Sawiak at Cambridge University, who used the following methodology, which he described below. 'Three rats in each group were anaesthetised with isoflurane (2-3% in 1l/min O2). MRI was performed at 4.7T using a Bruker BioSpec 47/40 system with an 86mm transmit/receive coil provided by the manufacturer (Bruker Inc., Germany). To separate signals from water and fat contributions, a three-point Dixon method based on IDEAL (404) was used with echo times of 5.44ms, 5.70ms and 6.21ms and a repetition of time of 12ms. The flip angle was 20° and the receiver bandwidth was 50kHz. Images were reconstructed using Matlab (Mathworks, Cambridge, UK) using iterative estimation of local field deviations to produce images showing water and fat'. A similar technique was used to perform cardiac MRI which has been described by Yang *et al*. (405).

2.2.4 Right heart catheter

Under isofluorane anaesthesia rats the right internal jugular vein was blunt dissected out and stretched in an anterior posterior orientation. A suture was placed around the proximal end of the vessel. A small hole was made in the vessel and a pressure catheter (Millar Mikrotip, Millar, Texas, USA) was introduced through this and advanced into the right ventricle. Pressure-volume curves and pressure-time traces were monitored throughout the procedure using Labchart 8 (ADI systems, Oxford, UK). A right ventricle trace was generated and right ventricular systolic pressure was recorded (406).

2.2.5 Dissection and tissue removal

Rats and mice were exsanguinated and blood was collected in SST or EDTA coated tubes and later spun down for removal of serum or plasma which was stored at -80^{0}C. Half of the lungs were

rendered in a distended state by infusion of low melting point agarose into the trachea for 1 minute and then were placed in 4% paraformaldehyde (Cellstore, Powys, UK) before being embedded in paraffin. The remaining lungs were immediately frozen in liquid nitrogen for protein and RNA isolation. The heart was dissected out for assessment of right ventricular and left ventricular weights. The TA and soleus muscles were identified (Figure 2.4) and dissected out bilaterally and weighed. One was immediately frozen in liquid nitrogen the other was cut longitudinally, placed in OCT (VWR, Leicester, UK) on a cork and then frozen in isopentane (ThermoFisher Scientific, MA, USA) dipped in liquid nitrogen (MCT) or placed in 4% paraformaldehyde (Cellstore, Powys, UK) (Sugen/hypoxia) for future analysis.

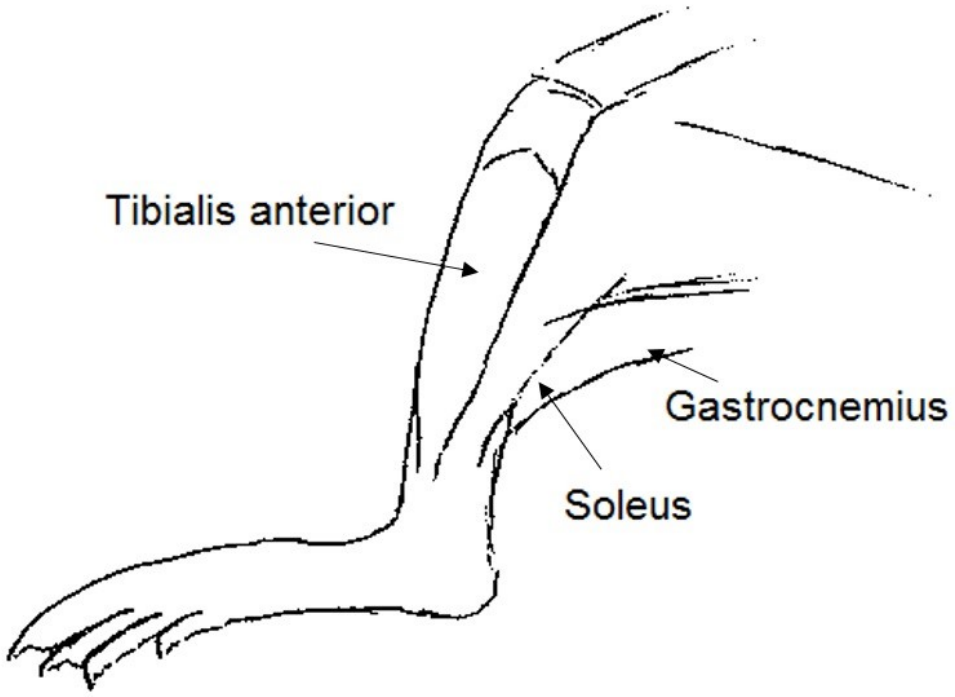

Figure 2.4 Sketch of the rat / mouse hind limb. This diagram shows the tibialis anterior muscle and the position of the soleus muscle deep to the gastrocnemius (407).

2.2.7 Right ventricular / Left ventricular plus septal weight (RV/LV+S)

To assess the extent of right ventricular hypertrophy (RVH), a marker of severity of pulmonary hypertension, the heart was removed, and the RV free wall was dissected from the left ventricle

and septum (LV+S) and weighed separately; the degree of RVH was determined from the ratio RV/LV+S.

2.2.8 Assessment of muscle mass

To assess muscle mass both right and left TA and soleus were weighed, prior to processing, and the average of the 2 weights was documented.

2.2.9 Tissue processing

Muscle and lung samples were homogenised using the Precellys 24 tissue homogeniser (Stretton Scientific, Derbyshire, UK) with 1.4mm ceramic beads (CDK-14, Stretton Scientific, Derbyshire, UK) in 2ml tubes. The machine was run twice for 15 seconds after which samples were assessed to see if they were homogenised. If the samples were not homogenised the process was repeated up to 3 times in total. RNA was extracted using trizol (Life Technologies, Carlsbad, CA, USA). The homogenised tissue in the trizol was mixed with chloroform (ThermoFisher Scientific, MA, USA) at a ratio of 5:1. To separate RNA from protein and DNA. The sample was centrifuged at 13000 rpm for 15 minutes at 4^{o}C. The top aqueous phase, which contains the RNA was removed and placed in a separate microcentrifuge tube. The RNA was precipitated with isopropyl alcohol (ThermoFisher Scientific, MA, USA), using 250µl of isopropyl alcohol per 500µl of trizol initially used. This mixture was vortexed and left at -80^{o}C overnight. The next day a RNA pellet was precipitated by centrifugation at 13000 rpm in a bench-top microcentrifuge for 10 minutes at 4^{o}C. The supernatant was removed and the pellet was washed twice in 75% ethanol (VWR, Leicester, UK) before being re-suspended in 30µl of RNAse free water. The RNA content of the extraction was quantified using a spectrophotometer (Nanodrop ND1000, Thermofisher, Waltham, MA, USA). RNA content was determined by measuring absorbance at 260nm and RNA purity estimated by quantifying the absorbance ratios 260nm:230nm and 260nm:280nm ratios.

Protein was extracted using cell lysis buffer (CLB) and phenylmethylsulfonyl fluoride (PMSF) (Cell signalling technologies, Danvers, MA, USA). Samples were homogenised in 497.5µl CLB with 2.5µl

PMSF. Protein content was analysed using Bio-rad protein assay reagent (Biorad, CA, USA) with absorbance at 595nm quantified on a plate reader (Biotek, Swindon, UK) and compared to known protein contents of bovine serum albumin standards (Sigma Aldrich, St Louis, MA, USA). Protein for ELISA was stored at -20^{o}C. The rest of the protein extracted was mixed with 3x loading buffer (Cell signalling technology, Danvers, MA, USA) and 10% 2-mercaptoethanol (Sigma Aldrich, St Louis, MA, USA), which was heated to 95^{o}C for 5 minutes, before being stored at -20^{o}C.

TA muscle from each animal was cut into 10µm sections (from OCT blocks in the MCT rat done by myself and from wax embedded blocks in the Sugen/hypoxia mouse done by Lorraine Lawrence in the histopathology department at Imperial College) and mounted by hand onto slides. The muscle was stained with haematoxylin and eosin (H&E) by Lorraine Lawrence in the histology department at Imperial College. Agarose inflated lung tissue samples that had been fixed in 4% paraformaldehyde (Cellstore, Powys, UK) were embedded in wax and sectioned at 6 microns prior to being mounted on slides by Lorraine Lawrence in the histology department at Imperial College.

2.3 Cell culture

2.3.1 C2C12 mouse myoblast cells

C2C12 myoblast cells were cultured in Dulbecco's modified eagle medium (DMEM) containing 4500 mg/L glucose, L-glutamine, and sodium bicarbonate, without sodium pyruvate (Sigma Aldrich, St Louis, MA, USA) supplemented with 10% (v/v) foetal calf serum (Sigma Aldrich, St Louis, MA, USA) and 1% penicillin/streptomycin (GIBCO, ThermoFisher Scientific, MA, USA) to a confluence of 70%. At this point cells were removed from the cell culture plastic with trypsin-EDTA 0.05% (GIBCO, ThermoFisher Scientific, MA, USA), counted with a haemocytometer and seeded in dishes or plates. The number of cells seeded per well in various plates and dishes and the experiments they were used in is outlined in Table 2.2. Some myoblasts were transfected for use in luciferase studies after which they were treated with agents as described in the appropriate section. Some myoblasts were transfected for myotube diameter experiments after which they were allowed to grow to 70% confluence and treated

with DMEM containing 4500 mg/L glucose, L-glutamine, and sodium bicarbonate, without sodium pyruvate (Sigma Aldrich, St Louis, MA, USA) supplemented with 2% (v/v) horse serum (Sigma Aldrich, St Louis, MA, USA) and 1% pencillin/streptomycin (GIBCO, ThermoFisher Scientific, MA, USA) to allow them to differentiate into myotubes. The media was changed every 2 days for a total of 10 days after which they were treated with agents as described in the appropriate section. Some untransfected myoblasts were also allowed to differentiate for 10 days in differentiation media prior to treatment as described above.

Plate size	Cells	Experiment
10cm	1000000	Western blot
6 well	100000	Myotube diameter / qPCR
12 well	50000	qPCR
24 well	25000	Luciferase / Nuclear localisation / Immunofluorescence
96 well	6250	Luciferase

Table 2.2 Number of C2C12 cells seeded per well in different plates.

2.3.2 C2C12 treatment

Cells for western blot and those for nuclear localisation of nuclear factor kappa B p65 (NFκB p65) were serum starved overnight prior to treatment. Myoblasts for luciferase, western blot and nuclear localisation of NFκB p65 were treated with the compounds listed below in serum free DMEM. For myotube diameter and quantitative PCR experiments, due to the longer time course employed, cells were treated with the compounds in DMEM supplemented with 1% penicillin/streptomycin with 10% (v/v) foetal calf serum or 2% (v/v) horse serum depending on their stage of differentiation. GDF-15 (R&D systems, Abingdon, UK) was dissolved in sterile 4 mM hydrochloric acid containing 0.1% bovine serum albumin (BSA) (Sigma Aldrich, St Louis, MA, USA) to a working concentration of 100 µg/mL. Cells were then treated at various concentrations from 0.5 to 50ng/ml by diluting GDF-15 in DMEM. Low dose was defined as 5ng/ml, whereas high dose was defined as 50 ng/ml (283). For some experiments cells were co-treated with GDF-15 and TGFβ1 or pre-treated with GDF-15 for 48 hours and then co-treated with GDF-15 and TGFβ1 and / or BMP-4. In some experiments cells were treated with the TGFβ activated kinase 1 inhibitor (TAK1i) (5Z)-7-oxozeaenol (Tocris bioscience, Bristol, UK), which was

dissolved in DMSO (Sigma Aldrich, St Louis, MA, USA) to a concentration of 25 mM and then further diluted in medium to give doses between 100 and 1000 nM. In some experiments cells were treated with the activin like kinase 5 (ALK-5) inhibitor SB431542 (Sigma Aldrich, St Louis, MA, USA), which was dissolved in DMSO (Sigma Aldrich, St Louis, MA, USA) to a concentration of 10 mM and then further diluted in DMEM (Sigma Aldrich, St Louis, MA, USA) to give doses of 10 µM, a dose used in other publications (408). As a positive control TGFβ1 (R&D systems, Abingdon, UK) dissolved in sterile 4 mM hydrochloric acid containing 0.1% BSA was used at various concentrations from 0.01 to 50 ng/ml. In experiments not requiring a dose response a dose of 2.5 ng/ml was used. Other positive controls used in the myoblast experiments include Myostatin (GDF-8) (R&D systems, Abingdon, UK) dissolved in sterile 4 mM hydrochloric acid containing 0.1% BSA, and used at 50 and 100 ng/ml, BMP-4 (R&D systems, Abingdon, UK) dissolved in sterile 4 mM hydrochloric acid containing 0.1% BSA, and used at 10 ng/ml and Tumour Necrosis Factor α (TNFα) dissolved in PBS and used at 10ng/ml. For negative control the appropriate diluent without active ingredients at the same volume used in the experimental condition was added to DMEM with or without serum.

2.3.3 Harvesting mRNA and protein from cell culture

At various time points after treatment cells were washed with cold Phosphate Buffered Saline (PBS) on ice. For RNA extraction between 250 and 500 µL of trizol (Life Technologies, Carlsbad, CA, USA) was added to the well after which the cells were scraped and trizol cell mix was placed in a microcentrifuge tube. From then on the RNA extraction process was undertaken as described previously. For protein extraction cells were scraped in ice cold PBS after which they were placed in a 15ml falcon tube and centrifuged at 1000 rpm for 5 minutes to form a pellet. The PBS was removed and the pellet was re-suspended in between 250 to 500 µL of CLB and PMSF (Cell signalling technologies, Danvers, MA, USA). The protein content was then analysed and stored as described above.

2.4 Plasmids, restriction digests, cloning and transfection

2.4.1 Plasmids, restriction digests and transformation of super-competent bacteria

Plasmids used throughout this thesis were cut with restriction enzymes to confirm their identity. NEB 5 alpha competent E-Coli bacteria (New England biolabs, MA, USA) were transformed with plasmids. 5 µl of plasmid was added to 40 µl of supercompetent cells and the samples were incubated on ice for 15 minutes. The sample was heat shocked for 90 seconds in a water bath at 42^{o}C after which it was returned to ice for 2 minutes. Thereafter 500µl of LB broth was added to the mixture and incubated for 45 minutes at 37^{o}C. After this 200µl of the plasmid bacteria mix was plated onto plates with ampicillin (100 µg/ml) (Sigma-Aldrich, St. Louis, MO, USA) and allowed to grow into colonies overnight at 37^{o}C. These colonies were picked and the plate was placed stored at 4^{o}C for future use. Picked colonies for future mini-prepping were added to LB broth with ampicillin 100 µg/ml and incubated at 37^{o}C overnight. The next day plasmids were mini-prepped using a QIAprep spin mini-prep kit (Qiagen, Hilden, Germany). Bacteria were pelleted by centrifugation at 8000 rpms for 3 minutes at room temperature. The pellet was re-suspended in 250 µl of P1 buffer (Qiagen, Hilden, Germany) and transferred to a microcentrifuge tube. Next 250 µl of P2 buffer (Qiagen, Hilden, Germany) was mixed in by inverting the tube 6 times, after which 350 µl of N3 buffer (Qiagen, Hilden, Germany) was added to the sample. The sample was before centrifuged the tube for 10 minutes at 13000 rpms. The supernatant was added to the QIAprep spin column and spun for 60 seconds at 13000 rpms. The flow-through was discarded and the process was repeated with 500 µl of PB buffer (Qiagen, Hilden, Germany) and then with 750 µl of PE buffer (Qiagen, Hilden, Germany) with ethanol. Residual wash buffer was removed with another spin and the column was placed in a fresh microcentrifuge tube after which 50 µL of EB buffer was added and spun for 1 minute. The resulting DNA was checked for concentration and purity using a spectrophotometer (Nanodrop ND1000, Thermofisher, Waltham, MA, USA). DNA content was determined by measuring absorbance at 260nm and purity was determined by

measuring the absorbance ratios 260nm:230nm and 260nm:280nm. The plasmids were then checked by restriction digest. In a PCR tube 4 µl of plasmid DNA was incubated with 12.5 µl of water, 2 µl of 10x buffer (dependant on the enzymes used), 0.5 µl of restriction enzyme one, 0.5 µl of restriction enzyme 2 and 0.5 µl of BSA (New England biolabs, MA, USA) for 1 hour at room temperature. A 1.5% agarose gel was prepared by adding 2.25 g of agarose (Bioline, London, UK) to TBE buffer, a 10 x stock of which is made from 108 g tris base (Sigma-Aldrich, St. Louis, MO, USA), 55 g of boric acid (Sigma-Aldrich, St. Louis, MO, USA) and 7.5 g of EDTA (Sigma-Aldrich, St. Louis, MO, USA) in 1 L of distilled water. This was heated in the microwave to allow the agarose to dissolve after which the mixture was cooled. At this point either 5 µl of ethidium bromide (ThermoFisher Scientific, MA, USA) or SYBR safe (ThermoFisher, MA, USA) was added to the mixture prior to it being made into a gel with lanes. The gel was placed in a gel electrophoresis tank (ThermoFisher Scientific, MA, USA) filled with 1x TBE and the wells were loaded with 10 µl of DNA with 5x loading buffer (Bioline, London, UK) or DNA ladders Hyperladder I or II (Bioline, London, UK). The gel was run in the tank at 120 volts for 40 minutes to allow band separation. The gel was then viewed on a Biorad chemidoc XRS+ running imagelab software (Biorad, CA, USA) and images saved and analysed for the size of DNA fragments. The plasmids, restriction enzymes and band sizes are listed in Table 2.3.

Plasmids	Restriction	Band sizes
pCDNA3	Pst1	4072, 1356
pRL-TK	EcoR1, BamH1	2582, 1463
pRL-TK no BRE	EcoR1, BglII	3680, 365
pCAGA12 luciferase	HindIII, BamH1	2471, 1574
pBRE luciferase	Nhe1	4370, 45
pCDNA3 hum TGFBR2	EcoR1, Pst1	4500, 4100
pCMV Sport 6.1 TGFBR2	EcoR1, Xho 1	3863, 1013
pCMV Sport 6.1 ACVR2B	EcoR1, Xho1	3863, 1762
pCMV Sport 6.1 BMPR2	EcoR1	4302, 3461, 74
pCDNA3 hum TTGBFR2	Pst1	3682, 1385, 379
pCAGGs-EGFP	BamH1	3734, 1471, 337

Table 2 .3 Plasmids. Plasmids used throughout my thesis, restriction enzymes and sizes of bands expected when run on a gel. All pCMV Sport 6.1 vectors coded for receptors of mouse origin.

2.4.2 Cloning the truncated TGFBR2

The plasmid map for plasmids coding for human and mouse TGFBR2 was examined and the sequence coding for the extracellular, transmembrane and intracellular portion of the receptor was identified using Uniprot (http://www.uniprot.org/). Primers were designed to encompass the extracellular area and transmembrane portion. For the human TGFBR2 these were forward GCGCTGGGGCTCGGTCTATGAC and reverse GCCGGTTTCCCAGGTTGAACTC and for the mouse TGFBR2 these were forward GCAGGCTGGTACCGGTCCGGAATTC and reverse CCTCCAGGATGATGGCACAATTGTC. The human TTGFBR2 was used in subsequent experiments and is therefore described below. PCR of the appropriate portion was carried out using HotStart HiFidelity polymerase kit (Qiagen, Hilden, Germany) and Taq DNA Polymerase HiFidelity kit (ThermoFisher, MA, USA). For the Qiagen kit 1 µl of TGFBR2 DNA was added to 5 µl of 10x buffer, 2 µl of 5 µM DNTPs, 2 µl Q buffer, 2.5 µl forward and 2.5 µl reverse primers, 1 µl Taq polymerase, and 36.5 µl of water (Qaigen, Hilden, Germany). For the ThermoFisher kit 1 µl of DNA was added to 5 µl of 10x buffer, 2 µl of DNTPs, 2 µl DMSO, 2.5 µl of forward and 2.5 µl or reverse primer, 1 µl of Taq polymerase and 37.0 µl of water (ThermoFisher, MA, USA). The mixes were placed on ice and the thermal cycler (ThermoFisher Scientific, MA, USA) was heated to 80^{o}C for a hot start. The machine was cycled to 95^{o}C for 1 minute, and then through 40 cycles of 95^{o}C for 30 seconds, 65^{o}C for 30 seconds and 72^{o}C for 1 minute. The resulting product was run on an agarose gel and imaged as above. An image showing a product of just over 800 bp that corresponds to the extracellular and transmembrane portion of the receptor is shown in Figure 2.5.

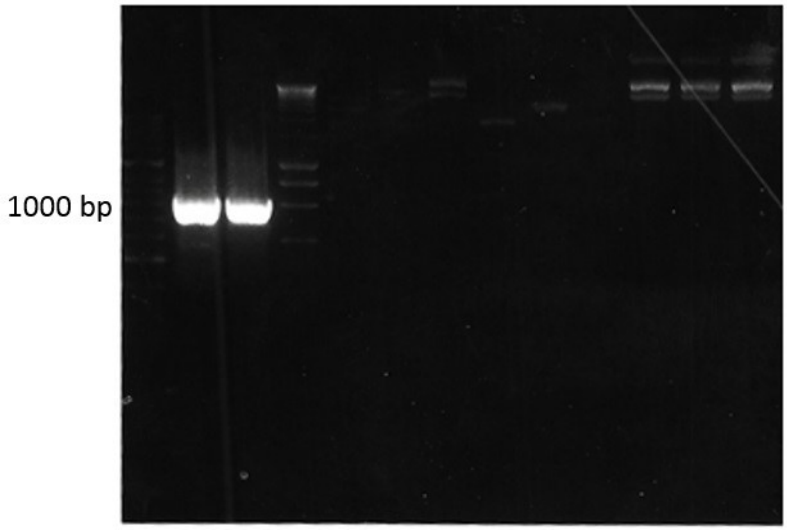

Figure 2.5 PCR product of the truncated TGFBR2 receptor. Image of agarose gel showing the PCR product of the truncated TGFBR2 primers (2 bright bands on the left)

The gel was imaged under ultra-violet light and the bands were cut out and placed in a microcentrifuge tube. The DNA was then gel extracted using a Qiagen gel extraction kit (Qiagen, Hilden, Germany). The agarose gel was suspended in QG buffer heated to 50^{o}C for 10 minutes after which isopropanol was added and solution was centrifuged in a QIAquick spin column for 1 minute at 13000 rpms. The flow through was discarded and the column was washed with PE buffer with ethanol and centrifuged again. The column was spun again and then 50 µl of EB buffer was added to elute the DNA into a new microcentrifuge tube (Qiagen, Hilden, Germany). The resulting DNA product was ligated into a pGEM-T Easy vector using the pGEM-T Easy vector kit (Promega, Wisconsin, USA). 3.5 µl of DNA insert, control or water negative control was added to 5 µl of 2x ligation buffer, 1 µl of pGEM-T vector and 0.5 µl of DNA ligase (Promega, Wisconsin, USA) and left overnight on the bench. The DNA was transformed into super-competent bacteria as described above. These were plated with 30 µl isopropyl β-D-1 thiogalactopyranoside (IPTG) (Sigma-Aldrich, St Louis, MO, USA) and 30 µl 5-Bromo-4-chloro-3-inodyl β-D-galactopyranoside (X-gal) (Sigma-Aldrich, St Louis, MO, USA) for blue white screening. Colonies were screened and white colonies, which contain recombinant DNA and not just vector, were picked. These were cultured overnight in LB-broth and mini-prepped using the technique described above. To

create an insert of truncated TGFBR2 with sticky ends the pGEM-T TTGFBR2 was cut with EcoR1 restriction enzyme. 16 µl of DNA was added to 5 µl of 10x EcoR1 buffer, 2 µl of EcoR1 restriction enzyme, and 0.5 µl of BSA, with water up to 50 µl (ThermoFisher Scientific, MA, USA). For the vector into which the TTGFBR2 was to be inserted pCDNA3 was also cut with EcoR1 and dephosphorylated to prevent self-ligation of the linearized vector. 10 µl of DNA was cut with 1 µl EcoR1, 3 µl of 10x EcoR1 buffer, 1.5 µl of BSA, 1 µl of alkaline phosphatase and 13.5 µl of water (ThermoFisher Scientific, MA, USA). The products were run on a gel, cut out, and the gel extracted using the technique described above (Qiagen, Hilden, Germany). The products were the ligated. 9 µl of DNA (7.2 µl insert and 1.8 µl of vector) were added to 4 µl of quickstick ligase buffer (Bioline, London, UK), 1 µl quickstick ligase enzyme (Bioline, London, UK) and 5 µl of water on the bench overnight as per protocol. The resulting DNA was transformed, plated with IPTG/X-gal and incubated overnight as above. Colonies were blue/white screened, picked and PCR screened. 5 µl of PCR buffer, 2.5 µl of forward and 2.5 µl of reverse primers (see earlier), 2 µl of DNTPs, 0.25 µl Taq polymerase and 5 µl of 10x buffer (Qiagen , Hilden, Germany) had a single colony re-suspended in TE buffer (ThermoFisher Scientific, MA, USA) dropped into it. PCR was performed on a thermal cycler (ThermoFisher Scientific, MA, USA) using the protocol, 94^{o}C for 3 minutes, and then 40 cycles of 94^{o}C for 30 seconds, 60^{o}C for 30 seconds and 72^{o}C for 2 minutes after which the solution was held at 72^{o}C for further 10 minutes before the end of the experiment. The resultant product was run on a gel which is shown in Figure 2.6.

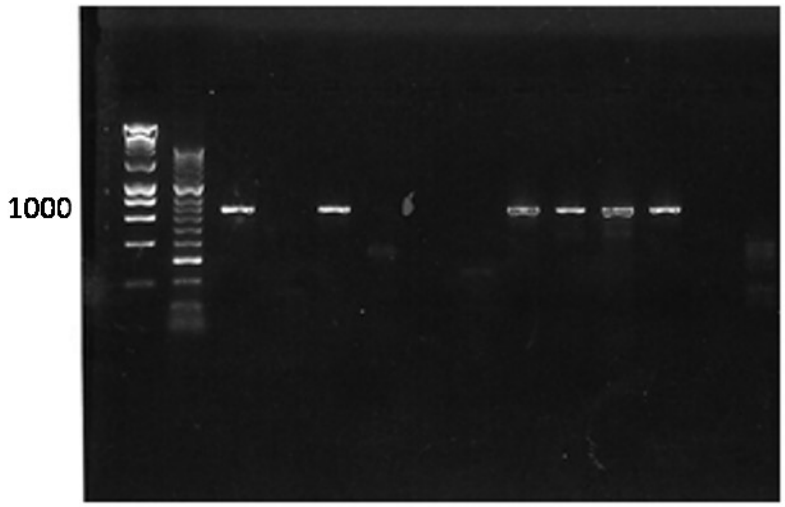

Figure 2.6 PCR screening for TTGFBR2 insert in pCDNA3. Gel showing PCR screen for TTGFBFR2 insert in pCDNA3 in colonies picked by blue / white screening. Lanes 1, 3, 7, 8, 9 and 10 were positive for the mutant vector.

The colonies that contained the product identified by PCR screening were transformed and resulting DNA from the mini-prep was cut with the restriction enzyme Pst1 to show directionality that the insert had been incorporated into the plasmid. If the insert had gone in forward the lowest band would be 379 base pairs, backwards the lowest band would be 246. The gel of pCDNA3 TTGFBR2 cut with Pst1 is shown in Figure 2.7. The DNA was sent for sequencing (Source Bioscience, Nottingham, UK) and the results showed 100% homology with the sequence of the TTGFBR2 (Appendix 2.3). This was used in subsequent experiments.

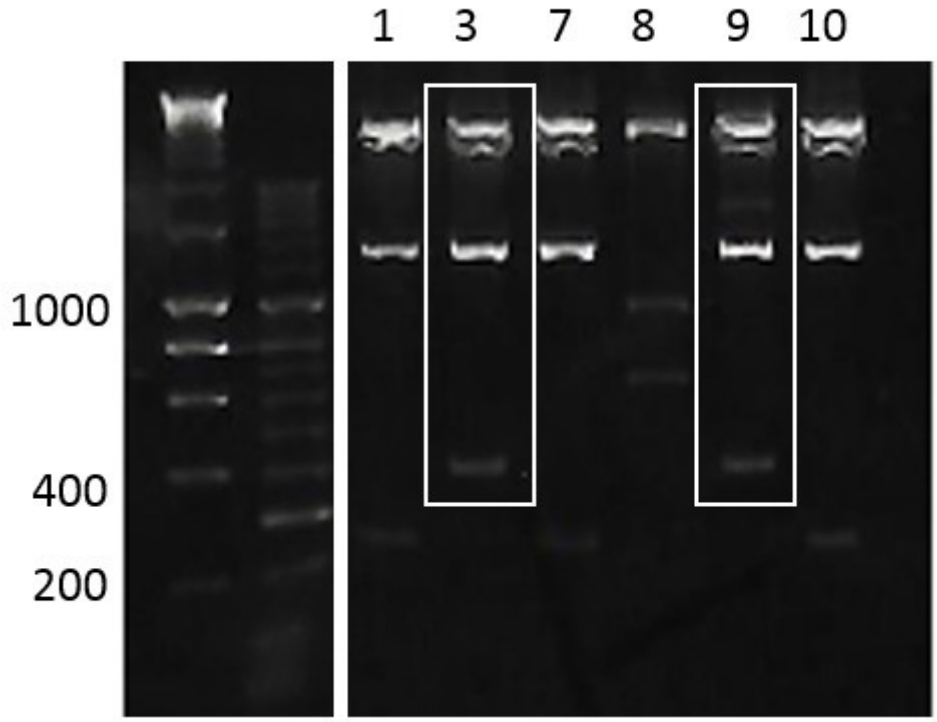

Figure 2.7. pCDNA3 hum TTGFBR2 plasmids cut with PST1 showing directionality. Highlighted samples 3 and 9 have a lowest band of 379 bp showing that the insert was in the appropriate orientation

2.4.3 Cloning a BMP responsive element (BRE) luciferase and removing a BRE from pRL-TK

The BMP responsive element luciferase vector was cloned using methods described by Korchynskyi and Dijke (409). Oligonucleotides (Sigma-Alrich, St Louis, MO, USA) CGCG GCGCCAGCCTGACAGCCCG, AGGACGGGCTGTCAGGCTGGCGC, TCCTGGCGTCTAACGGTCTGAG, CTAGCTCAGACCGTTAGACGCC were annealed by heating to 95^{o}C and cooled by 1^{o}C per minute to 50^{o}C. This created an insert with a 'NheI restriction site followed by 2 SMAD binding elements, 1 GGCG site, 2 CAGC sites, 2 GGCGCC palindromes, 2 CAGC sites, 1 GGCG site, 2 SBEs, and another NheI site' (409). The resulting product was phosphorylated with T4 polynucleotide kinase (PNK) (New England Biolabs, MA). The pGL5 luciferase reporter vector (Promega, CA, USA) was cut at the NheI site. 2 µl of DNA was added to 1 µl of 10x buffer, 1 µl of NheI restriction enzyme, 1µl of alkaline phosphatase and 1 µl of BSA (New England Biolabs, MA, USA). The linearised vector was run on an agarose gel, cut out and gel extracted as detailed above to remove the phosphatase. The insert and vector were ligated as

described above with Quick-stick ligase (Bioline, London, UK). The resulting DNA was transformed into bacteria (New England Biolabs, MA, USA) plated and colonies picked. These were cut with NheI and run on a gel to check for the presence of the insert (Figure 2.8). Those with the insert were then used in subsequent experiments.

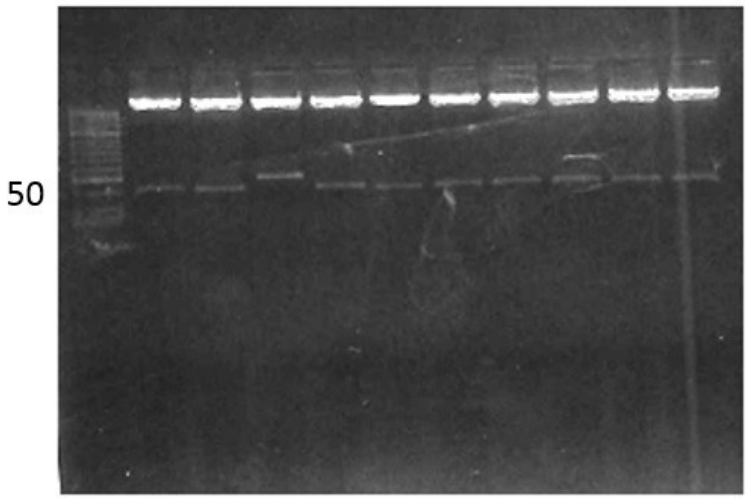

Figure 2.8 BRE luciferase cut with Nhe 1 to show the presence of the insert. The 3rd column was discarded as the band was higher than expected.

In the first experiments using the pGL5 BRE luc it was noted that BMP-4 treatment increased activity of the control pRL-TK luciferase (Figure 2.9). When the pRL-TK (Promega, CA, USA) sequence was examined a BMP responsive element in the HSV promoter of the vector was identified (Appendix 2.4). pRL-TK vector was therefore cut with BglII and SmaI restriction enzymes (New England Biolabs, MA, USA) as described above to remove 284 base pairs including those which contained the BMP responsive element. The DNA was run on a gel and the higher band was cut out. The sticky end of the BglII restriction site was filled in with T4 DNA polymerase (New England Biolabs, MA, USA). 10 µl of pRL-TK DNA was added to 20 µl of 5x T4 buffer, 1 µl of DNTPs, 2 µl DNA polymerase, 10 µl BSA and 67 µl water for 5 minutes at room temperature after which the mixture was heated to 75°C for 10 minutes to stop the reaction (New England Biolabs, MA, USA). The resulting linearised DNA with blunt ends was then ligated with Quick-stick ligase (Bioline, London, UK). It was then transformed,

cut with EcoR1 and BglII restriction enzymes run on an agarose gel and imaged to check for removal of the BRE from the pRL-TK. The resulting pRL-TK without the BRE was tested and showed no response to BMP-4 (Figure 2.9)

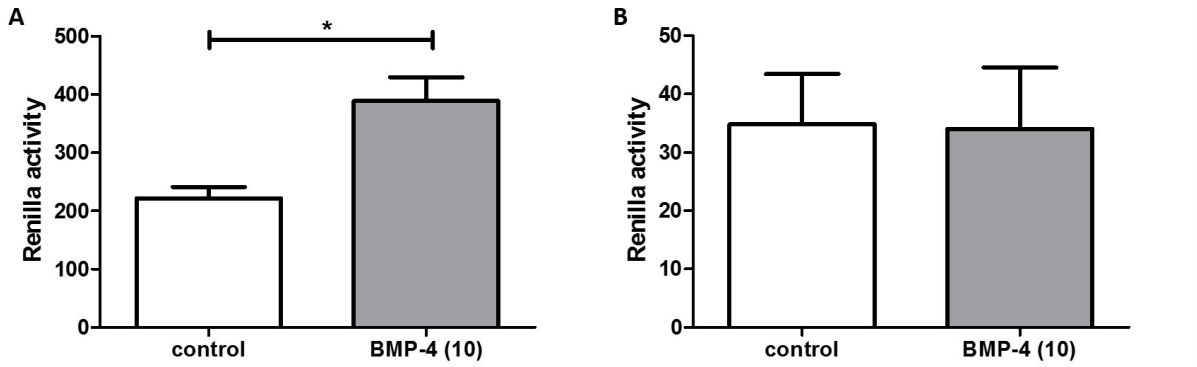

Figure 2.9 Renilla activity in BMP-4 treated cells transfected with pRL-TK with and without BRE. Example of raw data from renilla activity in cells transfected with pRL-TK treated with Bone morphogenetic protein 4 (BMP-4) at 10 ng/ml with **A.** the BMP responsive element included (Student's t-test p = 0.017) and **B.** with the BMP responsive element removed (Student's t-test p = 0.722).

2.4.4 Transfection of DNA for luciferase, immunofluorescence and fibre diameter

A total of 2 µg DNA was transfected per 4 wells of a 24 well plate and scaled up and down appropriately. For experiments involving SMAD 2, 3 dependant luciferase activity in the presence of various receptors 1 µg of p(CAGA)12-luc, 0.5 µg of pRL-TK and 0.25 µg of pCDNA3 with 0.25 µg of pCDNA3, pCDNA-TGFBR2 (Donated by P Kemp), pCDNA-TTGFBR2 (see cloning section) pCMV-mACVR2B (Sinobiological, Ludong, Beijing, China) or pCMV-Myc-BMPR2 (Sinobiological, Ludong, Beijing, China) was incubated with 10 µl of Lipofectamine (Invitrogen, ThermoFisher, MA, USA) in 200 µl of Optimem (GIBCO, Life technologies, CA, USA) for 15 minutes at room temperature. The cells were washed twice in serum free media. 600 µl of serum free media was added to the transfection mix at this point to bring the total volume added to each well of a 24 well plate to 200 µl. Cells were incubated in this transfection mix for 4.5 hours, after which the media was changed back to DMEM with 10% FCS. For experiments involving SMAD 1, 5 dependant luciferase activity in the presence of

various receptors cells were transfected in 24 well plates as above using pBRE-luc, and pRL-TK(no BRE) instead of p(CAGA)12-luc and pRL-TK and pCNDA3 or the receptors listed above at the same dose and using the same method described above. For experiments not requiring the addition of a plasmid coding for a receptor, cells were seeded in 96 well plates and transfected with 1.33µg of p(CAGA)12-luc or pBRE-luc and 0.66µg of pRL-TK or pRL-TK(no BRE) per 16 wells using the method described above.

Cells examining the effect of TTGFBR2 on myotube diameter were seeded in 6 well plates. The next day cells were transfected with 1µg of pCAGGs- enhanced green fluorescent protein (EGFP), 0.5µg of pCDNA3 and 0.5µg of pCDNA-TTGBR2 or 0.5 µg of pCDNA3 per well. Cells examining the effect of the TAK1 inhibitor, 5(Z)-7-oxozeaenol, on myotube diameter were transfected with 1 µg of pCAGGs-EGFP alone per well. These DNA mixes were combined with Optimem (GIBCO, Life technologies, CA, USA), Lipofectamine (Invitrogen, ThermoFisher, MA, USA) and DMEM in similar proportions to those used for other luciferase experiments scaled up appropriately. After transfection, cells were differentiated into myotubes until day 10, after which they were treated with control, GDF-15 and or 5(Z)-7-oxozeaenol (Tocris bioscience, Bristol, UK).

2.5 Molecular techniques

2.5.1 Luciferase assay

The Dual-Luciferase reporter assay system (Promega, Wisconsin, USA) was used as per manufacturer's instructions to measure SMAD 2, 3 and SMAD 1, 5 dependent luciferase activity. Cells were transfected and treated as detailed above. Cells were removed from the incubator, placed on ice and the media was removed by washing twice with PBS. Cells were incubated with passive lysis buffer (Promega, Wisconsin, USA) (125 µl/well of a 24 well plate and 50 µl/well of a 96 well plate) for 15 minutes on an orbital plate shaker. 10 µl of the lysate was placed in a 96 well plate for further analysis. A white plate was used to enhance luminescence. As per manufacturer's instructions 50µl of firefly assay substrate (Promega, Wisconsin, USA) was added to the lysate after which luminescence was read on a Luminark

spectrophotometer plate reader (BioRad, CA, USA) to define the SMAD 2, 3 or SMAD 1, 5 dependent luciferase activity. Next, 50µl of 'Stop and Glow' (Promega, Wisconsin, USA) substrate was added to the lysate and firefly assay substrate mix, after which luminescence was read again to define renilla activity. Firefly output was normalised to renilla output for each sample allowing adjustment of results for transfection efficiency.

2.5.2 cDNA synthesis and quantative PCR (qPCR) for mRNA.

150ng of mRNA was used for each reverse transcription reaction. The volume of sample containing 150 ng was made up to 11 µl with water. The mRNA was heated to 65^{o}C for 5 in a thermal cyler to denature it. Whilst cooling on ice a master mix of 2 µl water, 1 µl Omniscript (Qiagen, Hilden, Germany), 2 µl 5mM dNTPs (Qiagen, Hilden, Germany), 0.5 µl Ribolock (ThermoFisher Scientific, MA, USA), 0.5 µl random primers (Promega, Wisconsin, USA), 2 µl 10x buffer (Qiagen, Hilden, Germany) and 1 µl DTT (Qiagen, Hilden, Germany) was added to each sample. The samples were placed back in the thermal cycler where they were heated to 42^{o}C for 2 hours. The resulting cDNA was diluted with water up to a working volume of 200 µl before being frozen at -20^{O}C.

To test the relative expression of various genes involved in both TGFβ signalling and muscle wasting, appropriate primers were identified from the literature. These are listed in Table 2.4. Primer pairs were tested to ensure they were able to identify a single PCR product of appropriate size. A thermal cycler was used to undertake PCR. The resulting amplified DNA product was run on a 1.5% TBE agarose gel as described above to check for the presence of a single band.

An ABI 7500 fast thermal cycler (ABI, Life technologies, CA, USA) was used throughout the qPCR experiments. A master mix of 10 µl of fast SYBR green (Qiagen, Hilden, Germany) 2 µl of a 2 µM forward and reverse primer mix (Table 2.4) and 5 µl of water were added to each well of a 96 well fast optical plate. 3µl of cDNA from each sample was added to each well containing the master mix. Samples were analysed in duplicate and water negative controls were included on each plate. Plates were covered in a MicroAmp optical adhesive film (Life Technologies, CA, USA). Plates were then

centrifuged for 1 minute at 1000 rpms. The protocol for qPCR was to heat the samples to 95^{o}C for 5 minutes. This was followed by 40 cycles of 95^{o}C for 10 seconds and 60^{o}C for 30 seconds. A melt curve was included to pick up primer dimers, contamination and off target binding. The mean cycle threshold (CT) for each duplicated sample was recorded. Samples were excluded if the duplicates were not consistent or if the water in the plate had a measurable significant CT. Analysis was undertaken in valid samples using ΔCT method.

Primers	Sequence
Rat RPLPO F	ATGGGCAAGAACACCATGATG
Rat RPLPO R	CCTCCTTGGTGAACACAAAGC
Rat GAPDH F	ATGCCTTCCGTGTTCCTACCC
Rat GAPDH R	GCCTGCTTCACCACCTTCTTGAT
Rat GDF-15 F	AGC TGT CCG GAT ACT CAG TC
Rat GDF-15 R	GAG TCT CTT GGG TGC AAA TG
Rat TGFβ1 F	GCGCCTGCAGAGATTCAAG
Rat TGFβ1 R	GTATCAGTGGGGGTCAGCA
Rat GDF-8 F	TGGGCATGATCTTGCTGTAA
Rat GDF-8 R	TGTTACTTTGACCTTCTAAAAAGGGATT
Rat Atrogin-1 F	CCATCAGGAGAAGTGGATCTATGTT
Rat Atrogin-1 R	GCTTCCCCCAAAGTGCAGTA
Rat MuRF-1 F	TGGAGATGAATTGCTCAGT
Rat MuRF-1 R	GTGAAGTTGCCCCCTTACAA
Rat TAK1 F	TGCGATTTTGGTACAGCTTG
Rat TAK1 R	TGGTCGAGTGCCATTATGAA
Rat NFκB p65 F	GGTGGAGTTTGGGAAGGAT
Rat NFκB p65 R	TTTCTCCGAAGCTGAACA
Rat p38 MAPK F	CGAAATGACCGGCTACGTGG
Rat p38 MAPK R	CACTTCATCGTAGGTCAGGC
Mouse RPLPO F	GGACCCGAGAAGACCTCCTT
Mouse RPLPO R	TGCTGCCGTTGTCAAACACC
Mouse GAPDH F	ACTCCACTCCACGGCAAATTCA
Mouse GAPDH R	CGCTCCTGGAAGATGGTGAT
Mouse GDF-15 F	GGCTGCATGCCAACCAGAG
Mouse GDF-15 R	TCTCACCTCTGGACTGAGTATCC
Mouse TGFβ1 F	TGGAGCAACATGTGGAACTC
Mouse TGFβ1 R	GTCAGCAGCCGGTTACCA
Mouse GDF-8 F	CGGACGGTACATGCACTAATATTTC
Mouse GDF-8 R	GAGGGGAAGACCTTCCATGAC
Mouse atrogin-1 F	TCAGCCTCTGCATGATGTTC
Mouse atrogin-1 R	TGGGTGTATCGGATGGAGAC
Mouse MuRF-1 F	CGGGCAACGACCGAGTGCAGACGATC
Mouse MuRF-1 R	CCAGGATGGCGTAGAGGGTGTCAAAC
Mouse NFκB p65 F	ATCTTCACCATGGCAGACGAT
Mouse NFκB p65 R	TGAGTGAGTCAAAGCAGTGTTCAA

Table 2.4 Primers. Primers used in qPCR experiments. Large ribosomal protein (RPLPO), glyceraldehyde-3 phosphate dehydrogenase (GAPDH) are housekeeper genes

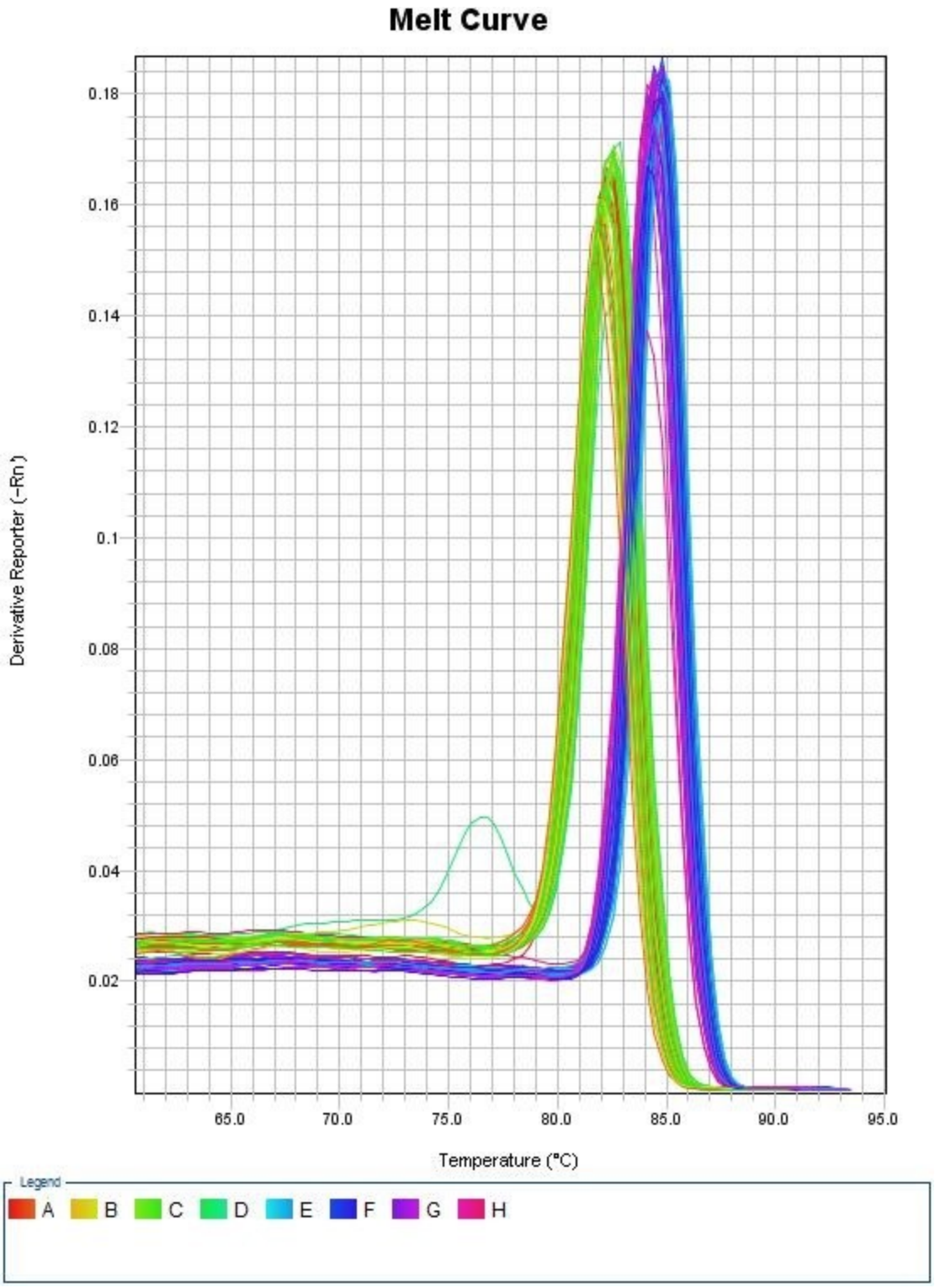

Figure 2.10 Example of melt curve generated by qPCR. Example of a melt curve of GAPDH and atrogin-1 genes from cells treated for 96 hours with GDF-15 at 5 ng/ml.

2.5.3 Western Blotting

Protein samples were collected and heated as documented above. Pre-cast gels (gradient 4-15%) with 10 wells each accommodating up to 50 µl (Biorad, CA, USA) were loaded with between 20 and 200 µg of protein, dependant on the protein of interest and the local expression level. The gel was run with at least one lane containing 'Precision Plus protein Dual Colour Standard' protein ladder (Biorad, CA, USA) to define the size of any product seen on the blot. The gels were run in a BioRad gel tank at 120 V until the samples could be seen to have run to the bottom of the gel in 1 x Tris glycine sodium dodecyl sulphate polyacrylamide gel electrophoresis (SDS-PAGE) buffer (National Diagnostics, GA, USA) normally taking between 60 and 90 minutes. A polyvinylidene difluoride (PVDF) membrane (GE healthcare, Little Chalfont, UK) was activated in 1 x Tris glycine SDS PAGE buffer (National Diagnostics, GA, USA) with 20% methanol (ThermoFisher, MA, USA). Transfer of the protein to this membrane was achieved using a wet transfer technique in 1 x Tris glycine SDS PAGE buffer (National Diagnostics, GA, USA) with 20% methanol (ThermoFisher, MA, USA) at 100 V (BioRad, CA, USA) for 75. Membranes were blocked in 5% milk (Marvel, UK) for non-phosho antibodies or 5% BSA (Sigma-Aldrich, St Louis, USA) for phospho antibodies in 1 x tris-buffered saline with 0.1% tween 20 (TBS-T) for 30 minutes on an orbital plate shaker. 10 x TBS was made with 24 g of Tris base (VWR, Leicester, UK) and 88 g of sodium chloride (VWR, Leicester, UK) dissolved in 900 ml of distilled water. The pH was brought down to 7.6 with hydrochloric acid (ThermoFisher Scientific, MA, USA) and the solution is made up to 1 L with water. The solution is diluted 1:10 and 1 ml of Tween 20 (Sigma-Aldrich, St. Louis, MO, USA) is added to 1 L of 1x solution to make TBS-T. After blocking, membranes were placed in sealed bags containing primary antibodies in 5% milk (non-phospho antibodies) or 5% BSA (phospho antibodies) in TBS-T overnight on an orbital plate shaker. The antibodies used are described in Table 2.5. The next day membranes were washed with TBS-T 3x for 5 minutes. Membranes were then placed in another plastic bag containing secondary horseradish peroxidise (HRP) conjugated antibodies in 5% milk in TBS-T for 1 hour. Membranes were washed again 3 x for 5 minutes in TBS-T. Membranes were then placed on cling film and Pierce enhanced chemoluminecence (ECL) reagent (Thermo Fisher Scientific,

MA, USA) was carefully pipetted on to ensure the entire blot was covered for 5 minutes. The membrane was then exposed to X-ray film (Life technologies, Carlsbad, CA, USA), for variable lengths of time, which was then developed on an automated film developing system in a dark room. Alternatively the membrane was exposed on an ettan dige imager (EDI) (GE Healthcare, Little Chalfont, UK). Proteins of interest probed with antibodies were identified by their molecular weight, which could be analysed by comparing band size to a known protein ladder. Protein and transfer efficiency can significantly alter band intensity across different lanes of a blot. In order to overcome this samples were probed for housekeeping proteins GAPDH, β-actin or the total non-phosphorylated protein of the protein of interest and or stained for Ponceau red (Biorad, CA, USA).

Xray films exposed to the blots were scanned and both this and the files generated by the EDI were analysed by ImageJ. A rectangle was drawn around each band and the density of each lane was plotted as a curve. A line was drawn under the curve and the area under the curve was calculated giving a numerical representation of the density of the band. This allowed comparison of the density of the bands across the blot. The target protein density level was then normalised to GAPDH, β-actin or the non-phosphorylated protein of the phosphorylated protein of interest.

For the quantification of phosphorylated TAK1 in rat tissue samples, 5 were quantified. These samples were the first five MCT and control animals in the first MCT TAK1 inhibitor study.

Antibody	Accession	Source	Concentration	Company
anti-phosphoTAK1 (Ser 412)	9339	Rabbit	1:500 - 1:1000	Cell signalling
anti-phospho NFκB p65 (Ser 536)	3031	Rabbit	1:500 - 1:1000	Cell signalling
anti-phospho p38 MAPK (Thr 180/ Tyr 182)	9311	Rabbit	1:1000	Cell signalling
anti-NFκB p65	sc 372	Rabbit	1:1000	Santa Cruz
anti-p38 MAPK	9212	Rabbit	1:1000	Cell signalling
anti-TGFBR2	sc 400	Rabbit	1:1000	Santa Cruz
anti-ACVR2B	sc 25453	Rabbit	1:1000	Santa Cruz
anti-BMPR2	6979	Rabbit	1:1000	Cell signalling
anti-β-actin	4967	Rabbit	1:1000	Cell signalling
anti-GAPDH	2118	Rabbit	1:1000	Cell signalling
anti-Rabbit IgG HRP linked secondary	7074	Goat	1:1000	Cell signalling

Table 2.5 Antibodies for western blot. Antibodies used in western blots throughout my thesis. Higher concentrations of antibody for phospho-TAK1 and phospho-NFκB p65 were required for animal experiments.

2.5.4 Enzyme-linked immunosorbent assay (ELISA).

GDF-15 protein levels in rat serum and lung and human plasma was analysed by commercially available rat/mouse and human ELISA kits (R&D systems, Abingdon, UK) as per manufacturer's instructions. 50 µl of assay diluent was added to each well, along with 50 µl of standard control or sample to each well. The samples were covered with a plate sealer and incubated at room temperature for 2 hours on an orbital microplate shaker. Wells were aspirated and washed. 100 µl of conjugate was then added to each well and after covering was incubated for 2 hours on the shaker. The samples were aspirated and washed 4 times. 100 µl of substrate solution was added to each and protected from light for 30 minutes. 100 µl of stop solution was then added to each well. ELISA plates were then read on a microplate spectrometer (BioTek Powerwave XS, Winooski, USA) at 450 nm with a background wavelength correction of 540 nm. Sample results were compared to the standard curve generated by the kit to give the final concentration of GDF-15. For serum and plasma samples neat samples were used. For lung samples homogenates in CLB and PMSF were analysed and normalised to total protein content measured by Bradford assay which was assessed at the time of protein extraction.

2.5.5 Muscle fibre and myotube diameter

An Olympus CKX41 microscope and Cell^D software (Olympus, Essex, UK) at 10x magnification was used to image H+E stained sections of rat and mouse muscle tissue. Three different images were taken per animal. Image J was used to assess fibre diameter. The minimal Feret's diameter, defined as 'the smallest distance between 2 parallel edges of the fibre', (265) was recorded for each fibre, after which the mean fibre diameter for each animal was calculated. The use of the Feret's diameter removes the potential variability seen in measuring cross sectional fibre area where fibres are not cut in the same orientation. Between 67 and 486 fibres were counted per animal. This large variability was due in part to ice crystal formation and in part due to the size of the sample embedded and cut. In the MCT TAK1i study the proportion of fibres below the 5 µm increments in diameter between 20 and 90 µm for each

animal was also calculated and analysed as previously described (410). In the MCT observational study 2 control and 5 MCT animal samples had to be completely excluded due to ice crystal formation within the samples. In the MCT TAK1 inhibitor study and the Sugen/hypoxia mouse study all samples were included.

After ten days myotubes transfected with pCAGGs-EGFP with or without pDNA3-TTGFBR2 were treated with GDF-15 (R&D systems, Abingdon, UK) with or without 5(Z)-7-oxozeaenol (Tocris bioscience, Bristol, UK) for 48 hours. Fluorescent images were taken on a Zeiss Axiovert 200 (Zeiss, Oberkochon, Germany) inverted microscope controlled by Improvision Volocity acquisition software (Perkin-Elmer, MA, USA) with a highly sensitive Hamamatsu Flash 4 (2048x2048 pixel) camera and a pE4000 CoolLed Led Illumination source. Using 10x magnification and a Green fluorescent protein (GFP) /Alexaflour 488 filter, 10 images were taken per well across 3 repeats, meaning for each condition studied there were between 154 and 367 myotubes for analysis. Myotube diameters were analysed using Image J. For each individual cell myotube diameter measurements were taken at 5 evenly distributed points along the length of the cell and the mean diameter was calculated. Raw data and relative change in myotube diameter for each experiment is presented. In order to show that the myotubes imaged, were single cells containing multiple nuclei one of the pCAGGs-EGFP transfected plates was fixed and stained with DAPI and imaged as above to reveal multinucleated myotubes, which are shown in Figure 2.11.

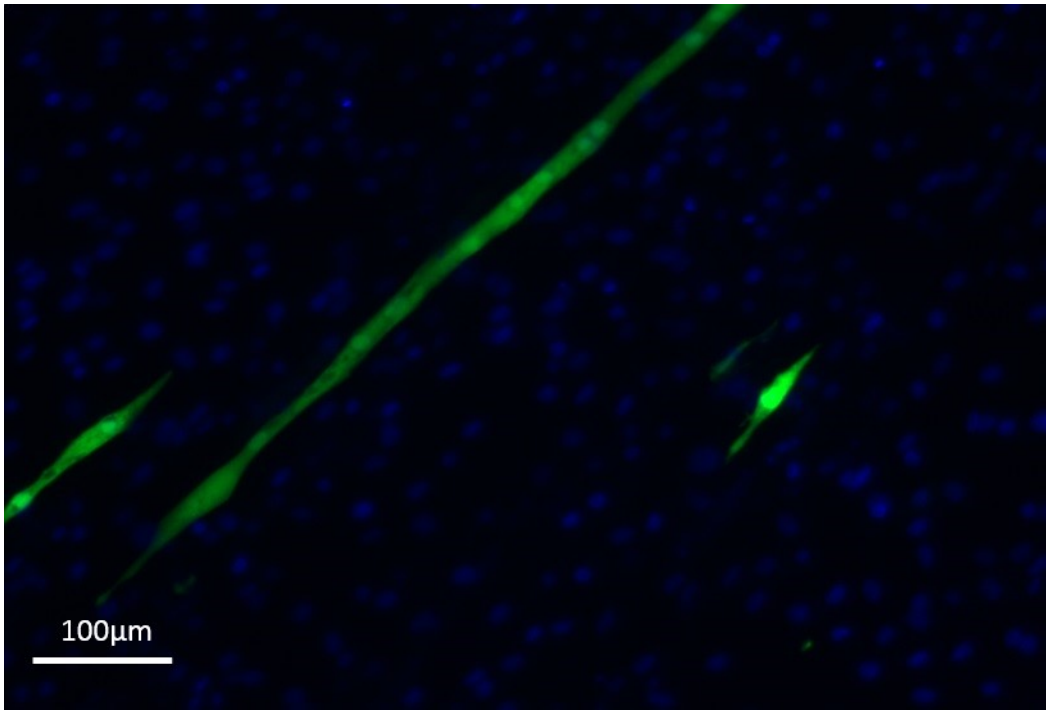

Figure 2.11 Immunofluorescent image of p-CAGGs-EGFP over-expressing myotube co-stained with DAPI. This allows visualisation of the multiple nuclei within the cell.

2.5.6 Immunohistochemistry

Slides from lung tissue from 5 MCT and 5 control rats were prepared by the histology department at Imperial College were washed twice in Histo-clear (National Diagnostics, GA, USA), 100% ethanol (ThermoFisher Scientific, MA, USA) and 95% ethanol (ThermoFisher Scientific, MA, USA) to de-parrafinise and rehydrate. Slides were then washed with water for 1 minute on a platform shaker. Next slides were placed in 10 mM sodium citrate pH 6 (Sigma-Aldrich, St. Louis, MO, USA) which was raised to boiling temperature for 40 minutes for heat induced epitope retrieval. The solution was topped up with water as needed and then left to cool for 2 minutes. The slides were then washed twice in distilled water for 3 minutes. Endogenous peroxidase activity was quenched in 3% hydrogen peroxidase (Sigma-Aldrich, St. Louis, MO, USA) for 20 minutes after which they were again washed in distilled water. Individual sections on each slide were then circled with a DAKO wax pen (DAKO, Glostrup, Denmark) and incubated in blocking solution, which contained 10ml of PBS (Sigma-Aldrich,

St. Louis, MO, USA) with 0.01% saponin (Sigma-Aldrich, MO, USA) and 3 drops of goat serum included in a Vectastain Elite kit ABC kit (Vectorlabs, CA, USA). This was removed and the sections were then incubated with primary antibody either rabbit anti-GDF-15 (orb2266633, Biorbyt, Cambridge, UK) at 1:100 dilution or mouse anti-α smooth muscle actin (MO851, DAKO, Glostrup, Denmark) at 1:400 dilution in PBS / 0.01% saponin with goat serum (2 drops per 10 ml of solution) as per manufacturer's instructions, overnight at 4^{o}C. After this the sections were washed twice for 5 minutes with PBS / 0.01% saponin. This was removed and the sections were incubated for 30 minutes with goat anti-rabbit or anti mouse biotinylated secondary provided in the Vectastain Elite kit (Vectorlabs, CA, USA). One drop of secondary antibody was added to 10mls of PBS / 0.01% saponin / goat serum (3 drops per 10mls) as per manufacturer's instructions. This was washed off as before. Vectastain ABC reagent was reconstituted by adding 2 drops of reagent A (Vectorlabs, CA, USA) and 2 drops of reagent B (Vectorlabs, CA, USA) to 5 ml of PBS which is then left for 30 minutes prior to being added to the slide and incubated for 30 minutes. Slides were washed again and then incubated with 3',3'-diaminobenzidine tetrahydrochloride (Sigma-Aldrich, St. Louis, MO, USA) for 6 minutes for GDF-15 sections and 4 minutes for smooth muscle actin sections after which the reaction was stopped by rinsing the slides in cold tap water. Slides were briefly counterstained with haematoxylin (VWR, Leicester, UK) for 15 seconds. After which they were washed in cold tap water. Sections were next dehydrated by placing them in 95% ethanol (ThermoFisher Scientific, MA, USA), 100% ethanol (ThermoFisher Scientific, MA, USA) and then Histo-clear (National Diagnostics, GA, USA) twice for 15 seconds each in the reverse of the hydration steps. Slides were then covered carefully in histomount (National Diagnostics, GA, USA) and mounted with a coverslip (VWR, Leicester, UK) and allowed to dry overnight. These slides were imaged using an Olympus CKX41 microscope (Olympus, Essex, UK) at 20x magnification and representative sections are presented in the results section. Negative controls where the sections were incubated with primary or secondary antibody alone are presented in Appendix 4.1.

2.5.7 Immunofluorescent staining for nuclear localisation of NFκB and over-expression of TGFβ receptors.

Cells were incubated overnight in serum free media and then treated for 1 hour with GDF-15, control or TNFα in serum free DMEM (Sigma-Aldrich, St. Louis, MO, USA) after which they were washed twice with ice cold PBS (Sigma-Aldrich, St. Louis, MO, USA) for 2 minutes. Cells were then fixed in 4% paraformaldehyde (Sigma-Aldrich, St Louis, MO, USA) in PBS for 10 minutes, after which they were washed three times with PBS with 0.05% Tween (PBS-T) (Sigma-Aldrich, St. Louis, MO, USA) for 5 minutes. Fixed cells were then permeabilised with 1% Triton X100 (Sigma-Aldrich, St. Louis, MO, USA) in PBS-T for 15 minutes. After this, the wash step was repeated and the cells were blocked in 5% milk in PBS-T for 30 minutes. Cells were incubated overnight with primary antibody in 5% milk at 4^{o}C. The next day cells were washed 3 times for 5 minutes with PBS-T, prior to incubation with Alexafluor-conjugated secondary antibody for 1 hour at room temperature in the dark. Primary and secondary antibodies used are outlined in table 2.6. As a negative control cells were incubated in only primary or secondary antibody. Cells were then washed with PBS-T 3 times for 5 minutes. Cells were incubated for 1 minute with 1:10000 4,6-diamidino-2-phenylindole (DAPI) in PBS. After which they were again washed in PBS-T before being imaged on a Zeiss Axiovert 200 (Zeiss, Oberkochon, Germany) inverted microscope controlled by Improvision Volocity acquisition software (Perkin-Elmer, MA, USA) with a highly sensitive Hamamatsu Flash 4 (2048x2048 pixel) camera and a pE4000 CoolLed Led Illumination source using 10 or 20x magnification and GFP/FITC/Alexafluor 488 (green) or Texas red (red) and DAPI/Hoechst (blue) filters. For NFκB p65 nuclear localisation one representative image per well was taken over the course of 3 experiments, meaning between 120 and 134 cells were analysed in total per condition. The exposure, brightness and thresholds were set at the same level for all images in the same experiment. ImageJ was used to calculate nuclear signal and total signal intensity for each individual cell as well as background signal (411). The background signal was subtracted from the 2 cell signal measurements and the nuclear signal was then normalised to the total signal to give a relative nuclear signal. For immunofluorescence showing over-expression of TGFβ receptors

representative images from each well were chosen and presented. Negative controls for the primary and secondary antibodies are shown in Appendix 5.2.

Antibody	Accession	Source	Concentration	Company
anti-TGFBR2	sc 400	Rabbit	1:100	Santa Cruz
anti-ACVR2B	sc 25453	Rabbit	1:100	Santa Cruz
anti-NFκB p65	sc 372	Rabbit	1:200	Santa Cruz
anti-Rabbit IgG (H+L) AlexaFluor488	A11008	Goat	1:500	Invitrogen
anti-Rabbit IgG (H+L) AlexaFluor568	A11036	Goat	1:500	Invitrogen

Table 2.6 Antibodies for immunofluorescence. Antibodies used in immunofluorescence throughout my thesis.

2.6 Data handling and statistical analysis

Data were handled and analysed using Graphpad Prisim 5 (Graphpad, CA, USA) or SPSS version 24 (IBM, New York, USA) software. Graphs were constructed using Graphpad Prism 5 (Graphpad, CA, USA). For each experiment normality was assessed visually using histograms and the Kolmogorov-Smirov, Shapiro-Wilk and D'Agosinto & Pearson normality tests available in Graphpad prism. N numbers (n) for each experiment are included in the figure for each experiment.

Data analysis methodology for the clinical study was discussed with Winston Banya (Medical statistician, NHLI, Imperial College). Demographic data are quoted as mean ± standard deviation (SD) or median and interquartile range (IQR). Student's t-tests or Mann-Whitney U tests were used to compare differences between 2 groups depending on the distribution of the data. When more than 2 groups were compared one way analysis of variance (ANOVA) with Bonferroni correction for multiple analysis or Kruskall-Wallace with Dunn's correction was used to determine differences between the groups of interest in normally and non-normally distributed data respectively. Correlations between different outcomes were assessed by Pearson or Spearman's tests depending on whether the data suggested linear or non-linear correlation. For linear regression to determine the independent predictors of exercise tolerance measured by 6MWD and QOL measured by SGRQ a model was constructed and analysed on SPSS version 24. Variables included in the model were Age, BMI, $USRF_{CSA}$, BNP, CRP and PAL. These variables were chosen as they were either important demographic details or

variables which measured one of muscle, cardiac function, inflammation or activity and were significantly correlated with the outcome of interest. All the variables were normally distributed except for BNP and CRP. Normally distributed variables were entered as continuous data whereas BNP and CRP had to be entered as dichotomous variables and cut off of 100 pmol/L and 10 mgl/L were chosen for BNP and CRP respectively. R^2 with p values for the strength of the overall model and β-coefficient with p values to show those variables that were independently associated with the outcome of interest were calculated and presented. ROC curves were constructed to determine whether one variable could predict an important outcome such as hospital admission, mortality or whether a questionnaire activity score could predict an objectively measured physical activity level. The outcomes for ROC curves included area under the curve as well as sensitivity and specificity analysis for the variable in predicting the outcome. The cut off given the highest sensitivity and specificity is presented. For mortality analysis Kaplein-Meier plots were constructed. Data was censured on the date the final patient included in mortality analysis completed 2 years of follow up. Transplant-free survival was defined as those patients who had not died or had a transplant at the time of assessment. Differences in mortality between 3 groups of patients based on FFMI of < 14, 14-19 and >19 and 2 groups of patients based on steps per day of > or < 2500 and SGRQ of < or > 70 was assessed by Log-rank Mantel-Cox Test as well as for FFMI the log rank test for trend.

For MCT, Sugen/hypoxia mouse and patient data presented in Chapter 4, similar techniques to those described above were employed to assess differences between groups, correlations and ROC curves. For mRNA data outcome genes of interest were normalised to the geomean of RPLPO and GAPDH using the ΔΔCT method, normalised to control values for the same gene in the same experiment and then logged to increase the normality of distribution of the data. The results from 2 rat experiments with the same conditions were pooled. In order to reduce variation between experiments and processing involving mRNA data, mRNA expression in individual animals were normalised only to the mean mRNA expression of control animals analysed at the same time. mRNA expression was analysed

in the TA of the Sugen/hypoxia and control mouse but not in the hypoxia mouse as circulating GDF-15 was not raised in the hypoxia alone treated group.

For cell experiments between 1 and 8 repeated experiments in singlicate to quadruplicate were included for analysis. The n's used in each experiment are included in the appropriate figure in the results section. Student's t-test, Mann Whitney U test, one way or repeated measures ANOVA with Bonferroni or Kruskall-Wallace with Dunn's correction were used. Where none of the above analyses were possible due to lack of variability in the control samples a one sample t-test or a Wilcoxon signed rank test was used. mRNA data was analysed similarly to that described above with the data from each experiment normalised to mean control data from that experiment and then log transformed to increase the normality of the data set. Luciferase data for each individual condition was normalised to control samples for that condition in individual experiments. Western blot data was determined by normalising results of protein of interest to β-actin in cells or GAPDH in animals or the total amount of the protein of interest. Relative activity or amount of protein was compared to control value in the same experiment and repeats were analysed. Myotube diameter data is presented as raw data and relative change in diameter across individual experiments.

For MCT TAK1 experiments ANOVA with Bonferroni or Kruskall Wallace with Dunn's was used. Rats who continued to grow were defined as those who reached their maximum weight on the last day of treatment without plateauing. Fisher's exact test was used to compare the proportion of rats still growing in the MCT and MCT TAK1i groups. Differences in TA atrogin-1 mRNA expression and circulating GDF-15 levels between those growing and not growing in the group overall and in the MCT and MCT TAK1i groups were analysed by Student's t test and Mann-Whitney U test. Correlations and ROC curves were performed and constructed as detailed above and mRNA and protein data analysis was handled as above. In the MCT TAK1 experiments fibre diameter was assessed as an average across each group and as a curve showing proportions of cells below cumulative 5 micron cut-offs, which were then assessed using ANOVA (410).

Chapter 3 Clinical outcomes pertaining to muscle wasting and physical activity in PAH

3.1 Background

Skeletal muscle dysfunction is emerging as an important complication in patients with PAH. Respiratory (154, 159) and peripheral muscle dysfunction (160, 161, 412) have been described in these patients, both of which have been associated with markers of prognosis, the 6MWD, and the cardio-pulmonary exercise test measured maximal oxygen uptake (159-161). Interestingly there was no direct association between muscle strength or size and haemodynamic parameters, in this group (160, 161).

Further indirect evidence of the importance of a peripheral muscle myopathy in PAH comes from studies looking at the effects of pulmonary rehabilitation. A number of studies have now shown that, contrary to previous thinking, rehabilitation was safe and effective in patients with PAH (164, 167, 172). Various forms of exercise programs have been able to improve QOL, functional status, peak oxygen consumption, muscle strength, size and oxidative capacity and 6MWD by between 0 and 110m, without changing haemodynamic parameters (164, 167, 172).

Physical inactivity in chronic cardio-respiratory disease is conceptually both a cause and effect of muscle wasting and contributes to the vicious cycle of disease progression (75). Physical activity has been infrequently measured in PAH but is emerging as both a target for intervention and an outcome measure in this group of patients. The latest European Society of Cardiology (ESC) / European Respiratory Society (ERS) guidelines have suggested that patients with PAH should be encouraged to remain as active as possible within symptom limits and that supervised rehabilitation is beneficial in terms of both exercise capacity and QOL (16). A small number of studies have shown that physical activity is reduced in patients with PAH when compared to healthy controls (173, 174, 176, 413). Furthermore, physical activity has been correlated with important prognostic markers, the 6MWD (173, 414) and WHO functional class (174, 415), as well as with QOL (413).

The association of muscle strength and physical activity have not been investigated together in a population of patients with PAH, and the effects of muscle strength and physical activity on outcomes like hospitalisation and mortality have not been directly measured. Furthermore the optimal way to practically measure physical activity in patients with PAH has not been investigated.

There are a number of ways in which physical activity can be quantified, each having its own advantages and disadvantages (177). The gold standards are calorimetry or double-labelled water, which are highly accurate but are time consuming, expensive and somewhat invasive (416). Accelerometers are considered accurate at measuring physical activity on an individual basis. They are able to pick up different modes of movement, not just walking, but they are expensive and must be worn over a number of days to collect accurate information, which may decrease patient compliance (417). One widely used accelerometer is the SWA. Its ability to measure physical activity has been validated in healthy individuals (376), in arthritis (418) and in COPD (419). It has been previously used to study physical activity in patients with PAH (173). Lastly physical activity questionnaires are quick to administer, cheap and non-invasive but they can be inaccurate, with over or under-estimation being reported (420). Indeed, we have previously noted the inaccuracy of a number of self-reported activity questionnaires when compared to objective activity monitors in patients with COPD (383).

Disease specific and general QOL questionnaires have been utilised to investigate interventions in PAH (387, 389, 413). Two of these questionnaires, the CAMPHOR, and the SGRQ, as well as generating data on overall QOL, allow investigators to calculate activity scores (385, 389). These activity scores have not been compared to objectively measured values of physical activity in patients with PAH.

3.2 Aims

To measure the associations of muscle strength and size and physical activity in a well characterised group of patients with PAH.

To determine the effects of muscle strength and size and physical activity on outcomes such as hospitalisation and mortality in patients with PAH

To investigate the association of physical outcome measures from QOL questionnaires with objectively measured physical activity.

3.3 Hypotheses

Muscle function and size and physical activity will correlate with prognostic markers, but not haemodynamic parameters and with outcomes such as mortality and hospitalisation in patients with PAH.

Physical activity scores will correlate only modestly, if at all, with objectively measured physical activity in patients with PAH.

3.4 Methods

For a full explanation of the methods please see Chapter 2 of this thesis

3.4.1 Participants

Thirty-three eligible patients over 16 years old with WHO class I-III PAH from the pulmonary hypertension clinic at the Royal Brompton hospital, were included in the study. Patients were excluded if they had other significant cardio-respiratory disease, a metabolic disorder or neurological condition, which would significantly affect their physical activity. The study was approved by the NRES ethics committee and all patients provided written informed consent.

3.4.2 Baseline measurements

All baseline measurements were undertaken at a single visit. Participants had their height, weight and BMI measured. They had their WHO functional status assessed, as well as undergoing a 6MWD (397), echocardiogram, C-reactive protein and BNP measurement. FFMI (370), QMVC (374) and $USRF_{CSA}$ were measured (28). Patients filled in the SGRQ (385) and CAMPHOR (389) questionnaires to document

QOL and activity scores. They were then provided with the SWA and wore it over the triceps of their right arm for 7 days after which it was delivered back to the researcher (376). At the time of the assessment the researcher and participant was blinded to the activity score of the QOL questionnaires, which was only calculated later.

3.4.3 Physical activity outcomes

The SWA was worn at all times for 7 days except when there was a risk of getting the armband wet. Analysis of the physical activity data was performed as previously described (378). Outputs from the SWA included in the analysis were: the physical activity level (PAL) (total energy expenditure per minute / basal metabolic rate), which gives a global assessment of physical activity (379); time spent in at least moderate physical activity defined as 3 metabolic equivalents (3.0 METs) (383) and steps per day. Data for physical activity level (PAL), time spent in greater than 3.0 metabolic equivalents and active energy expenditure was excluded from analysis if the SWA was worn for less than an average of 22.5 hours per day for 5 days including at least one weekend day as described by Watz *et al*. (378). Steps per day were excluded if the patient wore the armband for fewer than 8 hours for 4 days as has been previously described (380). For assessment of activity, low activity was defined as a PAL < 1.4 which has previously used to define extremely inactive individuals (382, 383). Active individuals were defined as those achieving 30 minutes of at least moderate activity (> 3.0 METs) as per current recommendations (384). The SGRQ and CAMPHOR total QOL and activity scores are expressed as arbitrary units with higher scores indicating lower QOL and lower levels of physical activity (385, 389).

3.4.4 Follow up period and measurements

Patients were followed up for at least 2 years after their initial assessment. They had their demographics, 6MWD, echocardiogram, BNP, functional status and QOL measured. QOL was measured by the Emphasis 10 questionnaire (391) at approximately 6 monthly intervals after their initial assessment. Average QOL score between 1 and 2.5 years was calculated. Transplant-free survival and overnight hospital admissions throughout the follow up period were documented.

3.4.5 Data Analysis

Statistics were performed using Graphpad prism version 5 (Graphpad, CA, USA) or SPSS version 24 (IBM, Portsmouth, UK). Demographic data is expressed as mean and standard deviation or median and inter-quartile range depending on whether the data was normally distributed; normal distribution was assessed using the Kolmogorov-Smirnov test and visually using histograms. Student's t-test or Mann Whitney U tests were used to compare experiments with 2 groups and ANOVA with Bonferroni correction or Kruskall-Wallace with Dunn's correction used to compare more than 2 groups. Pearson's or Spearman's test was used to assess correlations between scores. Survival curves were constructed to analyse the effect of muscle parameters and physical activity measures on transplant free survival and differences were analysed using the log-rank Mantel-Cox test. Data was censured on the day the final participant completed 2 years of follow up. Linear regression was used to determine the independent associations of various measured parameters with outcomes 6MWD and QOL. Receiver operator characteristic (ROC) curves and area under the curves (AUC) were used to assess the ability of the measured variables to predict outcomes including mortality, hospital admission and SWA measured physical activity.

3.5 Results

3.5.1 Demographics and compliance

The demographics with n numbers for the patients recruited to the study are shown in table 3.1. Measures of muscle function, size, physical activity and QOL and number of data points are included in Table 3.2. Follow up data is detailed in table 3.3.

Age	46.6 ± 13.6 years	n = 33
Sex		n = 33
Male	10	
Female	23	
Cause		n = 33
IPAH	25	
CHD	8	
BMI	25.2 (21.7 - 29.2) kg/m^2	n = 33
WHO		n =33
I	3	
II	20	
III	10	
6MWD	367.8 ± 131.4 m	n = 32
BNP	134.0 (53.5 - 278.0) pmol/L	n = 33
Echo		
RVSP	86.3 ± 26.9 mmHg	n = 26
TR velocity	409.6 ± 80.5 cm/s	n = 25
PAcT	83.8 ± 26.5 msec	n = 27
TAPSE	1.9 (1.5 - 2.1) cm	n = 32
CRP	3 (1 - 6) mg/L	n = 31

Table 3.1. Demographics. Demographic details of 33 eligible patients with pulmonary arterial hypertension enrolled in the study. Idiopathic pulmonary arterial hypertension (IPAH), Congential heart disease (CHD), World health organisation functional status (WHO), Right ventricular systolic pressure (RVSP) measured by echocardiogram (echo), tricuspid anterior posterior systolic excursion (TAPSE), tricuspid regurgitant (TR) velocity, pulmonary artery acceleration time (PAcT), Six minute walk distance (6MWD), plasma brain natriuretic peptide (BNP).

FFMI	17.1 ± 2.8 kg/m^2	n = 30
QMVC/BMI	1.30 ± 0.36	n = 30
USRF$_{CSA}$	481 ± 133 mm^2	n = 30
SWA		
Steps per day	5616 ± 3286	n = 30
AEE	243.5 (84.5 - 444.0) kcal	n = 26
Time in > 3.0 METs	49.0 (18.8 - 88.5) mins	n = 26
PAL	1.42 ± 0.19	n = 26
SGRQ		
Activity	63.8 ± 24.6	n = 31
Total	44.8 ± 19.6	n = 31
CAMPHOR		
Activity	9.62 ± 5.70	n = 29
Total	27.71 ± 13.72	n = 28

Table 3.2. Muscle bulk, physical activity and quality of life. Muscle bulk strength and size, physical activity and quality of life patients with pulmonary arterial hypertension Fat free mass index (FFMI) Quadriceps maximal volitional capacity / Body mass index (QMVC/BMI) Rectus femoris cross sectional area measured by ultrasound (USRF$_{CSA}$) Sensewear armband (SWA) Active energy expenditure (AEE). Metabolic equivalents (METs) St George's respiratory questionnaire (SGRQ).

Follow up		n = 31
Alive no transplant	25	
Alive with transplant	1	
Dead	5	
Dead after transplant	2	
Admission		n =31
Yes	16	
No	15	
Follow up QOL		
Emphasis 10	24.0 (16.8 - 35.0)	n = 29

Table 3.3. Follow up data. Follow up data in 31 patients with pulmonary arterial hypertension studied.

3.5.2 Muscle mass, strength and size and physical activity across WHO functional groups in patients with PAH

FFMI was not different between WHO functional classes, however quadriceps strength and size was significantly lower in patients in WHO class III than in class I or II (Figure 3.1 A, B and C). All measurements of physical activity including: steps per day; active energy expenditure; time spent in > 3.0 metabolic equivalents; and physical activity level were lower in patients in WHO functional class III than in class I / II (Figure 3.2 A-D).

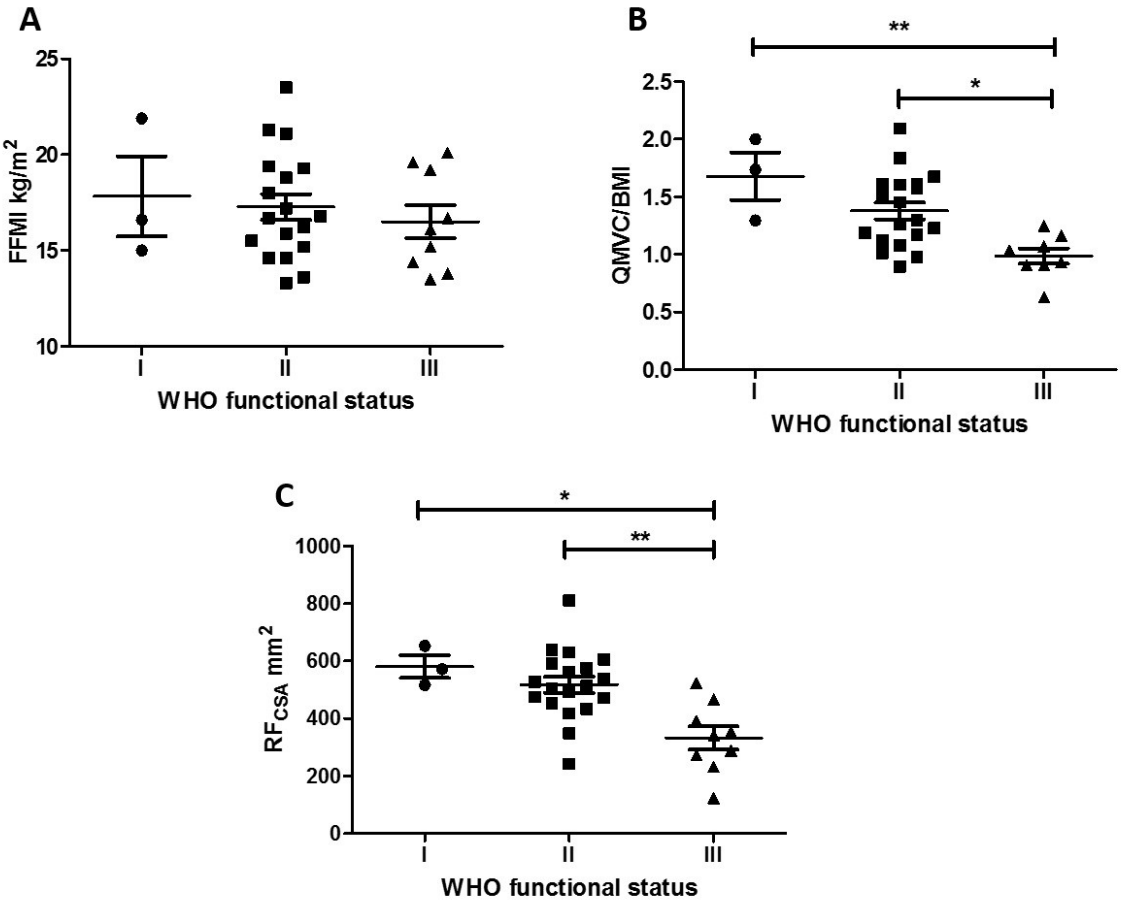

Figure 3.1 Muscle measurements across functional class. A. Fat free mass index (FFMI) across WHO functional class in patients with PAH (ANOVA p = 0.719) (WHO I n = 3, WHO II n = 18, WHO III n = 9). **B.** Quadriceps maximal volitional capacity normalised to Body mass index (QMVC/BMI) across WHO functional class in patients with PAH (ANOVA p = 0.002. (WHO I n = 3, WHO II n = 18, WHO III n = 9) **C.** Ultrasound measured rectus femoris cross sectional area (RF_{CSA}) across WHO functional class in patients with PAH (ANOVA p = 0.001) (WHO I n = 3, WHO II n = 18, WHO III n = 9).

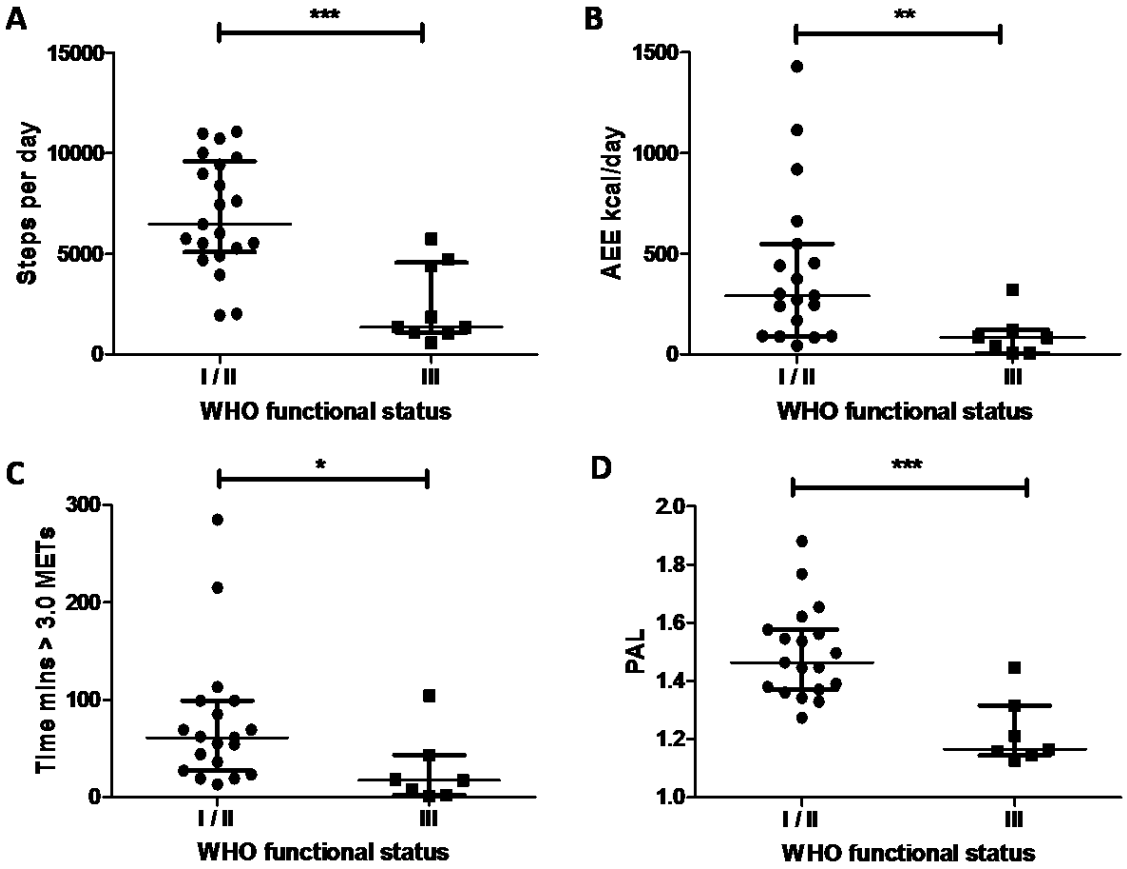

Figure 3.2 Physical activity across functional class. A. Steps per day across WHO functional class in patients with PAH (Mann Whitney U test p < 0.001, WHO class I/II n = 21, WHO class III n = 9). **B.** Active energy expenditure (AEE) across WHO functional class in patients with PAH (Mann Whitney U test p = 0.023, WHO class I/II n = 17, WHO class III n = 9). **C.** Time spent in activity of greater than 3.0 metabolic equivalents (METs) across WHO functional class in patients with PAH (Mann Whitney U test p = 0.015, WHO class I/II n = 17, WHO class III n = 9). **D.** Physical activity level (PAL) across WHO functional class in patients with PAH (Mann Whitney U test p = 0.001, WHO class I/II n = 17, WHO class III n = 9).

3.5.3 Correlations of muscle strength and size and physical activity in patients with PAH

In the cohort of PAH patients studied, 6MWD was associated with QMVC/BMI, $USRF_{CSA}$, PAL and BNP (Figure 3.3 A-D). No echocardiographic marker measured correlated significantly with 6MWD, however CRP did correlate non-linearly with 6MWD (Figure 3.3 E). A linear regression model using age, BMI, RFCSA, PAL, BNP (< 100) and CRP (<10) had an adjusted R^2 value of 0.37 in predicting 6MWD in patients with PAH with a p value of 0.031, suggesting that 37 percent of the variance in 6MWD was

explained by the model. The only independent variable making a significant unique contribution to the 6MWD was $USRF_{CSA}$, which had a β co-efficient of 0.72 ($p = 0.003$).

QOL measured by the SGRQ also correlated significantly with QMVC/BMI, $USRF_{CSA}$, PAL, and CRP (Figure 3.4 A-D) but failed to associate with any echocardiographic marker of disease severity or with BNP. Using the same inputs in a linear regression model, as above, the adjusted R^2 was 0.59 ($p = 0.002$) meaning 59% of the variance in SGRQ score was accounted for by the model. The only independent association of the SGRQ was again $USRF_{CSA}$ with a β co-efficient -0.82 and p value < 0.001.

QOL measured by the CAMPHOR also correlated significantly with Quads CSA, PAL and CRP but not with muscle strength, BNP or echocardiographic parameters (Figure 3.5 A-C).

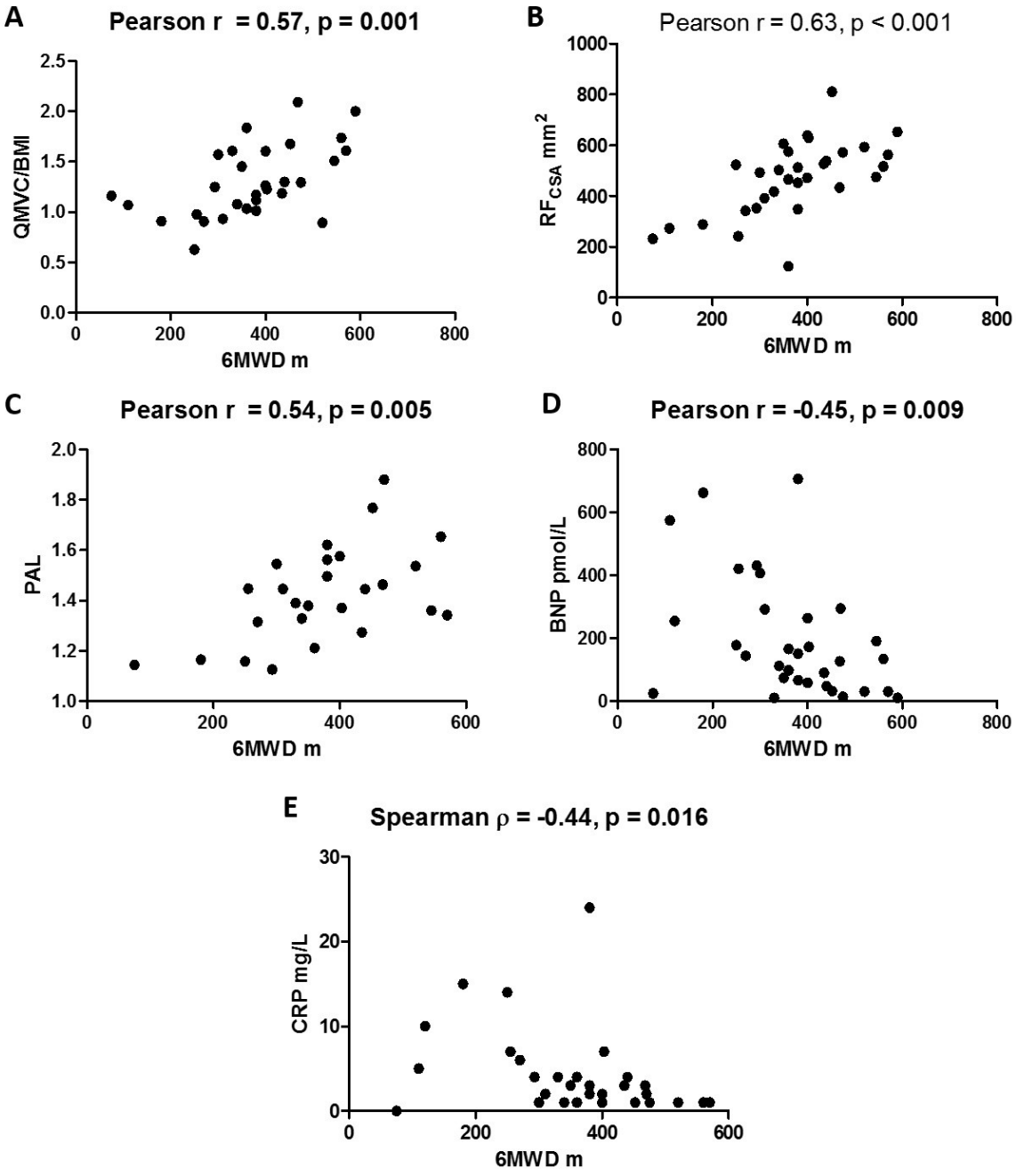

Figure 3.3 Correlations of six minute walk distance (6MWD). A. Quadriceps maximal volitional capacity / Body mass index (QMVC/BMI) plotted against 6MWD in patients with PAH (n=30). **B.** Ultrasound measured rectus femoris cross sectional area (RF_{CSA}) plotted against 6MWD in patients with PAH (n=30). **C.** Physical activity level (PAL) plotted against 6MWD in patients with PAH (n=26). **D.** Brain natriuretic peptide (BNP) plotted against 6MWD in patients with PAH (n=32). **E.** C-reactive protein plotted against 6MWD in patients with PAH (n=30).

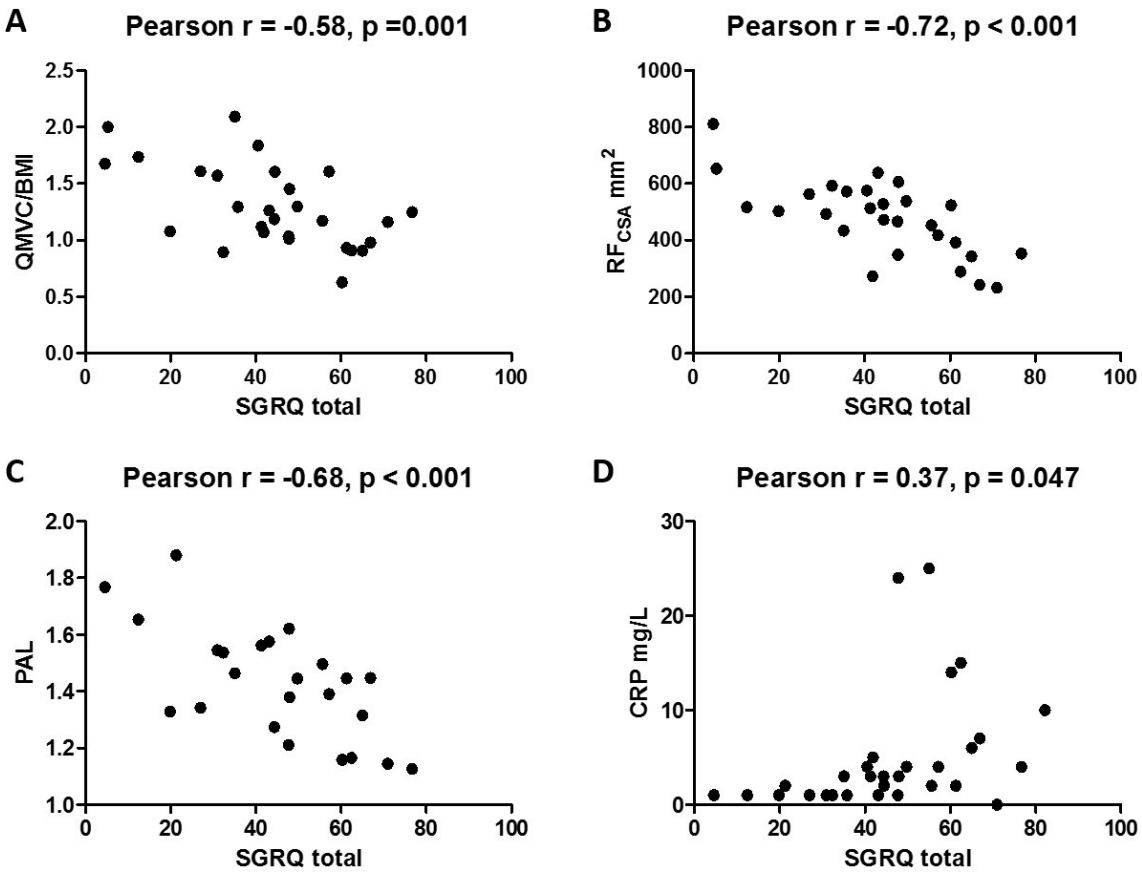

Figure 3.4 Correlations of St. George's respiratory questionnaire (SGRQ) quality of life. A. Quadriceps maximal volitional capacity / Body mass index (QMVC/BMI) plotted against total St. George's Respiratory questionnaire (SGRQ) score.in patients with PAH (n = 28). **B.** Ultrasound measured rectus femoris cross sectional area (RF_{CSA}) plotted against total SGRQ in patients with PAH (n = 28). **C.** Physical activity level (PAL) plotted against total SGRQ score in patients with PAH (n = 24). **D.** C-reactive protein (CRP) plotted against total SGRQ score in patients with PAH (n = 30).

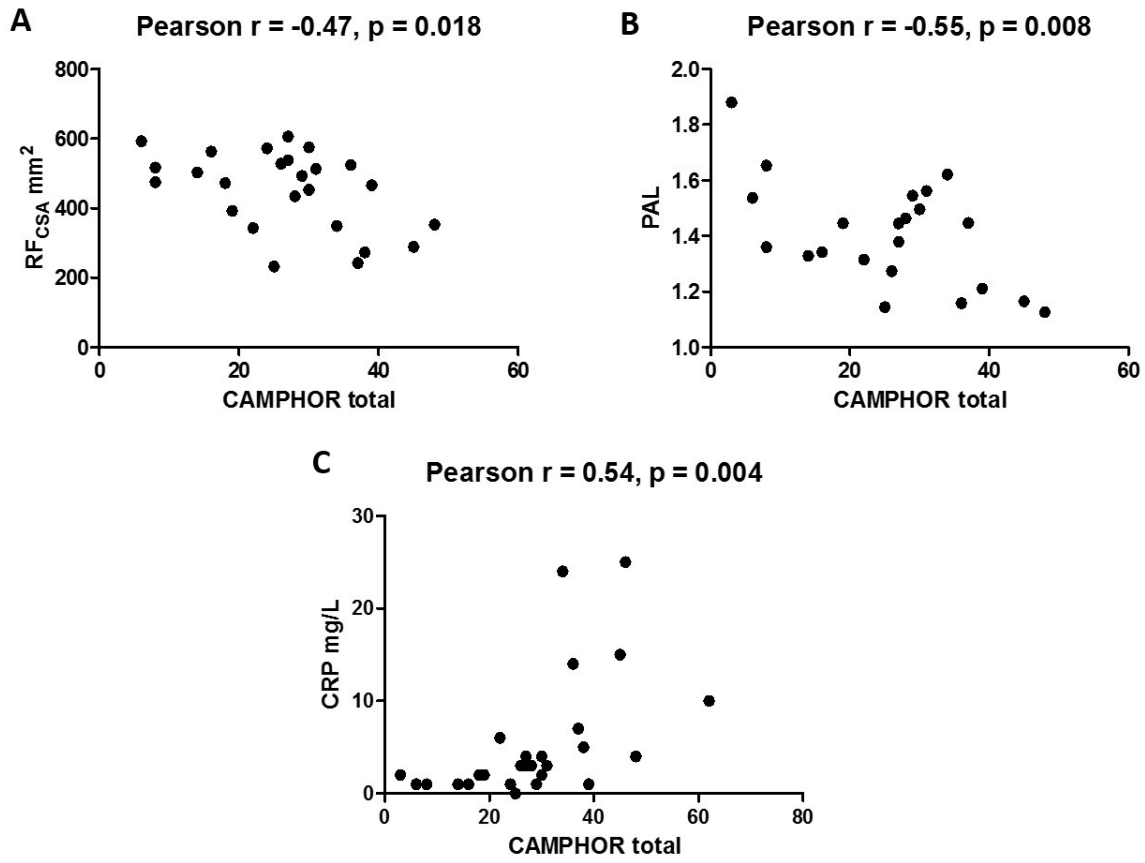

Figure 3.5 Correlations of CAMPHOR quality of life. A. Ultrasound measured rectus femoris cross sectional area (RF_{CSA}) plotted against total CAMPHOR score in patients with PAH (n=25). **B.** Physical activity level (PAL) plotted against total CAMPHOR score in patients with PAH (n=22). **C.** C-reactive protein (CRP) plotted against total CAMPHOR score in patients with PAH (n=27).

3.5.4 Association of muscle size, strength and cardiovascular markers with physical activity in PAH

Time spent in greater than 3.0 METs correlated with QMVC/BMI and RF_{CSA} (Figure 3.6 A and B), whilst PAL correlated only with RF_{CSA} (Figure 3.6 C). None of the measures of physical activity correlated with BNP or echocardiographic parameters.

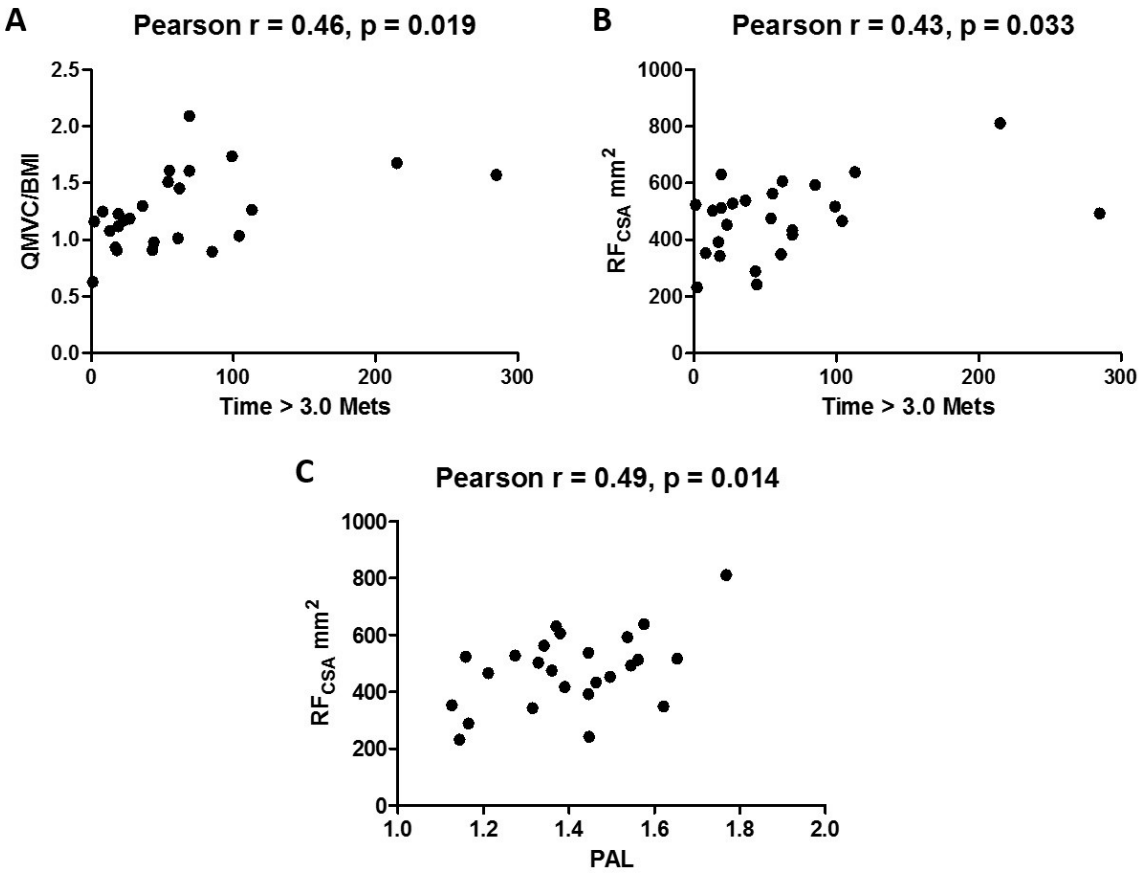

Figure 3.6 Correlations of physical activity and muscle parameters. A. QMVC/BMI plotted against SWA measured time in > 3.0 metabolic equivalents (METs)) (n = 25). **B.** Ultrasound measured rectus femoris cross sectional area (RFCSA) plotted against SWA measured time in > 3.0 METs (n=25). **C.** RFCSA plotted against SWA measured physical activity level in patients with PAH (n=25).

3.5.5 Muscle bulk and physical activity predict mortality in patients with PAH

Transplant-free survival curves for those patients with PAH for whom we had at least two year follow up data are shown in Figure 3.7. Comparing survival in patients with a FFMI < 14, 14-19 and > 19

demonstrated a Log-rank Mantel-Cox Test Chi squared of 6.40 (p = 0.041), whilst the log rank test for trend showed a Chi squared of 5.47 (p = 0.019) (Figure 3.7A). We also compared mortality between those patients taking < 2500 or > 2500 steps per day. In this case the Log-rank Mantel-Cox Test demonstrated a Chi squared of 11.0 (p < 0.001) (Figure 3.7B).

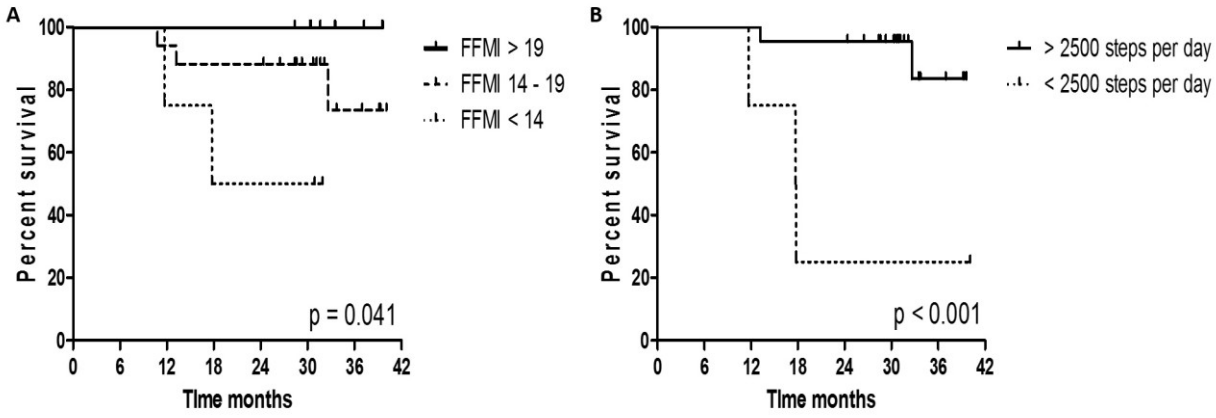

Figure 3.7 Survival in PAH by muscle bulk and activity. A. Kaplan-Meier plot showing survival in patients with pulmonary arterial hypertension and a fat free mass index (FFMI) in kg/m^2 of < 14 (n = 4), 14-19 (n = 17) and > 19 (n = 9). Log-rank Mantel-Cox Test Chi squared of 6.40 (p = 0.041). Log rank test for trend showed a Chi squared of 5.47 (p = 0.019). **B.** Kaplan-Meier plot showing survival in patients with pulmonary arterial hypertension and taking greater than (n = 22) or less than (n = 4) 2500 steps per day fat. Log-rank Mantel-Cox Test Chi squared of 11.0 (p < 0.001).

3.5.6 Muscle bulk and strength identify those patients with PAH at risk of hospital admission

As well as mortality, factors associated with overnight admission to hospital within 2 years of enrolment was examined. Age was significantly higher (p < 0.001), whilst FFMI and QMVC/BMI was significantly lower in those patients admitted to hospital in the follow up period compared to those not admitted (Figures 3.8 A and B). There was no difference in BNP, echocardiographic or physical activity parameters in those admitted and those not admitted. ROC curves were constructed for FFMI and QMVC/BMI in predicting admission over the follow up period. These are shown in Figure 3.8 C and D. Numerically, QMVC/BMI had a greater AUC compared to FFMI. The best sensitivity and specificity cut offs for each variable in predicting admission are shown in the Figures 3.8 C and D.

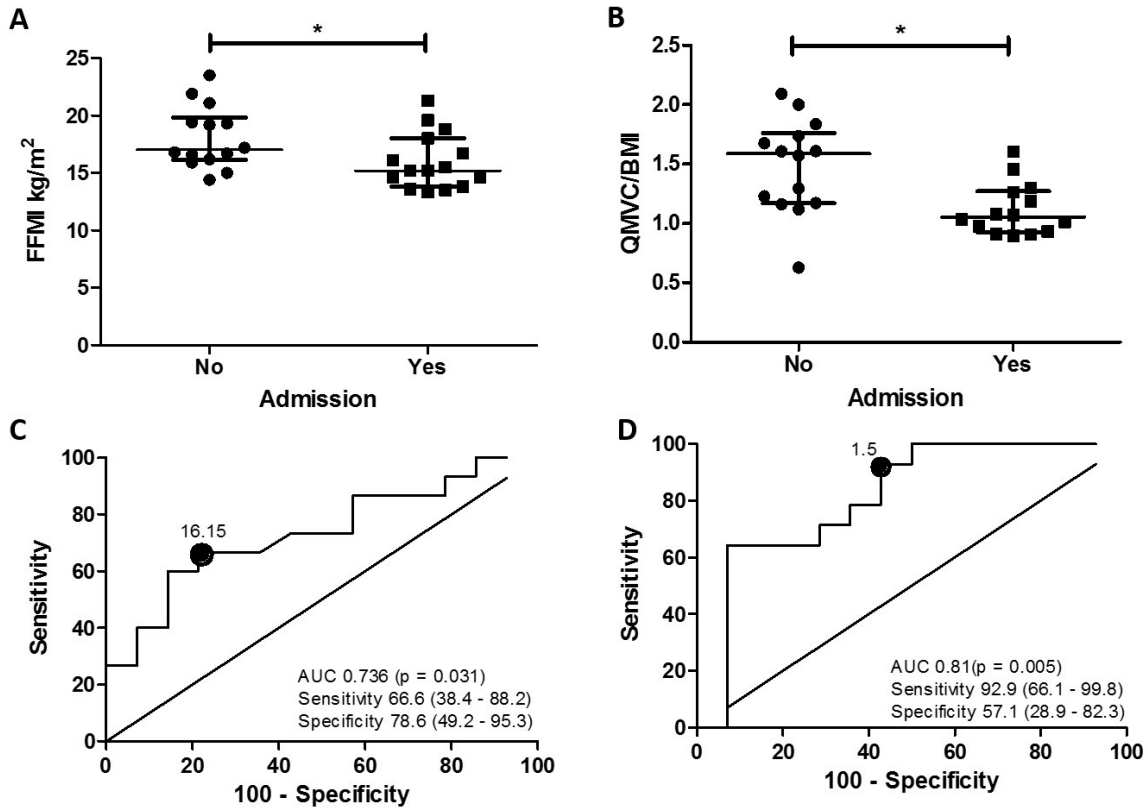

Figure 3.8 Muscle parameters predict hospitalisation in PAH A. Fat free mass index (FFMI) in those admitted (n = 15) and not admitted (n = 14) to hospital at 2 year follow up (Mann Whitney U test p = 0.037). **B.** Quadriceps maximal volitional capacity normalised to Body mass index (QMVC/BMI)) in those admitted (n = 14) and not admitted (n = 14) to hospital at 2 year follow up (Mann Whitney U test p = 0.006). **C**. Receiver operator characteristic (ROC) curve of FFMI in predicting those admitted to hospital at 2 years follow up. **D.** ROC curve of the QMVC/BMI in predicting those admitted to hospital at 2 years follow up.

3.5.7 Muscle strength and physical activity are correlated with future levels of quality of life in patients with PAH

Mean Emphasis 10 score on follow up was associated with QMVC/BMI, PAL and 6MWD and non-linearly with CRP (Figure 3.9 A - D) Neither BNP nor any echocardiographic measure correlated significantly with follow up QOL measured by EMPHASIS 10. A linear regression model including QMVC/BMI, PAL, 6MWD and CRP revealed an adjusted R^2 of 0.276, with a p of 0.042. This suggests the model accounted for 28 % the variance in follow up EMPHASIS 10 data. No one variable made a significant unique contribution to the EMPHASIS 10 score within this model.

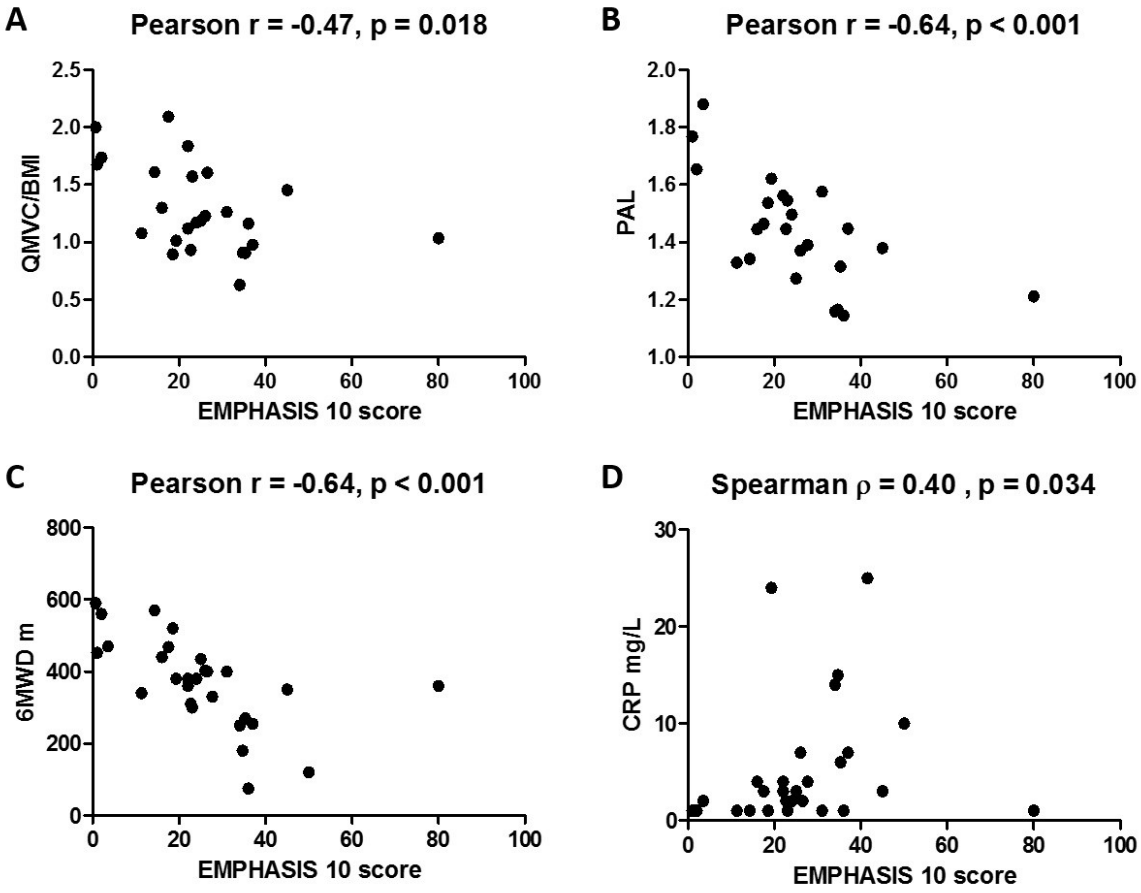

Figure 3.9 Correlates of future quality of life in PAH A. Quadriceps maximal volitional capacity / Body mass index (QMVC/BMI) plotted against average follow up EMPHASIS 10 score in patients with PAH (n=25). **B.** Sensewear armband measured physical activity level (PAL) plotted against average follow up EMPHASIS 10 score in patients with PAH (n=24) **C.** Six minute walk distance (6MWD) plotted against average follow up EMPHASIS 10 score in patients with PAH (n=28). **D.** C-reactive protein (CRP) plotted against average follow up EMPHASIS 10 score in patients with PAH (n=28).

3.5.8 Activity scores from QOL questionnaires can predict those patients with low physical activity in the context of PAH.

SGRQ measured activity levels correlated negatively with SWA derived steps per day, PAL and time spent in activity of > 3.0 METs (Figure 3.10 A, B and C). The CAMPHOR derived activity scores also correlated negatively and significantly with SWA steps per day, PAL and time spent in activity of > 3.0 METs (Figure 3.10 D, E and F).

ROC curves for the SGRQ activity, CAMPHOR activities and 6MWD in predicting patients who took < 2500 steps per day, are shown in Figure 3.11 A - C. The SGRQ activity score ROC curve AUC of 0.95, was numerically but not statistically better than the CAMPHOR and 6MWD in predicting those with a step count that I have shown to be associated with increased mortality.

Similar curves were generated for the SGRQ activity, CAMPHOR activities and 6MWD in predicting low physical activity, defined as a PAL < 1.4. These ROC curves and are shown in Figure 3.12 A - C. Again the SGRQ activity score performed best in predicting those with a PAL < 1.4 with an AUC of 0.78 ($p = 0.019$) when compared numerically to the CAMPHOR activities score and 6MWD.

ROC curves were also generated for the SGRQ activity, CAMPHOR activities and 6MWD in predicting those patients achieving the recommended amount of physical activity per week (30 minutes per day at > 3.0 METs). These ROC curves are shown in Figure 3.13 A - C. In this case neither SGRQ nor CAMPHOR activity scores, which had AUCs of 0.68 ($p = 0.116$) and 0.74 ($p = 0.062$) respectively, were numerically or statistically better than the 6MWD in predicting active individuals which had an AUC of 0.74 ($p = 0.040$).

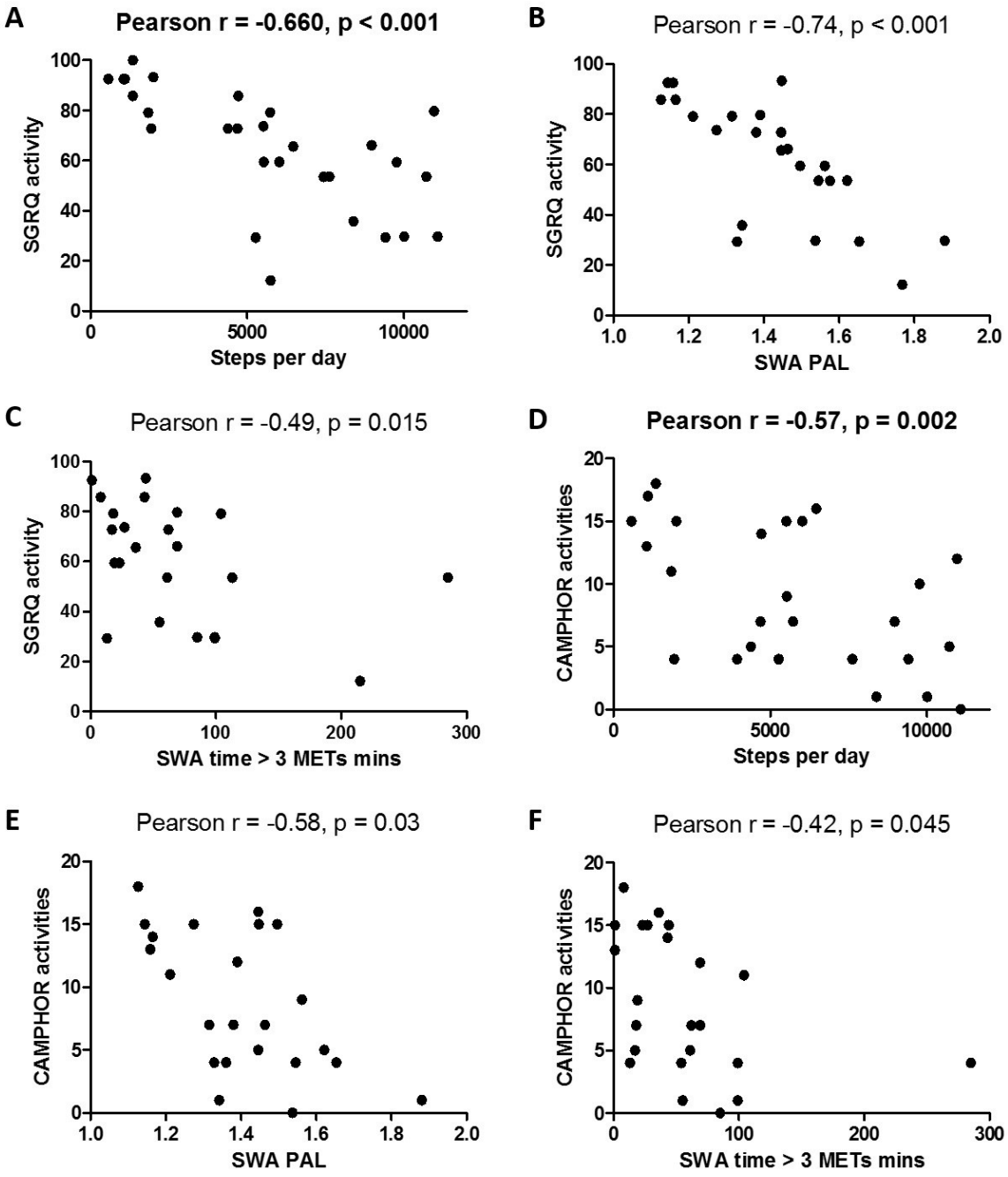

Figure 3.10. **SGRQ and CAMPHOR activity scores correlate with objectively measured physical activity**. Correlations of SGRQ activity score with: **A.** SWA measured steps per day (n = 28); **B.** SWA physical activity level (PAL – total daily energy expenditure / Basal metabolic rate) (n = 24); **C.** SWA measured time spent in greater than 3.0 metabolic equivalents (METs) (n = 24). Correlations of CAMPHOR activities score with: **D.** SWA measured steps per day (n = 27); **E.** SWA physical activity level (n = 23); **F.** SWA measured time spent in greater than 3.0 metabolic equivalents (METs) (n = 23).

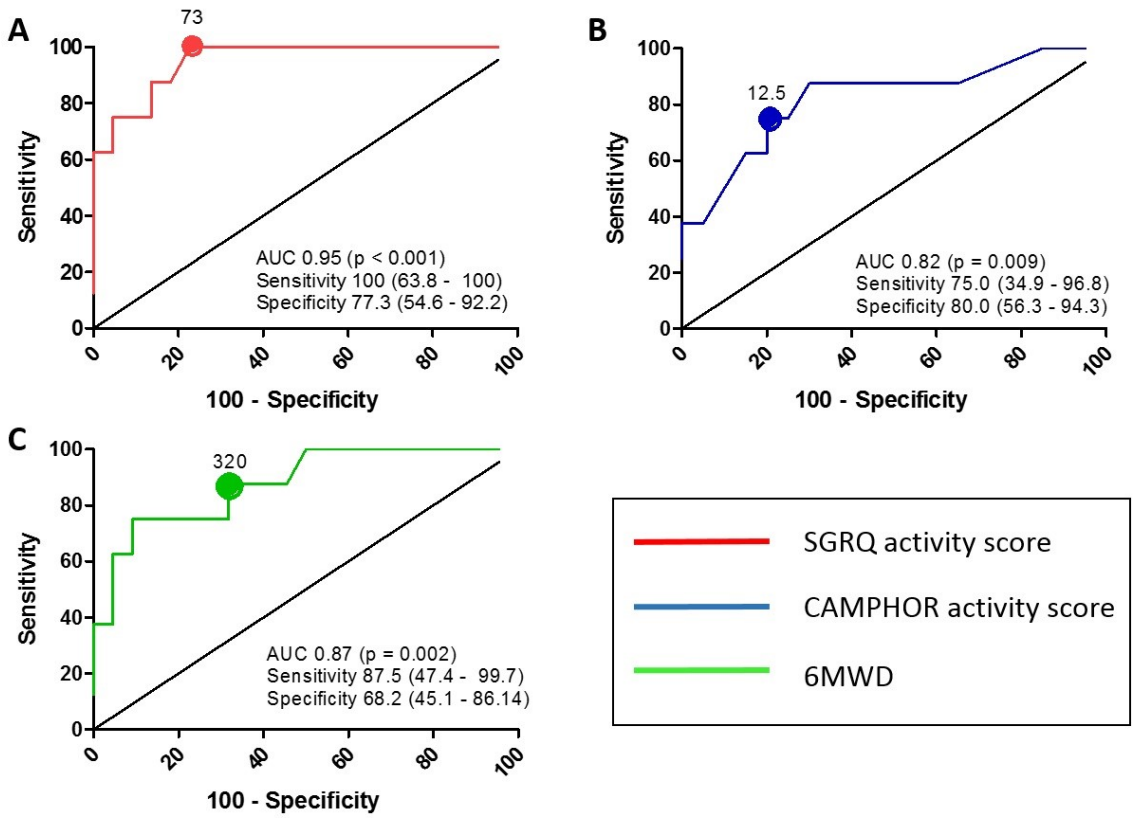

Figure 3.11 ROC curves of activity scores from the SGRQ, CAMPHOR and 6MWD in predicting low step count. **A.** Receiver operator characteristic (ROC) curve of the St. George's respiratory questionnaire (SGRQ) activity score in predicting those with low physical activity defined as <2500 steps per day (n = 28). **B.** ROC curve of the CAMPHOR questionnaire activity score in predicting those with low physical activity defined as <2500 steps per day (n = 27) **C.** ROC curve of the six minute walk distance (6MWD) in predicting those with low levels of physical activity defined as <2500 steps per day (n = 30).

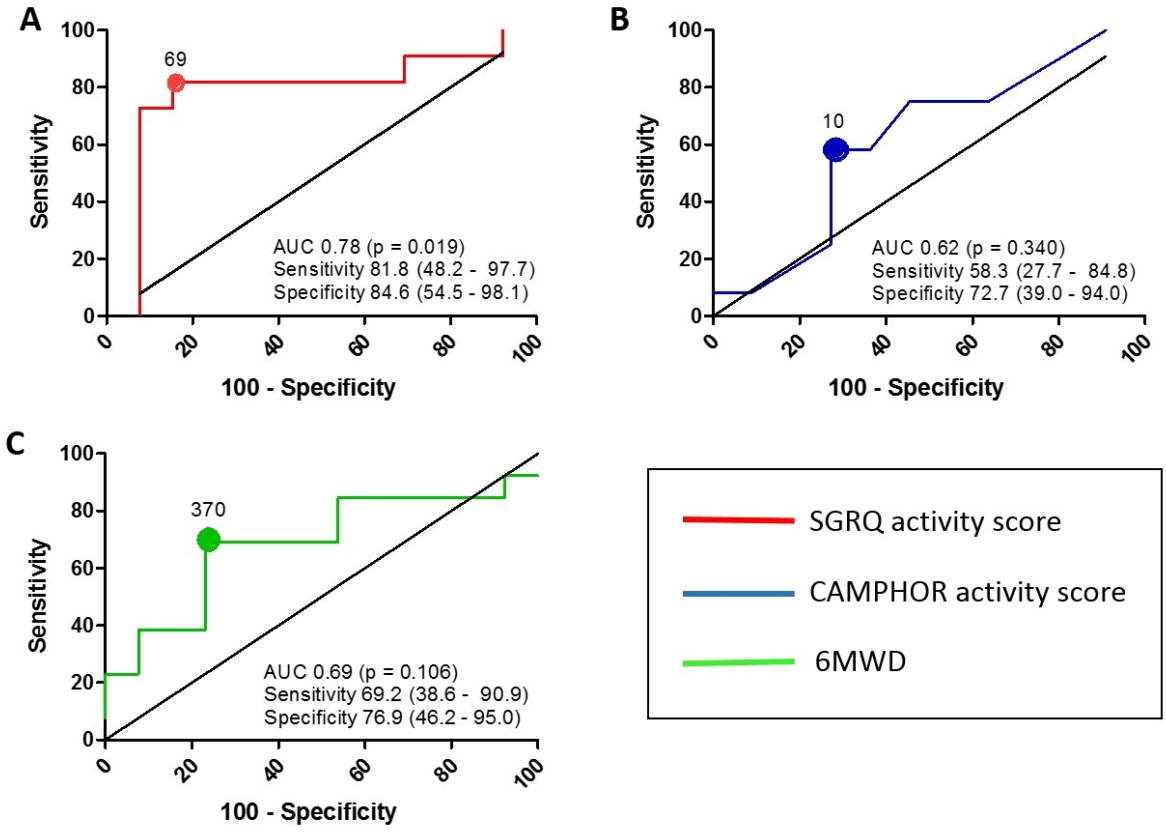

Figure 3.12 ROC curves of activity scores from the SGRQ, CAMPHOR and 6MWD in predicting low PAL A. ROC curve of the St. George's respiratory questionnaire (SGRQ) activity score in predicting those with low physical activity defined as a physical activity level (PAL) < 1.4 (n = 24)**. B.** ROC curve of the CAMPHOR questionnaire activity score in predicting those with low physical activity defined as a physical activity level (PAL) < 1.4 (n = 23). **C.** ROC curve of the six minute walk distance (6MWD) in predicting those with low levels of physical activity defined as a physical activity level (PAL) < 1.4 (n = 26).

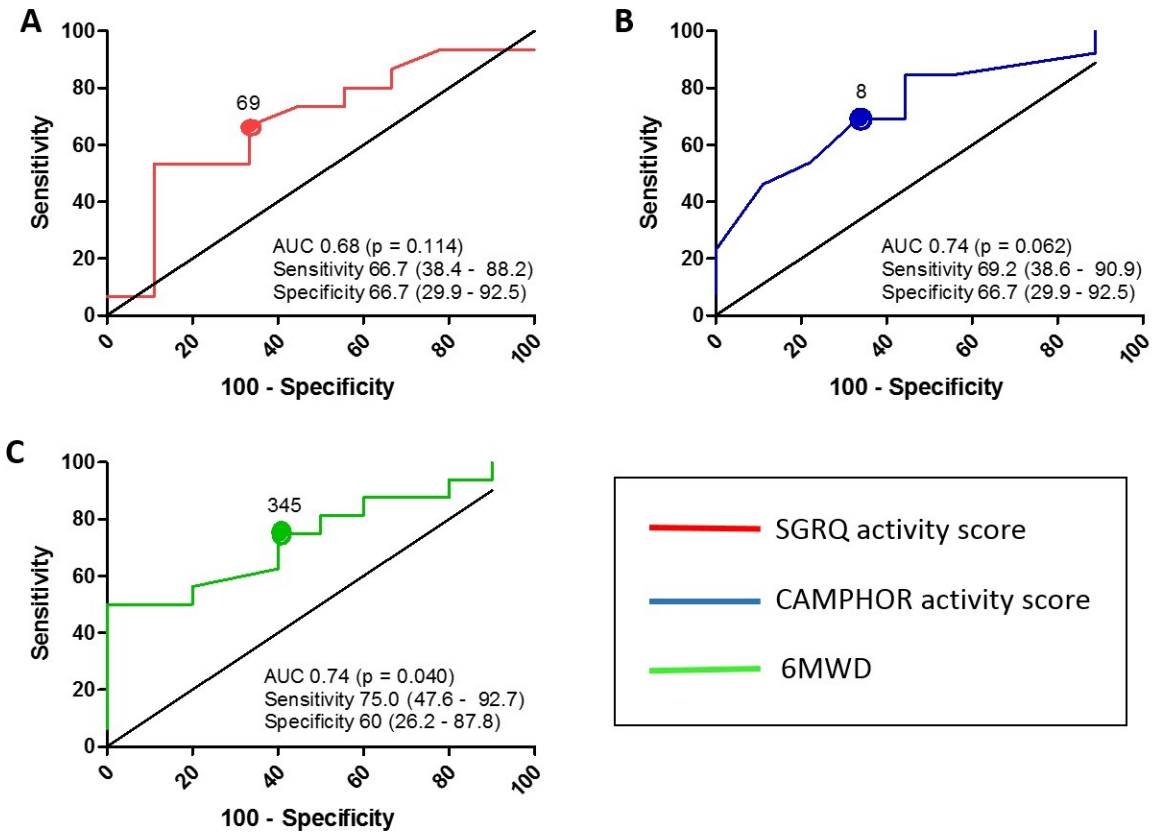

Figure 3.13 ROC curve of activity scores from the SGRQ, CAMPHOR and 6MWD in predicting active individuals

A. ROC curve of the St. George's respiratory questionnaire (SGRQ) activity score in predicting those achieving the recommended amount of physical activity defined as those spending at least 30 minutes in greater than 3.0 metabolic equivalents (METs) (n = 24). **B.** ROC curve of the CAMPHOR questionnaire activity score in predicting those achieving the recommended amount of physical activity defined as those spending at least 30 minutes in greater than 3.0 METs (n = 23). **C.** ROC curve of the six minute walk distance (6MWD) in predicting those achieving the recommended amount of physical activity defined as those spending at least 30 minutes in greater than 3.0 METs (n = 26).

Finally we have also shown that SGRQ activity score of > 70 can predict mortality in patients with PAH. The log-rank Mantel-Cox test chi squared was 5.60 (p = 0.018) (Figure 3.14 A). Furthermore a SGRQ activity score of > 69.5 was able to predict 2 year mortality / transplant with a sensitivity of 88% and a specificity of 63% (Figure 3.14 B).

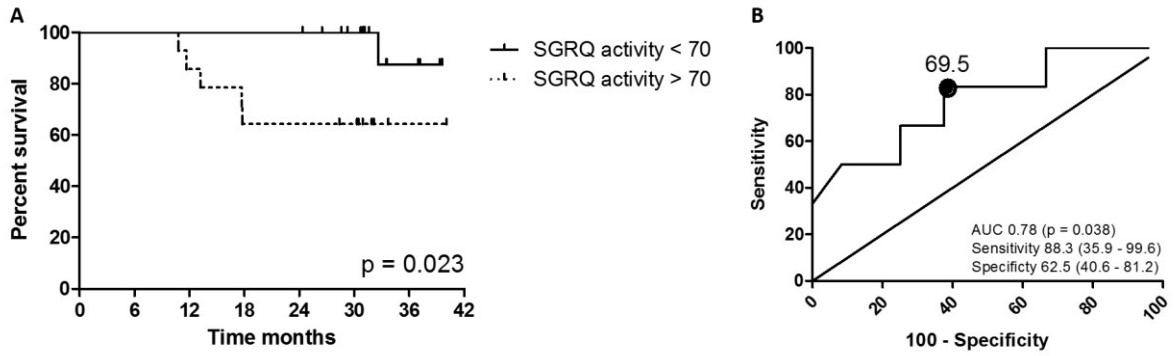

Figure 3.14 Kaplan-Meier and ROC curve predicting survival in patients based on SGRQ activity scores. A. measured by the SGRQ. Kaplan-Meier plot showing survival in patients with pulmonary arterial hypertension and a St George's respiratory questionnaire activity score of < (n = 16) or > (n = 14) 70. Log-rank Mantel-Cox Test Chi squared of 5.15 (p = 0.023 (n =30). **B.** Receiver operator characteristic (ROC) curve of the St. George's respiratory questionnaire (SGRQ) activity score in predicting 2 year mortality on patients with PAH (n = 30).

3.6 Discussion

The results documented above highlight the importance of both skeletal muscle and physical activity in patients with PAH. Skeletal muscle and physical activity parameters are associated with known markers of prognosis, the 6MWD and WHO functional status, current and future QOL; hospital admission; and mortality. The data also shows that the SGRQ activity score is a reasonable surrogate of more objectively measured physical activity, and is associated with mortality at 2 years.

We have shown that muscle strength and size and physical activity is lower in PAH patients with worse functional status. Objectively measured physical activity also was significantly lower in patients at higher WHO functional class. This is in keeping with the work from Mainguy *et al.* who demonstrated similar findings using the same activity monitor (173). The data also demonstrates that one of the most important markers of prognosis in patients with PAH, the 6MWD (421), is associated with muscle strength and size and with physical activity. This is in keeping with data published by other groups (160, 173). There was also an association of 6MWD and CRP and BNP, but no association with echocardiographic parameters, confirming the findings of other studies (160, 161). Using a linear regression analysis the only independent association with 6MWD in this group was the $USRF_{CSA}$. This

suggests that muscle size rather than the other variables included in this analysis, including age, BMI, PAL, CRP and BNP might influence 6MWD independently. QOL has been associated with physical activity (422) but not directly with muscle strength in patients with PAH. I found that lower QOL was associated with muscle strength, muscle size, CRP and PAL but not with markers of cardiovascular function as measured by BNP or echocardiographic parameters. Using the same inputs for linear regression, again, only the $USRF_{CSA}$ was independently associated with SGRQ measured QOL. Taken together this suggests that muscle size is an important factor that might influence outcomes in patients with PAH. This data is supported by studies showing that rehabilitation improves 6MWT, quadriceps function but not cardiovascular parameters in patients with PAH (164, 171, 172).

Muscle wasting and low physical activity have been linked to mortality in COPD (34, 423-425) and heart disease (425-427), but not previously in PAH. For the first time, as far as I am aware, I have shown that patients with PAH with lower FFMI and step counts have an increased mortality at 2 years. The cut offs of FFMI and steps per day predicting higher mortality in this cohort were very low. Epidemiological studies have suggested that the 5^{th} to 95^{th} percentile of FFMI was 16.8 -21.1 in young men and 13.8-17.6 in young women (370). This suggests that an FFMI of < 14, which has been identified as predicting the highest mortality, is well below average. Tudor-Locke suggested that people taking less than 5000 steps per day lived a sedentary lifestyle, whilst 2500 steps represented basal activity (428). In our cohort it was in those patients taking less than this basal activity who exhibited higher levels of mortality at 2 years.

In our cohort only one patient who underwent transplant for PAH survived. One of the major determinants of outcomes in transplant is pre-conditioning. If these patients had higher muscle strength and physical activity prior to assessment the outcomes may have improved (429).

Hospitalisation has been identified (430) and used as an important outcome measure in patients with PAH (431). The current cost of a hospital bed in the NHS in the UK is £400 per day (432). In a recent study in PAH patients in the USA the average length of stay for a hospital admission was 15 days,

compared to an average of 11 days for other diagnoses, with higher daily costs in the PAH population. Furthermore most of those re-admitted after their initial visit for PAH had at least one other admission in the follow up period (433). This suggests that the economic cost of admission for PAH is higher than the general population and avoiding admission might deliver higher economic benefits. Furthermore it has been shown that in a large unselected cohort of patients that hospitalisation was associated with deterioration in QOL (434) ; this is also likely to be true for patients with PAH. The data presented here suggests that patients with lower muscle strength and bulk are more likely to be admitted to hospital for an overnight stay for any reason within 2 years. Both FFMI and QMVC/BMI were able to predict those admitted to hospital within 2 years with reasonable AUC of their ROC curves. A QMVC/BMI of < 1.1 was particularly specific in defining those admitted over the 2 year follow up period. We have also shown that muscle strength and physical activity, as well as 6MWD and CRP correlated significantly with average follow up QOL using the PH specific EMPHASIS 10 questionnaire. As mentioned above, studies of rehabilitation have generally shown an improvement in 6MWD, a predictor of prognosis (421), through an improvement in muscle strength and without a change in cardiovascular function (18). This suggests that interventions aimed at altering muscle strength, size or bulk and physical activity may result in improved mortality, reduced hospital admission and improved QOL in patients with PAH.

Rehabilitation already has a theoretical if not an established practical role in the treatment of patients with PAH (18, 164, 171, 172). There is some emerging evidence of the mortality benefits of rehabilitation in a wide range of conditions as well as in a geriatric population (98, 435-438), and this is also likely to be true in PAH, especially given the data presented in this Chapter. This gives a rationale to support a more major role for rehabilitation in the management of pulmonary hypertension. The ideal method of rehabilitation in PAH, or for that matter in any chronic cardio-respiratory disease, has yet to be established and the method by which to transfer gains in exercise capacity into physical activity is as yet unknown, and these should be the focus of future research in this area (439).

There are a number of barriers to rehabilitation. Both low levels of baseline physical activity (440) and cachexia (441) have been associated with decrease uptake and or efficacy of rehabilitation in some studies. The data presented above suggests that it this group, who may respond less well to rehabilitation, and also have the worse prognosis, may benefit most from agents aimed at blocking muscle atrophy and promoting muscle gain. This may allow them to take part in rehabilitation and may alter their prognosis. At present international guidelines do not recommend the use of anabolic agents as adjuncts to rehabilitation (439) and there are currently no pharmacological agents aimed at improving muscle strength in chronic disease in established clinical use (442). Part of this may be due to a lack of clinical biomarkers of cachexia allowing the easy identification of patients at risk of muscle wasting. The authors of a recent review identify a number of biomarkers including GDF-15 as having potential to identify those with muscle loss (443). The issues of biomarkers and pharmacological treatment of muscle wasting in PAH are addressed in subsequent chapters of this thesis.

Our data suggests that objectively measured low physical activity is associated with increased mortality in patients with PAH. Assessment of physical activity is difficult. Screening tests which can be done quickly and cheaply are helpful in identifying those patients with low physical activity who may need more detailed assessment with expensive and time consuming activity monitors. Questionnaire based assessment is an attractive method to screen large populations for low physical activity levels (416). Our data suggests that a SGRQ physical activity score and, to a lesser extent a CAMPHOR physical activity score, can be used to determine those patients with PAH who are inactive. In addition, our data suggests that the SGRQ activity score outperforms the 6MWD in predicting inactive patients with PAH. In contrast to the above, we have found that these questionnaire generated activity scores were not as good at predicting those patients who achieved the recommended amount of moderate physical activity per day.

This study is the first to compare questionnaire-based assessment of physical activity against an objective measure in patients with PAH. Questionnaire based assessment of physical activity can be

unreliable with many researchers finding over and under-estimation. This bias may be due to patient factors including age, cultural differences and social desirability of physical activity, and questionnaire factors including length, complexity and whether it is self-report or interviewer led (444). The activity scores examined in our study were part of a wider assessment of QOL. The framing of a recall based activity assessment can have a significant influence over the results (444). Taking this into account, it may be that embedding an activity assessment in a general QOL questionnaire removes some of the bias, particularly that which relates to the social desirability of physical activity, conferring an advantage to both the SGRQ and CAMPHOR in assessing physical activity.

The SGRQ was superior to the CAMPHOR and 6MWD in predicting those patients with low physical activity based both on steps per day and PAL measured by the SWA. The SGRQ is a QOL questionnaire designed for use in in COPD although it has been used in other conditions including asthma (445). The activity component consists of 16 questions to which the subject answers yes or no (385) . Although not validated against any objective measure of activity, the activity score of the SGRQ has been shown to correlate with other questionnaire based assessments of physical activity (446) and to predict exacerbation frequency in COPD (447). The questionnaire has also been used to assess QOL in PAH (387). The CAMPHOR is a well-validated disease specific QOL questionnaire designed for use in patients with PAH (389). Its activity score is based on 15 questions in a single section. In the recent article by Matura *et al*. physical activity scores from the CAMPHOR correlated with accelerometer measured variability in physical activity but not with physical activity counts themselves, possibly due to the lower number of patients studied (413). Our data suggests that screening patients for low physical activity would be best done using the SGRQ.

Neither questionnaire's activity score was as good as the 6MWD in predicting those patients achieving their recommended amount of physical activity per day, defined as greater than 30 minutes and greater than 3.0 METs (384). This may be because these questionnaires ask patients what they can't

do rather than what they are doing and may be insensitive to light and moderate activity performed by the participant (448).

Importantly an SGRQ activity score of > 70 was able to define those patients at higher risk of mortality in the subsequent 2 years with reasonable sensitivity and specificity. This further supports the use of the SGRQ activity score to monitor patients' physical activity. Prospective studies should concentrate on whether improving activity scores are associated with improved long-term outcomes.

3.7 Limitations

One of the main limitations of this study is the small number of patients involved. It is difficult to make generalisations about the associations seen in our small cohort to a wider range of patients in other centres. I have undertaken multiple comparisons using the same data set and have not carried out Bonferroni corrections for multiple analysis. This is because the numbers needed to study would be higher than feasibly possible given the time and resources available and the rarity of the condition. This does leave us open to type 1 error but reduces the amount of type 2 error. As long as this is understood by the reader then this seems to be a reasonable approach and is supported in the wider literature when dealing with small sample sizes (449). The use of linear regression models in these small numbers to demonstrate independent associations of muscle, physical activity and other factors must be interpreted with caution. The data does however comply with the requirements of Austin *et al.* who suggested that only 2 subjects per variable were required for this analysis to be valid (450). This methodology was also discussed with a statistician. It should also be noted that PAH is a rare condition and the associations demonstrated in these small number are reasonably strong. A lager cohort might have demonstrated a statistical as well as numerical difference in area under the ROC curve analysis between the various measures, adding more weight to our arguments.

Another weakness of the study relates to missing data. This is particularly true with adequate SWA and questionnaire data. We have adopted the strategy of using all the valid data available to increase

the sample size. This was particularly important given the small sample size to begin with and is consistent with the approach taken by Dziura *et al.* (451)

The mortality and admission assessments undertaken were all cause and not PH specific. It would be interesting to split the admissions into those, which were for PH and those for other reasons. The numbers, again, were too small to attempt this assessment in our cohort.

Although we have addressed the subject of validity of questionnaires in our study we have not assessed the reliability or reproducibility of these questionnaires in PAH patients both of which need to be assessed prior to making firm conclusions on the effectiveness of the questionnaires as screening tools for low physical activity. Furthermore, although the SWA has been validated in other chronic diseases such as COPD (419), it has not been validated in PAH and we have not compared the SWA outputs to the gold standard calorimetry or DLW in this cohort.

Finally this study does not address whether the primary deficit accounting for the association of poor outcomes is low physical activity due to breathlessness leading to muscle loss or whether cachexia due to muscle loss from inflammation and hypoxia is a primary driver of low physical activity. Only longitudinal observational and multi-armed interventional studies with adequate follow would be able to address this issue. Whichever is true, breaking the vicious cycle of breathlessness, low activity and muscle loss at any point is likely to have positive effects on outcomes in these patients (75).

3.8 Conclusions

The main findings of this study were that muscle strength and size and physical activity were associated with functional status, exercise capacity, and QOL both at time of measurement and at follow-up in patients with PAH. Quadriceps muscle size was independently associated with both 6MWD and QOL in this cohort.

The data demonstrates for the first time that extremely low FFMI and physical activity was associated with increased mortality in patients with PAH, whilst low FFMI and muscle strength was associated with increased risk of hospital admission.

In this study we have demonstrated for the first time a moderately strong association between the activity scores generated by two commonly used QOL questionnaires and physical activity measured objectively by the SWA in a fully characterised group of patients with PAH. The questionnaires may be effective screening tests for low physical activity for use in larger population studies, to guide intervention or for enrolment in clinical trials.

Chapter 4 TGFβ signalling in muscle wasting in pulmonary hypertension

4.1 Background

TGFβ signalling has been implicated in both the development of muscle wasting (182) and PH (402). The MCT rat has been used for many years as a model of PH associated cachexia (133, 136). The role of TGFβ signalling in the development of PH in the MCT rat model has been studied extensively (402). However the part that the TGFβ super-family plays in muscle wasting in this model is poorly understood, being limited to one study showing raised circulating levels of GDF-8 associated with muscle loss (153). Another animal model of PH, the Sugen/hypoxia mouse (452), has been shown to have similar fibre type changes in the diaphragm as the MCT rat (162) but has not been examined for peripheral muscle wasting.

The TGFβ super-family protein, GDF-15, which is a marker of prognosis in PAH (207), has been implicated in the development of muscle wasting in ICU acquired weakness (218, 265), COPD (266), cancer (269) and in a healthy elderly population (263). Originally, it was thought that GDF-15 caused muscle loss exclusively through appetite suppression (260), but our group has shown, both *in vitro* and *in vivo*, that GDF-15 treatment or over-expression can cause direct myotube and myofibre atrophy (265, 453). In ICU patients and in those with COPD, both local and circulating GDF-15 levels were associated with levels of muscle wasting (265, 453). Other groups have shown that the source of GDF-15 in patients with PAH was the pulmonary endothelial cells and plexiform lesions (283). It is known that GDF-8 can cause muscle wasting in both a paracrine and endocrine manner (182) and that GDF-15 producing tumours can cause a reduction in weight (269) but it is not clear whether local or systemic GDF-15 is most important in influencing muscle wasting.

4.2 Aims

To define the association of GDF-15 with muscle function and size in animal models and in patients with PAH.

To identify the source of GDF-15 in animal models of PAH

4.3 Hypotheses

Circulating GDF-15 is associated with muscle strength and size in animal models and in patients with PAH.

The source of circulating GDF-15 is the pulmonary vasculature and not the skeletal muscle

4.4 Methods

For a full explanation of the methods please see Chapter 2 of this thesis

4.4.1 Animal models

Thirty male Sprague-Dawley rats were treated with 40mg/kg MCT (16) or PBS (14) to induce PH (401). Some animals underwent MRI of the hind limb and the heart at the outset of the experiment and then 4 weeks later (405). At this time all animals were humanely killed by exsanguination, at which time blood was collected, after cardiac catheterisation. The heart was dissected for RV / LV+S weight. Half the lung was agarose inflated and placed into formalin and the other half was flash frozen (402). The TA and soleus muscles from one leg were snap frozen, whilst those from the other leg were embedded in OCT and frozen in isopentane, cooled in liquid nitrogen.

10 Male C57BL/6J mice were injected subcutaneously with the VEGF antagonist, SU5416 (Sugen), or vehicle control at a dose of 20mg/kg per dose on a weekly basis. Mice were exposed to either room air or chronic normobaric hypoxia for 3 weeks. After this, the mice underwent cardiac catheterisation, and were humanely killed by exsanguination, at which time blood was taken. The heart, lung, TA and soleus were processed as described above, except the muscle was fixed in formalin and embedded in wax ready to be cut into slides (403)

4.4.2 Tissue processing and analysis

Lung and muscle tissue was homogenised for mRNA and protein using methods described in full in Chapter 2. Blood was spun down for serum and/or plasma. Lung and muscle tissue was sectioned and mounted on slides. Muscle tissue was stained with haematoxylin and eosin and fibre diameter was assessed as previously described. Lung tissue was stained for GDF-15 and α smooth muscle actin. Blood samples and lung tissue protein were analysed for GDF-15 by ELISA as per manufacturer's instructions. Lung and muscle tissue was analysed by qPCR using primers listed in Chapter 2 as previously described and fully explained in Chapter 2 (265).

4.4.3 Clinical study

Thirty patients with PAH, recruited from PH clinics at the Royal Brompton Hospital were included in this portion of the study. They underwent 6MWD according to American Thoracic Society guidelines (397) and had their QMVC measured (374) which was expressed as a function of BMI (34). These patients also had their USRF$_{CSA}$ measured using the ultrasound technique described by Seymour *et al*. (67). All patients initially enrolled also underwent physical activity monitoring for 7 days with the SWA (376). Twenty-six had adequate data defined as wearing the armband for 22.5 hours for at least 5 days including both Saturday and Sunday (378). The primary output from the SWA we examined against GDF-15 was the PAL (378). All patients also underwent echocardiographic assessment (394). Blood was taken and plasma was extracted for analysis of GDF-15 levels, which were measured by ELISA (R&D systems, Abingdon, UK). This study was approved by the REC and the Royal Brompton hospital. The REC study number was 13/LO/0481. All patients gave full written informed consent for participation in this study.

4.4.4 Statistics

Differences between control and PH groups or those with high and low muscle strength were assessed using Student's t-test or Mann-Whitney U test depending on the distribution of the data. Normality was assessed using the Kolmogorov-Smirov, D'Agostino and Pearson test and the Shapiro-Wilk test as

well as visually using histograms. Correlations were assessed using Pearson or Spearman analysis depending on the linearity of the association of the data sets. ROC curve analysis was used to define the ability of GDF-15 to predict patients with preserved muscle strength defined by a QMVC/BMI > 1.5.

4.5 Results

4.5.1 The MCT rat is a model of PH and muscle loss

Four weeks after a single injection of MCT, all the treated rats had developed PH. MCT rats had a higher RV/LV+S weight ratio when compared to controls (Figure 4.1 A) and, in those that had cardiac catheter data available , right ventricular systolic pressure was also raised (Figure 4.1 B). MRI revealed a number of abnormalities in the MCT group when compared to controls (n=3). These changes include right ventricular hypertrophy and dilation as well as bowing of the septum in systole (Figure 4.1 C). At 4 weeks the MCT rats weighed less, (Figure 4.2 A) had grown less (Figure 4.2 B) and, on average, had eaten less (Figure 4.2 C) than their control counterparts. Both TA (predominantly fast twitch) and soleus (predominantly slow twitch) muscle weight was lower in MCT compared to control treated rats (Figure 4.2 D and E). MRI of the hind limb of the animals (n=3) showed a general reduction in muscle bulk in the MCT animals compared to controls (Figure 4.3). In view of evidence from previous studies suggesting that the atrophy in the skeletal muscle of the MCT rat is type II fibre specific, the fibre diameter of the type II fibre rich TA was analysed. The mean fibre diameter of the TA was lower in the MCT rat when compared to controls (Figure 4.4 A and B).

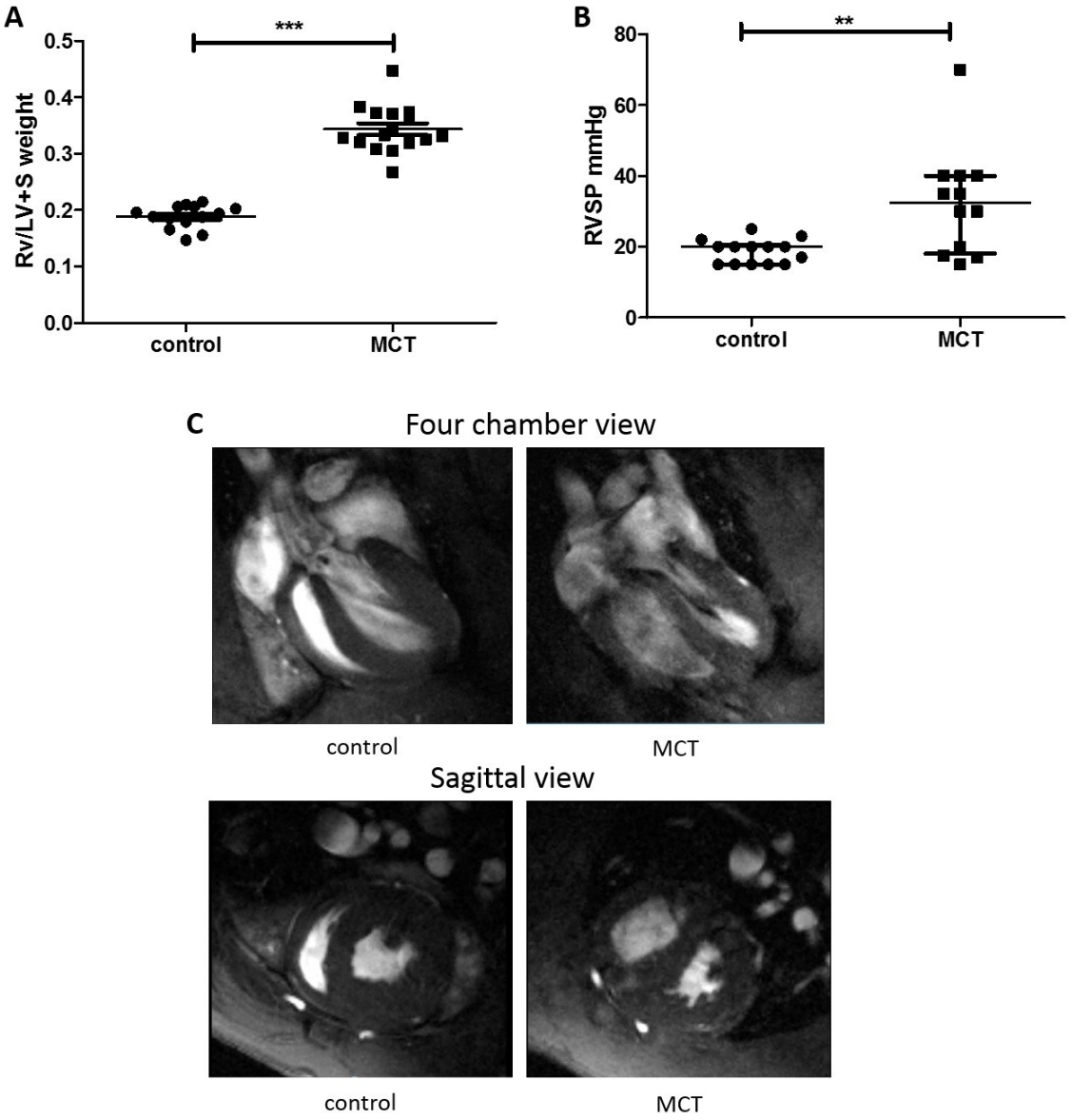

Figure 4.1 The monocrotaline (MCT) rat is a model of pulmonary hypertension. A. Right Ventricular / Left Ventricular + Septal (RV/LV+S) weight in control (n=14) and MCT (n=16) rats (student's t-test $p < 0.001$). **B.** Right ventricular systolic pressure in mmHg in control (n=14) and MCT (n=12) rats (Mann Whitney U test $p = 0.009$). **C.** Representative four chamber and sagittal magnetic resonance image views of control (n=3) and MCT (n=3) rat heart in systole demonstrating a thickened and dilated right ventricle and bowing of the interventricular septum.

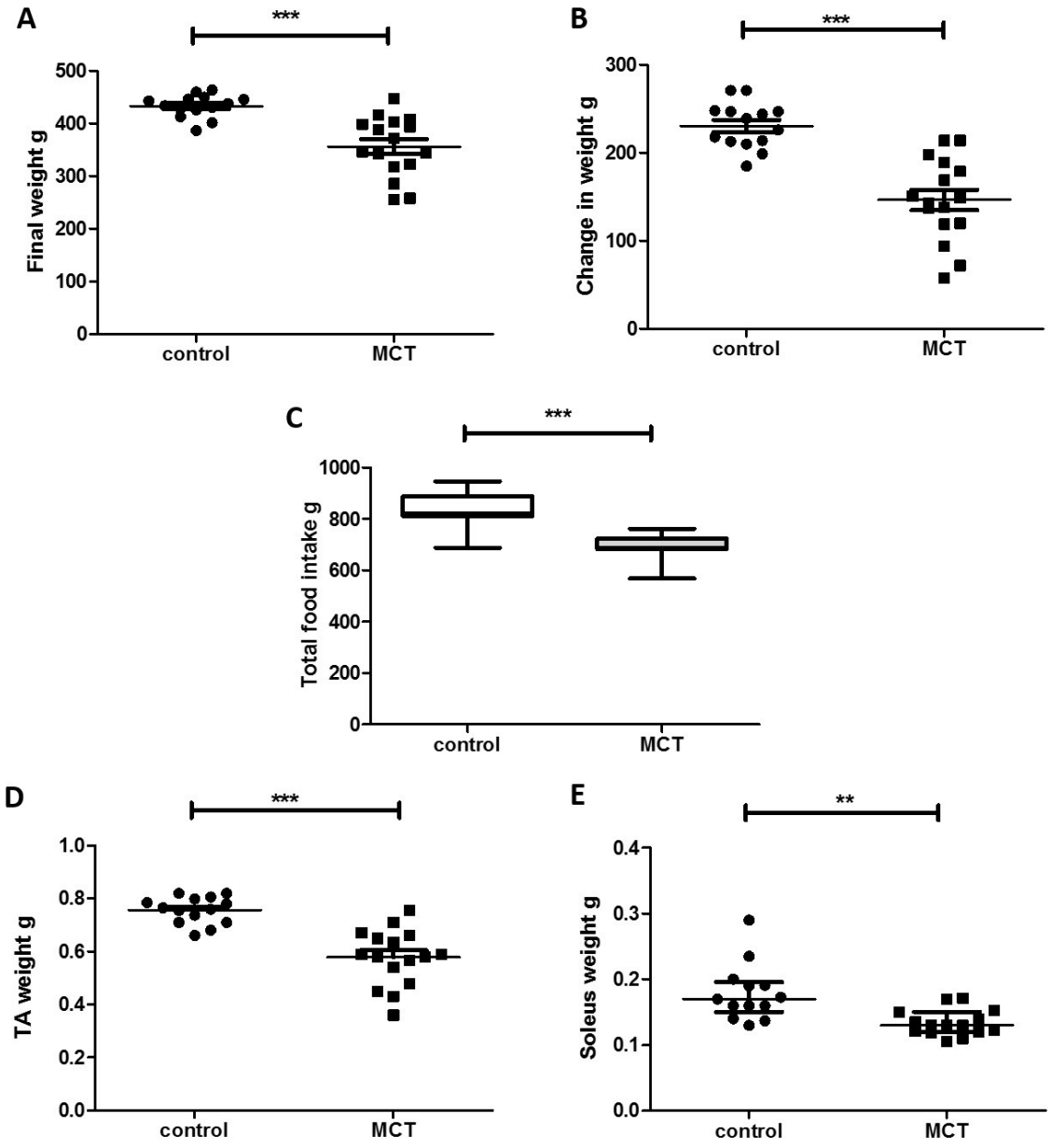

Figure 4.2 Growth, body weight, muscle weight and food intake in the monocrotaline (MCT) rat. A. Final weight in grams (g) in control (n=14) or MCT (n=16) rats (student's t-test $p < 0.001$). **B.** Change in weight in grams (g) in control (n=14) or MCT (n=16) rats (student's t-test $p < 0.001$). **C.** Average food intake per animal in control (n=13) or MCT (n=15) rats (Mann Whitney U test $p < 0.001$). **D.** Tibialis anterior (TA) muscle (predominantly fast twitch) weight in grams (g) in control (n=14) or MCT (n=16) rats (student's t-test $p < 0.001$). **E.** Soleus muscle (predominantly slow twitch) weight in grams (g) in control (n=13) or MCT (n=15) (Mann Whitney U test $p < 0.001$).

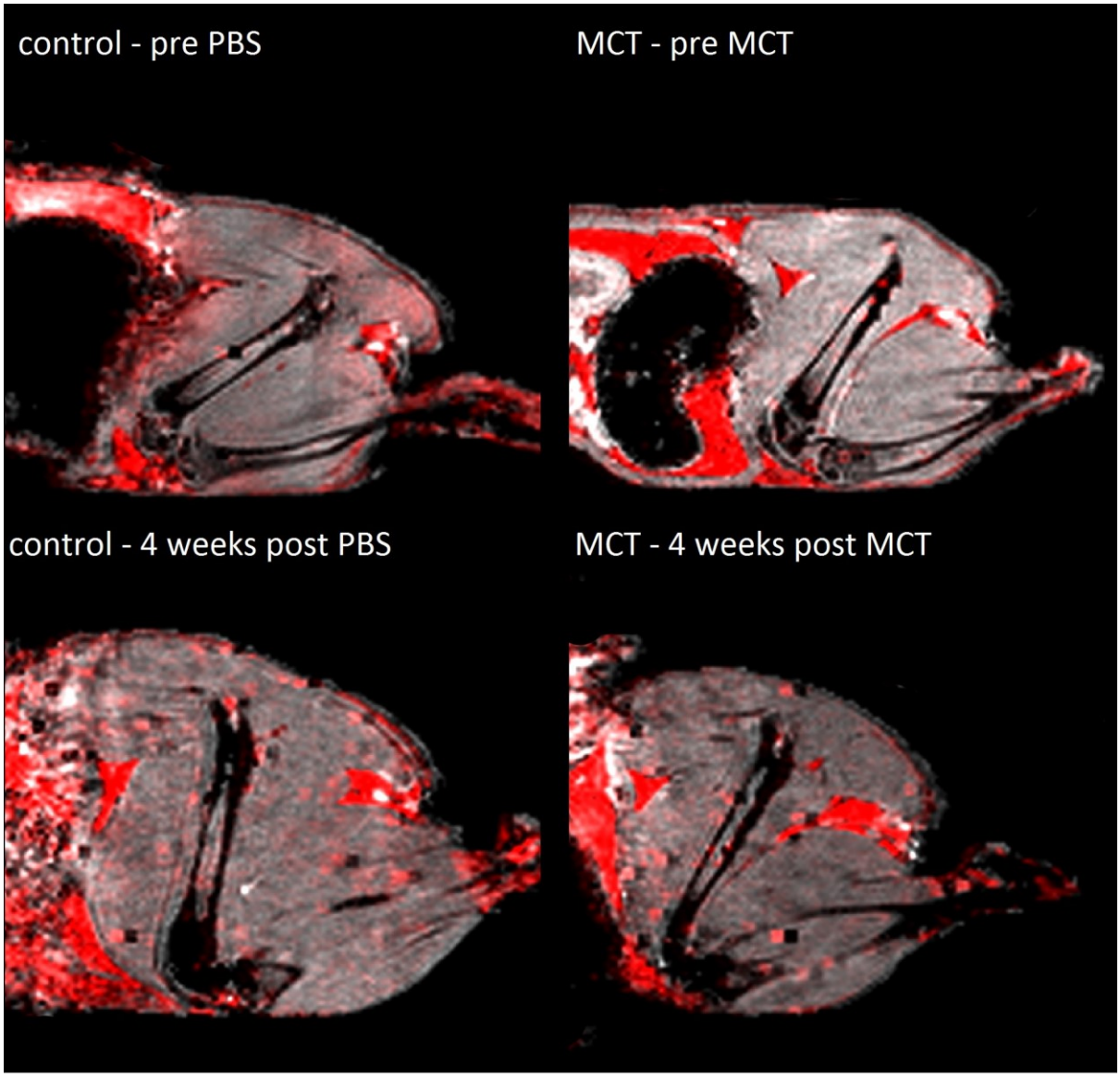

Figure 4.3 MRI imaging of the hind limb of the monocrotaline (MCT) rat. Representative cross sectional MRI showing the muscle bulk of the hind limb of control and MCT rats taken through the femur before and after control or MCT injection (n=3).

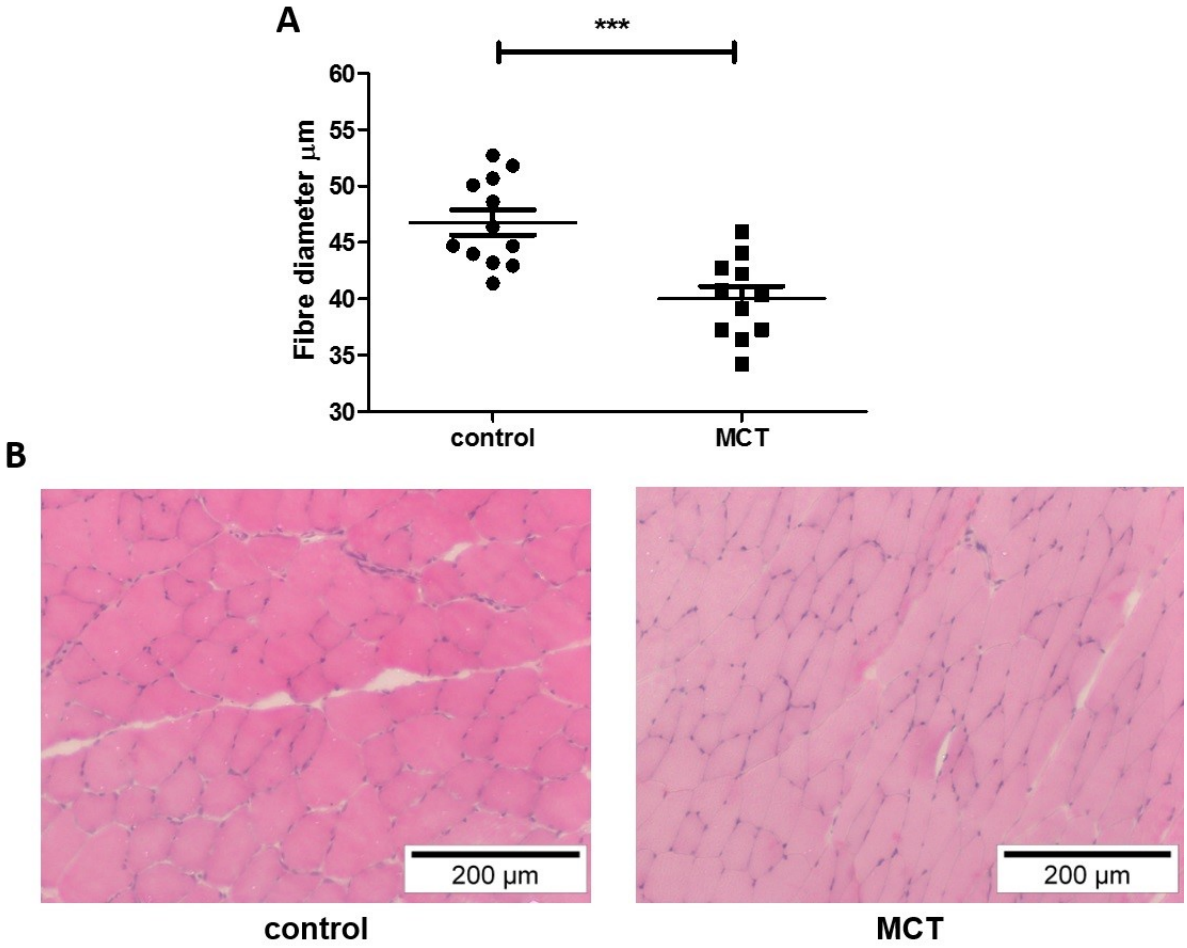

Figure 4.4 Tibialis fibre diameter in the monocrotaline (MCT) rat. A. TA fibre diameter in micrometres (µm) in control (n=12) or MCT (n=11) rats (student's t-test $p < 0.001$). **B.** Representative bright-field image of rat muscle tissue stained with haematoxylin and eosin from which average fibre diameter was determined by Image J.

4.5.2 TGFβ super-family member expression in the muscle and blood in the MCT rat

mRNA expression of a number of TGFβ ligands was analysed in the TA of the MCT rat. There was no difference in the expression levels of TGFβ1 (Figure 4.5 A) or GDF-15 (Figure 4.5 B) between MCT and control treated animals. There was, however, a significant increase in GDF-8 expression within the TA of the MCT rat compared to controls (Figure 4.5 C). Next, serum levels of GDF-15 were analysed. GDF-15 levels were raised in the serum of MCT rats when compared to controls (Figure 4.6 A). GDF-15 protein levels were undetectable in the TA of the MCT rat, by this same

ELISA (data not shown). Across both MCT and control rats, circulating GDF-15 levels were negatively correlated with final animal weight TA weight and TA fibre diameter (Figure 4.6 B, C and D).

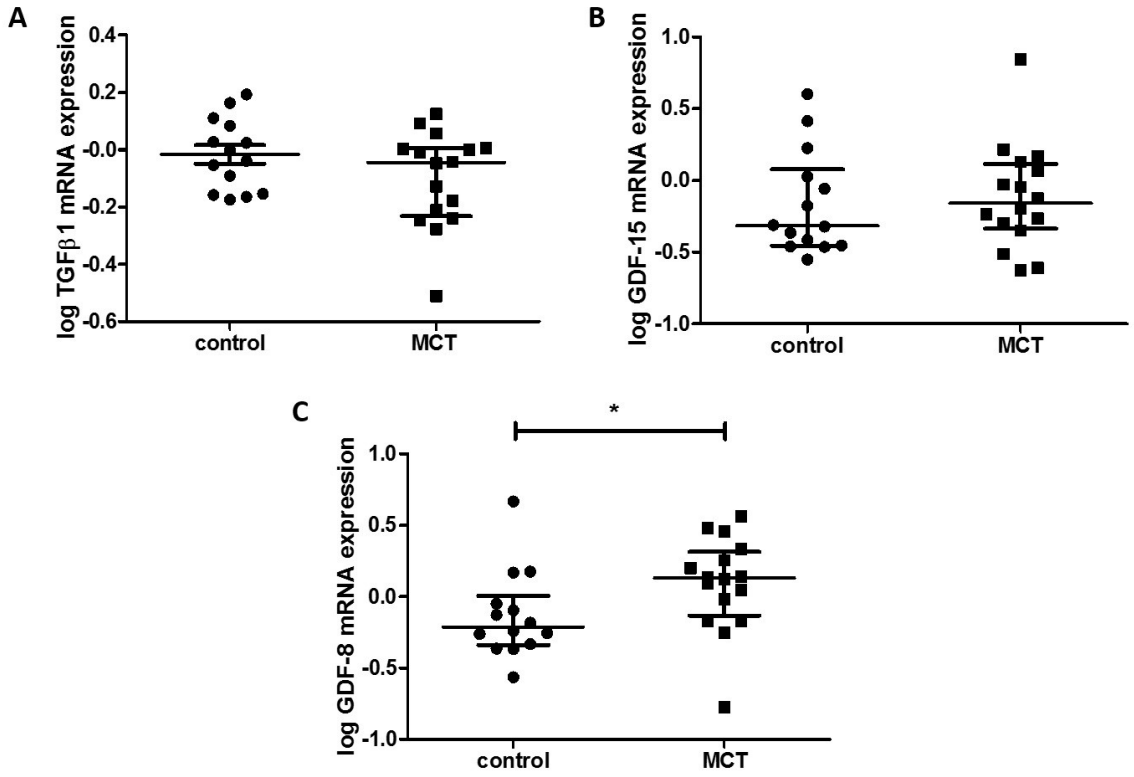

Figure 4.5 TGFβ super-family member mRNA expression in the muscle of the monocrotaline (MCT) rat. A. log TGFβ1 mRNA expression in the TA of control (n=14) and MCT (n=16) treated rats (Mann Whitney U test p = 0.190). **B.** log GDF-15 mRNA expression in the TA of control (n=14) and MCT (n=16) treated rats (Mann Whitney U test p = 0.575). **C.** log GDF-8 mRNA expression in the TA of control (n=14) and MCT (n=16) treated rats (Mann Whitney U test p = 0.026).

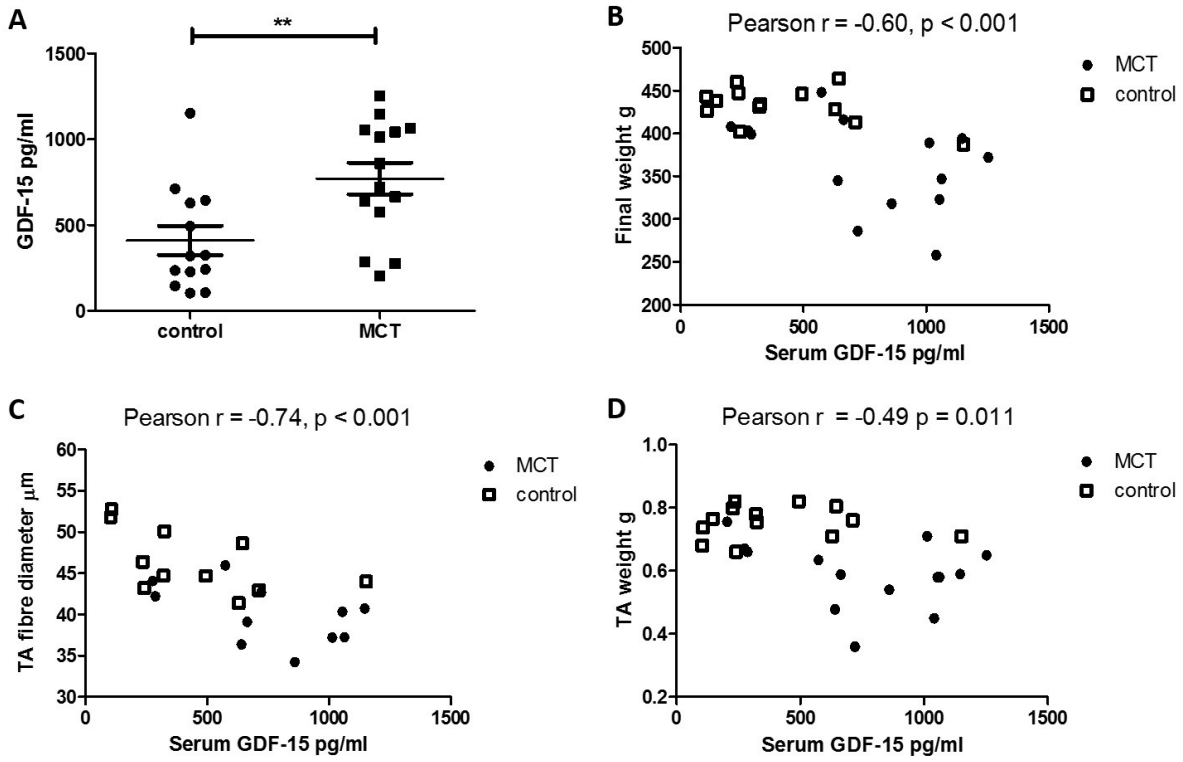

Figure 4.6 Circulating GDF-15 and muscle loss in the monocrotaline (MCT) rat A. GDF-15 levels in the serum of control (n=13) and MCT (n=14) treated rats (Student's t-test p = 0.008). **B**. Serum GDF-15 levels plotted against final animal weight in control (n=13) and MCT (n=14) treated rats. **C.** Serum GDF-15 levels plotted against tibialis anterior (TA) weight in control (n=13) and MCT (n=14) treated rats. **D.** Serum GDF-15 levels plotted against TA fibre diameter in control (n=11) and MCT (n=11) treated rats.

4.5.3 The pulmonary vasculature is a source of circulating GDF-15 in the MCT rat

qPCR revealed a significant increase in expression of GDF-15 mRNA in the lungs of the MCT rat compared to control (Figure 4.7 A). GDF-15 mRNA levels correlated with serum levels of the protein suggesting that the lung is an important source of GDF-15 production in this model (Figure 4.7 B). ELISA also showed an increase in GDF-15 protein expression in lung homogenates from MCT rats when compared to controls (Figure 4.7 C). Immunohistochemistry revealed that GDF-15 production was localised in the pulmonary vasculature and particularly in the endothelial and to a lesser extent the smooth muscle cell layer of the vessels (Figure 4.8).

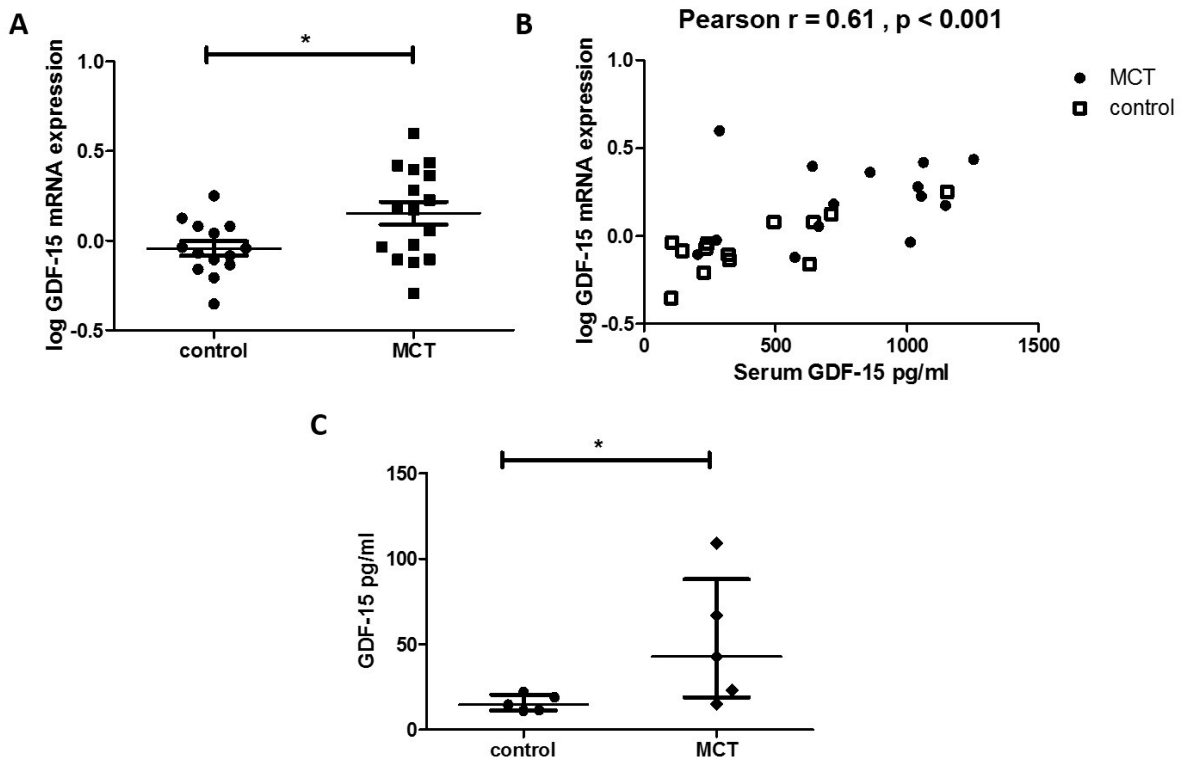

Figure 4.7 GDF-15 mRNA and protein in the lung of the MCT rat. A. GDF-15 mRNA expression in the lung of control (n=14) and MCT (n=16) treated rats (Student's t-test p = 0.017) **B.** Serum GDF-15 levels plotted against GDF-15 mRNA expression in the lung of control (n=13) and MCT (n=14) treated rats. **C.** GDF-15 protein expression normalised to loading 100 μg of protein in the lung of control (n=5) and MCT (n=5) treated rats (Mann-Whitney U test p = 0.032).

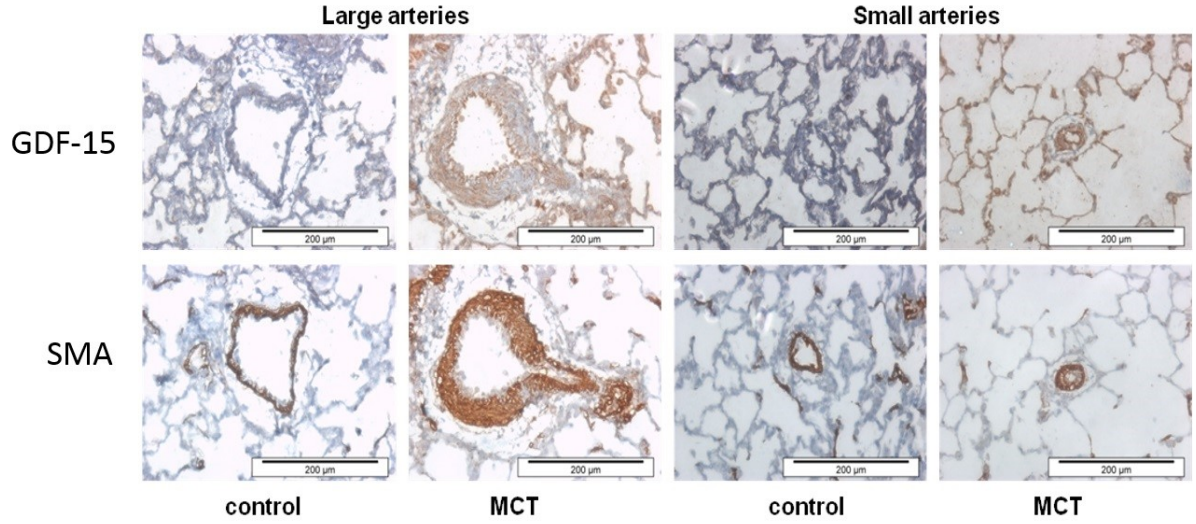

Figure 4.8. GDF-15 in the pulmonary vasculature of the monocrotaline (MCT) rat. GDF-15 produced in the pulmonary vasculature Representative immunohistochemistry of lung sections showing large and small pulmonary arteries stained for GDF-15 or Smooth muscle actin (SMA) in control (n=5) and MCT treated rats (n=5).

4.5.4 Sugen/hypoxia mice develop PAH and associated muscle loss

Sugen/hypoxia treated animals had a median RVSP of 38 (36, 42) mmHg and RV/LV+S weight of 0.36 (0.38, 0.43), whilst hypoxia treated animals had a median RVSP of 36 (30, 42) and a median RV/LV+S weight of 0.43 (0.27, 0.53). The Sugen/hypoxia treated mouse TA weighed less than that of control animals (Figure 4.9 A). The Sugen/hypoxia mice also had significantly smaller TA fibre diameters than the normoxic mice (Figures 4.9 B and C). Hypoxic mice had intermediate TA weights and TA fibre diameters that did not differ statistical from either the normoxic of Sugen/hypoxia mouse groups (Figures 4.9 A-C).

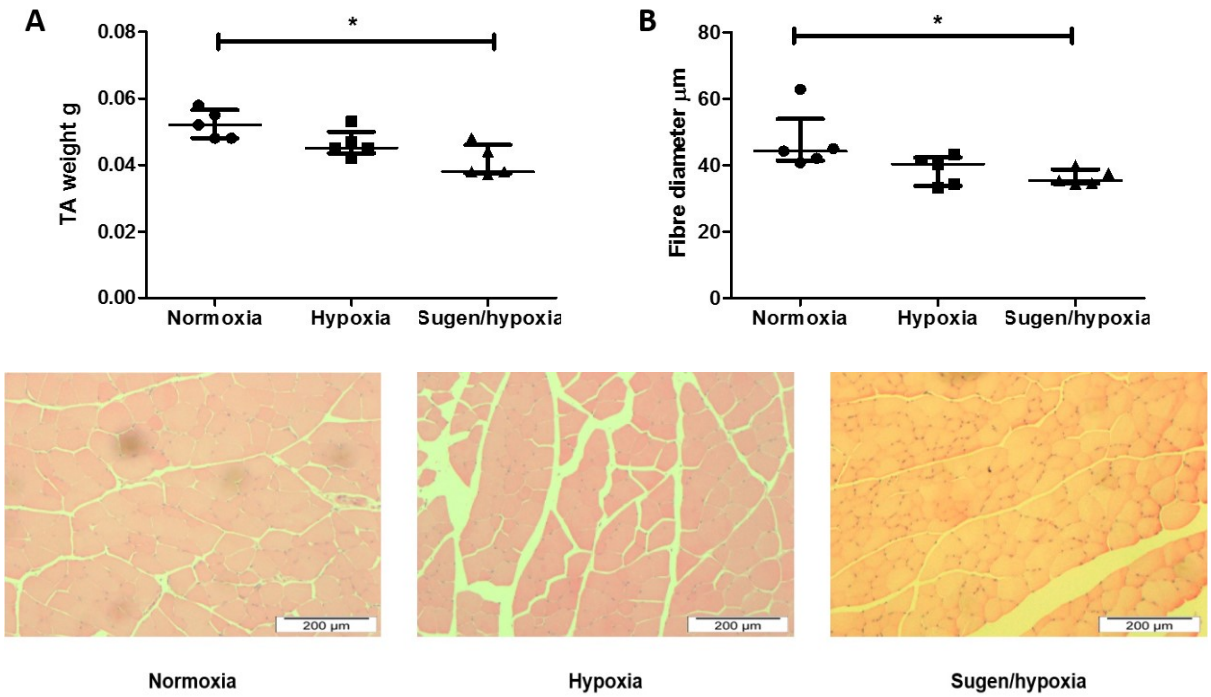

Figure 4.9. Tibialis anterior (TA) weight and fibre diameter in Normoxic, Hypoxic and Sugen/hypoxia mouse. **A.** TA weight in grams (g) in normoxic (n=5), hypoxic (n=5) or Sugen/hypoxia (n=5) mice (Kruskall-Wallace with Dunn's correction p = 0.017) **B.** TA fibre diameter in micrometres (µm) in normoxic (n=5), hypoxic (n=5) or Sugen/hypoxia (n=5) mice (Kruskall-Wallace with Dunn's correction p = 0.023). **C.** Representative bright-field image of rat muscle tissue stained with haematoxylin and eosin from which average fibre diameter was determined by Image J.

4.5.5 GDF-15 and other TGFβ super-family members in the muscle and circulation of the Sugen/hypoxia mouse

GDF-15 levels were significantly raised in the plasma of the Sugen/hypoxia mice when compared to both normoxic controls and to hypoxic mice (Figure 4.10 A). Plasma GDF-15 levels correlated significantly with TA weight and non-linearly with TA fibre diameter in this model (Figures 4.10 B and C). Further analysis of the muscle was limited to the Sugen/hypoxia and normoxia mice as a model of GDF-15 induced wasting. There was no difference in TA mRNA expression of TGβ1, GDF-15 or GDF-8 between normoxic and Sugen/hypoxia treated animals (Figures 4.11 A – C).

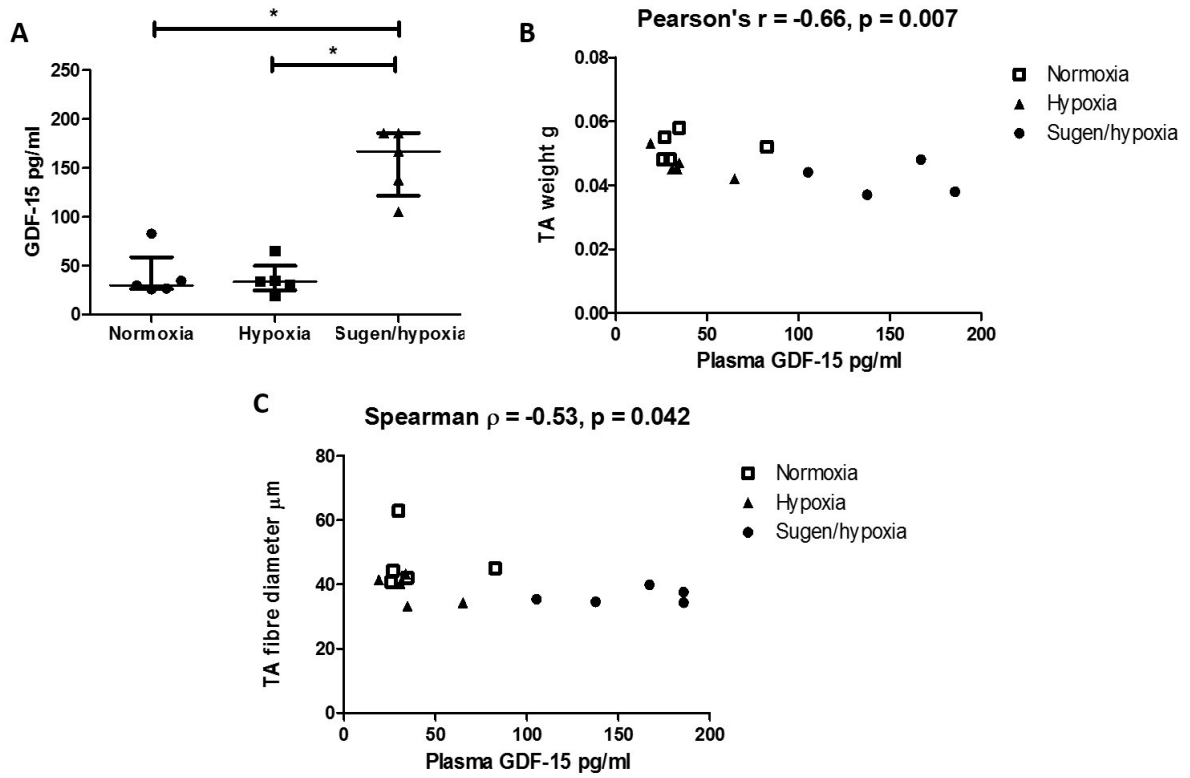

Figure 4.10 Circulating GDF-15 and muscle loss in the Sugen/hypoxia mouse. A. Plasma GDF-15 levels were higher in the Sugen/hypoxia mouse than in mice held in normoxic or hypoxic conditions (Kruskall-Wallace with Dunn's correction p = 0.009, control (n=5), hypoxic (n=5) and Sugen/hypoxia (n=5)). **B.** Plasma GDF-15 levels plotted against TA weight in grams (g) in control (n=5), hypoxic (n=5) and Sugen/hypoxia (n=5) treated mice. **C.** Plasma GDF-15 levels plotted against TA fibre diameter in control (n=5), hypoxic (n=5) and Sugen/hypoxia (n=5) treated mice.

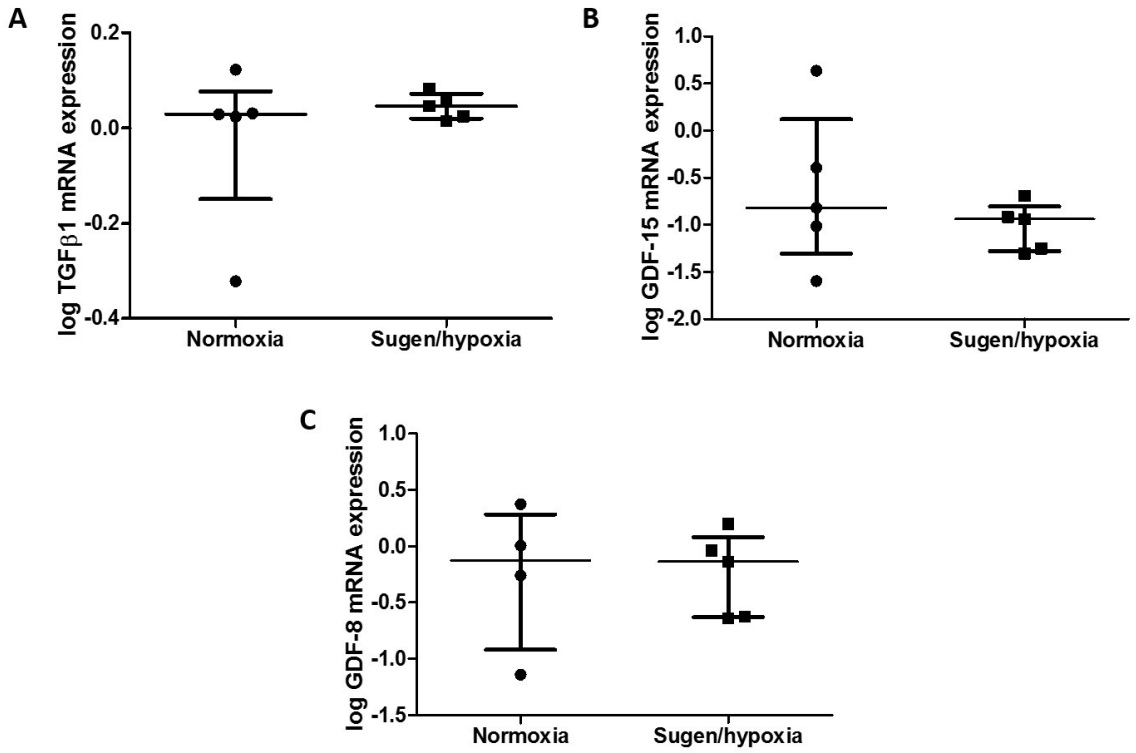

Figure 4.11 TGFβ super-family member mRNA expression in the muscle of the Sugen/hypoxia mouse A. log TGFβ1 mRNA expression in the TA of normoxic (n=5) and Sugen/hypoxia (n=5) treated mice (Mann Whitney U test p = 0.691). **B.** log GDF-15 mRNA expression in the TA of normoxic (n=5) and Sugen/hypoxia (n=5) treated mice (Mann Whitney U test p = 0.547). **C.** log GDF-8 mRNA expression in the TA of control (n=4) and MCT (n=5) treated rats (Mann Whitney U test p = 0.905).

4.5.7 The Sugen/hypoxia mouse also over-expresses GDF-15 in the lung

Analysis of lung tissue by qPCR revealed an increase in mRNA expression of GDF-15 in the Sugen/hypoxia model of PH compared to normoxic controls. Again there was intermediate expression of GDF-15 in the lung of the hypoxia treated mice that did not differ from either other group (Figure 4.12A). Lung GDF-15 mRNA expression correlated significantly, but non-linearly with plasma GDF-15 levels in this model (Figure 4.12B).

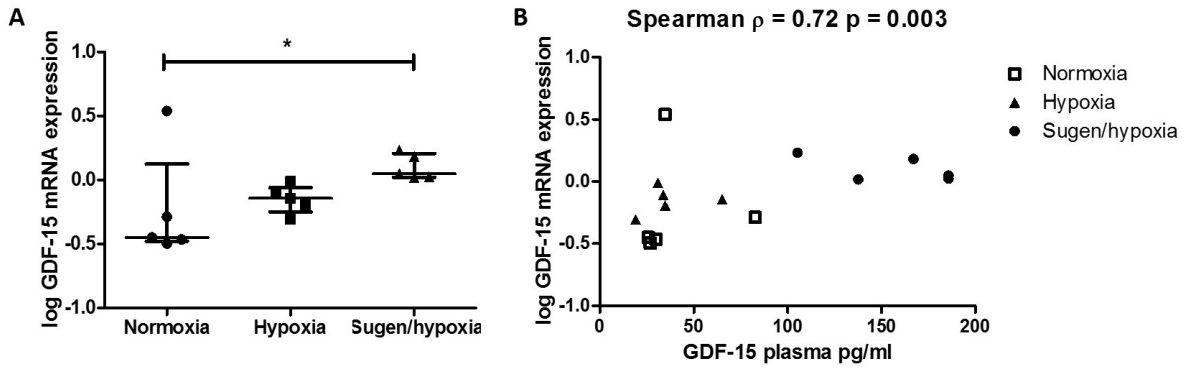

Figure 4.12 GDF-15 mRNA expression in the lung of the Sugen/hypoxia mouse. A. log GDF-15 mRNA expression in the lung of control (n=5), hypoxia (n=5) and Sugen/hypoxia (n=5) (Kruskall-Wallace with Dunn's correction p = 0.042) **B.** Serum GDF-15 levels plotted against GDF-15 mRNA expression in the lung of control (n=5), hypoxia (n=5) and Sugen/hypoxia (n=5) mice.

4.5.8 Circulating GDF-15 is negatively correlated with physical activity, muscle strength and size in patients with PAH

The demographics of thirty patients with concurrently measured muscle size, strength, physical activity, echocardiogram, BNP and GDF-15 are shown in Table 4.1. In this group of patients, at various points in their treatment course, median plasma GDF-15 was 862 (459, 1635) pg/ml. Plasma GDF-15 correlated with general markers of severity in PAH including 6MWD (Pearson r = -0.45, p = 0.013) and plasma BNP levels (Pearson r = 0.52, p = 0.003). GDF-15 also correlated linearly with $USRF_{CSA}$ and PAL and non-linearly with QMVC/BMI Figure (4.13 A-C). GDF-15 plasma levels were significantly lower in those patients with preserved muscle strength defined as a QMVC/BMI of > 1.5 (Figure 4.13 D). This cut off was associated with a lower risk of admission to hospital (see Chapter 3). A ROC curve for GDF-15 plasma levels predicting those with preserved muscle mass had an AUC of 0.74 (p = 0.035). The most useful cut-off was a GDF-15 concentration of < 564 pg/ml and had an 80 (44 - 97) % sensitivity and 84 (62 - 97) % specificity in identifying those patients with preserved muscle strength (Figure 4.13 E).

Demographics	n = 30
Age	46.8 (± 13.9) years
Female	20
Height	167 (± 8) cm
Weight	67.3 (58.8 - 77.7) kg
Diagnosis	
IPAH	23
Congenital heart disease	7
Echocardiogram	
RVSP	88.5 (± 26.8) mmHg
TAPSE	1.9 (1.5, 2.1) mm
TR velocity	408 (± 84) cm/sec
PAcT	83.8 (± 26.5) msec
Exercise, WHO, BNP	
6MWD	373 (± 126) m
WHO I : II : III	3 : 19 : 8
BNP	131 (44, 271) pmol/L

Table 4.1 Demographics. Demographic details of 30 patients with pulmonary arterial hypertension investigated for circulating growth and differentiation factor 15 (GDF-15) levels and muscle loss. World health organisation functional status (WHO), Idiopathic pulmonary arterial hypertension (IPAH), Right ventricular systolic pressure (RVSP) measured by echocardiogram (echo), tricuspid anterior posterior systolic excursion (TAPSE), tricuspid regurgitant (TR) velocity, pulmonary artery acceleration time (PAcT), Six minute walk distance (6MWD), plasma brain natriuretic peptide (BNP).

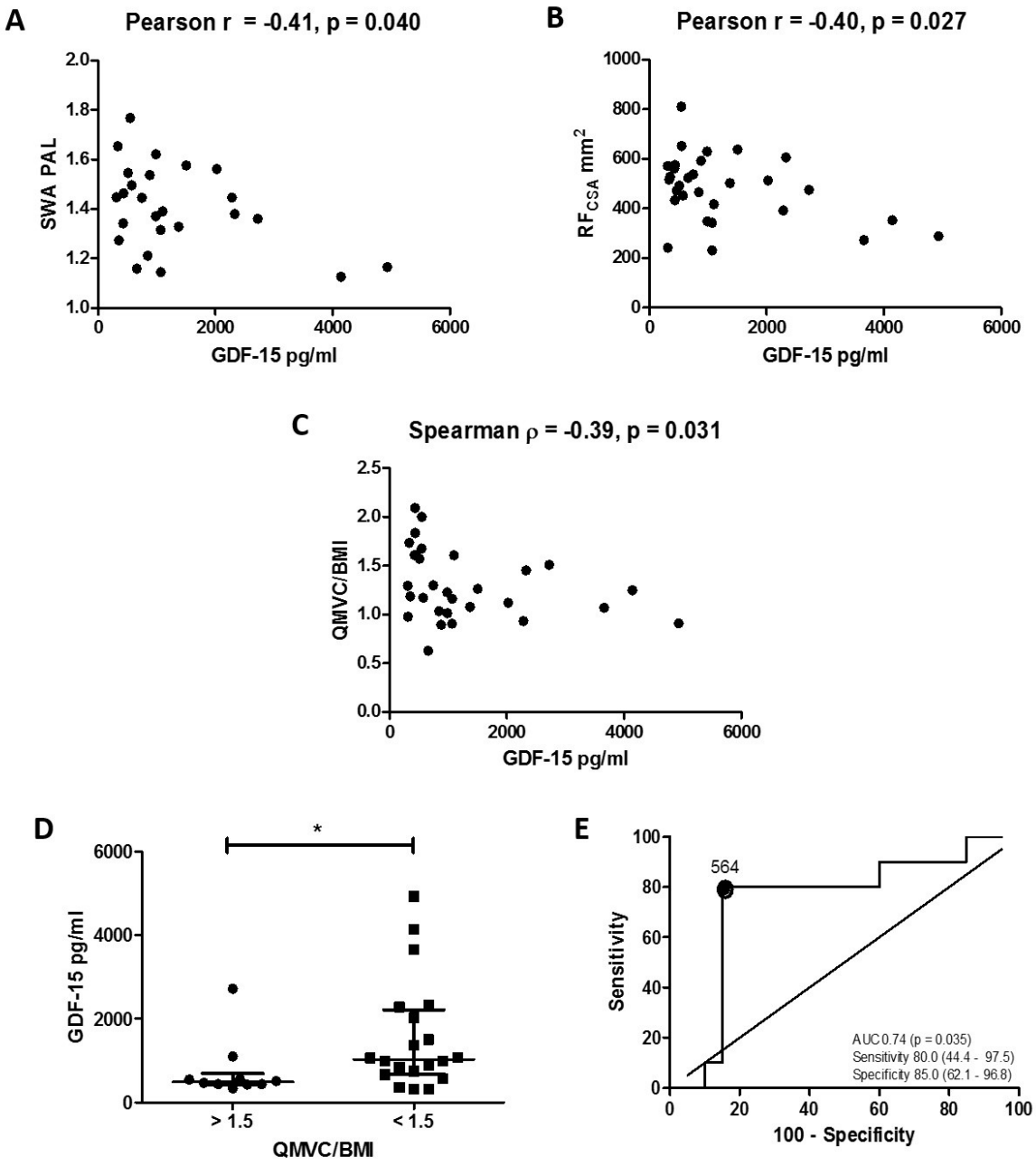

Figure 4.13 Circulating GDF-15, muscle wasting and physical activity in patients with PAH. A. Quadriceps maximal volitional capacity (QMVC) / Body mass index (BMI) plotted against plasma GDF-15 levels in 30 patients with PAH. **B.** Ultrasound measured rectus femoris cross sectional area (USRF$_{CSA}$) plotted against plasma GDF-15 levels in 30 patients with PAH **C.** SWA measured physical activity level (PAL) plotted against plasma GDF-15 levels in 25 patients with PAH. **D.** GDF-15 levels in patients with high and low muscle strength defined by a QMVC/BMI of < or > 1.5 (Mann-Whitney U test p = 0.037). **E.** ROC curve of GDF-15's ability to predict those with a QMVC < 1.5 or > 1.5 (AUC 0.74, p = 0.036).

4.6 Discussion

In these experiments I have shown that circulating GDF-15 levels are associated with muscle loss in 2 animal models of PH and that in patients with PAH, GDF-15 is negatively associated with lower limb muscle function and size. These data suggest that GDF-15 could be used as a biomarker of muscle loss in PAH. Consistent with this suggestion, we have shown that GDF-15 levels less than 564 pg/ml are indicative of a clinically significant preservation of proportional strength. My data also suggests that the pulmonary vasculature is a major source of circulating GDF-15 in animal models of PH, thereby linking the primary disease to the muscle wasting. Other novel findings include: that the addition of Sugen to hypoxia was required to stimulate a rise in circulating GDF-15 levels in the mouse models of PH and that TA GDF-8 mRNA production is raised in the MCT treated rat compared to controls and may therefore contribute to muscle wasting in this model.

MCT treatment of rats is a well-established model for studying skeletal muscle atrophy in association with heart failure and PH. The observation of reduced TA and soleus weight in association with increased pulmonary artery pressures is consistent with these earlier studies (132). Previous studies have also shown that after 3 weeks Sugen/hypoxia treated mice exhibited weight loss (452) and similar diaphragm changes to those seen in the MCT rat model (162). Here we show for the first time a loss of TA muscle weight and fibre diameter in this model of PH, which mimics the changes seen in the MCT rat.

Circulating GDF-15 has been shown to be raised in patients with PAH when compared to controls. It is also a recognised marker of prognosis (207). This is the first work to show GDF-15 levels are raised in the serum or plasma of the both the MCT rat and Sugen/hypoxia mouse. Circulating GDF-15 has been identified as a biomarker and potential regulator of muscle wasting in a number of conditions including in COPD (453) as well as in elderly women, where circulating GDF-15 was significantly negatively correlated with handgrip strength (263). The results presented here confirm this association in patients with PAH. They also show that GDF-15 levels are reduced in patients with preserved QMVC/BMI of > 1.5, which has been associated with a lower risk of

hospitalisation (see Chapter 3). Furthermore I have demonstrated that physical activity level, measured by the SWA, were associated with circulating GDF-15 levels. Physical activity has rarely been studied alongside GDF-15 levels. Transgenic and knockout mice data have yielded conflicting results (260, 270, 271, 273), whilst a study in patients with ischaemic heart disease showed that 6 months of rehabilitation after coronary artery stenting had no effect on GDF-15 levels (257). Further data is needed to establish the usefulness of GDF-15 as a clinical or research biomarker of muscle loss. Future work should therefore focus on demonstrating how GDF-15 responds to a variety of treatments aimed both at the primary disease as well as muscle wasting itself.

Studies in ICU acquired weakness have shown an increase in GDF-15 expression in the quadriceps, raising the possibility of an autocrine or paracrine effect of the protein on muscle mass (265). Recently it has been demonstrated that GDF-8 can exert its negative effect on muscle mass through autocrine, paracrine and endocrine mechanisms (182). In this study there was no change in GDF-15 expression in the TA of the MCT rat or Sugen/hypoxia mouse indicating that elevated circulating GDF-15 was derived from another tissue. Previous studies have shown that GDF-15 is expressed in the vascular endothelium and plexiform lesions in the lung of patients with PAH (283). We found that GDF-15 was over-expressed in the lung of MCT treated rats. GDF-15 was predominantly associated with the vascular endothelium but also to a lesser extent with the pulmonary artery smooth muscle cells in this MCT model of PH. Furthermore mRNA expression of GDF-15 was strongly correlated with circulating GDF-15 protein levels suggesting that the lung is a major source of GDF-15 in this animal model. Whether there is a local increase in GDF-15 expression in the skeletal muscle of patients with PAH remains to be determined, but the association of muscle mass with circulating GDF-15 in both the animal models and in patients strongly implies that the protein can act in an endocrine fashion. Our hypothesis is supported by recent work showing GDF-15 secreting tumours can cause muscle loss that is antagonised by a GDF-15 neutralising antibody (269).

Our data has implications outside PAH. GDF-15 has been identified as a marker of all-cause mortality in a wide range of different conditions including cardiovascular disease, cancer, renal failure and even a healthy elderly population (454). Sarcopaenia and cachexia are also almost universally associated with increased risk of morbidity and mortality across all disease states (455) suggesting that our data showing an association of GDF-15 and muscle may be more generalizable to all chronic diseases.

GDF-15 is known to be a stress response protein produced by a number of different stimuli including but not limited to inflammation, UV light and hypoxia (227). This study also demonstrated that after 3 weeks of hypoxia there was no significant increase in GDF-15 in the mouse model of pulmonary hypertension. This was in contrast to the Sugen/hypoxia mouse, which did exhibit raised circulating levels of GDF-15. It can therefore be concluded that SU5416 is required to stimulate GDF-15 secretion into the circulation in this model. Whether SU5416 alone is enough to stimulate GDF-15 production has not been tested. Whether hypoxic mice get an initial rise in circulating GDF-15 that then falls back to normal has, again, not been addressed by this work. SU5416 is a vascular endothelial growth factor antagonist, which causes greater increases in PH in mice over hypoxia alone (452). The interaction of VEGF and GDF-15 has been examined in a small number of studies. GDF-15 was shown to be important for increasing VEGF expression by HIF1α in HUVEC cells (284) and is responsible for a VEGF type neo-vascularisation response in malignant melanoma tumours (456). GDF-15 is known to prevent apoptosis in HPMECs (283) and VEGF inhibition in hypoxic rats leads to general endothelial cell apoptosis but also to emergence of a pool of apoptosis resistant endothelial cells (457). It may be that GDF-15 is produced in response to hypoxia in both hypoxia and Sugen/hypoxia mouse endothelium but is downregulated when its target, VEGF, is elevated in the hypoxic mouse, due to the adaptive effects of neo-vascularisation. The lack of VEGF response in SU5416 treated mice and subsequent unchecked GDF-15 in this model may contribute to the excess pulmonary hypertension seen in this model.

GDF-8 has been identified as a major negative regulator of muscle mass. It is known to activate both SMAD and non-SMAD pathways (458). Circulating levels of the protein have been shown to be raised i11n the MCT rat (153). We have shown that GDF-8 expression is raised in the TA of the MCT rat. Being a TGFβ super-family member means that GDF-8 is likely to activate some of the same pathways as GDF-15. This highlights the potential difficulty in attempting to antagonise only one molecule in a system with so much redundancy and is one of the reasons why GDF-8 antagonists may failed to have significant clinical effects in large studies (459). It is therefore important to identify common downstream points that are activated by a number of different pathways. These can then be targeted to improve clinical outcomes.

4.7 Limitations

The main limitation of these studies is the small sample size. This is especially true for the mouse model of PH. Despite this, GDF-15 levels in the circulation were consistently associated with muscle wasting in these models. We have limited biopsy data in patients with PAH and therefore it is not clear whether the models we used accurately represent what is going on in the muscle and pulmonary circulation of patients. GDF-15 has been linked to muscle wasting directly (453) through pro-atrophic processes and through appetite suppression (260). The MCT rat did eat less than its control counterparts meaning we cannot exclude nutrition as a contributing cause of loss of muscle mass in this model. Finally, although we found an excess of GDF-15 in the pulmonary vascular endothelium of the MCT rat, other tissues as a source of significant GDF-15 production in these models cannot be ruled out.

4.8 Conclusions

Circulating GDF-15, a major source of which is likely to be the pulmonary vascular endothelium, is associated with muscle wasting in 2 animal models and in patients with PAH. Low GDF-15 levels may be used as a biomarker of preserved muscle mass in this population.

Chapter 5 GDF-15 causes muscle atrophy *in vitro* through actions on TAK1

5.1 Background

GDF-15 is secreted as a 25kda protein. It is considered to be the first and only member of a sub-group of TGFβ super-family of cytokines due to its lack of structural homology to any other family members. GDF-15 has generally low expression levels during periods without cellular stress, but on stimulation by hypoxia, inflammation, short wavelength light exposure, tissue injury and cancer progression levels can substantially increase (227). The role of GDF-15 in health and disease remains to be fully elucidated. GDF-15 has been found to be expressed in high levels: in the placenta suggesting it may have a role in pregnancy and embryonic development (220); in seminal fluid, suggesting it has a role in fertility (231); and in macrophages where it exerts anti-inflammatory effects (219). Studies defining the role of GDF-15 in neurological, cardiac, and cancerous tissue both in vitro and in vivo have produced varied and contrasting results (237-239, 258).

Our group has previously shown that addition of GDF-15 to differentiated myotubes causes atrophy (218), possibly through an increase in expression of ubiquitin ligases atrogin-1 and MuRF-1 (265).We have also demonstrated that over-expression of GDF-15 in the TA of mice through electroporation causes muscle fibre atrophy (460).

Generally, TGFβ super-family member proteins are secreted and stored in the extracellular matrix as inactive pro-peptides which are cleaved by proteases to adopt their active form, which then bind to their target receptors (183). The receptors are classed as type 1 and 2 (184). The ligand binds to its receptor which forms a hetero-tetrameric complex consisting of 2 type 1 and 2 type 2 receptors (185). The type 2 receptor is a constitutively active serine threonine kinase which is able to phosphorylate the type 1 receptor (184), which, in turn, phosphorylates intracellular SMAD molecules (186). The TGFβ / activin ligands tend to activate SMAD 2 and 3, whilst BMPs activate SMAD 1, 5, 8 but there is significant overlap within the system (187). These SMADs combine with the co-SMAD, SMAD 4, which translocates them to the nucleus to stimulate gene transcription (188). All SMADs recognise the binding site CAGAC whilst SMADs 1 and 5 have higher affinity for GC rich areas of DNA (179). Despite

nearly 40 TGFβ ligands being identified, there are only 5 type 2 receptors and 7 type 1 receptors meaning that most ligands can bind to different combinations of receptors with different affinities, altering the consequences for downstream signalling (178). As well as classical SMAD signalling, it has been established that TGFβ super-family members can interact directly and indirectly with a number of other pathways. Particularly important pathways include the TAK, Ikκ-β, NFκB axis (190) p38 MAPK (191), ERK 1 and 2 (192), JNK (193) and PI3 kinase - AKT(194). These non-canonical pathways are often involved in antagonising or augmenting the effects of classical SMAD signalling, suggesting that, by activation of a number of competing pathways, the TGFβ super-family can fine tune its effects in a cell, time and environment dependent manner (178, 179).

The signalling pathways activated by GDF-15 are still under investigation. The receptor through which GDF-15 acts is unclear. In neural tissue, very recently, it has been established that GDF-15 acts through the GFRAL to regulate appetite (292-294, 296). This receptor is not present in skeletal muscle (295). Some data shows that in some cells, at least, the TGFBR2 and ALK-5 receptors are required for GDF-15 activity (288, 301), whilst others have shown that GDF-15's activity is independent of TGFBR2 (243, 260) and ALK-5 (243, 289, 460). Other TGFβ receptors implicated in GDF-15 response include ALK1, (291) ALK4, 6 or 7 (290). GDF-8, the archetypal TGFβ super-family member involved in muscle wasting, acts through the ACVR2B (73). The affinity of GDF-15 for this receptor has not been investigated.

Some authors have shown that stimulation with GDF-15 can result in the activation of SMAD 2, 3 (235, 290, 297), whilst others have shown that SMAD 1, 5, 8 (238, 291, 300) are involved, both through western blot and luciferase assay. Others still have shown no SMAD activation in response to GDF-15 (260, 299), with some finding that GDF-15 actually caused a reduction in a TGFβ1 mediated SMAD response (298).

Similar findings of a cell type, context and dose dependant response to GDF-15 are applicable to non-canonical pathways. Most researchers have shown that GDF-15 increases the phosphorylation of ERK and AKT in a number of different cell lines (238, 243, 245, 294, 304, 308, 315). However this is not a

universal phenomenon (313). Data regarding P38-MAPK phosphorylation is less clear with some showing an upregulation (303, 304, 314, 315) and other showing a downregulation in the signal (312, 317). The effect of GDF-15 on the TAK1, IKK, NFκB axis has also yielded conflicting results. In HCT-8 intestinal epithelial cells, infection with enteropathic E-coli caused an up-regulation of GDF-15. Recombinant GDF-15 was also able to directly stimulate TAK1 phosphorylation in these cells. Furthermore enteropathic E-coli effects on TAK1 were shown to be GDF-15 dependant, whilst enteropathic E-coli effects on NFκB were inhibited in the presence of the TAK1i 5(Z)-7-oxozeaenol (318). Similar results were generated in HCT-116 colorectal cancer cells where enteropathic E-coli infection caused GDF-15 dependent TAK1 activation and TAK1 dependent increases in RhoA protein levels with an increase in cell detachment and possible migration (319). In contrast in human umbilical vein endothelial cells GDF-15 knockout seemed to have an enhancing effect on glucose mediated NFκB activation (316).

5.2 Aims

To define the pathway through which GDF-15 might cause muscle wasting *in vitro* with a view to antagonising its effects.

5.3 Hypotheses

GDF-15 acts through the TGFBR2 and a non-canonical pathway in C2C12 cells. Antagonising this pathway will prevent GDF-15 mediated myotube atrophy in vitro.

5.4 Methods

For a full explanation of the methods please see Chapter 2 of this thesis

5.4.1 C2C12 cells

C2C12 myoblast DMEM with 10% foetal calf serum were seeded in 96, 24, 12 or 6 well plates. Some cells were transfected with various receptors, luciferase reporters and or pCAGGs-EGFP. Some cells for western blot, qPCR and myotube diameter studies were differentiated into myotubes for 10 days.

This was achieved by incubating myoblasts in DMEM supplemented with 2% horse serum. Cells were then treated at various concentrations of: GDF-15, TAK1i (5Z)-7-oxozeaenol and or the ALK-5 inhibitor SB431542 (408). For some experiments cells were co-treated with GDF-15 and TGFβ1 or pre-treated with GDF-15 for 48 hours and then co-treated with GDF-15 and TGFβ1 and / or BMP-4. TGFβ1, GDF-8, BMP-4 and TNFα were used as positive controls.

5.4.2 Animal experiments

The details of experiments for the MCT rat and Sugen/hypoxia mouse are documented in Chapter 2 and 4.

5.4.3 Human Samples

A small subset of PAH patients from the clinical study detailed in Chapter 3 underwent muscle biopsy by the Bergstrom technique detailed in Chapter 2. (265).

5.4.4 Cloning

5.4.4.1 Truncated TGFBR2 (TTGFBR2)

A TTGFBR2 was constructed with an active extracellular domain but only a short intracellular tail lacking the kinase domain meaning it was capable of binding TGFβ super-family members but not able to partake in intracellular signal transduction. The extracellular and trans-membrane portion of the TGFBR2 was identified. Primers were designed to isolate this portion, PCR, and cloning techniques were then used to drop the TTGFBR2 sequence into the pCDNA3 expression vector.

5.4.4.2 BMP responsive element BRE

A SMAD 1, 5 BRE binding element was cloned into pGL4luc vector using the technique described by Korchynskyi *et al*.(409).

5.4.4.3 pRL-TK without BRE

A BMP responsive element in the promoter region of the pRL-TK vector was removed using restriction digests, T4 DNA polymerase and relegation of blunt ends.

5.4.5 Luciferase experiments

5.4.5.1 Transfection

Cells were transfected with a SMAD 2, 3 dependent ($CAGA_{12}$) luciferase reporter or a SMAD 1, 5 dependent (BRE) luciferase reporter and pRL-TK or pR-LTK without BRE luciferase reporter. In experiments involving the interaction between TGFβ super-family members and receptors, cells were also transfected with a combination pCDNA3 with or without TGFBR2, ACVR2B, BMPR2 or a TTGFBR2 vector. Cells were treated with GDF-15, TGFβ-1, GDF-8 or BMP4.

5.4.5.2 Luciferase Activity

Luciferase activity was determined using a dual luciferase reporting system (Promega, Wisconsin, USA) and Luminark plate reader according to manufacturer's instructions. $CAGA_{12}$ or BRE dependent luminescence was divided by pRLTK luminescence.

5.4.6 Myotube Diameter

Cells were seeded in 6 well plates. The next day they were transfected as above with pCAGGS-EGFP with or without pCDNA3 or TTGBFR2. The next day cells were differentiated as above. After 10 days cells were treated with GDF-15 with or without 5(Z)-7-oxozeaenol or control. At 48 hours myotubes were visualized using a Fluorescent microscope at 10x magnification. Twenty representative images were taken at random from each of the 6 wells and myotubes identified by identifying multinucleated cells. Only myotubes transfected with pCAGGS-EGFP were included. Using Image J the average of 5 discreet measurements were taken across the length of the myotube to estimate its diameter (218).

5.4.7 Western blotting

Transfected and un-transfected myoblasts and myotubes were treated with GDF-15, TGFβ1 or TNFα at a number of different doses, with or without 5(Z)-7-oxozeaenol. Cells for phospho-protein analysis were serum starved overnight prior to treatment. Cells, animal TA muscle and PAH patient and control muscle biopsies were lysed with CLB and PMSF. Protein content was analysed using Bradford reagent against a known set of standards. Samples were analysed a described in Chapter 2 and membranes were cut at 55KDa so that they could be interrogated for 2 different proteins on the same blot. Membranes were then incubated with primary antibody in BSA or milk overnight at 4^{o}C. Blots were then washed with 0.05% TBS-T and incubated with secondary antibody conjugated with horseradish peroxidase for 1 hour at room temperature. They were washed again and exposed to Pierce enhanced chemiluminecence (ECL) detection reagent and imaged on an Ettan dige-imager (EDI) or with radiographic film using a photo-developer. Blots were then analysed by densitometry using Image J software.

5.4.8 Quantitative real time polymerase chain reaction (qPCR)

qPCR was carried out as previously described using primers detailed in Chapter 2 (265). Samples from myoblasts and myotubes treated with GDF-15, 5(Z)-7-oxozeaenol, SB431542 or vehicle control and TA samples from animal experiments were analysed using primers listed below. All mRNA levels were normalised to levels of housekeeping genes RPLPO and GAPDH within the samples.

5.4.9 Immunofluorescence

Myoblasts were serum starved overnight and then treated with GDF-15, TNFα or vehicle control or transfected with TGFBR2 or ACVR2B. Cells were then fixed in 4% PFA and lysed with 1% triton. Cells were then blocked for in 5% milk before being incubated in PBS-T with 5% milk containing with antibodies listed in Chapter 2 overnight at 4^{o}C. Cells were again washed in PBS-T and then incubated in secondary antibody and then in DAPI. Cells were washed and stored in PBS and were then imaged

on a widefield fluorescent microscope at 10x magnification, using filters set at to pick up green, red and blue light. Images were analysed using Image J software to calculate relative nuclear fluorescence.

5.4.10 Statistics

Results were expressed as mean and standard error of the mean or median and range dependant on the distribution of the data, which was assessed by Kolmogorov-Smirov, D'Agostino and Pearson test and the Shapiro-Wilk test normality tests as well as visually using histograms. Student's t-test with or without Welch's correction or Mann-Whitney U test were used to compare differences between 2 groups. When more than one group was to be compared a one way or repeated measures ANOVA with Bonferroni correction or Kruskall-Wallace with Dunn's correction was used. Repeated measures ANOVA was specifically employed for the analysis of time course experiments where a single passage of cells was treated with the same dose of GDF-15 for differing times on the same day. Where the above analyses were not possible due to lack of variability in the control samples a one sample t-test or a Wilcoxon signed rank test was used.

5.5 Results

5.5.1 In myoblasts GDF-15 does not stimulate SMAD 2, 3 and decreases SMAD 1, 5 response

GDF-15 caused no change in SMAD 2, 3 dependent luciferase activity at high or low dose when compared to control. In fact at 5 ng/ml there was a trend to a decrease in SMAD 2, 3 dependent luciferase activity (Figures 5.1 A and B). As a positive control TGFβ1 caused a significant increase in SMAD 2, 3 dependent luciferase activity at very low dose, down to 0.1 ng/ml (Figure 5.1C). GDF-15 also caused no significant change in SMAD 1, 5 dependent luciferase activity in myoblasts treated with 5 or at 50 ng/ml of GDF-15 for 24 hours. BMP-4 at 10 ng/ml acted as a positive control (Figure 5.2 A, B and C).

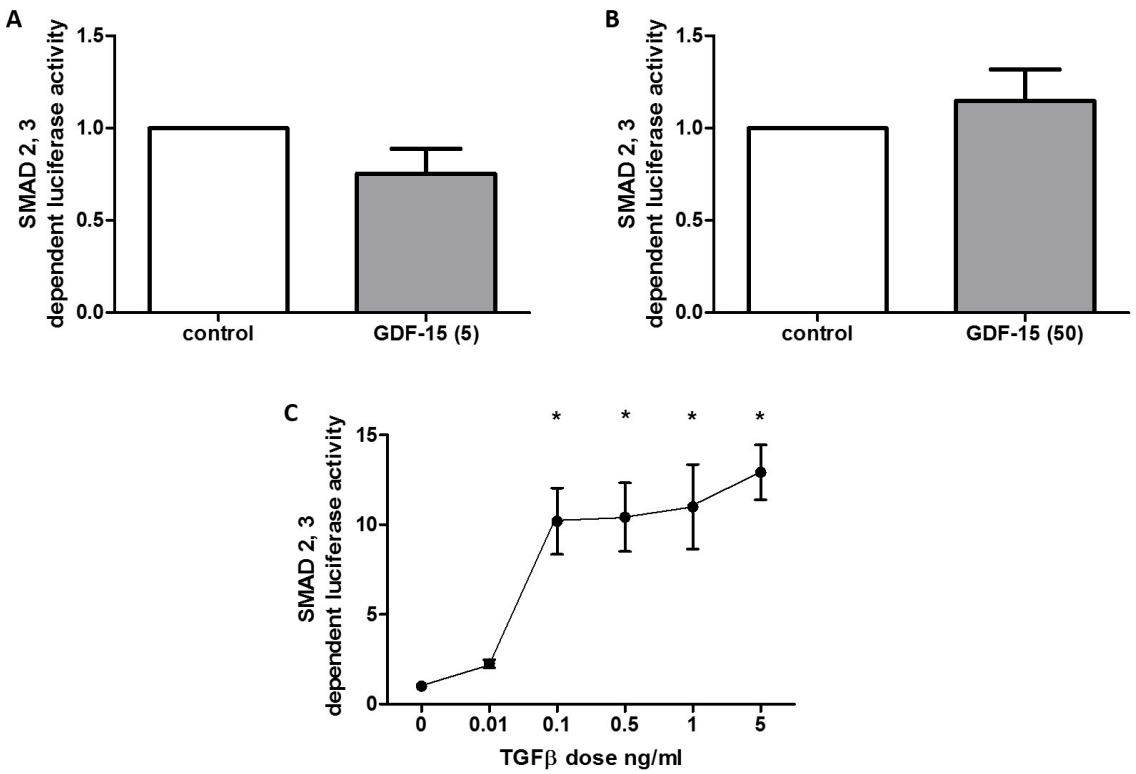

Figure 5.1 SMAD 2, 3 dependent luciferase activity in C2C12 myoblasts treated with growth and differentiation 15 (GDF-15). **A.** GDF-15 at 5ng/ml for 6 hours (n = 7) (One sample t test p = 0.118). **B.** GDF-15 at 50ng/ml for 6 hours (n = 7) (One sample t test p = 0.416). **C.** Transforming growth factor β 1 (TGFβ1) at a number of different doses for 6 hours (n=3) (One way ANOVA p = 0.018).

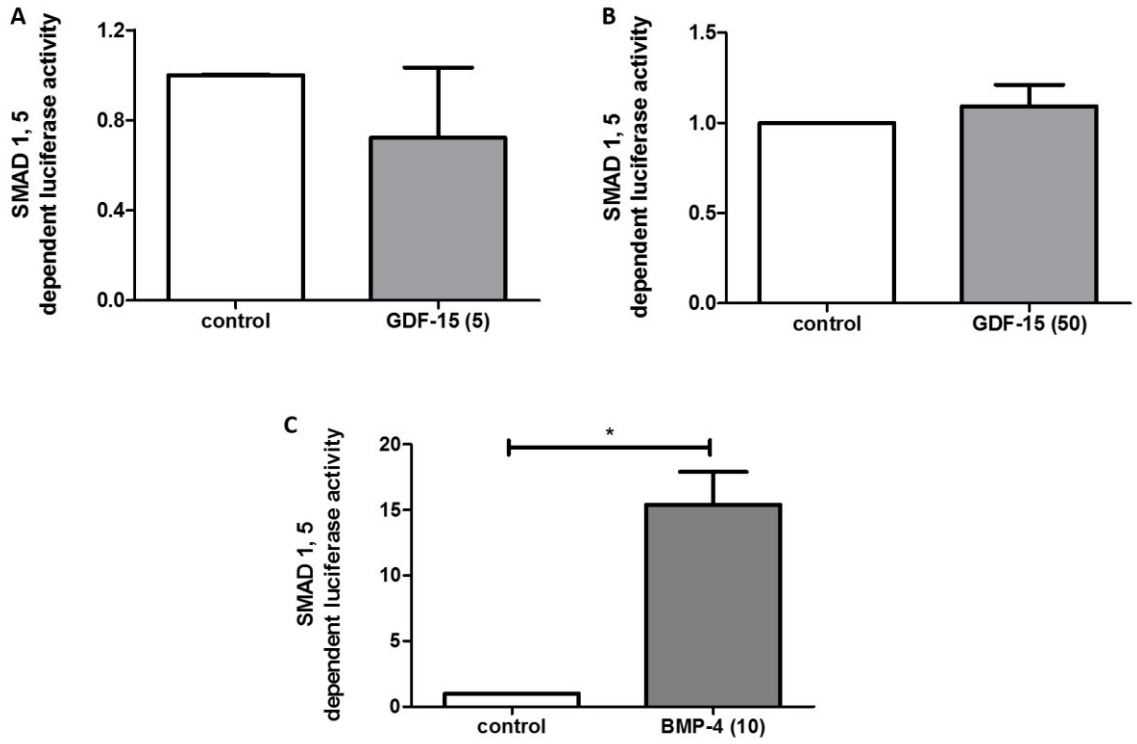

Figure 5.2. SMAD 1, 5 dependent luciferase activity in C2C12 myoblasts treated with growth and differentiation 15 (GDF-15). A. Growth and differentiation factor (GDF-15) at 5ng/ml for 24 hours (n = 4) (Wilcoxon signed rank test p = 0.875). **B.** GDF-15 at 50ng/ml for 24 hours (n = 14) (Wilcoxon signed rank test p = 0.950).**C.** Bone morphogenetic protein 4 (BMP) at 10ng/ml for 24 hours as a positive control caused a significant increase in SMAD 1, 5 dependent luciferase response (n = 4) (One sample t-test p = 0.010).

5.5.2 GDF-15 causes a significant increase in significant increase in SMAD 2, 3 dependent response in TGFBR2 over-expressing cells.

Over-expression of the TGFBR2, the ACVR2B and the BMPR2 receptors was demonstrated using western blot (Figure 5.3 A - C) Over-expression of the TGFBR2 and ACVR2B was also shown using immunofluorescence (Figure 5.4 A and B) (Negative controls are shown in appendix 5.1).

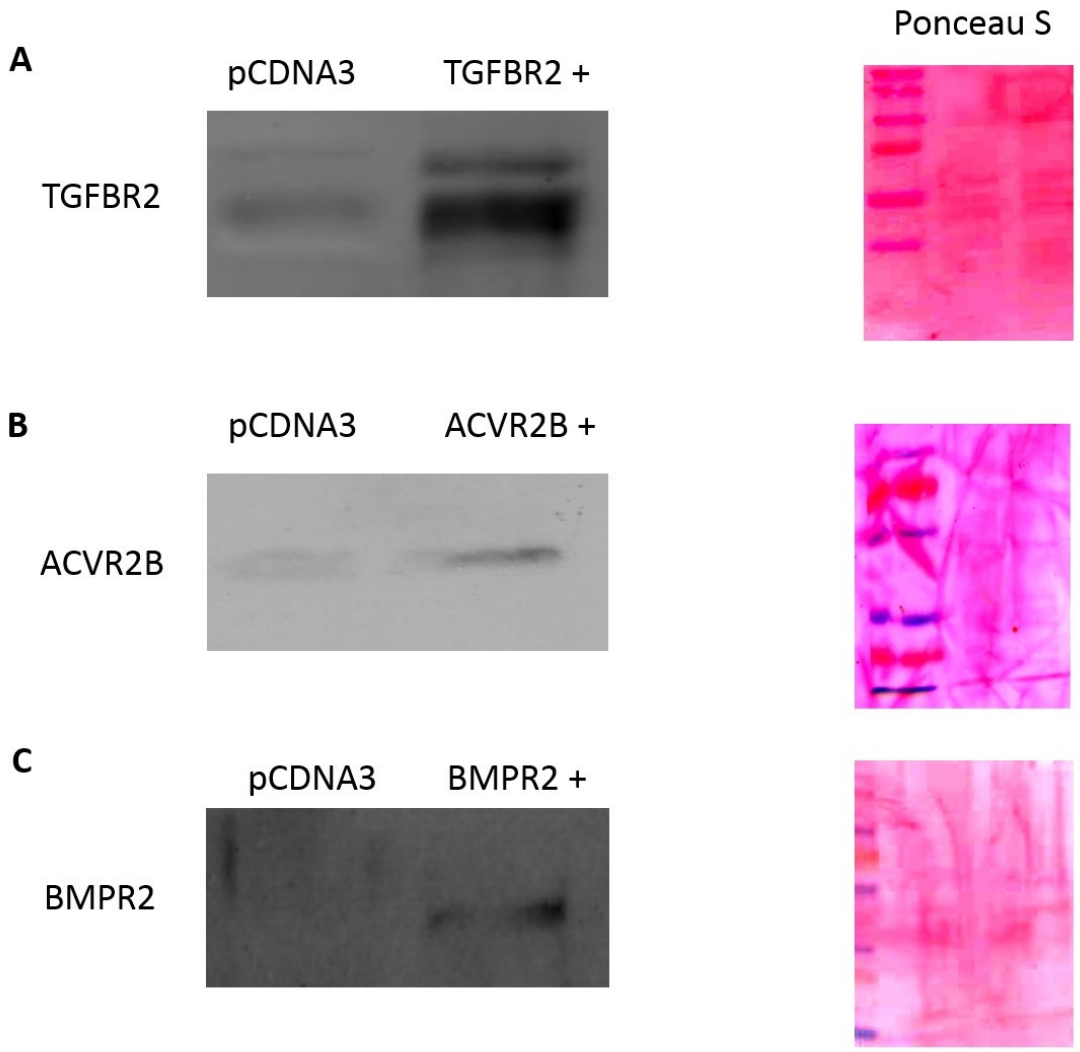

Figure 5.3. Western blot showing over-expression of receptors in C2C12 cells. A. pCDNA3 or the Transforming growth factor β receptor 2 (TGFBR2) probed with anti-TGFBR2 antibody with accompanying Ponceau S of the blot (n = 1); **B.** pCDNA3 or the Activin receptor 2B (ACVR2B) probed with anti-ACVR2B antibody with accompanying Ponceau S of the blot (n = 1); **C.** pCDNA3 or the Bone morphogenetic protein receptor 2 (BMPR2) probed with anti-BMPR2 antibody with accompanying Ponceau S of the blot (n = 1).

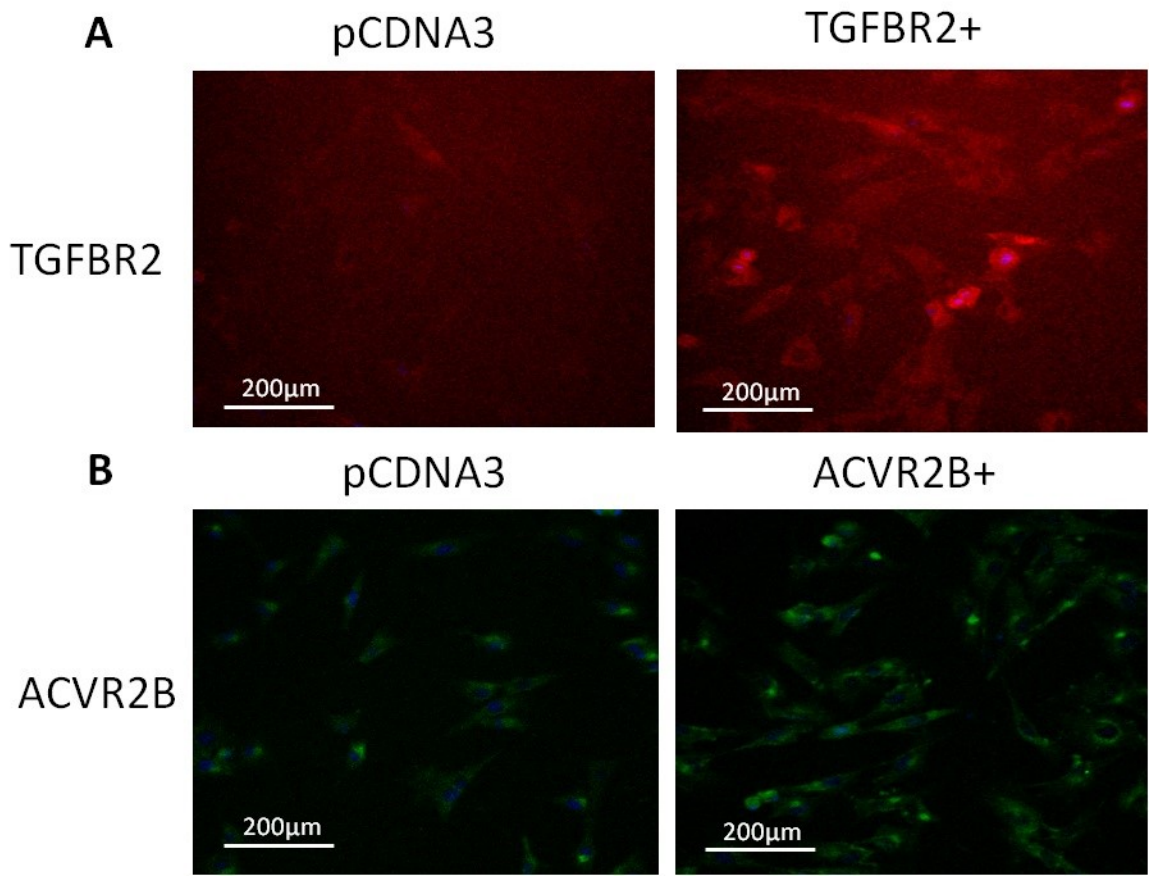

Figure 5.4. Immunofluorescence showing over-expression of receptors in C2C12 cells A. Immunofluorescence of cells over-expressing pCDNA3 or the Transforming growth factor β receptor 2 (TGFBR2) probed with anti-TGFBR2 antibody and Alexa-Fluor 568 and DAPI (n = 1). **B.** Immunofluorescence of cells over-expressing pCNDA3 or the Activin receptor 2B (ACVR2B) probed with anti-ACVR2B antibody and Alexa-Fluor 488 and DAPI (n = 1).

Over-expression of the TGFBR2 caused a significant upregulation in SMAD 2, 3 and a significant reduction in SMAD 1, 5 dependent luciferase responses (Figure 5.5 A). Over-expression of the ACVR2B caused a significant reduction in SMAD 2, 3 response but a significant increase in SMAD 1, 5 luciferase response, whilst over-expression of the BMPR2 caused a significant increase in SMAD 1, 5 responses (Figures 5.5 A and B). Because SMAD 2, 3 responses to over-expression of the ACVR2B showed a downregulation in signal I attempted to prove that the ACVR2B that we overexpressed was functional by stimulating the cells with their natural ligand and known upstream mediator of SMAD 2,3 signalling, GDF-8. At 50ng/ml no SMAD 2, 3 dependent luciferase activity was seen in pCDNA3 transfected cells but there was a significant increase in SMAD 2, 3 dependent luciferase activity in response to GDF-8

stimulation in the presence of the ACVR2B at this dose. At higher doses GDF-8 could stimulate SMAD 2, 3 dependent luciferase activity in pCDNA3 transfected cells (Figure 5.5 C).

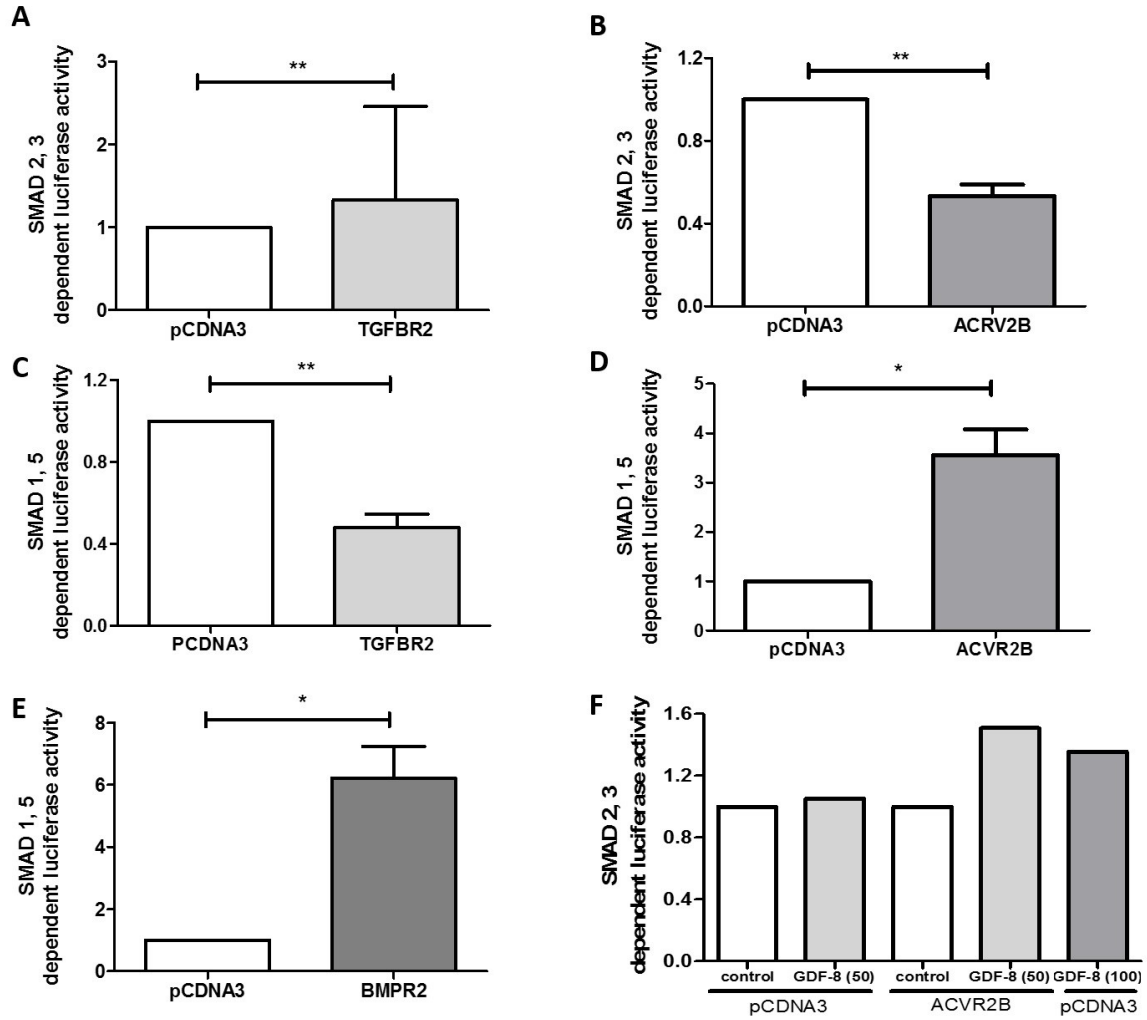

Figure 5.5 Effect of receptor over-expression on SMAD 2, 3 and SMAD 1, 5 dependent luciferase activity in C2C12 cells. Difference in SMAD 2, 3 dependent luciferase activity in: **A.** pCDNA3 and TGFBR2 over-expressing C2C12 myoblasts (n = 9) (Wilcoxon signed rank test p = 0.008); **B.** pCDNA3 and ACVR2B over-expressing C2C12 myoblasts (n = 4) (One sample t test p = 0.003) Difference in SMAD 1, 5 dependent luciferase activity in: **C.** pCDNA3 and TGFBR2 over-expressing C2C12 myoblasts (n = 4) (One sample t test p = 0.004); **D.** pCDNA3 and ACVR2B over-expressing C2C12 myoblasts (n = 4) (One sample t test p = 0.016); **E.** pCNDA3 and BMPR2 over-expressing C2C12 myoblasts (n = 4) (One sample t test p = 0.015)**. F.** SMAD 2, 3 dependent luciferase responses to GDF-8 treatment for 6 hours at 50 ng/ml and at 100 ng/ml in C2C12 myoblasts in pCDNA3 and ACVR2B transfected cells (n = 1).

GDF-15 at 50ng/ml caused no significant increase in SMAD 2, 3 dependent luciferase activity in pCDNA3 transfected cells. However, in cells over-expressing the TGFBR2, GDF-15 at 50ng/ml caused a significant increase in SMAD 2, 3 dependent luciferase activity (Figure 5.6 A). No similar change was seen in cells over-expressing the ACVR2B (Figures 5.6 B). When cells over-expressing the TGFBR2 were treated with low dose GDF-15 (5ng/ml) this effect on SMAD 2, 3 dependent luciferase activity was not seen (Figures 5.7). Over-expression of the TGFBR2, ACVR2B or BMPR2 and treatment with GDF-15 at 50ng/ml resulted in a small but significant increase in SMAD 1, 5 dependent luciferase activity over that seen in pCDNA3 transfected GDF-15 treated cells (Figure 5.8 B).

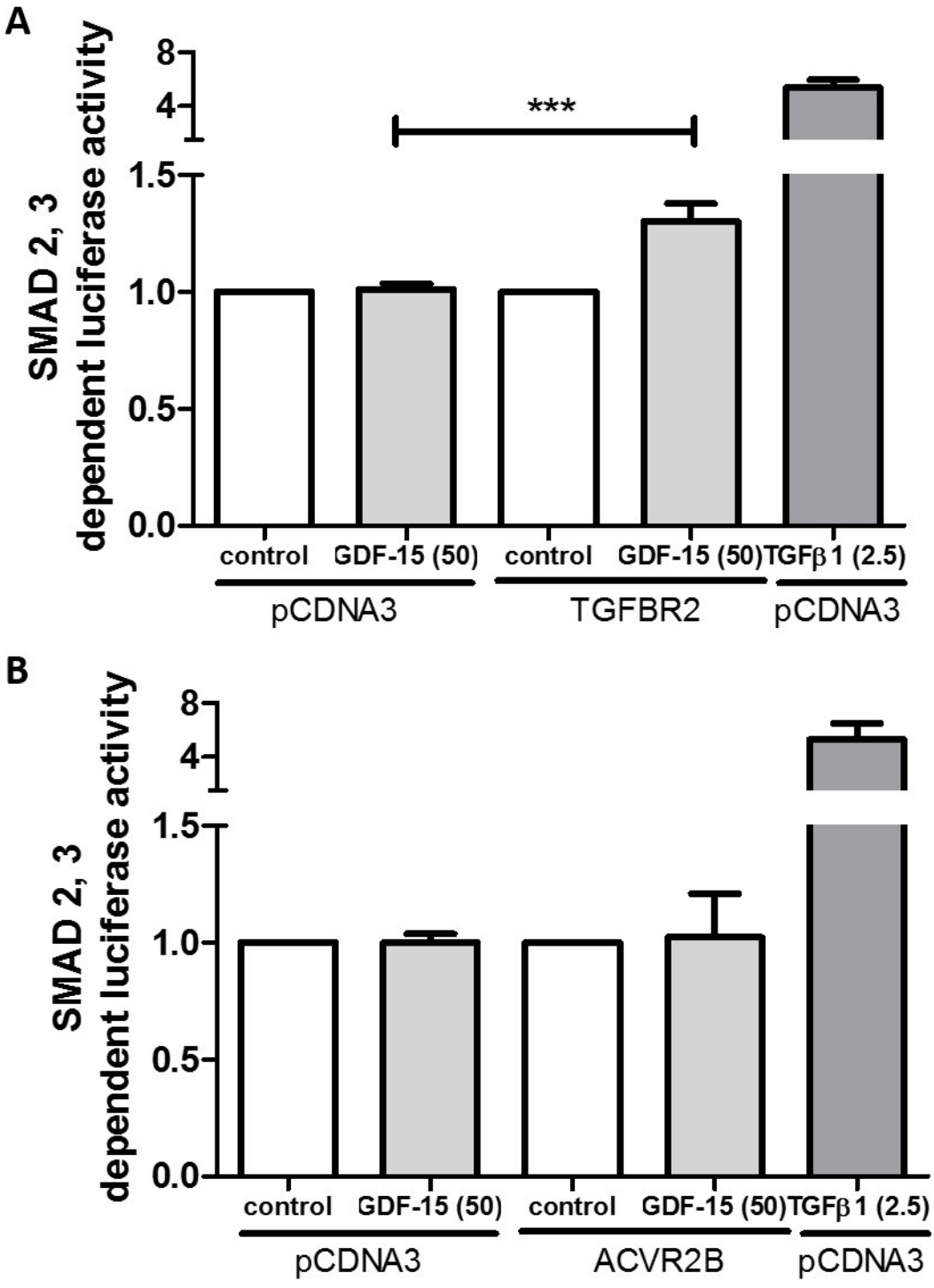

Figure 5.6. SMAD 2, 3 dependent luciferase activity in C2C12 myoblasts over-expressing pCDNA3, TGFBR2, or ACVR2B treated with vehicle control or GDF-15 at 50 ng/ml for 6 hours. Results were normalised to luciferase activity of control treatment for each individual receptor. TGFβ1 at 2.5 ng/ml was used as a positive control **A.** GDF-15 resulted in a significant up-regulation in SMAD 2, 3 dependent luciferase dependent activity in TGFBR2 over-expressing cells (n = 12) (One way ANOVA $p < 0.001$) **B.** GDF-15 caused no significant change in SMAD 2, 3 dependent luciferase activity in cells transfected with the ACVR2B (n = 8) (Kruskall-Wallace $p = 0.032$, but no difference between the groups).

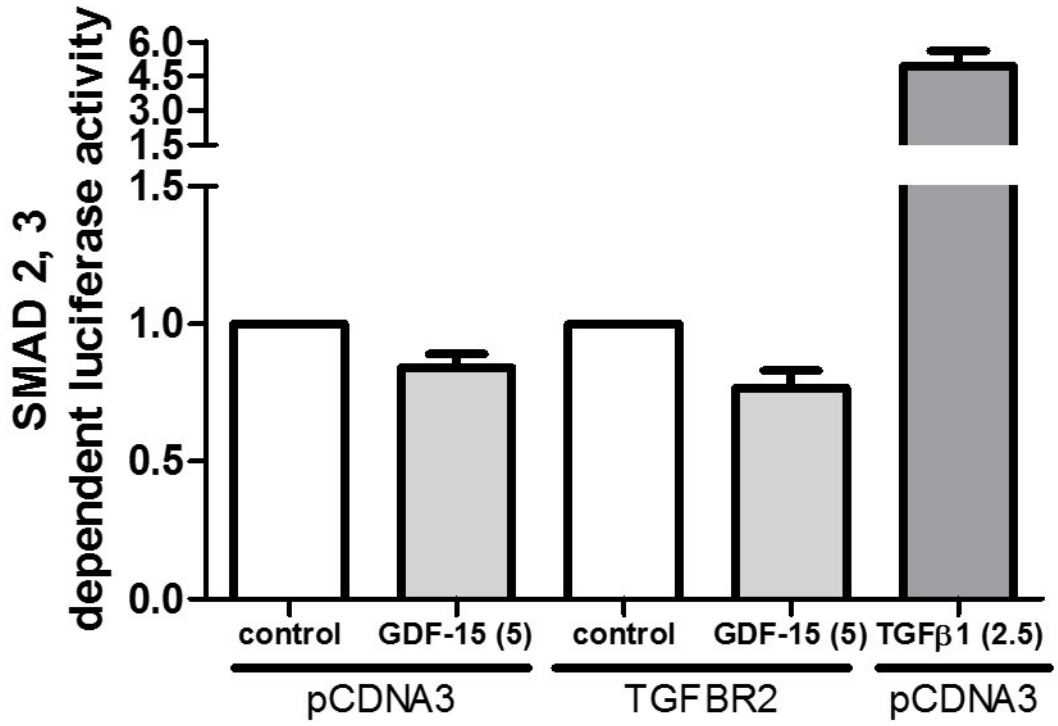

Figure 5.7. SMAD 2, 3 dependent luciferase activity in C2C12 myoblasts over-expressing pCDNA3 or TGFBR2 with vehicle control or GDF-15 at 5 ng/ml for 6 hours. Results were normalised to luciferase activity of control treatment for each individual receptor. TGFβ1 at 2.5 ng/ml was used as a positive control. GDF-15 caused no significant change in SMAD 2, 3 dependent luciferase activity in TGFBR2 over-expressing cells when compared to GDF-15's effects in pCDNA3 transfected cells (n = 3) (One way ANOVA p = 0.007, but no difference between PCDNA3 GDF-15 and TGFBR2 GDF-15).

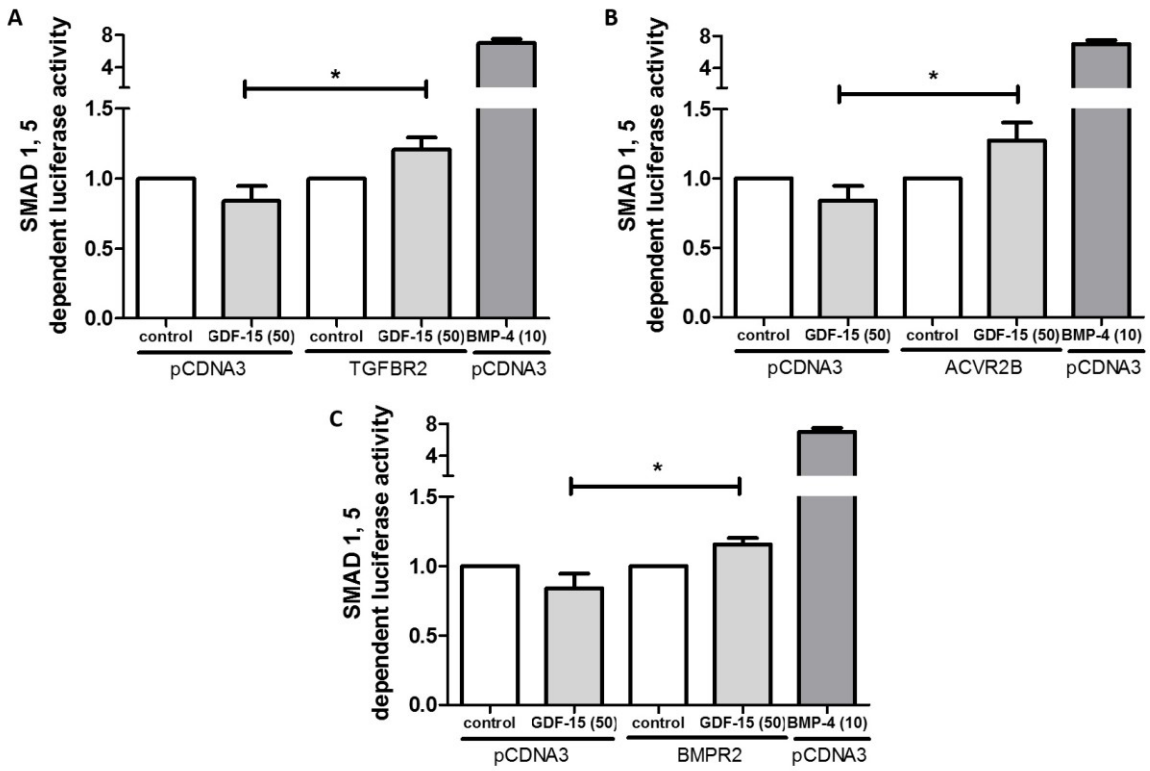

Figure 5.8. SMAD 1, 5 dependent luciferase activity in C2C12 myoblasts over-expressing pCDNA3, TGFBR2, ACVR2B or BMPR2 treated with vehicle control or GDF-15 at 50 ng/ml for 24 hours. Results were then normalised to control treatment for each individual receptor. BMP4 at 10 ng/ml was used as a positive control **A.** GDF-15 caused a significant increase in SMAD 1, 5 dependent luciferase activity in TGFBR2 over-expressing cells (n = 3) (One way ANOVA p = 0.034). **B.** GDF-15 caused a significant increase in SMAD 1, 5 dependent luciferase activity in ACVR2B over-expressing cells (n = 3) (One way ANOVA p = 0.038). **C.** GDF-15 caused a significant increase in SMAD 1, 5 dependent luciferase activity in BMPR2 over-expressing cells (n = 3) (One way ANOVA p = 0.030).

5.5.3 In myoblasts longer term treatment with GDF-15 failed to alter TGFβ1 or BMP-4 dose responses

We have previously shown that GDF-15 may augment TGFβ1 activity through actions on miR-181 (265). The effects of GDF-15 on SMAD 2, 3 dependent luciferase activity in TGFβ1 treated cells and SMAD 1, 5 dependent luciferase activity in BMP-4 treated cells were therefore examined. There was no difference in SMAD 2, 3 dependent luciferase responses to TGFβ1 in the presence or absence of co-treatment with GDF-15 (Figure 5.9 A and B). Cells were then pre-treated with GDF-15 (50ng/ml) for 48 hours and then incubated for 6 hours with fresh GDF-15 with or without TGFβ1 or BMP4 at a number of doses. At the 54 hour time point mean SMAD 2, 3 dependent luciferase activity was higher in response to GDF-15 alone but this difference did not reach statistical significance (Figure 5.9 C). There was no difference in the subsequent dose response curve to TGFβ1 in these pre-treated cells (Figure 5.9 D). Similarly mean SMAD 1, 5 dependent luciferase activity was higher at 54 hours in GDF-15 pre-treated cells (Figure 5.9 E) but did not reach statistical significance and no difference in SMAD 1, 5 dependent responses to BMP-4 was observed with GDF-15 pre-treatment at any dose used (Figure 5.9 F).

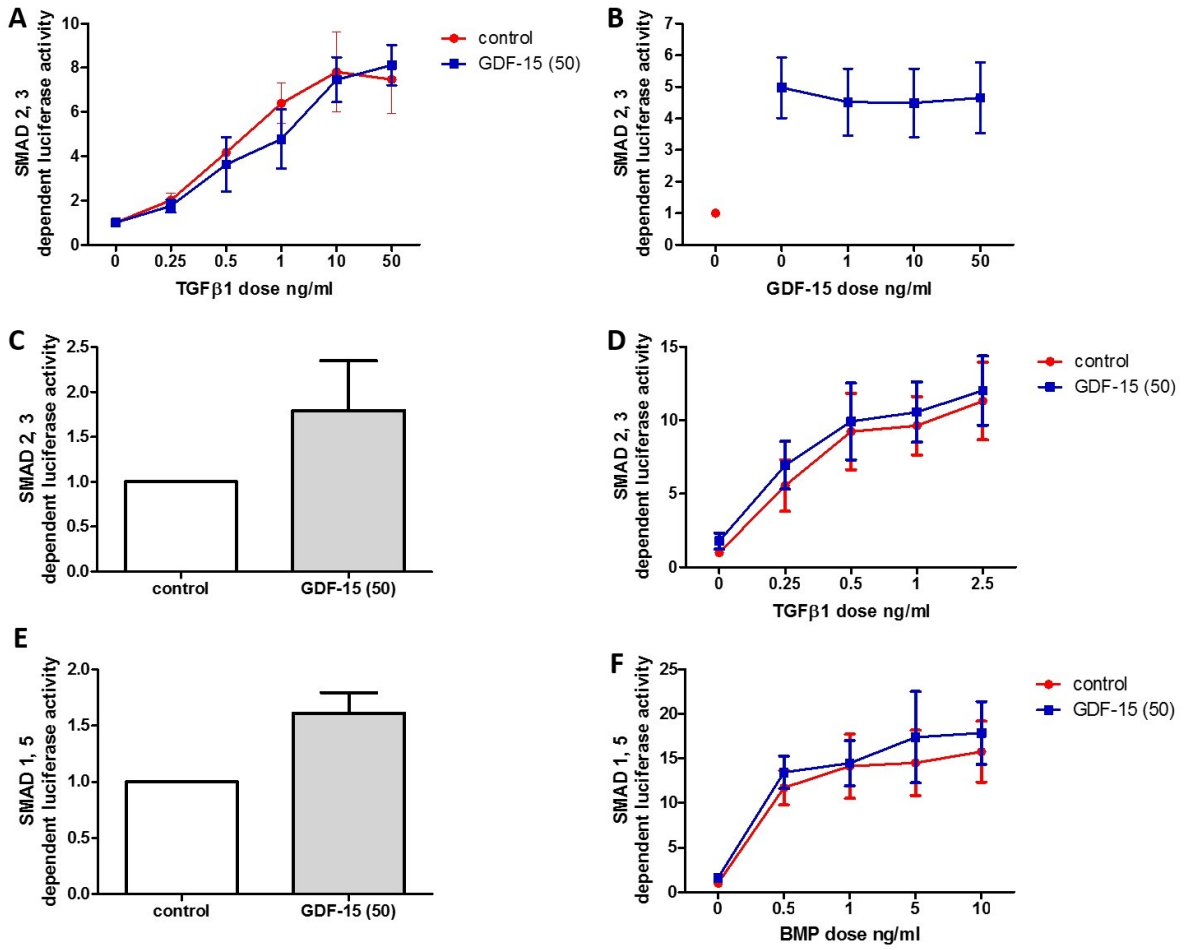

Figure 5.9. SMAD 2, 3 and SMAD 1, 5 dependent luciferase activity in cells co-treated with GDF-15 and TGFβ1 / BMP-4. A. SMAD 2, 3 dependent luciferase activity in C2C12 myoblasts treated for 6 hours with various doses of TGFβ1 in the presence or absence of GDF-15 at 50 ng/ml. There was no difference in response between GDF-15 and control treated cells (n = 3) (Two way ANOVA p = 0.515). **B.** SMAD 2, 3 dependent luciferase activity in cells treated with GDF-15 at a number of doses for 6 hours in the presence of TGFβ1 at 2.5 ng/ml. There was no+ difference in response with GDF-15 at any dose (n = 4) (One way ANOVA p = 0.987). **C.** SMAD 2, 3 dependent luciferase activity in C2C12 myoblasts treated with GDF-15 at 50 ng/ml for 54 hours (n = 3) (One sample t test p = 0.285). **D.** SMAD 2, 3 dependent luciferase activity in cells pre-treated with GDF-15 at 50 ng/ml for 48 hours then co-treated with TGFβ1 at various doses and GDF-15 at 50 ng/ml for 6 hours, There was no difference in response between GDF-15 and control pre-treated cells (n = 3) (Two way ANOVA p = 0.485). **E.** SMAD 1, 5 dependent luciferase response in C2C12 myoblasts treated with GDF-15 at 50 ng/ml for 54 hours (n = 3) (One sample t test p = 0.079). **F.** SMAD 1, 5 dependent luciferase activity in cells pre-treated with GDF-15 at 50 ng/ml for 48 hours then co-treated with BMP4 at various doses and GDF-15 at 50 ng/ml for 6 hours, There was no difference in response between GDF-15 and control pre-treated cells (n = 3) (Two way ANOVA p = 0.431).

5.5.4 A truncated TGFBR2 (TTGBFR2) failed to prevent GDF-15 mediated atrophy in myotubes.

A truncated TGFBR2 expression vector was then cloned, which lacked part of the intra-cellular portion of the protein essential for signal propagation but still allowing ligand binding. When over-expressed* the TTGFBR2 reduced SMAD 2, 3 dependent luciferase activity when compared to pCDNA3 transfected cells (Figure 5.10 A). When examining the effects of the TTGFBR2 on the response to GDF-15, there was a significant increase in SMAD 2, 3 dependent luciferase responses to GDF-15 at 5ng/ml in TTGFBR2 over-expressing cells when compared to responses in pCDNA3 transfected cells (Figures 5.10 B). There was no such change in cells over-expressing TTGFBR2 and treated with GDF-15 at 50ng/ml (Figure 5.10 C). GDF-15 (50 ng/ml) is known to cause a reduction in myotube diameter in 10 day differentiated myotubes (218). In pCAGGS-EGFP pCDNA3 transfected C2C12 cells, GDF-15 at high dose mean and relative myotube diameter was lower than in control treated cells, but this reduction did not meet statistical significance. This reduction in diameter was unaltered by over-expression of the TTGFBR2 (Figures 5.11 A - C).

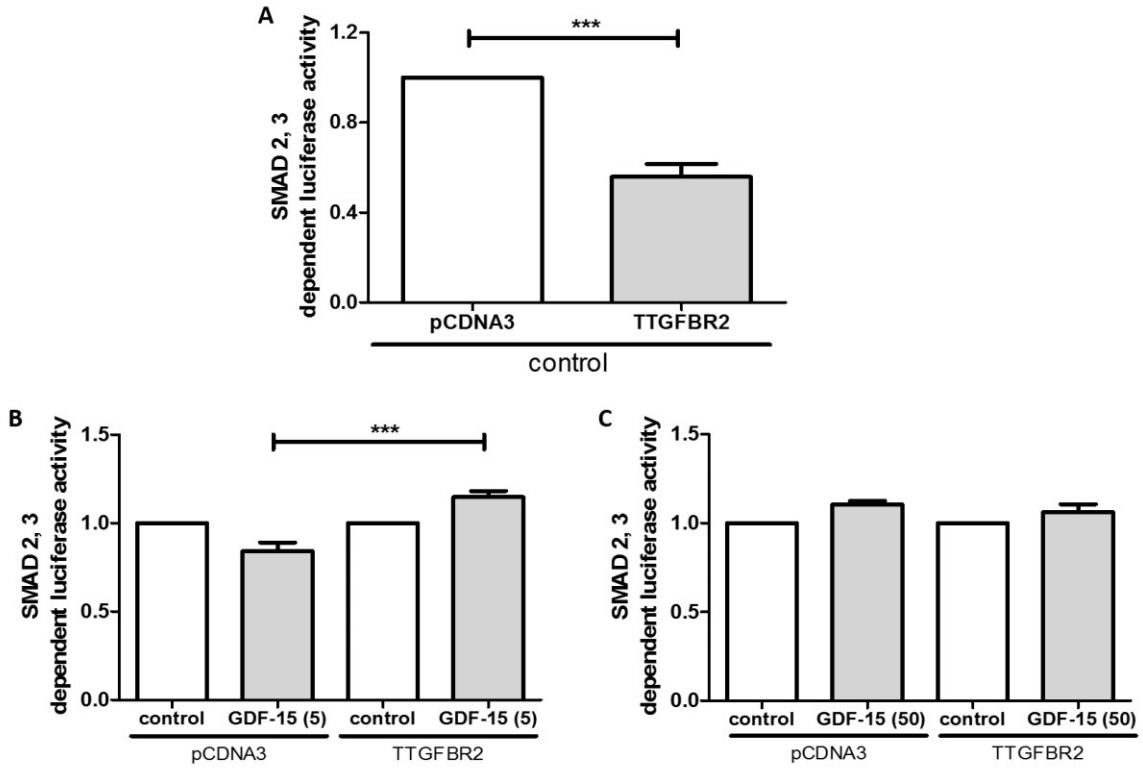

Figure 5.10 SMAD 2, 3 dependent luciferase responses in TTGFBR2 over-expressing cells A. SMAD 2, 3 dependent luciferase activity in pCDNA3 or TTGFBR2 transfected cells. TTGFBR2 caused a significant reduction in SMAD 2, 3 dependent luciferase activity when compared to pCDNA3 transfection in control treated cells (n = 8) (One sample t test $p < 0.001$). **B.** SMAD 2, 3 dependent luciferase activity in pCDNA3 and TTGFBR2 over-expressing cells treated with GDF-15 at 5 ng/ml for 6 hours. There was no a significant increase in GDF-15 responses in TTGFBR2 over-expressing cells when compared to those over-expressing pCDNA3 (n = 3) (One way ANOVA $p < 0.001$). **C.** SMAD 2, 3 dependent luciferase activity in pCDNA3 and TTGFBR2 over-expressing cells treated with GDF-15 at 50 ng/ml for 6 hours. There was no difference in GDF-15 responses in pCDNA3 and TTGFBR2 over-expressing cells (n = 3) (One way ANOVA test $p = 0.044$, but no difference between the groups).

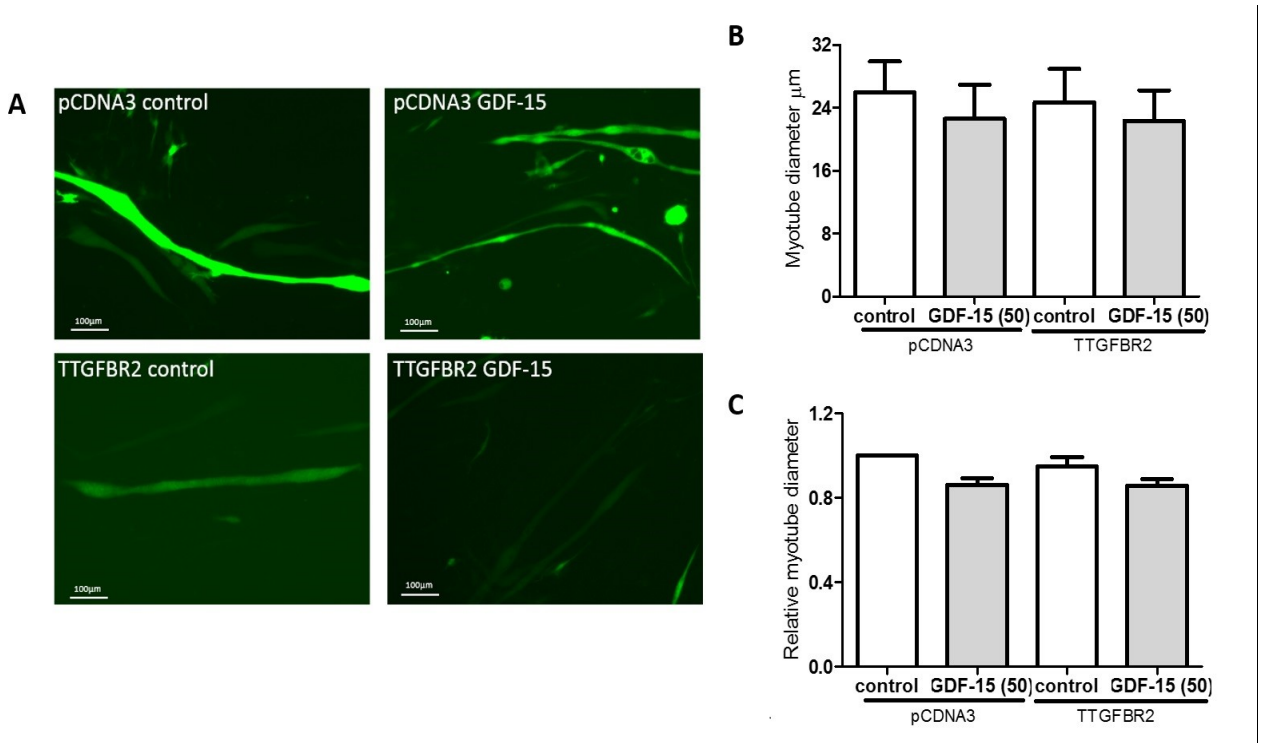

Figure 5.11 Myotube diameter in TTGFBR2 over-expressing GDF-15 treated cells. A. Representative GFP images of pCAGGS-EGFP expressing cells transfected with pCDNA3 or TTGFBR2 and treated with GDF-15 (50ng/ml) or vehicle control from which myotube diameters were measured. **B.** Myotube diameter in pCDNA3 or TTGFBR2 over-expressing cells treated with GDF-15 (50ng/ml) or vehicle control (n=3) (One way ANOVA p = 0.981). **C.** Fold change in myotube diameter in pCDNA3 or TTGFBR2 over-expressing cells treated with GDF-15 (50ng/ml) or vehicle control normalised to control myotube diameter (n=3) (One way ANOVA p = 0.035, No difference between groups).

5.5.5 GDF-15 may act through non-canonical TGFβ pathways, which is best studied in myotubes

The above results suggest that any SMAD response to GDF-15 in myoblasts is at most small. GDF-15's effects on non-canonical signalling in C2C12 myoblasts was studied next. Of particular interest was GDF-15's effects on the NFκB p65 pathway. GDF-15 (50ng/ml) caused an increase in nuclear localisation of NFκB p65 at 60 minutes post treatment (Figures 5.12A and B) (Negative controls are shown in appendix 5.1). GDF-15 treatment, also, caused a significant up-regulation in mRNA production of NFκB p65 in myoblasts after 48 hours (Figure 5.13 A). In order to see if TAK1 was an important intermediate in GDF-15's ability to increase mRNA production of NFκB p65 I treated C2C12 myoblasts with GDF-15 in the presence and absence of the TAK1 inhibitor 5(Z)-7-oxozeaenol (1000nM). There was a significant reduction in NFκB p65 mRNA expression in GDF-15 and TAK1i co-treated cells when compared to those treated with GDF-15 alone (Figure 5.13B).

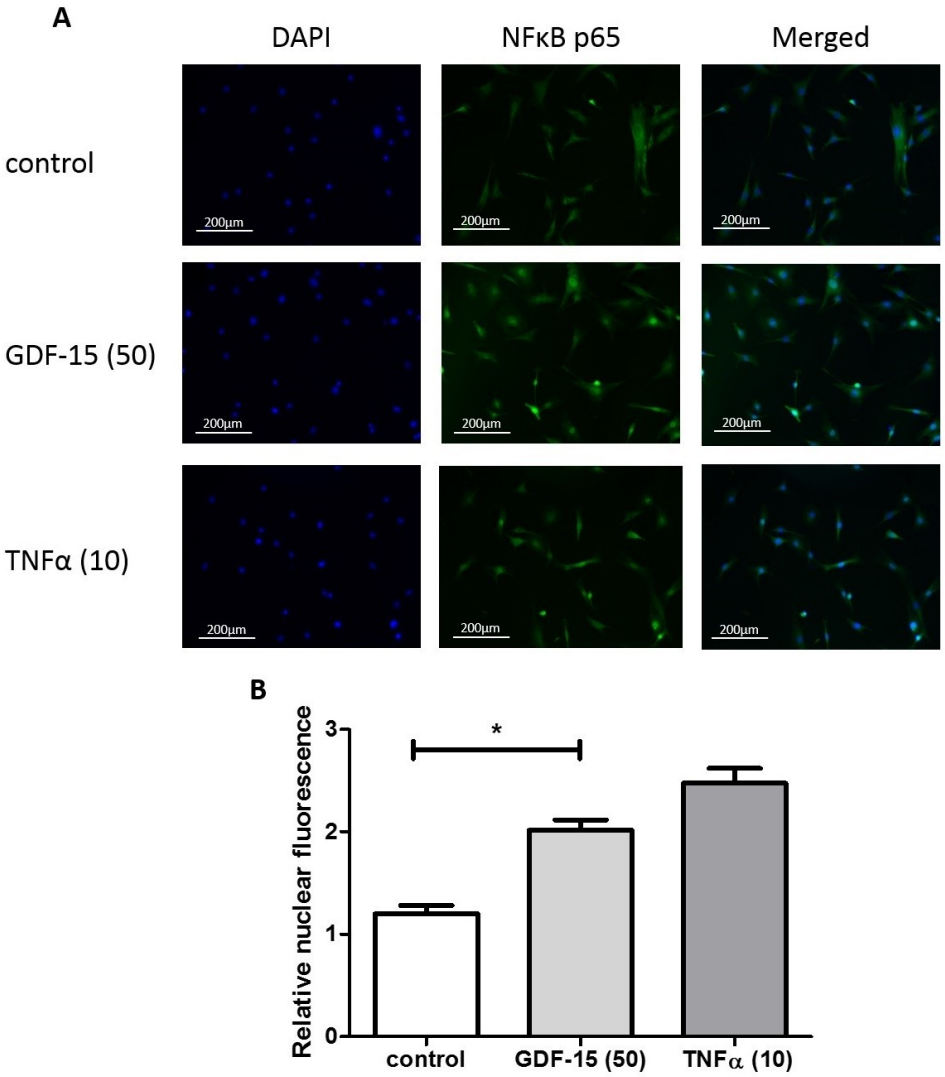

Figure 5.12 Nuclear localisation of NFκB p65 in response to GDF-15 treatment. A. Representative immunofluorescent images of C2C12 cells treated with control, GDF-15 50ng/ml or TNFα 10ng/ml for 1 hour and stained with anti-NFκB p65 and Alexa-Fluor 488 and DAPI. Images showing nuclear DAPI staining. NFκB p65 staining and a merged image are shown. **B.** Difference in relative immunofluorescent nuclear signal compared to total cell fluorescent signal in cells treated with control or GDF-15 50 ng/ml (n = 3) (Student's t test p = 0.003). TNF α acted as a positive control.

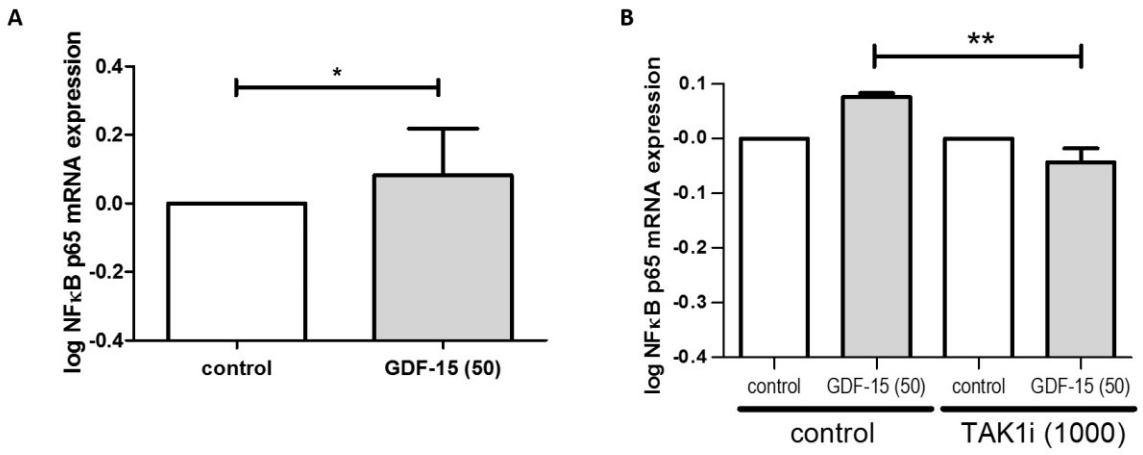

Figure 5.13. mRNA expression of NFκB p65 in response to GDF-15 and TAK inhibition A. log NFκB p65 mRNA expression in C2C12 myoblasts treated with control or GDF-15 50 ng/ml for 48 hours (n = 6) (Wilcoxon signed rank test p = 0.031). **B.** Differences in relative log NFκB p65 mRNA expression in C2C12 myoblast treated with GDF-15 in the presence or absence TAK1 inhibitor 5(Z)-7-oxozeaeol at 1000 nM (TAK1i) (n = 3) (One way ANOVA p = 0.001).

The effects of GDF-15 on phosphorylation of TAK1 in myoblasts was next examined by western blotting. TAK1 was shown to be constitutively active in myoblasts (Figure 5.14 A). When protein lysates from myoblasts were compared to those from myotubes a decrease in phospho-TAK1 and phospho-NFκB p65 activity was seen (figure 5.14 B). Furthermore, during serum starvation NFκB p65 was shown to be located in the nucleus of day 2 C2C12 myoblasts (Figure 5.14 C). This is in keeping with data from Bhatnagar *et al.* (361). The role of TAK1 and NFκB in propagating the effects of GDF-15 was therefore examined in myotubes rather than in myoblasts and was the focus of further investigations.

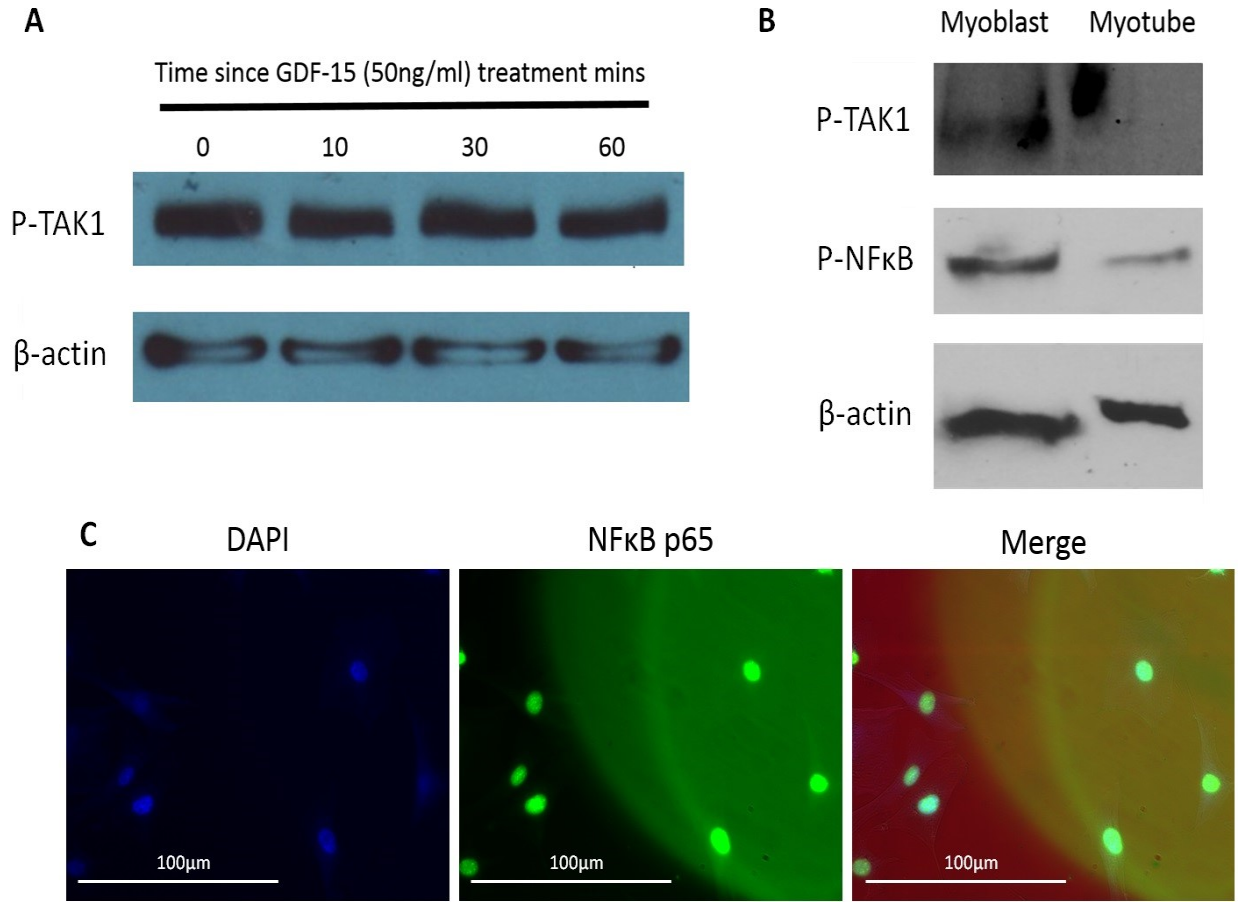

Figure 5.14 Non-canonical GDF-15 signalling in myoblasts versus myotubes. A. Western blot of Phospho-TGFβ activated kinase 1 (P-TAK1) and B-actin in myoblasts treated for 0, 10, 30 and 60 minutes with GDF-15 50 ng/ml (n = 1). **B**. Western blot of P-TAK1, phospho-nuclear factor Kappa B p65 (P-NFκB p65), and β-actin levels in myoblasts and myotubes (n = 1). **C.** Representative images of serum starved day 2 myoblasts stained with anti-NFκB p65, Alexa-Fluor 488 goat anti-rabbit secondary and DAPI imaged and merged to show nuclear localisation (n = 3).

5.5.6 GDF-15 activated TAK1 and NFκB p65 at high and low dose in C2C12 myotubes

In 10 day C2C12 myotubes GDF-15 at high dose (50ng/ml) caused phosphorylation of TAK1 which peaked at 60 minutes. GDF-15 treatment also caused phosphorylation of NFκB p65 which peaked at 120 minutes after treatment and caused a reduction in phosphorylation of p38MAPK which reached its nadir at 60 minutes (Figures 5.15 A-F). As a positive control TGFβ1 (0.5ng/ml) also caused a rapid phosphorylation of TAK1 (Figure 5.15 G and H). Having established the effects of GDF-15 at high dose, a dose response was performed. The maximum TAK1 phosphorylation effect was seen at 5ng/ml (Figure 5.16 A and B). NFκB p65 phosphorylation was also increased by 5ng/ml GDF-15 at 60 minutes (5.16 C and D). Although there was a trend to increase in P-p38 MAPK levels at this lower dose of 5ng/ml it did not meet statistical significance (Figure 5.16 E and F).

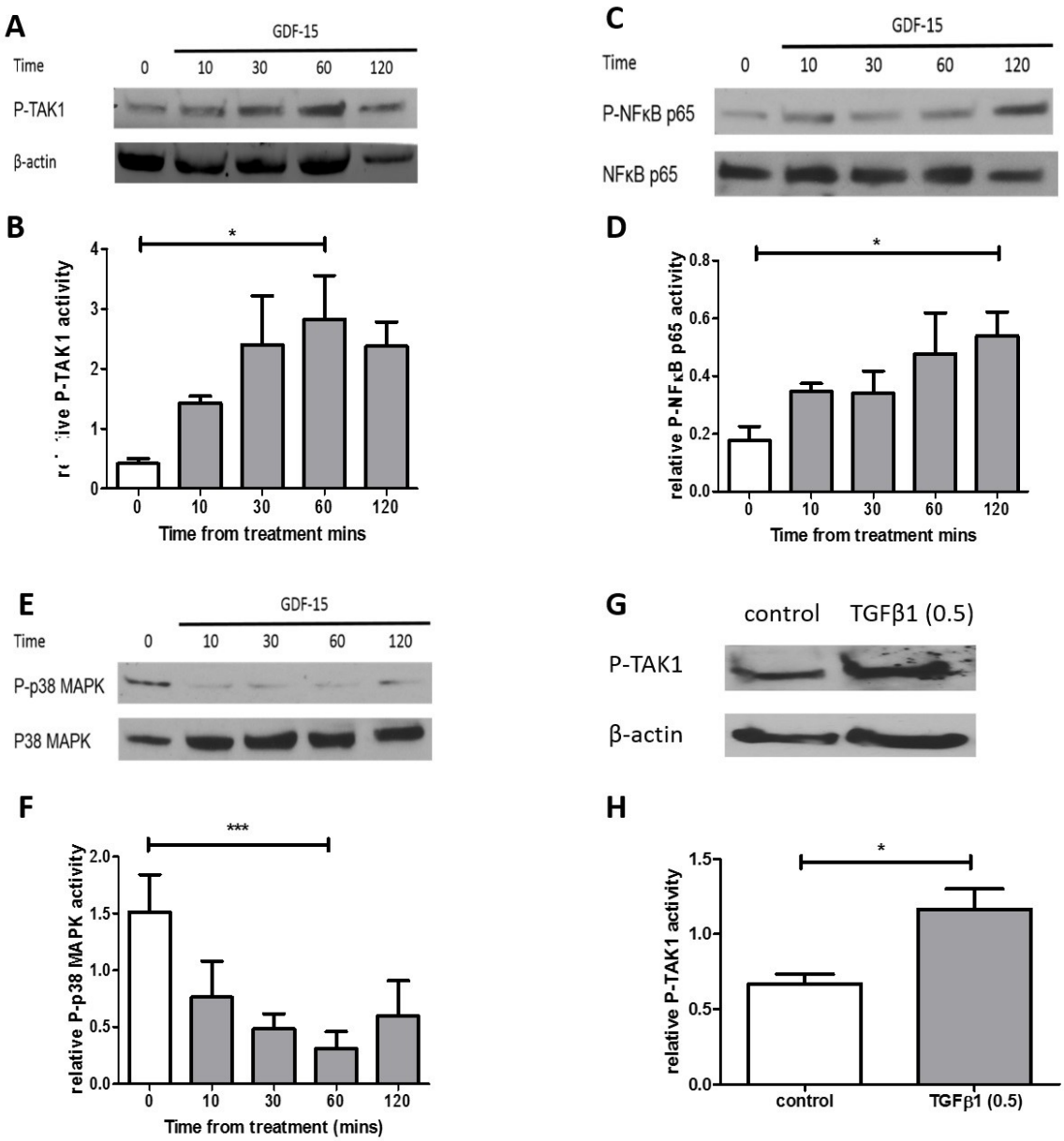

Figure 5.15. Western blots of day 10 myotubes treated for 0, 10, 30, 60 and 120 minutes with 50 ng/ml of GDF-15. The time at which GDF-15 caused its maximal response for each phosphorylated protein was used for statistical comparison. **A.** Phosphorylated TAK1 (P-TAK1) activity and β actin levels in GDF-15 treated myotubes (Representative blot n = 4). **B.** Relative intensity of P-TAK1 activity normalised to β-actin (Repeated measures ANOVA p = 0.020). **C.** Phosphorylated p65 NFκB (P-NFκB) activity and total NFκB levels in GDF-15 treated myotubes (Representative blot n = 4). **D.** Relative intensity of P-NFκB activity normalised to total NFκB (Repeated measured ANOVA p = 0.046). **E.** Phosphorylated p38 MAP kinase activity in GDF-15 treated myotubes (P-p38 MAPK) and total p38 MAPK levels inGDF-15 treated myotubes (Representative blot n = 4). **F.** Relative intensity of P-p38 MAPK activity normalised to total p38 MAPK (Repeated measures ANOVA p < 0.001). **H.** P-TAK1 activity and β-actin levels in TGFβ1 treated myotubes for 60 minutes (Representative blot n = 3). **H.** Relative intensity of P-TAK1 activity normalised to β-actin (Student's t-test p = 0.047).

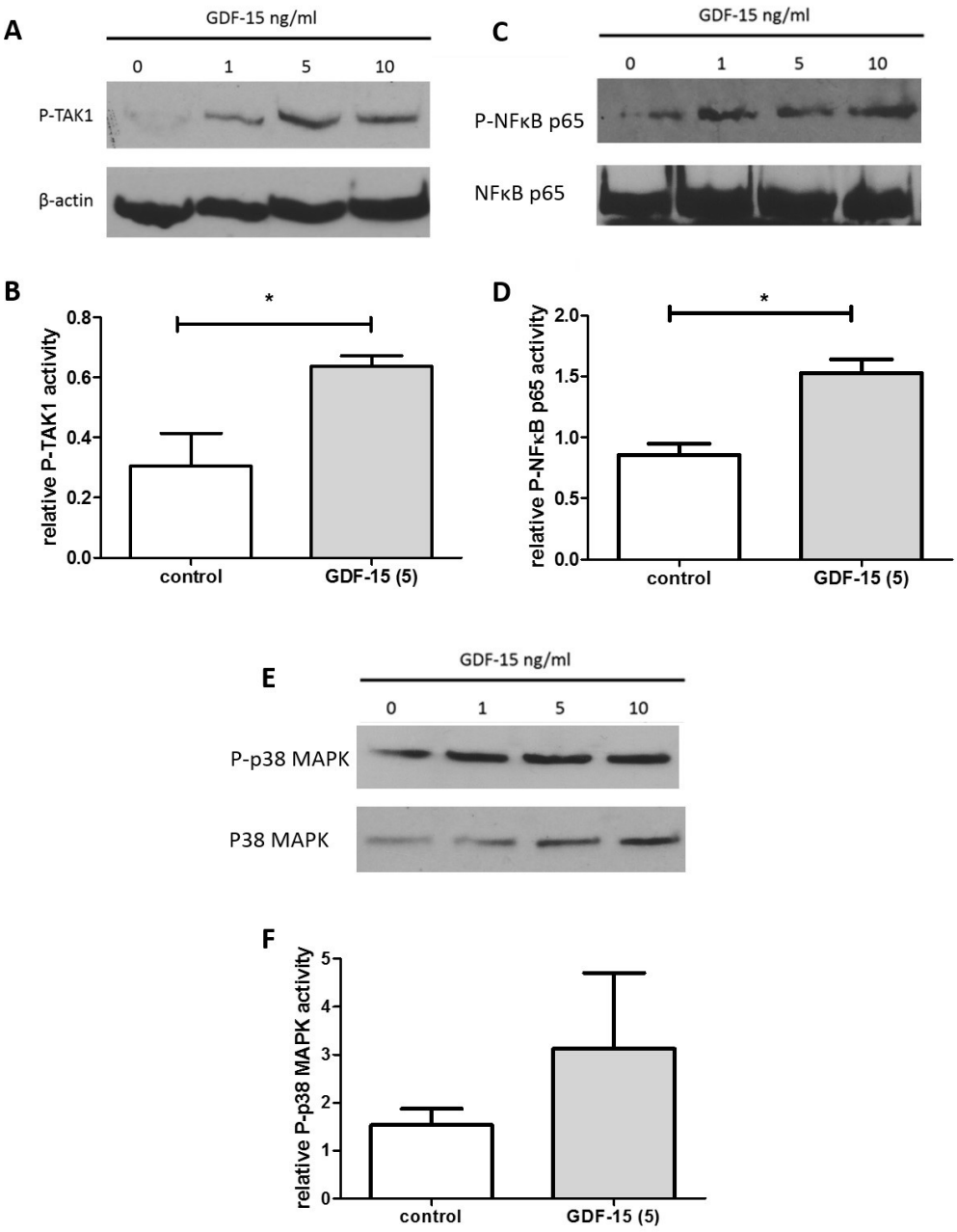

Figure 5.16. Western blot of day 10 myotubes treated for 60 minutes with 0, 1, 5 or 10 ng/ml of GDF-15. The western of the dose response is presented but only the treatment with 5 ng/ml was repeated 3 times for statistical analysis. **A.** Phosphorylated TAK1 (P-TAK1) activity and β actin levels in GDF-15 treated cells (n = 3). **B.** Relative intensity of P-TAK1 activity normalised to β-actin in cells treated with vehicle control and GDF-15 (5 ng/ml) (Student's t-test p = 0.045). **C.** Phosphorylated p65 NFκB (P-NFκB) activity and total NFκB levels in GDF-15 treated cells (n = 3). **D.** Relative intensity of P-NFκB activity normalised to total NFκB in cells treated with vehicle control and GDF-15 (5 ng/ml) (Student's t-test p = 0.011). **E.** Phosphorylated p38 MAP kinase activity in GDF-15 treated cells (P-p38 MAPK) and total p38 MAPK levels inGDF-15 treated cells (n = 3). **F.** Relative intensity of P-p38 MAPK activity normalised to total p38 MAPK in cells treated with vehicle control and GDF-15 (5 ng/ml) (Student's t-test p = 0.378).

5.5.7 GDF-15 mediated myotube atrophy can be antagonised by the TAK1 inhibitor 5(Z)-7-oxozeaenol

Our group has previously shown that GDF-15 (50ng/ml) can cause the up-regulation of atrogin-1 and MuRF-1 mRNA (265) and cause a reduction in myotube diameter in vitro (218). The data above suggest that GDF-15 can activate TAK1, therefore the effects of the TAK1 inhibitor, 5(Z)-7-oxozeaenol, on GDF-15 mediated atrophy was investigated. *In vitro* 5(Z)-7-oxozeaenol at 1000nM prevented TNFα mediated increases in NFκB p65 activity (Appendix 5.2), acting as a positive control. TAK1 inhibition with 5(Z)-7-oxozeaenol was able to partially prevent the GDF-15 mediated reduction in myotube diameter seen at 48 hours at low dose (100 nM) and completely block GDF-15's effects at high dose (1000nM) (Figure 5.17 B and C). Furthermore myotubes treated with GDF-15 (50ng/ml) for 96 hours showed an increase in atrogin-1 mRNA expression. The increase in atrogin-1 mRNA expression was inhibited by co-treatment with 5(Z)-7-oxozeaenol at both 100nM and 1000nM (Figure 5.18 A). There was no significant change in MuRF-1 mRNA in TAK1i treated cells with high dose GDF-15 (Figure 5.18 B).

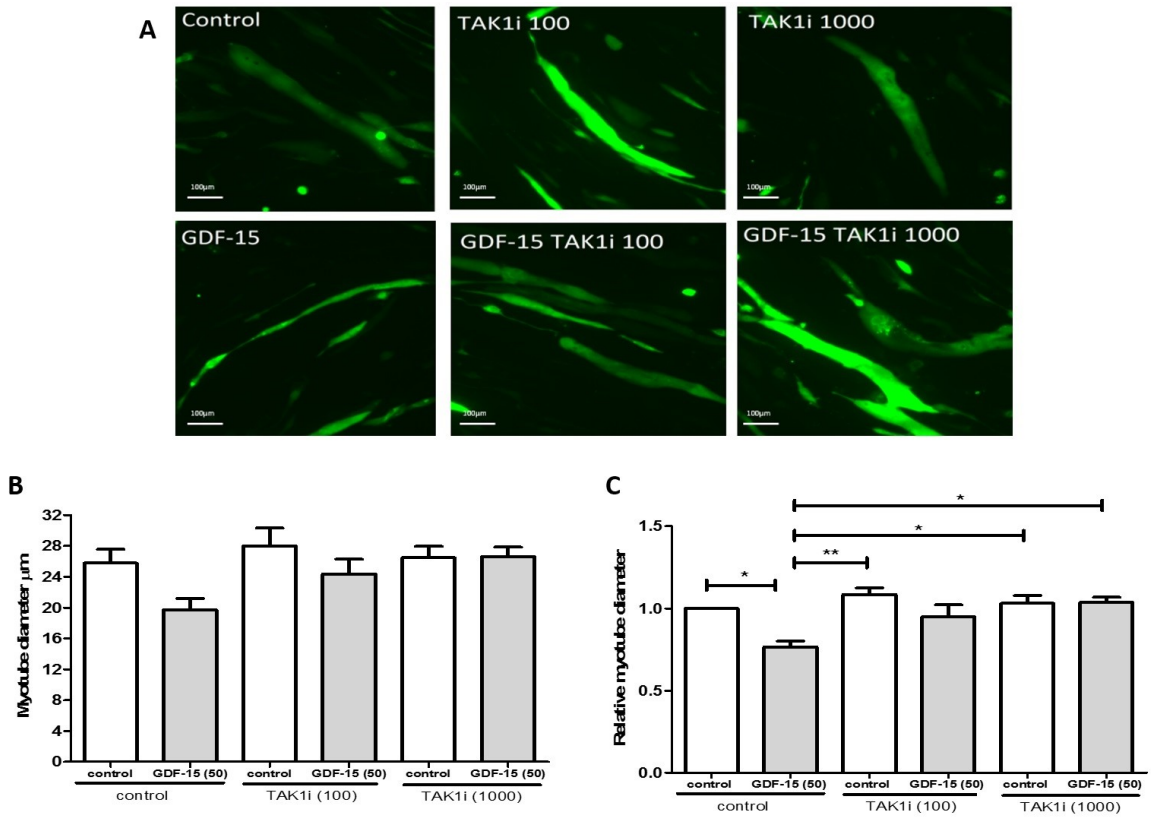

Figure 5.17 Myotube diameter in high dose GDF-15 / 5(Z)-7-oxozeaenol treated cells A. Representative Green fluorescent images of pCAGGS-EGFP expressing cells treated with GDF-15 (50ng/ml) or vehicle control with or without TAK1i at 100 or 1000 nM. **B.** Comparison of myotube diameter in cells treated for 48 hours with GDF-15 (50ng/ml) or vehicle control with or without the TAK1 inhibitor 5(Z)-7-oxozeaenol (TAK1i) at 100 or 1000 nM (n = 3) (One way ANOVA p = 0.068). **C.** Fold change in myotube diameter compared to baseline in cells treated for 48 hours with GDF-15 (50ng/ml) or vehicle control with or without the TAK1 inhibitor 5(Z)-7-oxozeaenol (TAK1i) at 100 or 1000 nM. TAK1i rescued GDF-15 mediated atrophy partially at 100 nM and completely at 1000 nM (n =3) (One way ANOVA p = 0.003).

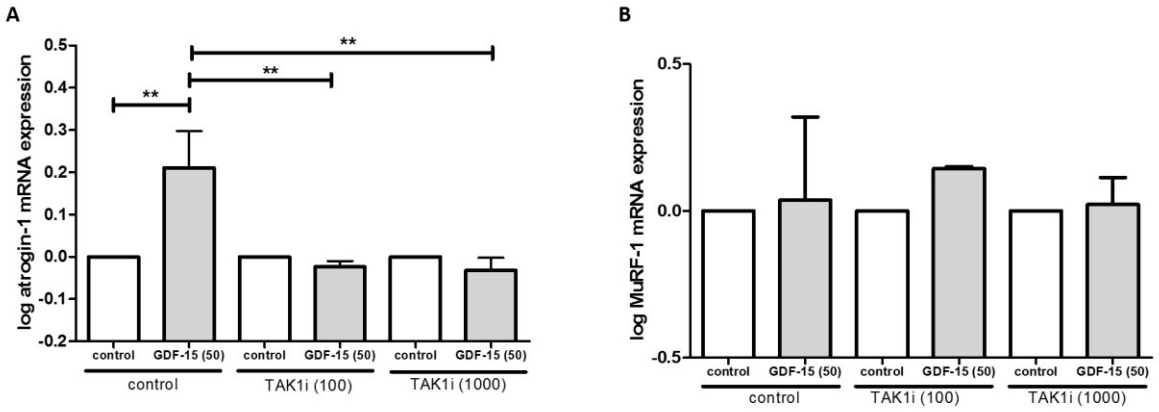

Figure 5.18 Ubiquitin ligase expression high dose GDF-15 / 5(Z)-7-oxozeaenol treated cells. C2C12 myotubes were treated with control or GDF-15 50 ng/ml with or without 5Z-7-oxozeaenol (TAK1i) at 100 or 1000nm for 96 hours after which RNA was extracted for qPCR. **A.** GDF-15 caused a small but significant increase in mRNA expression of atrogin-1. TAK1i co-treatment at 100 nM and 1000 nM reduced GDF-15 induced increases in atrogin-1 levels (n = 5) (One way ANOVA p = 0.001). **B.** Neither GDF-15 nor TAK1i in this experiment had an effect on MuRF-1 mRNA levels (n = 5) (Kruskall-Wallace p = 0.011).

Low dose GDF-15 (5ng/ml) had similar effects on myotube diameter as high dose. Again 5(Z)-7-oxozeaenol was able to inhibit GDF-15 mediated myotube atrophy (Figure 5.19 A and B). Low dose GDF-15 (5ng/ml) mediated atrogin-1 and MuRF-1 mRNA expression was inhibited by 1000nM but not 100nM doses of 5(Z)-7-oxozeaenol (Figured 5.20 A and B).

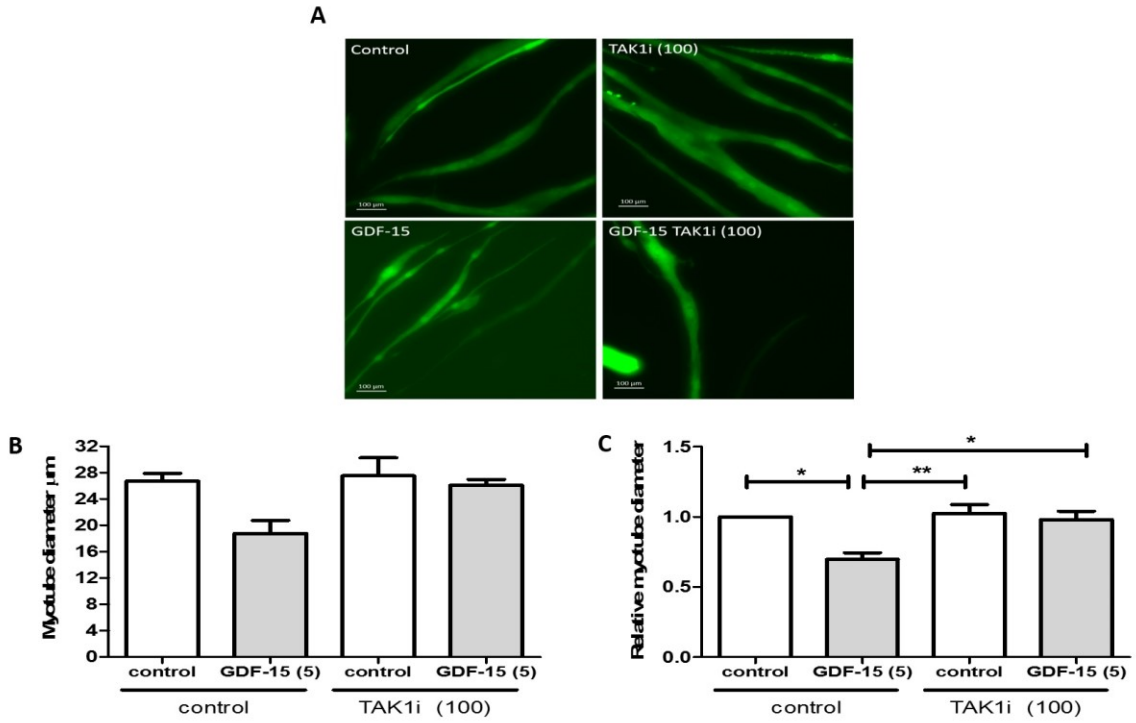

Figure 5.19 Myotube diameter in low dose GDF-15 / 5(Z)-7-oxozeaenol treated cells A. Representative Green fluorescent images of pCAGGS-EGFP expressing myotubes treated with GDF-15 (5ng/ml) or vehicle control with or without TAK1i at 100 nM for 48 hours. **B.** Myotube diameter in cells treated with GDF-15 (5g/ml) or vehicle control with or without TAK1i at 100 nM (n = 3) (One way ANOVA p = 0.033, No difference between the groups). **C.** Fold change in myotube diameter compared to baseline in cells treated for 48 hours with GDF-15 (5ng/ml) or vehicle control with or without the TAK1 inhibitor 5(Z)-7-oxozeaenol (TAK1i) at 100. TAK1i rescued GDF-15 mediated atrophy (n = 3) (One way ANOVA p = 0.005).

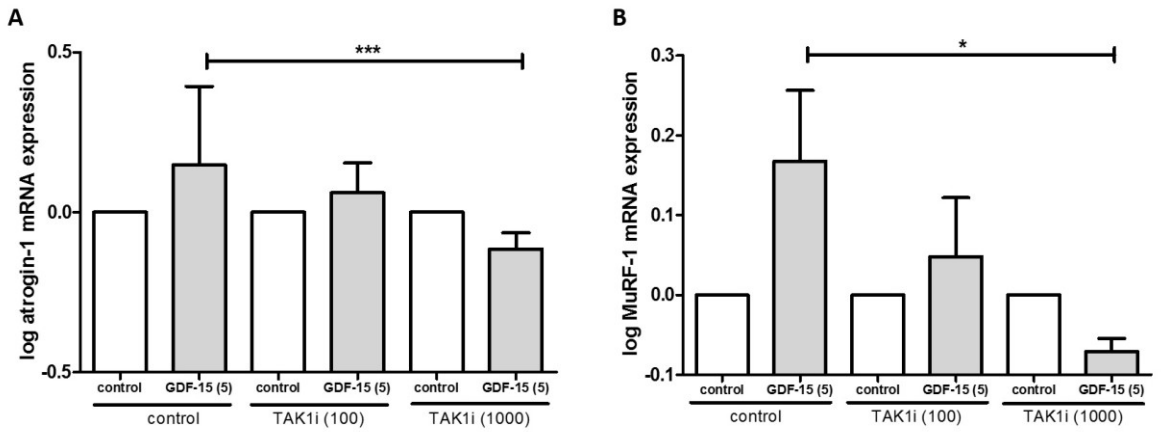

Figure 5.20 Ubiquitin ligase expression in low dose GDF-15 / 5(Z)-7-oxozeaenol treated cells. C2C12 myotubes were treated with control or GDF-15 5 ng/ml with or without 5Z-7-oxozeaenol (TAK1i) at 100 or 1000nm for 96 hours after which RNA was extracted for qPCR. **A.** TAK1i (1000nM) treatment caused a reduction in GDF-15 induced Atrogin-1 mRNA expression (n = 5) (Kruskall-Wallace with Dunn's correction p = 0.001) **B.** TAK1i (1000nM) treatment also caused a reduction in GDF-15 induced MuRF-1 mRNA expression (n = 5) (One way ANOVA p = 0.039).

It has been reported that GDF-15 may act through the ALK-5 type 1 TGFβ receptor (243). Myotubes treated with GDF-15 (50ng/ml) were co-treated for 96 hours with the ALK5 inhibitor SB-431542 (10 μM) (461). ALK-5 inhibition prevented the rises in atrogin-1 mRNA expression induced by GDF-15. (Figure 5.21 A and B).

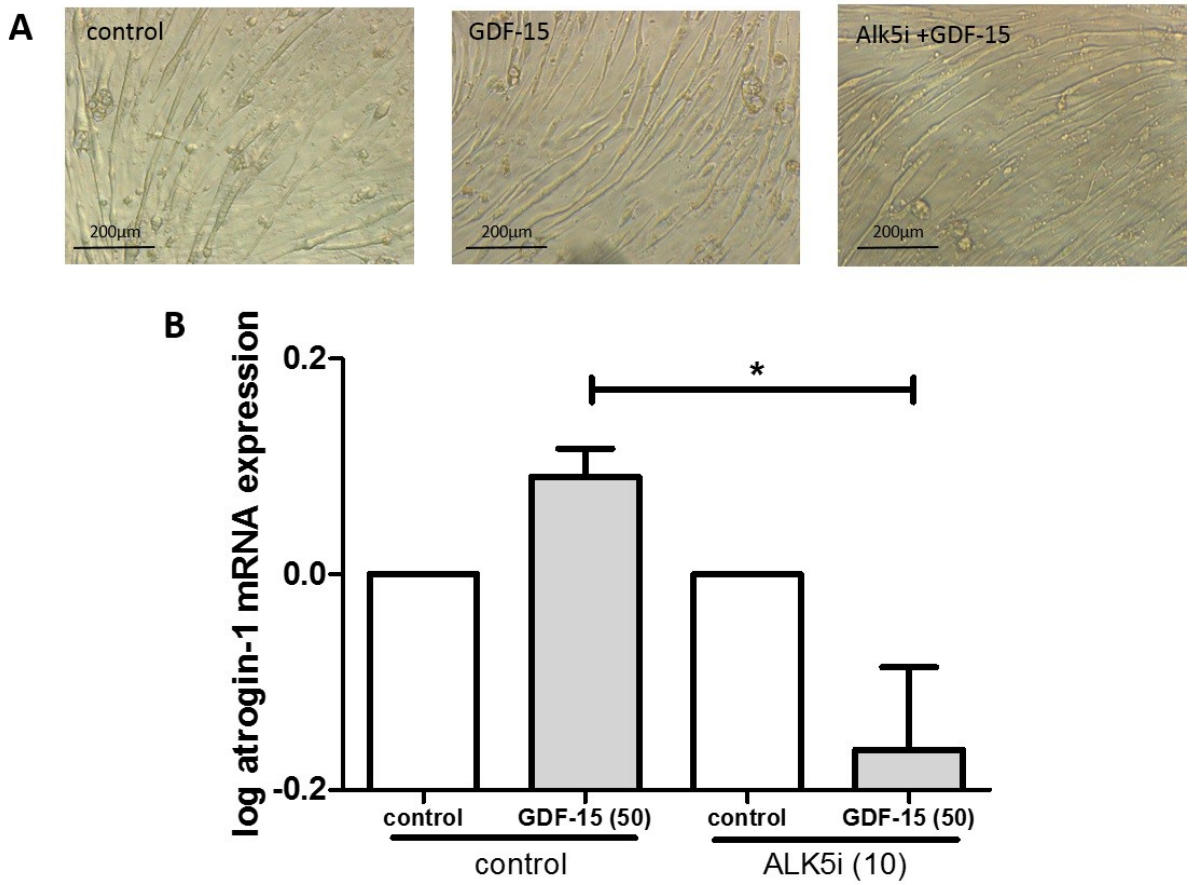

Figure 5.21. Atrogin-1 mRNA expression in high dose GDF-15/ ALK5 inhibitor treated cells. C2C12 myotubes were treated with control or GDF-15 50 ng/ml with or without SB-431542 (ALK5i) at 10µM for 96 hours after which RNA was extracted for qPCR. **A.** Representative brightfield images of myoblasts treated with control, GDF-15 and GDF-15 / ALK5i. **B.** ALK5i prevented GDF-15 mediated increases in atrogin-1 mRNA expression (n = 3) (One way ANOVA p = 0.014).

5.5.8 Downstream mediators of GDF-15 are up-regulated in the muscle of the MCT rat

In the MCT rat TA at 4 weeks post treatment there was no significant increase in MuRF-1 mRNA expression (Figure 5.22A). There was a trend to increase in atrogin-1 mRNA expression that did not reach statistical significance (p = 0.08) (Figure 5.22B). However in the MCT rat TA atrogin-1 mRNA expression correlated with both animal growth (Figure 5.22C) and TA weight (Figure 5.22D). In the Sugen/hypoxia mouse there was no significant increase in MuRF-1 or atrogin-1 mRNA expression within the TA (Figures 5.23 A and B). In the MCT model, TAK1, NFκB p65 and p38 MAPK mRNA levels

remained stable between control and MCT treated animals (Figures 5.24 A-C). However, we did find at the earlier time point used in the MCT TAK1 inhibitor study that phospho-TAK1 was upregulated in the MCT rat TA compared to the control treated animals (Figure 25 A and B). Furthermore there was a suggestion, from the limited data available, that phospho-TAK1 was also increased in skeletal muscle biopsies of patients with PAH compared to controls (Figure 5.25 C)

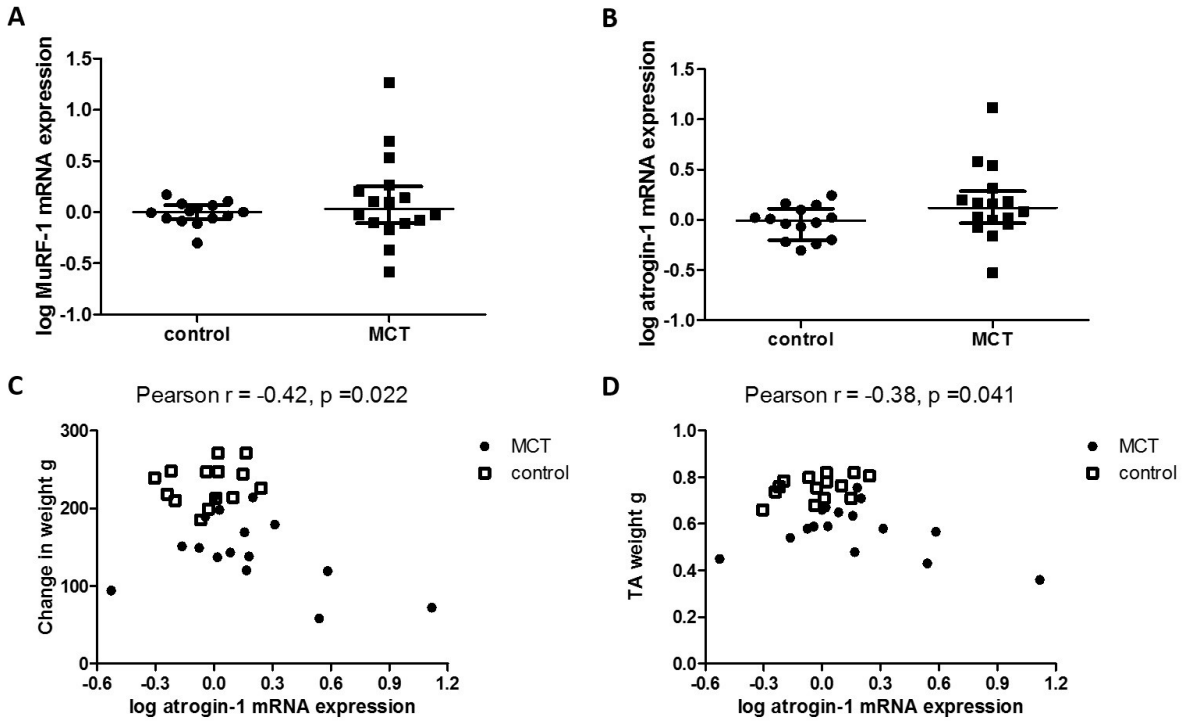

Figure 5.22. Ubiquitin ligase mRNA expression in the TA of the MCT rat. A. log MuRF-1 expression in the TA of control and MCT and control treated rats (control n = 14, MCT n = 16, Student's t-test p = 0.298). **B.** log Atrogin-1 mRNA expression in the TA of control and MCT treated rats (control n = 14, MCT n = 16, Student's t-test p = 0.077). **C.** log TA atrogin-1 mRNA expression plotted against change in weight in control and MCT treated rats (control n = 14, MCT n = 16). **D.** log TA atrogin-1 mRNA expression plotted against TA weight in MCT and control treated rats (control n = 14, MCT n = 16).

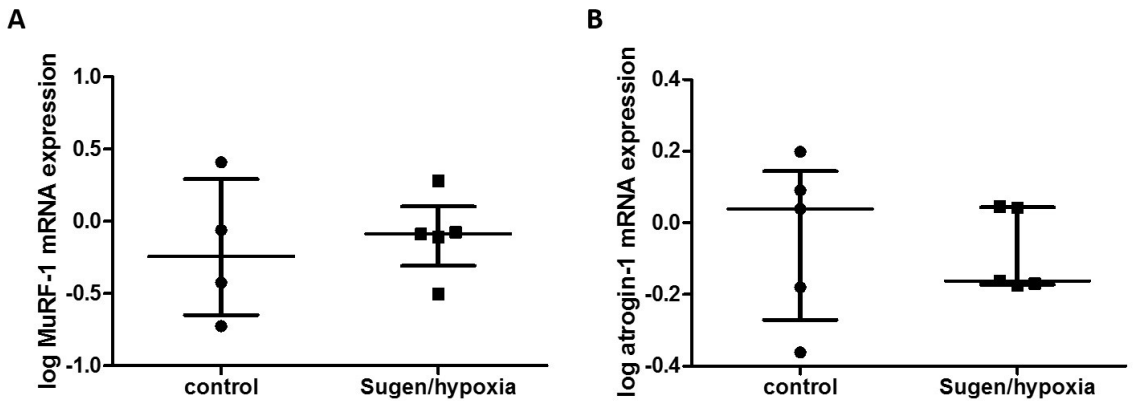

Figure 5.23. Ubiquitin ligase mRNA expression in the TA of the Sugen/hypoxia mouse. A. log MuRF-1 mRNA expression in the TA of the control and Sugen/hypoxia treated mice (control n = 4, MCT n = 5, Mann Whitney U test p = 1.00). **B.** log Atrogin-1 mRNA expression in the TA of control and Sugen/hypoxia treated mice (control n = 5, MCT n = 5, Mann Whitney U test p = 1.00).

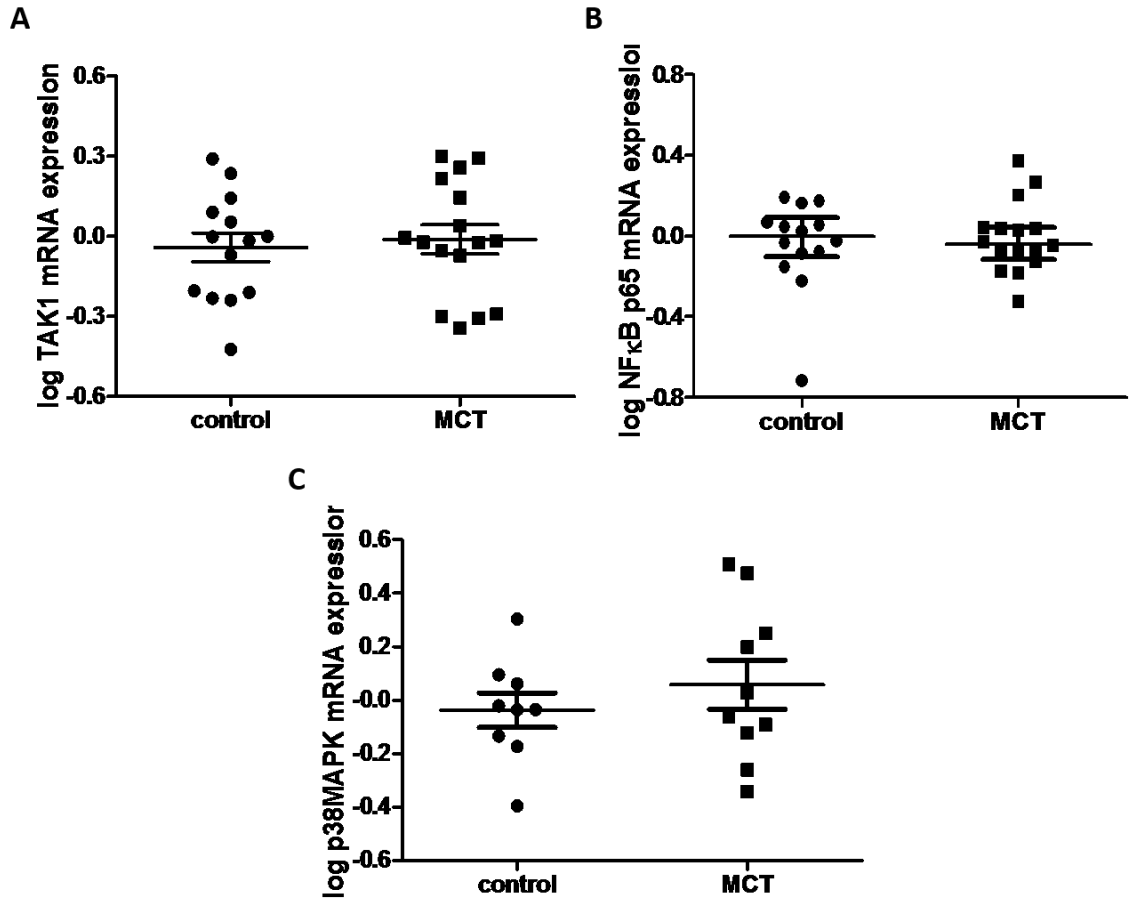

Figure 5.24. mRNA expression of TAK1, NFκB p65 and p38 MAPK in the TA of the MCT rat. A. log TGFβ activated kinase 1 (TAK1) mRNA expression in the TA of control and MCT treated rats (control n = 14, MCT n = 16, Student's t-test p = 0.699). **B.** log NFκB p65 mRNA expression in the TA of control and MCT treated rats (control n = 14, MCT n = 16, Mann Whitney U test p = 0.643). **C.** log p38MAPK mRNA expression in the TA of control and MCT treated rats (control n = 9, MCT n = 10, Student's t-test p = 0.419).

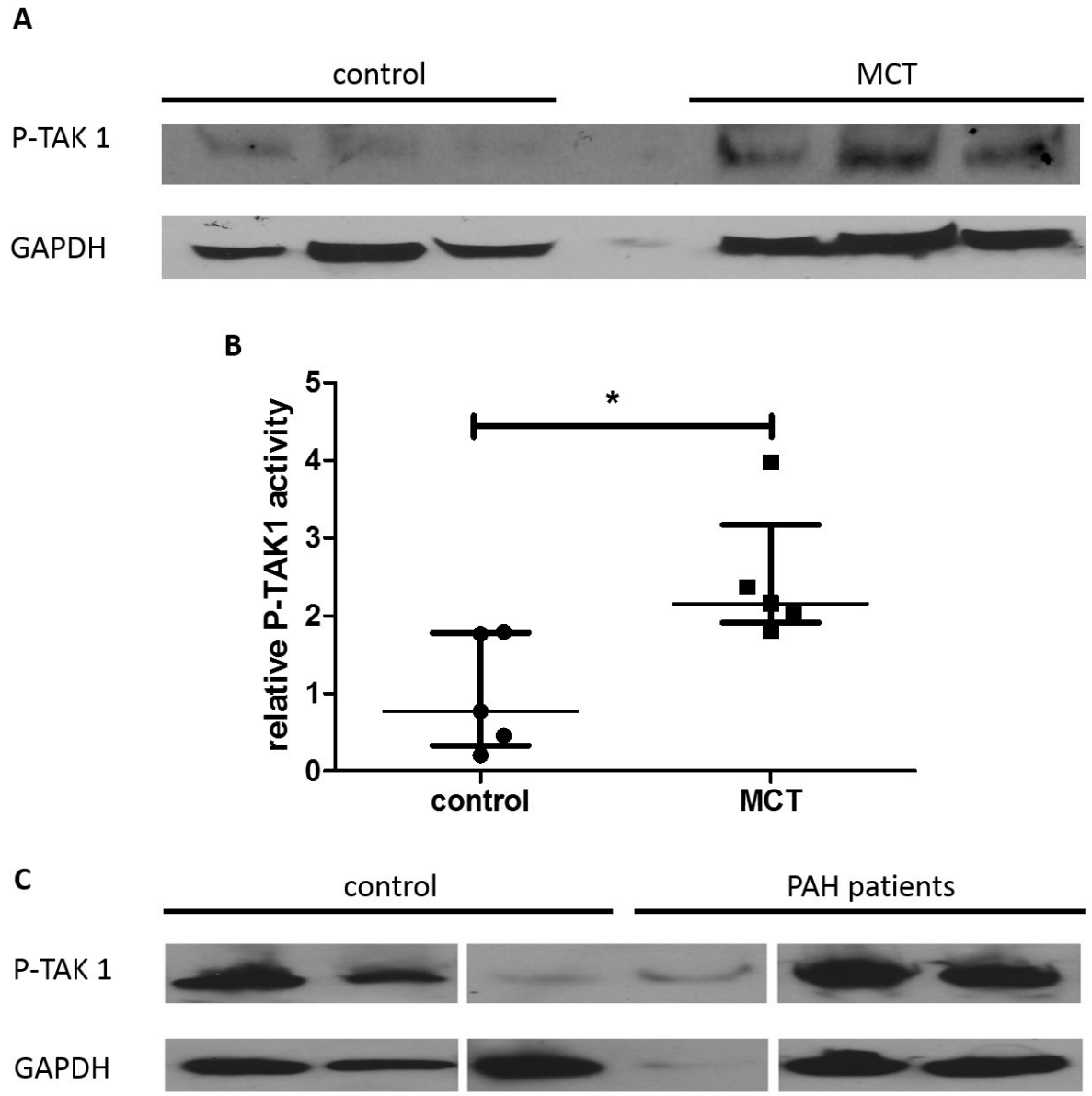

Figure 5.25. Phospho-TAK1 in the TA of the MCT rat and in the rectus femoris of patients with PAH. A. Representative western blot of P-TAK1 and GAPDH in homogenates from the TA of control and MCT treated rats. **B.** Relative intensity of P-TAK1 activity normalised to GAPDH in TA homogenates from control and monocrotaline (MCT) treated rats (control n = 5, MCT n = 5, Mann Whitney U test p = 0.008). **B.** Western blot of P-TAK1 and GAPDH in quadriceps homogenates from control volunteers and patients with PAH.

5.6 Discussion

The above results show that GDF-15 can interact with both the TGFBR2 and ALK5 receptors. GDF-15 treatment did not seem to have any effect on SMAD 1, 5 or SMAD 2, 3 dependent luciferase activity at either high or low dose. The clinical significance and relevance of this interaction between GDF-15 and TGFBR2 in both myoblasts and mature muscle cells is difficult to interpret. The TTGFBR2 changed GDF-15 induced SMAD 2, 3 dependent luciferase activity but had no effect on GDF-15 induced myotube atrophy. Larger changes are seen in the effects of GDF-15 on non-canonical pathways, particularly the up-regulation in TAK1 and NFκB p65 activity. The main findings of this chapter suggest that GDF-15 activates TAK1 and that TAK1 inhibition can prevent GDF-15 mediated myotube atrophy possibly by preventing up-regulation in pro-atrophic ubiquitin ligases atrogin-1 and MuRF-1. Finally the results demonstrate that these non-canonical pathways are potentially important in the development of muscle wasting in the MCT rat model of PH induced muscle loss, and may therefore be targets for future therapeutic intervention.

GDF-15 caused no significant change in SMAD 2, 3 dependent luciferase activity at any dose used at 6 hours, although there was a trend at lower doses (5 ng/ml) to inhibition of SMAD signalling. This is in keeping with data presented by Johnen *et al*. who could see no evidence of SMAD 2, 3 signalling in response to GDF-15 in mouse hypothalamus (260), but is in contrast to data showing an increase in SMAD 2, 3 dependent luciferase activity in conditioned media from GDF-15 over-expressing cells (235). The latter is not direct evidence of the positive effect of GDF-15 on SMAD 2, 3 activity as an alternative protein in the conditioned media may have caused this effect and the 3TP promoter that they used in their luciferase may have mis-identified a TAK1 effect through 3TP-Luc binding. GDF-15 also had no effect on SMAD 1, 5 dependent luciferase activity in myoblasts.

The purity of recombinant human GDF-15 has been called into question (Email from S. Breit Appendix 5.3) and concerns have been raised about contamination of GDF-15 with TGFβ1. My experiments have shown that the batch of GDF-15 we used was not significantly contaminated with TGFβ1. There was

an up-regulation in SMAD2, 3 dependent luciferase activity with as little as 0.1 ng/ml of TGFβ1. The maximum dose of GDF-15 used was 50 ng/ml. Even at this high dose there was no SMAD 2, 3 dependent luciferase effect. We can therefore conclude that if contamination of GDF-15 with TGFβ1 was present then it was in the order of less than 0.2%. Furthermore GDF-15 at 5 ng/ml caused a similar upregulation in P-TAK1 activity to TGFβ1 at 0.5 ng/ml meaning that contamination with TGFβ1 would have to reach 10% if this was solely responsible for the changes seen with GDF-15, ruling out this possibility.

Recent data suggests that GDF-15 acts in the central nervous system through the GFRAL receptor (294). This receptor is not present in skeletal muscle (295). A number of other groups have shown that GDF-15's effects are mediated by the TGFBR2 and ALK5 (288, 301). In TGFBR2 over-expressing cells GDF-15 (50ng/ml) caused a small but significant increase in SMAD 2, 3 activity above baseline. This change was not seen at lower doses of GDF-15 (5 ng/ml). It seems therefore that in the presence of excess receptor and high dose ligand, GDF-15 can be forced to bind to the TGFBR2 to stimulate SMAD 2, 3 responses, but the physiological relevance of this *in vivo* and in patients is yet to be elucidated. GDF-15 at 50 ng/ml could also be shown to stimulate small increases in relative SMAD 1, 5 responses above that seen in pCDNA3 transfected cells, in the presence of excess TGFBR2, ACVR2B or BMPR2. The fold change of this up-regulation was again small. This demonstrates that GDF-15 has some affinity to bind to all these receptors. However the small fold change means the results presented here must be interpreted with caution. The ALK-5 inhibitor SB-431542 was able to prevent GDF-15 mediated increases in atrogin-1 expression, suggesting that the ALK-5 is involved in GDF-15 signalling. However, SB-431542, as well as ALK-5 has some activity against ALK-4 and ALK-7, meaning GDF-15 may act through these receptors as well. (462). Interestingly, in the presence of ALK5 inhibition, GDF-15 actually caused a decrease in atrogin-1 expression compared to ALK-5 alone. This suggests that, as we have seen with the type II receptors, GDF-15 can act with a number of type I activin receptor like kinase receptors with contrasting effects on gene expression. This serves to further highlight the high levels of receptor promiscuity within TGFβ signalling pathways (178).

GDF-15 had no significant effect on the dose response curves of TGFβ1 or BMP-4 on their relevant SMAD luciferase assay, suggesting that the ligand does not act as a competitive antagonist to these ligands by binding out their receptors but not contributing to downstream signalling.

In view of the fact that the TGFBR2 has previously been identified as a potential receptor through which GDF-15 might signal (260) and the findings that there was some interaction between the TGFBR2 and GDF-15, a TTGFBR2 was cloned. This was effective in reducing baseline SMAD 2, 3 luciferase activity (178). TTGFBR2 over-expression was also able to influence SMAD 2, 3 responses to GDF-15 at 5 but not 50ng/ml. TTGFB2 over-expression had no effect on GDF-15 mediated myotube atrophy. This is in contrast to data showing TGFBR2 antagonism with a truncated receptor was able to prevent the formation of a dystrophic phenotype in δ-sacroglycan-null mice and reduced inflammation and increased regeneration in a mouse model of muscle injury (463). The results presented here should be treated with caution as the effects of the TTGFBR2 are not necessarily GDF-15 specific and in fact may be mediated through antagonism of a number of different potential ligands resulting in no net change in the balance between protein synthesis and degradation.

There was no evidence that GDF-15 caused any change in SMAD responses in C2C12 myoblasts. GDF-15 did however cause an increase nuclear localisation of NFκB p65 activity measured by immunofluorescence. GDF-15 treatment also increased mRNA expression of NFκB p65 in C2C12 myoblasts, a phenomenon inhibited by co-treatment with the TAK1 inhibitor 5(Z)-7-oxozeaenol. This provided some evidence that GDF-15 may signal through the TAK1 - NFκB p65 axis in muscle cells. This pathway has already been shown to be important in mediating GDF-15 signalling in Ecoli infected gastric epithelial cells (318, 319). TAK1 and its downstream target NFκB p65 are constitutively active in C2C12 myoblasts and this activity is lost during differentiation (361, 464), meaning investigation of factors which upregulate this signalling pathway is difficult in these immature cells. Therefore in order to determine the relevance of this pathway further we concentrated on myotubes where only low level baseline TAK1 and NFκB activity was exhibited. This also had the advantage of being a more representative population of mature muscle cells seen in adults with chronic disease such as PH.

As we have already shown, GDF-15, like other TGFβ super-family members, acts in a dose and environment dependant manner (227). In myotubes GDF-15 treatment caused phosphorylation of TAK1 and NFκB p65 at a number of times and doses. It also caused a significant decrease in p38 MAPK phosphorylation which was only seen with high dose treatment. In other cells GDF-15 has been shown to both activate and prevent activation of TAK1, NFκB and p38 MAPK (312, 317-319), adding validity to our results but also providing more evidence of the context dependant nature of pathways activated by TGFβ proteins. It is well established that TAK1 is upstream of NFκB and p38 MAPK, both of which have been associated with muscle atrophy through activation of ubiquitin ligases (465-467). Previous work from our group showed that GDF-15 can up-regulate atrogin-1 and MuRF-1 expression (265) and cause myotube atrophy (218). It is generally accepted that activation of p38 MAPK is associated with up-regulation of both MuRF-1 and atrogin-1, whilst NFκB has generally been associated with upregulation of MuRF-1 alone (467). TAK1 inhibition with 5(Z)-7-oxozeaenol prevented GDF-15 mediated relative myotube atrophy and expression of atrogin-1 mRNA. It also prevented MuRF-1 mRNA expression caused by low but not high dose GDF-15. Taken together these results suggest that GDF-15 may phosphorylate TAK1, activating NFκB and up-regulating mRNA expression of MuRF-1. The increase in atrogin-1 demonstrated also seems to be dependent on TAK1 but is likely to be independent of both NFκB, which is not thought to be in involved in up-regulation of atrogin-1 expression (467) and p38 MAPK, activation of which was, if anything, was inhibited by GDF-15, at high doses in these experiments.

Downstream mediators of GDF-15 effects are elevated in the muscle of the MCT rats, a model of cachexia associated with raised GDF-15 levels. Although expression of neither ubiquitin ligase were elevated in the TA of the MCT rat in this experiment, atrogin-1 mRNA levels trended to increase with a p value of 0.08. Furthermore Atrogin-1 mRNA expression was associated with both a change in animal weight and final TA weight of the animal. Atrogin-1 mRNA and protein have both previously been shown to be raised in the gastrocnemius of the MCT rat (153, 468). MuRF-1 mRNA expression remained unchanged at the time point studied in my experiment, but this does not rule out its

involvement in the muscle wasting process. Previous work has shown that as well as Atrogin-1 mRNA, MuRF-1 mRNA levels are also raised in the gastrocnemius of the MCT rat at 21-22 days (60, 468) a week prior to the time point at which the rats in our experiment were investigated. It is interesting to note that variation in ubiquitin ligase expression with time have also been observed in man (469) and that in an animal model of burns induced muscle wasting whilst atrogin-1 mRNA remained persistently elevated at 5 days post insult MuRF-1 mRNA levels fell to baseline after 5 days (470). This suggests that atrogin-1 and MuRF-1 mRNA may have peaked prior to the time at which the animals were humanely killed explaining why we don't necessarily see an increase in expression at the time point we investigated. This may also be the reason we don't see any change in ubiquitin ligase expression in the Sugen/hypoxia mouse.

TAK1 seems to have a dual role in the balance between atrophy and hypertrophy as, whilst is seems to be a vital component of satellite stem cell function in regenerating muscle or in muscle development in immature animals (363, 364) it is also an essential requirement in allowing myostatin to propagate its growth inhibitory signal in muscle cells (67, 366). Its role in chronic disease *in vivo* has not been investigated and the finding of elevated levels of phosphorylated TAK1 in the TA of the MCT model and the preliminary data in patients with PAH confirms it as a potential future therapeutic target for intervention.

5.7 Conclusion

GDF-15 may act through ALK-5 and possibly through TGFBR2 to stimulate TAK1 and NFκB which leads to increased expression of ubiquitin ligases, including but not limited to Atrogin-1 and MuRF-1, resulting in muscle loss. This pathway seems to be active in an animal model of PAH. TAK1 inhibition may be a target for therapeutic intervention aimed at antagonising the muscle weakness found in PAH.

Chapter 6 The effect of 5(Z)-7-oxozeaenol on muscle wasting in the MCT rat.

6.1 Background

Data from previous chapters has shown that TAK1 might be involved in GDF-15 mediated muscle atrophy in PAH. TAK1 is a mitogen activated protein kinase kinase kinase and a serine threonine kinase, which is found in the cell as a hetero-tetramer bound to its adapter proteins TAB1 and TAB2/3. TAK1 is activated by a number of different signalling factors including the IL-1 and TNFα. This activation results from the interaction of receptor associated factors with TAB2/3. Other factors known to stimulate TAK1 activity include lipopolysaccharide and TGFβ1. Activation of TAK1 involves phosphorylation at Thr184/187 sites, which in turn results in phosphorylation of JNK, NFκB and p38 MAPK resulting in a pro-inflammatory state through transcription of cytokines and an increase in inflammatory cell recruitment (344, 345). Recent data has suggested that for full activation of TAK1 and propagation of down-stream signals phosphorylation at Ser412 is also required. Whether this is dependent or independent of Thr 184/187 phosphorylation remains to be elucidated (335, 471).

Although essential for embryonic development, innate and adaptive immunity and homeostasis of essential organ function (344-346) excessive TAK1 activity has also been associated with inflammatory conditions, cancers (347), cardiovascular disease (348), and fibrosis (349, 350). TAK1 has become an exciting potential therapeutic target in a wide range of conditions and a number of compounds, aimed at antagonising its actions, are in development. These include: covalent cysteine binders such as 5(Z)-7-oxozeaenol and hypothemycin, which act on the cysteine residue in the Asp-Phe-Gly / DFG 1 region on the N-terminal of the activation loop of the kinase; type I molecules which interact directly with ATP binding site of the kinase which is not dependent on the conformation of the kinase, known as DFG-in binders, e.g. AZ-TAK1; and type II DFG out-binders, like PF-04358168, which also bind to the nearby ‘allosteric’ site of the protein, only when the kinase is in inactive form, called DFG out (351, 472). All the mechanisms by which it might be possible to inhibit TAK1 have advantages and

disadvantages with some compounds being potent but having off-target effects whilst others may be more specific but less effective (351).

5(Z)-7-oxozeaenol was the first TAK1 inhibitor characterised (352) and has been the most widely used to inhibit TAK1 *in vitro* and *in vivo*. It is a resorcyclic acid lactone naturally produced by a fungus (352). It acts as an irreversible kinase inhibitor by forming a covalent bond between the cis-enone group of 5(Z)-7-oxozeaenol and the functional thiol group of the cysteine residue of TAK1 resulting in alkylation of the protein and preventing the binding of TAK1 and ATP at its DFG site. The compound is highly specific for TAK1, with very few off target effects (353). *In vivo* 5(Z)-7-oxozeaenol has been shown to: enhance chemotherapeutic effect of doxorubicin on neuroblastoma tumours in mice (354); prevent diabetes in a mouse model of the disease (355); reduce the severity of nephropathy in in diabetic mice (356); increase neuronal survival and decrease seizure duration in epileptic rats (357); reduce the size of infarct after stroke (358); and prevent neo-intimal formation in wire induced vascular injury (359). Its effects on muscle wasting has not been investigated. 5(Z)-7-oxozeaenol has been used intra-peritoneally at doses of between 0.5 – 5 mg/kg/day (356, 358, 359).

The data presented in Chapter 5 suggests that *in vitro* GDF-15 mediated muscle loss is antagonised by blocking TAK1 activation, which to a certain extent prevents the upregulation of atrogin-1 and MuRF-1. The validity of this pathway is supported by data from others showing GDF-15 can activate TAK1 (318, 319) and that GDF-15 mediated muscle loss involves the up-regulation of the aforementioned ubiquitin ligases (265). In Chapter 4 and 5, muscle wasting in the MCT rat was shown to be associated with both an upregulation of circulating GDF-15 and local TAK1 activation. Consistent with these observations, muscle wasting in the MCT rat is also associated with up-regulation of atrogin-1 and MuRF-1 (60).

GDF-15 is not the only upstream mediator of TAK1 signalling that is involved in the development of muscle wasting in the MCT rat. Both GDF-8 and TNFα can activate TAK1 (67, 345) and are over-expressed (136, 153) in this rodent model of PAH and muscle wasting. This observation suggests that

TAK1 may be more effective than other inhibitors of muscle wasting in this model as it blocks a number of different synergistic pathways. Furthermore, data from a cohort of patients undergoing rehabilitation after a fractured neck of femur has shown that TAK1 levels drop after exercise suggesting a protective role for TAK1 inhibition in an adult population (473), backing up the limited muscle biopsy data on TAK1 phosphorylation shown in Chapter 5.

6.2 Aim

To determine whether TAK1 inhibition prevented muscle loss in the MCT rat model of PAH

6.3 Hypothesis

TAK1 inhibition with 5(Z)-7-oxozeaenol will prevent muscle loss and weight loss in the MCT rat model of PAH by altering the mRNA levels of ubiquitin ligases.

6.4 Methods

For a full explanation of the methods please see Chapter 2 of this thesis

6.4.1 Animal experiments

Twenty rats were treated with MCT and 10 with control injections as before. After 2 weeks, 10 of the animals in the MCT group were treated with 5(Z)-7-oxozeaenol, 0.5mg/kg/day, (dissolved in 10% DMSO/90% PBS) intra-peritoneally for 9 days as previously described, after which they were humanely killed (358, 402). During the experiment rats were weighed regularly. One animal in the MCT TAK1i group was excluded from analysis as it had to be humanely killed before the treatment end point. Blood was collected, after cardiac catheterisation. The heart was dissected for and RV/LV+S weight measured. Half the lung was agarose inflated and dropped into formalin. The other half was flash frozen. The TA and soleus muscles from one leg were snap frozen, whilst those from the other leg were embedded in OCT and frozen in isopentane cooled in liquid nitrogen.

6.4.2 Tissue processing and analysis

Lung and muscle tissue was homogenised for mRNA and protein as previously described (See Chapter 2). Blood was spun down for serum. Lung and muscle tissue was sectioned and mounted on slides. Muscle tissue was stained with haematoxylin and eosin and fibre diameter was assessed as previously described. Blood samples were analysed for GDF-15 by ELISA as per manufacturer's instructions. Lung and muscle tissue was analysed by qPCR and western blot using primers and antibodies fully explained in Chapter 2 (265).

6.4.4 Statistics

The 3 treatment groups were compared using ANOVA with Bonferroni correction or Kruskall-Wallace with Dunn's correction depending on the distribution of the data. When only 2 groups were compared, Student's t-test or Mann Whitney U test was used depending on the distribution of the data. Normality was assessed using the Kolmogorov-Smirov, D'Agostino and Pearson test and the Shapiro-Wilk test as well as visually using histograms. Rats were defined as continuing to grow if they reached their maximum weight on the last day of the experiment and had not plateaued. Fisher's exact test was used to compare the proportions of MCT treated rats continuing to grow or not growing after 9 days treatment with 5(Z)-7-oxozeaenol. A ROC curve was constructed to define GDF-15's ability to predict those animals growing or not growing at the end of the experiment. The number of fibres in 5 micron groups were determined for each animal. The cumulative number of fibres below each 5 micron diameter cut off was determined and expressed as a percentage of the total number of fibres counted. Two way ANOVA with Bonferroni correction was used to compare the proportion of fibres in the control, MCT and MCT TAK1 group at each diameter cut off.

6.5 Results

6.5.1 TAK1 inhibition prevents weight loss in the MCT rat model of PAH

Two weeks after MCT treatment, rats were treated with 9 days of 5(Z)-7 oxozeaenol. Both MCT control and MCT TAK1 inhibitor rats had similar final weights, overall growth, growth since initiation of TAK1 inhibitor treatment, and change from maximum weight (Figure 6.1 A-D). Examining the growth curves of the animals completing 9 days of treatment there was a trend to stabilisation of weight in the MCT TAK1i group that did not meet statistical significance (Figure 6.2 A). In the MCT TAK1i rat group, 4/9 continued to gain weight on the last day of treatment compared to 0/10 of the MCT control treated rats (Fisher's exact test $p = 0.033$) (Figure 6.2 B). There was no difference in overall or weekly food intake between MCT and MCT TAK1 inhibitor rats, which ate, as expected, less on average than their control treated counterparts (control 477g; MCT 389g; MCT TAK1i 387g).

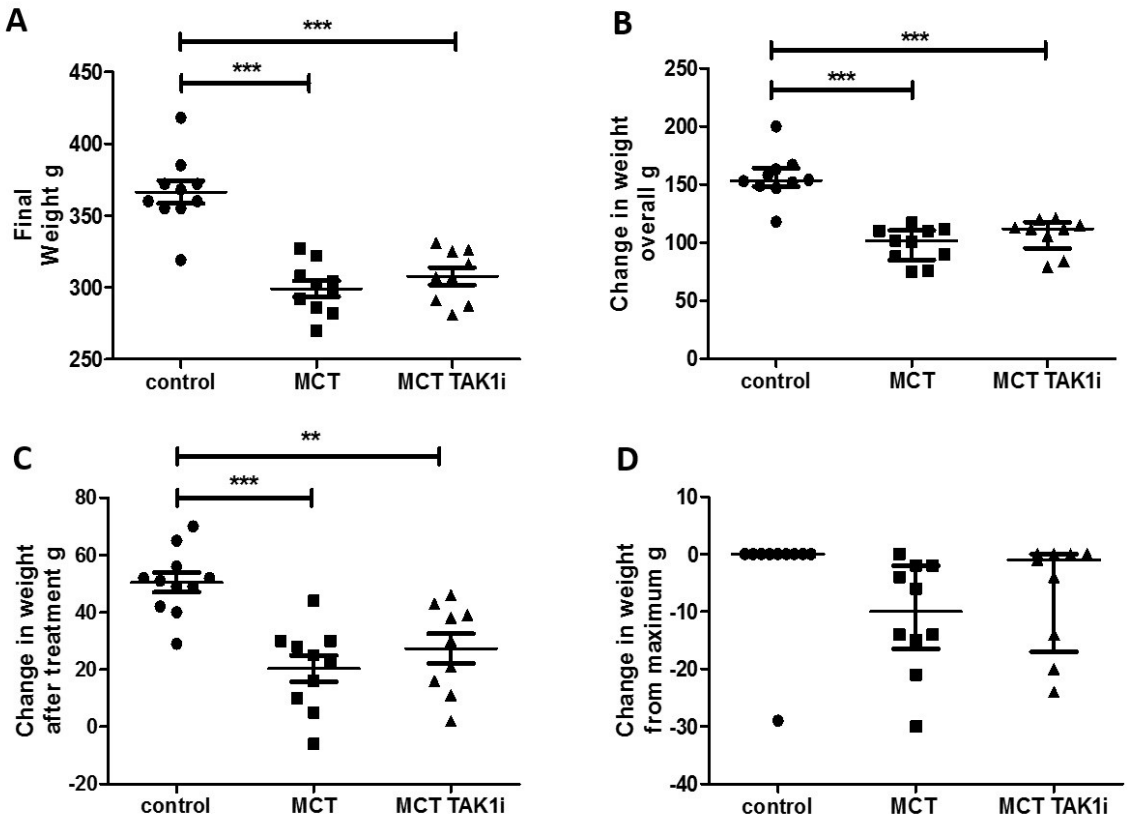

Figure 6.1 Weight in the MCT rat treated with 5(Z)-7-oxozeaenol. A. Final weight in grams (g) in control (n=10), MCT (n=10) and MCT TAK1i (n=9) treated rats (ANOVA $p < 0.001$). **B.** Change in weight in grams (g) in control (n=10), MCT (n=10) and MCT TAK1i (n=9) rats over the entire experiment (ANOVA $p < 0.001$). **C.** Change in weight in grams (g) after treatment with TAK1i of PBS/DMSO in control (n=10), MCT (n=10) and MCT TAK1i rats (n=9) (ANOVA $p < 0.001$). **D.** Change in weight in grams (g) from maximum in control (n=10), MCT (n=10) and MCT TAK1i rats (n=9) (ANOVA $p = 0.195$).

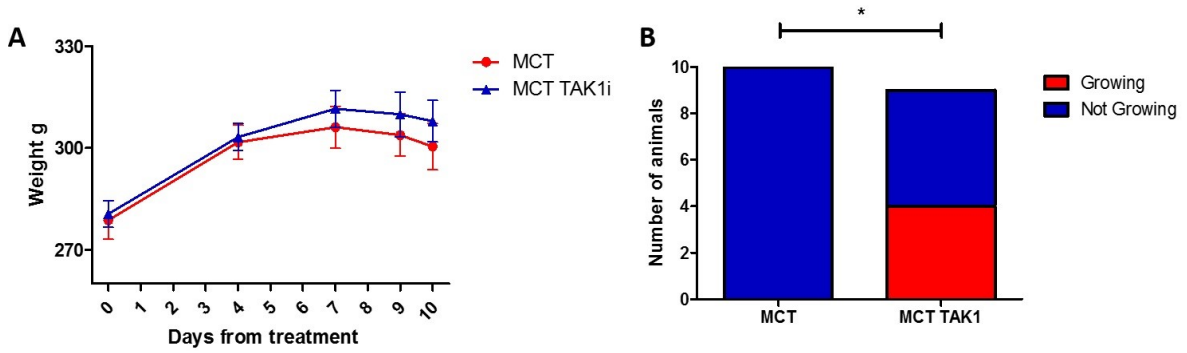

Figure 6.2 Growth in the MCT rat treated with 5(Z)-7-oxozeaenol. A. Growth curves showing mean and standard error of the mean in weight of MCT (n=10) and MCT TAK1i (n=9) treated MCT rats after initiation of PBS/DMSO or TAK1i. **B.** Number of MCT animals growing and not growing at the end of the experiment in the MCT (n=10) and MCT TAK1i (n=9) groups Fisher's exact test p = 0.033).

6.5.2 TAK1 inhibition may partially prevent loss of TA fibre diameter and prevents MCT induced increases in activated NFκB and atrogin-1 expression

TAK1 inhibitor treated MCT rats had significantly heavier TAs than MCT control treated animals (Figure 6.3 A). There was no difference in soleus weight between MCT control and MCT TAK1i treated animals (Figure 6.3B). In this model TAK1i inhibition prevented MCT induced fibre atrophy, as shown by the fact that MCT TAK1i rats had a lower proportion of fibres with diameters between 30 – 50 µm (Figure 6.4 A, B and C).

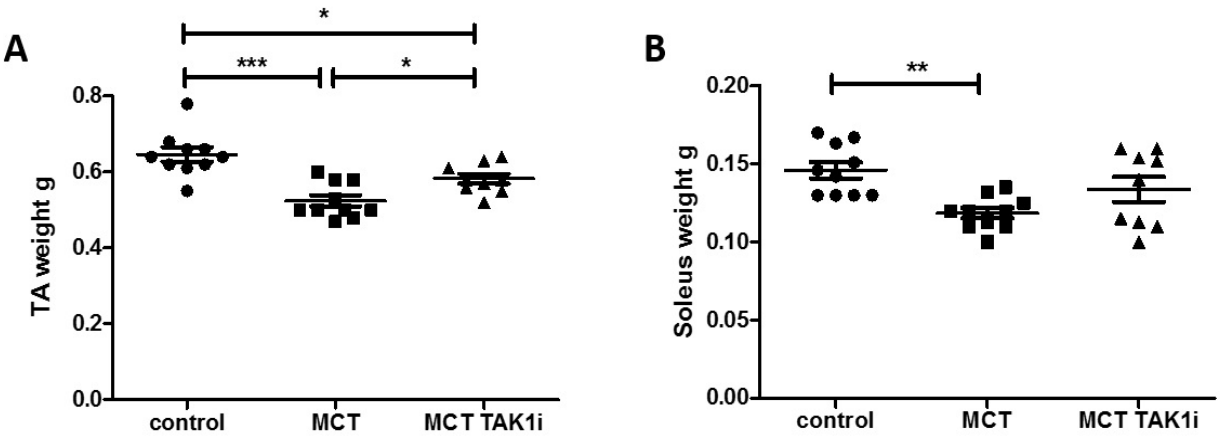

Figure 6.3 Muscle wasting in the MCT rat treated with 5(Z)-7-oxozeaenol. A. Tibialis Anterior (TA) weight in grams (g) in control (n=10), MCT (n=10) and MCT TAK1i (n=9) treated animals (ANOVA $p < 0.001$). **B.** Soleus weight in grams (g) in control (n=10), MCT (n=10) and MCT TAK1i (n=9) treated animals (ANOVA p = 0.007)

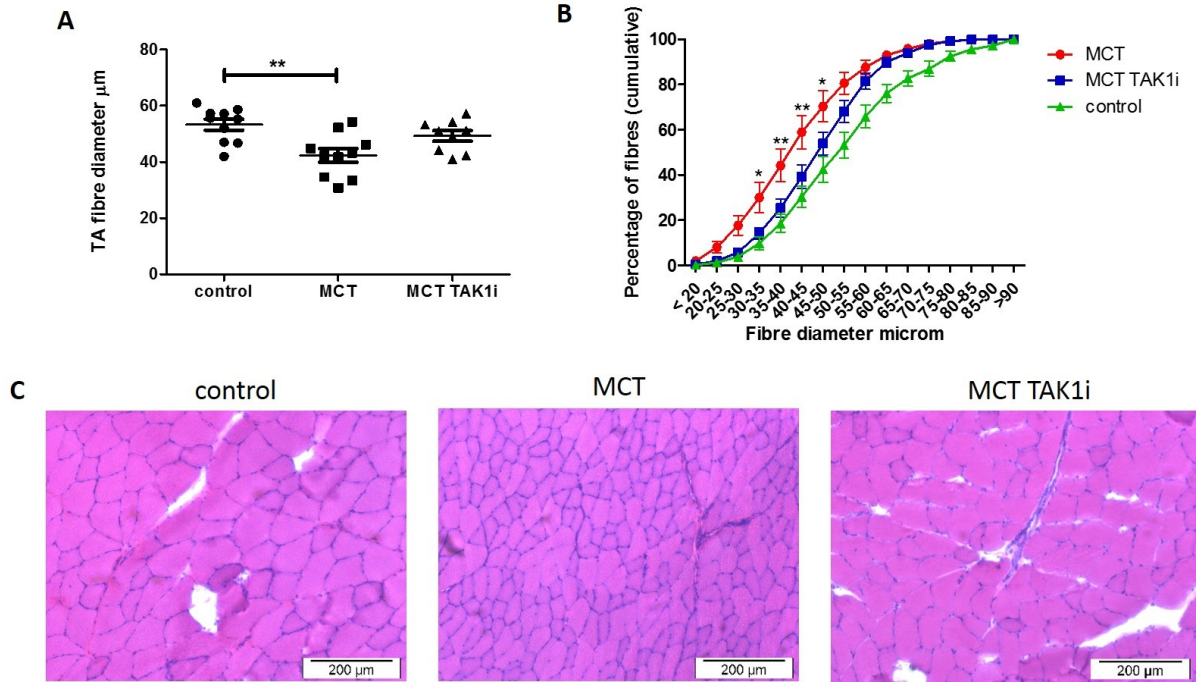

6.4 TA Fibre diameter in the MCT rat treated with 5(Z)-7-oxozeaenol A. TA fibre diameter in micrometres (µm) in control (n=10), MCT (n=10) and MCT TAK1i (n=9) treated animals (ANOVA p = 0.004). **B.** Fibre profiles of control (n = 10), MCT (n = 10), and MCT TAK1i (n = 9) plotted as mean and standard error of the mean of proportion of fibres below the indicated fibre diameter in 5 µm increments (Two way ANOVA p < 0.001 for row, column and interaction, * and ** represent a significant difference between MCT and MCT TAK1 proportions at each 5µm fibre intervals by Bonferroni). **C.** Representative bright-field image of rat muscle tissue stained with haematoxylin and eosin from which average fibre diameter was determined by Image J.

5(Z)-7-oxozeaenol treatment prevented increases in phospho-NFκB p65 protein levels in the TA of the MCT rat (Figure 6.5). There was a trend to a reduction in atrogin-1 and MuRF-1 mRNA levels in the TA of the MCT rat treated with TAK1 inhibition at this time point that did not meet statistical significance. (Figure 6.6 A and B). TA Atrogin-1 mRNA expression was, however, lower in animals which continued to grow at the end of the experiment when analysed in the group as a whole (Figure 6.6 C) and when the MCT treated animals were analysed alone (Figure 6.6 D).

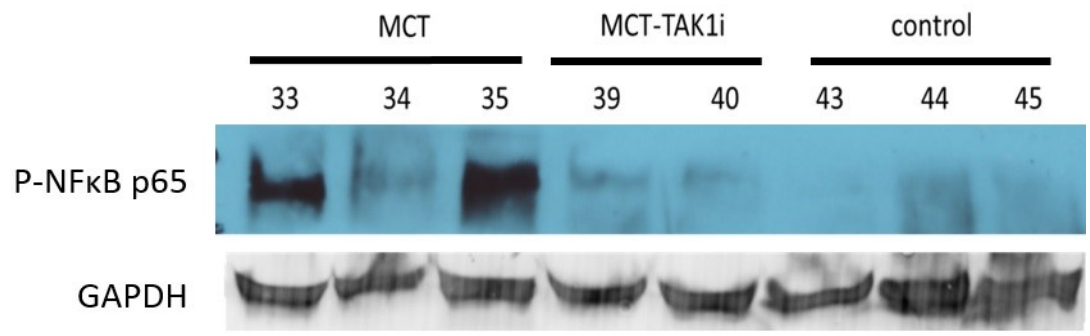

Figure 6.5 Phospho-NFκB p65 in the TA of the MCT rat treated with 5(Z)-7-oxozeaenol. Representative western blot of TA homogenates probed for phospho-NFκB p65 normalised to GAPDH in monocrotaline (MCT), MCT 5(Z)-7-oxozeaenol (MCT TAK1i) and control treated rats (n=5 MCT and control and n = 4 MCT TAKi).

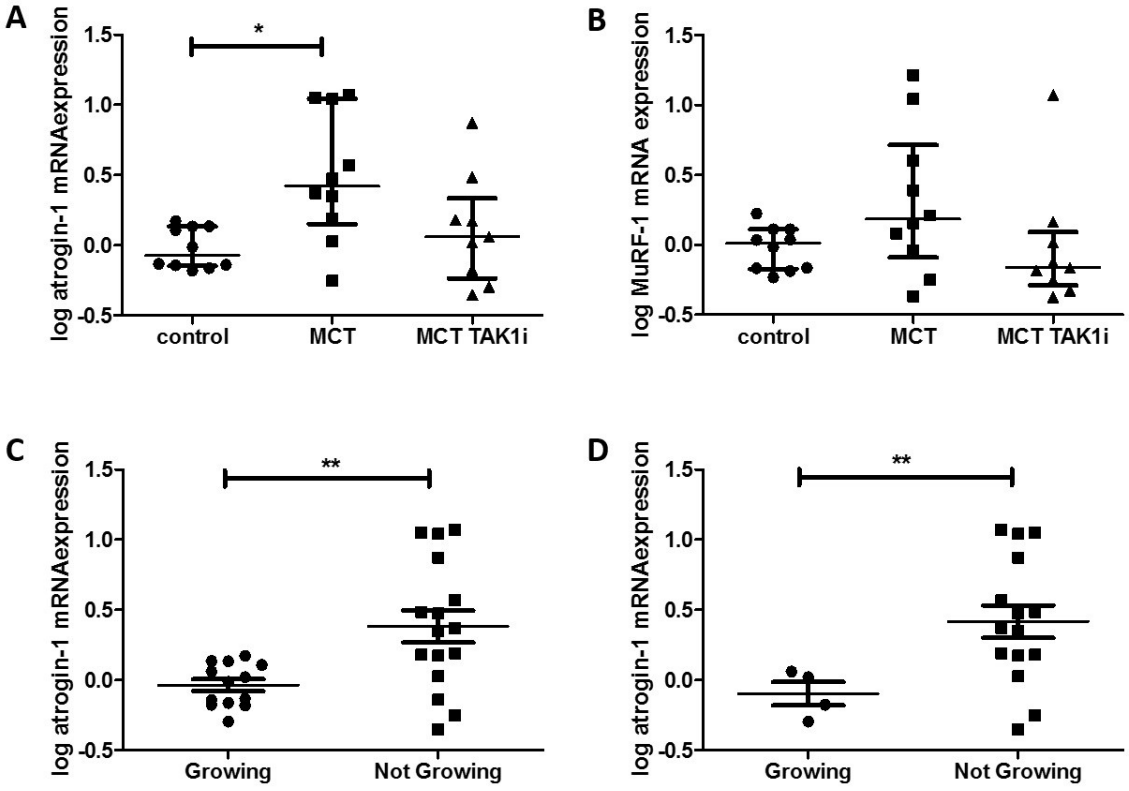

Figure 6.6 Ubiquitin ligase mRNA expression in the TA of the MCT rat treated with 5(Z)-7-oxozeaenol. A. log atrogin-1 mRNA expression in the TA of control (n=10), MCT (n=10) and MCT TAK1i (n=9) treated rats (Kruskall-Wallace p = 0.018). **B.** log MuRF-1 mRNA expression in the TA of control (n=10), MCT (n=10) and MCT TAK1i (n=9) treated rats (Kruskall-Wallace p = 0.177). **C.** log atrogin-1 mRNA expression in the TA of rats that were growing (n = 13) and not growing (n = 16) at the end of the experiment across the group as a whole (Student's t-test p = 0.003). **D.** log atrogin-1 mRNA expression in the TA of rats that were growing (n = 4) and not growing (n = 15) at the end of the experiment across the MCT treated animals alone (Student's t test p = 0.041).

6.5.3 TAK1 inhibition did not significantly change pulmonary pressure, right ventricular remodelling or GDF-15 levels in the MCT rat.

TAK1 inhibition, at the concentration used, had no discernible effect on RVSP or RV/LV+S weight (Figure 6.7A and 6.7B). Serum levels of GDF-15 in control, MCT and MCT TAK1i treated rats are shown in Figure 6.8A. Treatment with the TAK1 inhibitor caused a reduction in circulating GDF-15 levels in some animals, a trend that did not reach statistical significance (Figure 6.8A). GDF-15 mRNA expression in the lung of the control, MCT and MCT TAK1 inhibitor treated rats followed a similar pattern to serum levels in this model (Figure 6.8B).

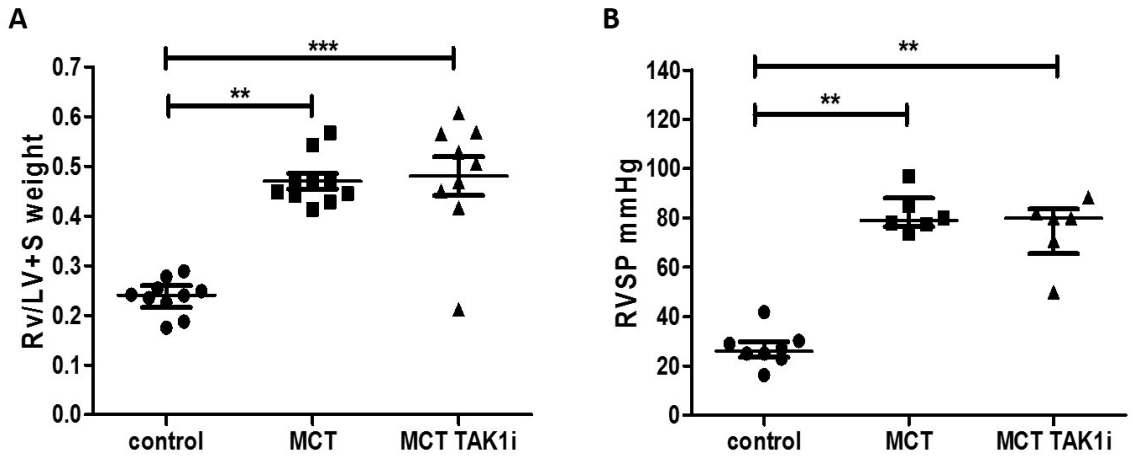

Figure 6.7 Pulmonary hypertension in the MCT rat treated with 5(Z)-7-oxozeaenol. A. Right ventricle / Left ventricle plus septal weight (RV/LV+S) in control (n=10), MCT (n=10) and MCT TAK1i (n=9) treated rats (Kruskall-Wallace $p < 0.001$). **B.** Right ventricular systolic pressure (RVSP) in mmHg in control (n=8), MCT (n=6) and MCT TAK1i (n=6) rats (Kruskall-Wallace $p = 0.001$).

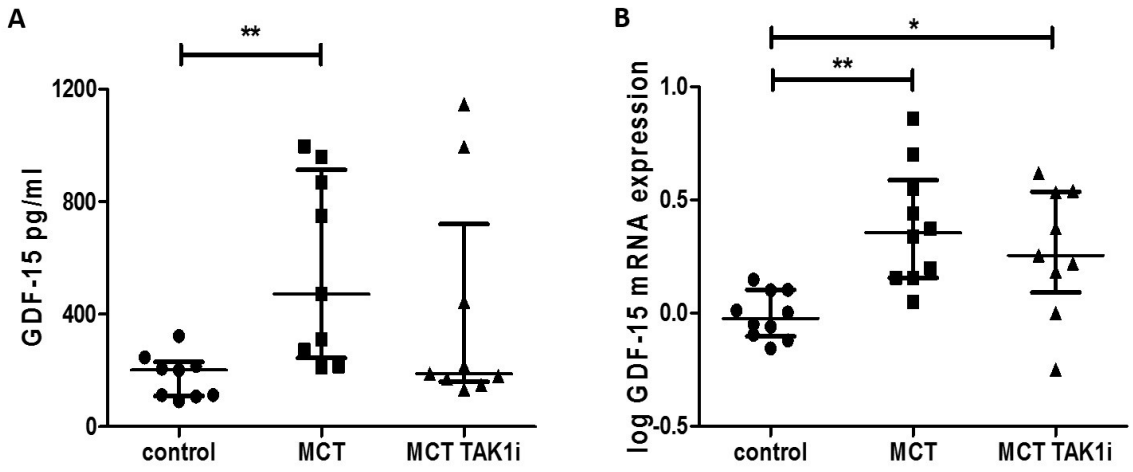

Figure 6.8 GDF-15 in the MCT rat treated with 5(Z)-7-oxozeaenol A. Circulating GDF-15 in pg/ml in control (n=9), MCT (n=9) and MCT TAK1i (n=9) treated rats (Kruskall-Wallace p = 0.013). **B.** log GDF-15 mRNA expression in the lung of control (n=10), MCT (n=10) and MCT TAK1i (n=9) rats (Kruskall-Wallace p = 0.002).

6.5.4 Circulating GDF-15 levels were associated with markers of muscle loss as well as continued growth in MCT rats treated with 5(Z)-7-oxozeaenol.

GDF-15 levels were correlated linearly and significantly with change in weight and TA atrogin-1 mRNA expression in this model (Figures 6.9 A and C). GDF-15 also correlated non-linearly with TA weight (Figure 6.9 B). Circulating GDF-15 levels were significantly lower in those animals which continued to grow at the end of the experiment compared with those that didn't. This was true across the group as a whole (Figure 6.10 A) and within the MCT treated group alone (Figure 6.10 B). GDF-15 had an AUC of 0.82 (p = 0.005) in predicting those animals which continued to grow at the end of this experiment. A GDF-15 cut off of < 260 pg/ml had a sensitivity of 83% and a specificity of 73% in predicting those animals which continued to grow (Figure 6.10 C).

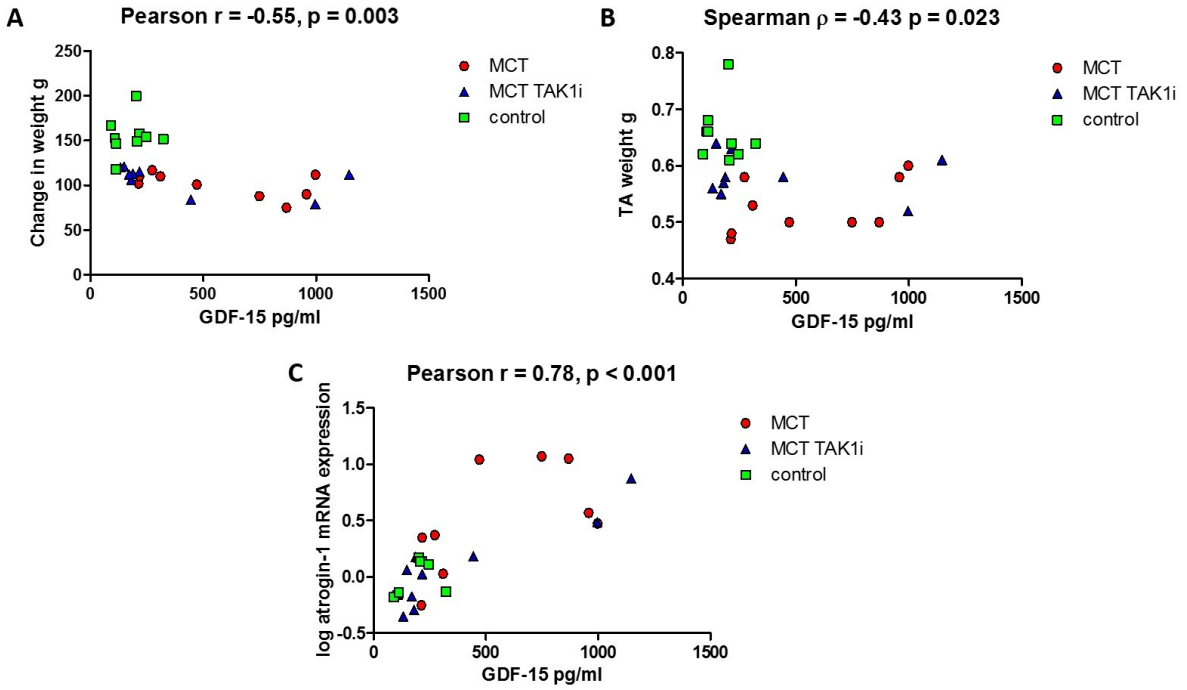

Figure 6.9 Correlations of circulating GDF-15 levels in MCT rats treated with 5(Z)-7-oxozeaenol. A. Plasma GDF-15 levels plotted against changed in weight in grams (g) in control (n=9) MCT (n=9) and MCT TAK1i (n=9) treated rats. **B.** Plasma GDF-15 levels plotted against TA weight in grams (g) in control (n=9) MCT (n=9) and MCT TAK1i (n=9) treated rats. **C.** Plasma GDF-15 levels plotted against log atrogin-1 mRNA expression changed in weight in grams (g) in control (n=9) MCT (n=9) and MCT TAK1i (n=9) treated rats.

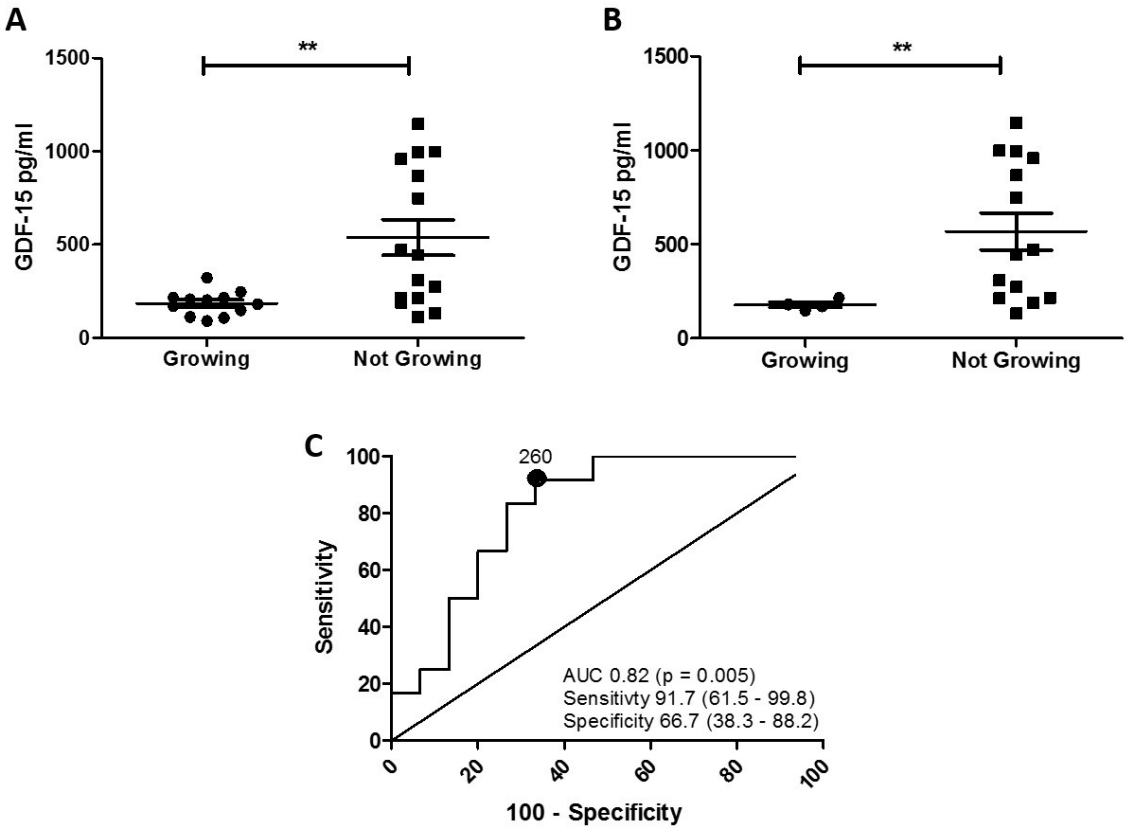

Figure 6.10 GDF-15 as a biomarker of continued growth in MCT rats treated with 5(Z)-7-oxozeaenol. A. GDF-15 levels in control (n = 10), MCT (n = 10) and MCT TAK1i (n = 9) treated animals growing and not growing at the end of the experiment (Student's t-test p = 0.003). **B.** GDF-15 levels in MCT (n = 10) and MCT TAK1i (n = 9) treated animals not growing and growing at the end of the experiment (Student's t test p = 0.002). **C.** ROC curve of GDF-15's ability to predict those still growing at the end of the experiment across all animals (n = 29) (AUC 0.82 p = 0.005).

6.6 Discussion

Inhibiting TAK1 with 5(Z)-7-oxozeaenol partially reversed MCT induced TA muscle wasting and prevented weight loss in some animals potentially in part by preventing increases in atrogin-1 mRNA expression. Interestingly circulating GDF-15 levels were able to predict those animals still growing at the end of the experiment confirming its utility as a biomarker of cachexia.

5(Z)-7-oxozeaenol treatment in the MCT rat did not change the final weight of the animals but did seem to prevent some of the muscle wasting seen in this model. Looking at previous work on growth

of the MCT rat weight loss does not occur until between the 3rd and 4th week, depending on the dose of MCT used, although growth inhibition occurs immediately after dosing (474, 475). This may go some way to explain why we only see the beginning of divergence in growth curves in the data presented and why the only difference in growth is in the proportion of animals still putting on weight at the end of the experiment.

TAK1 is an important mediator of NFκB activity (476). 5(Z)-7-oxozeaenol was able to significantly inhibit increases in phosphorylated NFκB p65 activity in the TA of the MCT rat, suggesting that the compound had the desired activity i*n vivo*. This does not, however, confirm that inhibition of NFκB signalling is definitively involved in reversal of wasting seen with 5(Z)-7-oxozeaenol treatment, especially as NFκB is not felt to be involved in increase in atrogin-1 expression (467).

GDF-15 has previously been shown to cause muscle wasting and to elevate expression of atrogin-1 and MuRF-1 (265). The data presented in Chapter 5 suggests that GDF-15 may mediate this effect through TAK1, a mechanism supported by others (318, 319). In the data shown above atrogin-1 mRNA there was a trend to a reduction in atrogin-1 mRNA the TA of the MCT TAK1i treated rats when compared to their MCT control treated counterparts, which did not meet statistical significance. These rats had larger TAs and on average an increase in proportion of larger TA fibre. Furthermore there was a significant decrease in the atrogin-1 mRNA expression in the TA of the animals treated with MCT and TAK1i that continued to grow at the end of the experiment compared to those that lost weight across the MCT group as a whole. Taken together this supports a role for GDF-15 and TAK1 in the muscle wasting seen in the MCT rat and suggests that 5(Z)-7-oxozeaenol *in vivo* may prevent GDF-15 mediated muscle atrophy, possibly through actions on atrogin-1. As previously mentioned, other mediators, such as GDF-8 and TNFα, may act through TAK1 to cause muscle loss (67, 136, 153, 345). Anti-TNF α treatment with a soluble receptor antagonist and pentoxyfylline, a general inhibitor of TNFα activity, have been shown to prevent cachexia in the MCT rat through a reduction in mRNA expression of atrogin-1 (136), whilst GDF-8 and GDF-15 neutralising antibodies have had some success in animal

models of cancer in reducing muscle wasting (269, 477). 5(Z)-7-oxozeaenol is likely to have blocked the effects of GDF-15, GDF-8 and TNFα signalling pathways in this model, acting synergistically to prevent muscle loss.

Some researchers have shown that, rather than being solely detrimental, activity in the TAK1 pathway is vital for maintenance of normal muscle homeostasis through its actions on satellite stem cell function. Genetically modified mice lacking TAK1 expression in satellite stem cells cannot regenerate after acute injury and actually exhibit smaller muscle fibres and increased atrogin-1 mRNA expression than wild type animals(363). It has also been shown that selective TAK1 knockout in mouse skeletal muscle impairs growth in the first few weeks of life (364). This is not surprising given the vital role that TAK1 has in preventing differentiation of myoblast and therefore maintaining a population of cells able to allow regeneration (478). The relevance of this action in muscle wasting in chronic disease, where TAK1 activity may be dysregulated is, however, unclear. The majority of muscle cells in the MCT rat model of PAH are mature and therefore have very low intrinsic TAK1 activity. TAK1 inhibition at low dose, aiming to bring the TAK1 activity levels back to baseline, rather than abolishing it all together, is likely to prevent inflammatory signalling in these cells resulting in the reduction in muscle wasting seen with this drug. The effect of high dose 5(Z)-7-oxozeaenol treatment may be very different from low dose therapy and may result, as with knockout models, in complete obliteration of TAK1 signalling causing a worsening rather than an improvement in the rate of muscle loss. Careful pharmacokinetic studies are needed to define the role of TAK1 inhibition in muscle wasting in patients with chronic disease and this should be a focus of future in vivo research. It is also not clear from the data whether the reason for the lack of response in some animals in the MCT TAK1i group in terms of prevention of weight loss is due to under or over-suppression of TAK1 activity, both of which is a possibility given its dual actions in myoblasts and mature cells.

TAK1 activity has been previously linked directly to disease activity in pulmonary hypertension, with excess levels of the phosphorylated protein being found in the lung homogenates of the MCT rat.

Furthermore TAK1 inhibition with 5(Z)-7-oxozeaenol has been shown to reduce the excess pulmonary artery smooth muscle cell proliferation seen in BMPR2 knockout cells suggesting a central role in the pulmonary vascular remodelling of PAH (360). 5(Z)-7-oxozeaenol can prevent neo-intimal formation in a wire induced vascular injury model, supporting a potential therapeutic role for TAK1 inhibition in vascular remodelling (359). The data presented above, however, shows that at low dose TAK1 inhibition has no effect of pulmonary pressure or right ventricular hypertrophy. This may be due to the timing of the intervention; after 2 weeks, the observed pulmonary vascular remodelling is already established and cannot be reversed. It may also be due to the low dose of 5(Z)-7-oxozeaenol used in this study. Although 0.5mg/kg doses of 5(Z)-7-oxozeaenol have been shown to be successful in some studies (359), in others they have not altered outcomes, where higher doses of 5mg/kg have been more effective (358).

There was no significant difference in GDF-15 levels in the circulation or in the lung homogenates of MCT control and MCT TAK1i treated rats. However, there was a trend to lower levels in the animals treated with 5(Z)-7-oxozeaenol. As in Chapter 4 circulating GDF-15 levels were associated with animal growth, TA weight and TA atrogin-1 mRNA expression. Furthermore GDF-15 levels in the blood were lower in those rats who continued to grow at the end of the experiment compared to those that didn't in the group as a whole. This was also true when the MCT group were analysed alone. These results suggest a complex interplay between GDF-15 and TAK1 *in vivo*.

We have shown that GDF-15 may act through TAK1 and that 5(Z)-7-oxozeaenol can inhibit GDF-15 mediated atrophy adding to the work of Bloch *et al*. (265) and Choi *et al.* (319). GDF-15 mRNA production is known to be a p53 dependant process (479). It has recently been shown that over-expression of TAK1 has been associated with increased expression of p53 mRNA and accumulation of the protein in the intracellular space (480). This may go some way to explaining why TAK1 inhibition with 5(Z)-7-oxozeaenol was able to inhibit production of GDF-15 in at least some animals, and could be confirmed by examining co-localisation of GDF-15 and p53 mRNA and protein expression in the

endothelial cell layer of the pulmonary vasculature of MCT rats treated with control or 5(Z)-7-oxozeaenol.

Finally, we have added to the body of research showing that GDF-15 is an effective biomarker of muscle wasting in acute and chronic disease. Our group has previously shown that GDF-15 is associated with muscle loss in AICU acquired weakness (218) and in COPD (266). In Chapter 4 this association was demonstrated in patients with PAH. A good biomarker needs to be valid, reliable and responsive (481). Data presented above shows that GDF-15 levels are decreased in animals that continued to grow who were treated with 5(Z)-7-oxozeaenol. This suggests that GDF-15 is responsive to change and might have be a useful biomarker of response to treatment and could be used as a surrogate end-point in drug trials (482).

6.7 Limitations

The main limitations of the study is the number of animals investigated, which meant that it was difficult to show a statistically significant difference between the groups studied. Other limitations included the requirement to humanely kill the animals on different days. Part of this is unavoidable to prevent a breach of the severity limits of the Home Office license, however, some was also practical as it was not possible to undertake cardiac catheters on all the animals in just one day. The lack of pharmaco-dynamic and pharmaco-kinetic assessment of the therapy also detracts from the validity of our study, although the fact that local NFκB p65 activity was lower in the TA of the TAK1i treated MCT rats than their MCT control treated counterparts was reassuring. Only one dose of 5(Z)-7-oxozeaenol was used and the effect of a higher dose and a trial of its use in a preventative model of MCT induced disease was not investigated.

6.8 Conclusions

The results presented above suggest that inhibiting TAKi with 5(Z)-7-oxozeaenol at low dose can prevent muscle loss, atrophy and weight loss in, at least, some animals in a MCT model of cachexia. This research suggests GDF-15, working with GDF-8 and TNFα, acting through TAK1 and possibly atrogin-1 may cause muscle wasting, a process that may be blocked by a TAK1i. Therefore, TAK1 may be a future target for therapeutic intervention in muscle wasting in PAH and other conditions associated with excess GDF-15 production.

Chapter 7 Discussion

7.1 Summary

I have shown in this thesis that:

1. Skeletal muscle wasting and physical inactivity are associated with poor outcomes in patients with PAH
2. Circulating GDF-15 levels are associated with skeletal muscle wasting both in animal models and in patients with PAH and thus may be a useful biomarker to identify those at risk of muscle loss.
3. GDF-15 causes myotube atrophy in vitro and also activates TAK1.
4. TAK 1 inhibition with 5(Z)-7-oxozeaenol reduced GDF-15 mediated muscle atrophy in vitro and reduces muscle loss but had no effect on the PAH phenotype in MCT rat.

7.2 My findings in context

A number of different groups have found that peripheral muscle function is impaired in patients with PAH and that this is associated with functional status and 6MWD but not necessarily with cardiovascular parameters (160, 161). We can draw the same conclusions from my data. Muscle strength and size are closely correlated with 6MWD and WHO functional status but not with echocardiographic parameters. The data presented here goes further, since I have shown that quadriceps cross sectional area is an independent predictor of 6MWD, suggesting muscle size exerts a major influence over exercise capacity, supporting data from studies of rehabilitation (164, 171, 172). Although associations can be inferred from studies of rehabilitation (18), to the best of my knowledge QOL has not been measured in the same population of PAH patients as muscle strength and size. The data presented in this thesis therefore sheds new light on the potential influence of skeletal muscle mass on QOL, demonstrating that larger quadriceps muscle size was independently associated with improved SGRQ scores. Furthermore muscle strength has been shown to associate

with average follow up QOL suggesting that changes in muscle function over time could be translated into long term benefits in these patients.

Physical activity has been rarely studied in PAH. Unsurprisingly, low physical activity has been associated with worse functional class, decreased exercise capacity (173) and lower quality life (483) in PAH, all findings which are corroborated by my data set, including associations with follow up QOL. It is interesting that physical activity, unlike muscle size, was not independently associated with either 6MWD or SGRQ score, suggesting that at the time of measuring current muscle size had more influence than current activity level on these outcomes. My results also confirm the close association of muscle strength, size and physical activity seen in other conditions (484) in PAH. What we cannot tell from this study is whether a reduction in muscle size and function, or low physical activity due to breathlessness is the primary driver of the 'vicious cycle' of breathlessness, deconditioning and skeletal muscle weakness seen in chronic cardio-respiratory disease (75).

The 6MWD is one of the most important prognostic indicators in PAH (421). The findings above suggest that locomotor muscle function and physical activity are closely linked to 6MWD. In contrast to COPD and heart failure, where both outcomes have been linked to mortality, (34, 423-427) neither muscle strength or size nor physical activity has previously been associated with mortality in PAH. In this cohort, patients exhibiting both lower FFMIs and steps per day had an increased mortality. This suggests that improving muscle strength and/or physical activity in patients with PAH may reduce mortality in this group. As mentioned in Chapter 3 the cut offs of these measures associated with poor prognosis were very low (370, 428). These patients might have the most to gain but are also the potentially the least likely to take up exercise (440, 441, 485). Whether rehabilitation is as effective in these patients remains to be seen and whether there is greater potential for anti-atrophic and pro-anabolic adjuncts in this particular group should be the focus of future research.

Hospitalisation for patients with PAH is likely to be associated with lower QOL and increases in healthcare costs (431, 433, 434). The data presented here suggest that patients with lower muscle

strength and bulk are more likely to be admitted to hospital. In fact 90% those patients with a QMVC/BMI of < 1.1 were admitted within 2 years of enrolment, compared to 50% in the overall cohort. This observation suggests that improving muscle strength might prevent admission and thereby improve both QOL and reduce healthcare costs.

The findings of this study and data from studies of rehabilitation (18, 164, 171, 172) reinforce the virtues of exercise training in patients with PAH, which may well also deliver the benefits seen in other populations (98, 435-438). A number of challenges remain. Firstly, the ideal method of delivering rehabilitation and transferring gains in muscle strength into sustained improvements in physical activity is unknown (439). Secondly, the method for identifying those patients with low physical activity and low muscle strength without doing expensive tests and without the requirement for specialist equipment is not established. Clinical biomarkers of cachexia (443) and simple and effective screening tests for low physical activity (416) are required to identify those who might benefit most from interventions aimed at increasing these modifiable risk factors. Thirdly, as mentioned above, those patients with especially low muscle mass may benefit from anabolic agents. There is currently no such agent in clinical use (439) meaning novel pathways need to be identified and new drugs are required in this area.

Screening tests are required to determine those patients with PAH who are at risk of low physical activity for targeted intervention and enrolment in clinical trials. The SGRQ and CAMPHOR are QOL questionnaires from which activity scores can be calculated, both of which have been used in PAH (387, 389). The SGRQ but not the CAMPHOR activity score has been validated against other activity questionnaires (446). No previous studies have attempted to compare objectively measured physical activity with questionnaire based assessment in this population. I have previously shown, in patients with COPD, that some physical activity questionnaires outcomes are associated with objectively measured activity (383). My data suggests that a SGRQ and to a lesser extent a CAMPHOR physical activity score can be used to determine those patients with PAH who are inactive. Questionnaire based

assessment of physical activity can be unreliable (444) but embedding activity scores in a QOL questionnaire may reduce recall bias through framing (444). Interestingly, higher (i.e. worse) SGRQ activity scores were associated with increased mortality adding weight to the argument that the SGRQ might be used to screen and even monitor activity in patients with PAH.

GDF-15 is emerging as a potential biomarker of cachexia and muscle loss, although it is not in clinical use at present (443), although an antibody for human use is in development. We used 2 animal models of PAH to determine the association of circulating GDF-15 with muscle loss. The MCT treated rat is a well-established model of cardiac cachexia (132), and I have shown that Sugen/hypoxia treatment in mice, which has previously been associated with weight loss (452) and diaphragmatic changes (162), also exhibited a similar pattern of skeletal muscle wasting.

My data shows that, like in patients with PAH (207), circulating GDF-15 levels are raised in the MCT rat and Sugen/hypoxia mouse compared to controls. Interestingly there was no increase in GDF-15 in the hypoxia alone treated animals. This suggests that Sugen, a vascular endothelial growth factor antagonist, is required for GDF-15 production in a hypoxic mouse model of PAH.

Circulating GDF-15 has been identified as a biomarker of skeletal muscle loss in COPD (453) in healthy elderly women (263), in cancer (269) and in ICU acquired weakness (218). The results presented here confirm the association of GDF-15 and skeletal muscle wasting in animal models and in patients with PAH. They also show that low GDF-15 levels can be used as a reasonable biomarker of preserved muscle strength in these patients. I have also shown that circulating GDF-15 levels are associated with objectively measured physical activity in patients with PAH, with previous work done in animal and rehabilitation studies yielding either conflicting or negative results (257, 260, 270, 271, 273).

As well as being a marker of muscle loss there is emerging evidence that GDF-15 is also a cause of low muscle mass. Initially felt to exert its actions by suppressing appetite (260) our group has also shown that GDF-15 can have a direct effect on muscle size *in vitro* (218) and *in vivo* (453). TGFβ super-family proteins, including GDF-8, have been shown to act in an autocrine, paracrine and

endocrine manner (182, 486). Studies in ICU acquired weakness have shown an increase in local GDF-15 expression in the quadriceps of patients who exhibit muscle wasting. This suggested that GDF-15's actions may be autocrine or paracrine (265). In my study there was no change in TA GDF-15 expression in either animal model examined. Like in patients with PAH I have shown that GDF-15 in these animals is over-expressed in the pulmonary vascular endothelium (283), supporting the hypothesis that GDF-15 acts in a predominantly endocrine manner. This data is further supported by a recent study showing GDF-15 secreting tumours can cause muscle loss that is antagonised by a GDF-15 neutralising antibody (269).

GDF-15 is not the only TGFβ super-family member that I have identified as potentially being important in regulating muscle mass in the MCT rat. GDF-8 levels are raised in the circulation of the MCT rat (153). I have shown that GDF-8 is also up-regulated in the skeletal muscle of this model. Unlike GDF-15, GDF-8 primarily acts locally (182) and is almost exclusively produced by muscle cells (487). The fact that there are a number of different proteins which can stimulate muscle wasting in this model highlights the importance of identifying common pathways which co-ordinate this process, so these can be targeted by effective therapeutic intervention.

Despite identifying GFRAL receptor as the receptor for GDF-15 in the central nervous system (292) the downstream signalling pathway and receptors through which GDF-15 acts in muscle is as yet unknown (227, 295). Both canonical and non-canonical pathways have been identified as important in propagating GDF-15's signals in different cells lines.

In C2C12 skeletal muscle cells GDF-15 caused no significant upregulation in SMAD 2, 3 or SMAD 1, 5 dependent luciferase activity at 6 hours. This finding is similar to some (260, 299) but in contrast to others (235, 290, 297).

Other groups have found that GDF-15 effects are mediated through the TGFBR2 and ALK-5 receptors (288, 301). I found in TGFBR2 over-expressing cells, GDF-15 (50 ng/ml) caused an increase in SMAD 2, 3 activity, suggesting a potential interaction with this receptor. This demonstrates that GDF-15 has

some affinity to bind to the TGFBR2, however the small fold change and the dose of both receptors and ligand required to elicit these changes brings the physiological relevance of these results in to question. The ALK-5 inhibitor SB-431542 was able to reduce GDF-15 mediated atrogin-1 mRNA expression, suggesting that the ALK-5 receptor may be involved in GDF-15 signalling. This result is complicated by the fact that SB-431542, has some activity against ALK-4 and ALK-7 (462) and that ALK5 inhibition did not just abolish GDF-15's actions but actually reversed its effects on atrogin-1. This highlights some of the difficulties investigating pathways with high levels of receptor promiscuity (178).

Next I cloned a truncated version of the TGFBR2. Others have shown the beneficial effects the TTGFBR2 in reducing inflammation and promoting regeneration in skeletal muscle (463). In my experiments TTGBFR2 over-expression failed to prevent high dose GDF-15 (50ng/ml) mediated myotube atrophy, leaving the question as to whether the TGFBR2 is the binding receptor for GDF-15 unanswered.

The evidence collected by luciferase assay suggested that up-regulation of SMAD responses did not play a major role in GDF-15 signalling in myoblasts. This led us to investigate the non-canonical TGFβ signalling pathway. GDF-15 has previously been shown to signal through the TAK1 - NFκB p65 axis in Ecoli infected gastric epithelial cells (318, 319). In myoblasts GDF-15 caused an increase in NFκB p65 nuclear localisation and overexpression of NFκB p65 mRNA, the latter of which was antagonised by co-treatment with TAK1 inhibitor 5(Z)-7-oxozeaenol.

For the remainder of the experiments mature myoblasts with low intrinsic TAK1 and NFκB p65 activity (361, 464) were used. In these cells GDF-15 treatment caused phosphorylation of TAK1 and NFκB p65 at a number of times and doses. Bloch et al. has previously shown that GDF-15 up-regulated atrogin-1 and MuRF-1 mRNA expression (265) and caused myotube atrophy (218). I have shown that TAK1 inhibition with 5(Z)-7-oxozeaenol (1000 nM) prevented relative GDF-15 mediated myotube atrophy and reduced GDF-15 mediated expression of atrogin-1. It also prevented GDF-15 mediated MuRF-1 expression caused by low but not high dose GDF-15.This suggests that GDF-15 promotes TAK1

phosphorylation, thereby activating NFκB and up-regulating mRNA expression of MuRF-1. The increase in atrogin-1 demonstrated also seems to be dependent on TAK1 but is likely to be independent of NFκB p65, which is not thought to be in involved in up-regulation of atrogin-1 expression (467).

I next examined whether the downstream mediators of GDF-15 activity were raised in the muscle of the MCT rat. Previous work has shown that both atrogin-1 and MURF-1 mRNA levels are raised in the skeletal muscle of the MCT rat at 21-22 days (60, 468). My data showed a trend to increase in atrogin-1 mRNA in the MCT rat TA and an association between atrogin-1 mRNA expression and the animal's change in weight and TA weight at 4 weeks. MuRF-1 mRNA was not elevated in these animals. The differences between my data and that of others could be accounted for by the time course at which the levels of ubiquitin ligases were assessed, meaning the time of the peak mRNA levels were missed in my experiments. This hypothesis is supported by the facts that MuRF-1 has been shown to peak earlier than atrogin-1 in a model of burns induced muscle wasting (470), that variation in ubiquitin ligase expression over time has been observed in man (469) and that the rats in previous experiments showing increases in ubiquitin ligases were assessed at 3 and not 4 weeks (60, 468). This hypothesis is supported by data presented in Chapter 6 where there was a significant increase in atrogin-1 mRNA expression at the earlier time point studied.

TAK1 has been found to be vital for the development and regeneration of healthy muscle through its actions on satellite stem cell function (363, 364). It is also an essential downstream mediator of GDF-8, allowing it to prevent hypertrophy in muscle cells (67, 366). This suggests that TAK1 regulation must be carefully controlled in order to prevent an imbalance between protein synthesis and degradation. I have shown that TAK1 activity is increased in the skeletal muscle of the MCT rat and have presented some limited evidence that it also raised in the quadriceps biopsy of patients with PAH. GDF-15 activates TAK1 *in vitro* and antagonising TAK1 may be a potential method by which GDF-15's actions can be blocked *in vivo*. This may have the advantage, unlike other more specific treatment, like

monoclonal antibodies of GDF-15 (269), of blocking the signalling of a number of molecules involved in muscle wasting including but not limited to GDF-15, GDF-8 and TNFα (67, 136, 153, 345).

5(Z)-7-oxozeaenol inhibited increases in phosphorylated NFκB p65 activity, a known downstream mediator of TAK1 (476) in the TA of the MCT rat, suggesting that the compound had the desired activity i*n vivo*. NFκB is not felt to be involved in increases in atrogin-1 expression (467), suggesting that there are other downstream protein involved in TAK1 mediated muscle loss, that were not identified in this study.

5(Z)-7-oxozeaenol treatment at 0.5 mg/kg/day for 9 days starting at 2 weeks after MCT treatment seemed to prevent muscle wasting in this animal model of PAH in at least some animals. GDF-15 has previously been shown to cause muscle wasting through atrogin-1 and MuRF-1 over-expression (265). I have presented data that suggests that GDF-15 may act through TAK1 in muscle cells similar to its effect in Ecoli infected gastric epithelial cells (318, 319). I demonstrated that atrogin-1 mRNA was reduced in the TA of the MCT TAK1i treated rats that continued to grow at the end of the experiment. The rats in the intervention group had larger TAs and a decrease in proportion of smaller and an increase proportion of larger TA fibres.

This supports a role for TAK1 in the muscle wasting seen in the MCT rat and suggests that 5(Z)-7-oxozeaenol may prevent GDF-15 induced muscle loss in this model of chronic muscle wasting. Antagonising TAK1 has the advantage of potentially targeting a number of other mediators of muscle loss, like GDF-8 and TNFα (67, 136, 153, 345). Both anti-GDF-8 and GDF-15 monoclonal antibodies have been associated with a reduction in muscle wasting in animal models of cancer cachexia (269, 477), whilst anti-TNF α treatment has been shown to prevent cachexia in the MCT rat through a reduction in mRNA expression of atrogin-1 (136), closely mimicking my work. 5(Z)-7-oxozeaenol is likely to have blocked the effects of GDF-15, GDF-8 and TNFα signalling pathways in this model, acting synergistically to prevent muscle loss.

As mentioned above, the TAK1 pathway is vital for maintenance of normal muscle homeostasis through its actions on satellite stem cell function. Therefore antagonising TAK1 must be done with great care. Genetically modified satellite stem cell TAK1 knockout mice cannot regenerate after acute injury and actually exhibit smaller muscle fibres and increased atrogin-1 mRNA expression when compared to wild type animals (363). It has also been shown that selective TAK1 knockout in mouse skeletal muscle impairs growth in the first few weeks of life (364). This is not surprising given the vital role that TAK1 has in preventing differentiation of myoblast and therefore maintaining a population of cells able to allow regeneration (478). The relevance of TAK1's action in muscle wasting in chronic disease, where there may be excess TAK1 activity has not been previously defined. The majority of muscle cells in the MCT rat model of PAH are mature and therefore have very low intrinsic TAK1 activity. Despite this we have shown that phosphorylated TAK1 expression is raised in these animals. TAK1 inhibition at low dose, like we have used here, is aimed at reducing TAK1 activity levels back to baseline, rather than abolishing them completely. This strategy has proven to be effective with a reduction in muscle atrophy and a decreased in atrogin-1 expression in the intervention group. The next step would be to carry out careful pharmacokinetic studies of both low and high dose TAK1 inhibition in the MCT rat with a careful focus both on inhibition of regeneration (363) and on off target effects of the drug (345).

TAK1 activity has been previously linked directly to disease activity in PH, with excess levels of the phosphorylated protein being found in the lung homogenates of the MCT rat. Furthermore TAK1 inhibition with 5(Z)-7-oxozeaenol has been shown to reduce the excess pulmonary artery smooth muscle cell proliferation seen in BMPR2 knockout cells suggesting a central role in the pulmonary vascular remodelling of PAH (360). 5(Z)-7-oxozeaenol can prevent neo-intimal formation in a wire induced vascular injury model, supporting a potential therapeutic role for TAK1 inhibition in vascular remodelling (359). The data presented in my thesis, however, shows that at low dose TAK1 inhibition has no effect of pulmonary pressure or right ventricular hypertrophy. This may be due to the timing of the intervention; that after 2 weeks the pulmonary vascular remodelling seen is already established

and cannot be reversed. It may also be due to the low dose of 5(Z)-7-oxozeaenol used in this study. Although 0.5mg/kg doses of 5(Z)-7-oxozeaenol have been shown to be successful in some studies (359) in others they have not altered outcomes, where higher doses of 5mg/kg have been more effective (358).

There was no significant difference in GDF-15 levels in the circulation or in the lung homogenates of MCT control and MCT TAK1i treated rats. However there was a trend to lower levels in the animals treated with 5(Z)-7-oxozeaenol. Circulating GDF-15 levels were associated with animal growth, TA weight and TA atrogin-1 mRNA expression. Furthermore GDF-15 levels in the blood were lower in those rats who continued to grow at the end of the experiment compared to those that didn't in the group as a whole and when the MCT group were analysed alone. These results confirm the complex interaction between GDF-15 and TAK1 which seems to be both up and downstream of the ligand. Increased TAK1 activity may drive increased GDF-15 production, as over-expression of TAK1 has been shown to lead to the accumulation of p53 a known activator of the GDF-15 expression (479, 480). This may go some way to explaining why TAK1 inhibition with 5(Z)-7-oxozeaenol was able to inhibit production of GDF-15 in at least some animals. This data also further demonstrates GDF-15's role as an effective biomarker of muscle wasting, which is responsive to change and might have utility as a surrogate end-point in drug trials (482).

7.3 Limitations

7.3.1 Sample size

Small sample size was a problem for the clinical study, the Sugen/hypoxia mouse study and to a certain extent the TAK1 inhibitor MCT rat study. There were a number of reasons for this. PAH is a rare disease with a limited pool of patients from which to recruit (10). Even so, this is the largest cohort of patients to undergo muscle testing in this condition. The Sugen/hypoxia mouse model we used had far lower circulating GDF-15 levels than the MCT rat, so with limited resources was not a major focus of investigation. The interventional model was studied in collaboration with Cambridge University, and

delays and animal licensing issues in our collaborators laboratory meant that work was delayed. Due to these small numbers it is difficult to make generalisations about the associations seen in our cohorts. Only relative and not absolute change in myotube diameter was statistically different between GDF-15 and TAK1i treated cells. This is again likely due to the small sample numbers. Our group has previously published myotube diameter findings using only 2 repeats but including all the cell data (218). The methodology used in this thesis, showing consistent changes in average relative diameter across all three experiments, adds weight, rather than detracts from the validity of the data presented. Throughout this thesis I have undertaken multiple comparisons using the same data set and have not carried out Bonferroni corrections for multiple analysis. This is because the numbers needed to study would be higher than feasible given the time and resources available. This does leave us open to type 1 error but reduces the amount of type 2 error. As long as this is understood by the reader then this seems to be a reasonable approach and is supported in the wider literature when dealing with small sample sizes (449), even when using linear regression (450).

7.3.2 Missing data

Both animal models and the clinical study had some missing data. This particularly effected the SWA and questionnaire data. I adopted the strategy of using all the valid data available to increase the sample size. This was particularly important given the small sample size to begin with and is supported by the paper by Dziura *et al.* (451)

7.3.3 Validity of equipment

In the clinical study although it has been used previously (173), and been validated in COPD (419), the SWA has not been validated in PAH.

7.3.4 Animal Licensing and Assessment

In the animal experiments a number of animals had to be humanely killed to prevent them from reaching their severity limits. If this had not been the case longer time courses may have been possible

and these may have generated a stronger signal particularly in the interventional model. There was some requirement to humanely kill the animals on different days. Part of this is unavoidable to prevent a breach of the severity limits of the Home Office license, as mentioned above, however some was also practical as it not possible to undertake cardiac catheters on all the animals in just one day. The lack of a time course of assessment of the TA gene expression means we may have missed the time at which maximal mRNA expression of various genes peaked.

7.3.5 The primary deficit causing muscle loss, GDF-15 production and its actions

This study leaves a number of important unanswered questions. I have not established the primary problem causing low muscle mass in patients with PAH, whether this be low physical activity due to breathlessness or a direct myo-toxic response to increases in inflammatory mediators and hypoxia seen in the disease. I have not established the relative contribution that nutrition, physical inactivity and direct pro-atrophic signalling play in propagating GDF-15's effects on muscle mass in PAH. Although I have demonstrated like others that GDF-15 is produced in the pulmonary vascular endothelial cells in PAH (283), I have not ruled out alternative sites of over-expression in the MCT rat. *In vitro* I have established that GDF-15 can cause muscle atrophy and activate TAK1 at a number of doses and time points. I have shown that TAK1 inhibition, with a selective inhibitor, can prevent these actions, however there is always a possibility of off target effects with a small molecule inhibitor(488). I have not performed experiments in TAK1 siRNA C2C12 cells and in muscle specific conditional knockout animals which would add weight to my arguments.

7.4 Conclusions (Figure 7.1)

In this thesis I aimed to: define the association between GDF-15 and muscle parameters in patients and in animal models of PAH; investigate the source of production of GDF-15 in animal models of PAH; define the pathway through which GDF-15 acts to cause muscle wasting *in vitro*, with a view to antagonising its effects *in vitro* and *in vivo*; examine GDF-15's usefulness as a biomarker of muscle

loss; and assess the association of muscle loss with outcomes in PAH like QOL, hospitalisation and mortality.

I have shown that circulating but not local GDF-15 levels, likely to be released from the pulmonary vasculature, are associated with measures of muscle function and size in 2 animal models and in patients with PAH. I have shown that GDF-15 levels in the circulation are a reasonable biomarker of muscle loss in PAH, which, along with physical activity is associated with poor outcomes in the disease. I demonstrated that GDF-15 may act through TAK1 activation to increase the expression of ubiquitin ligases atrogin-1 and MuRF-1 in the muscle of the MCT rat. This process may be partly, but is unlikely to be fully, dependant on NFκB activation. GDF-15's effects are likely to result in an imbalance between protein synthesis and degradation leading to a reduction in muscle mass and a decrease in function. I have also demonstrated that other target molecules such as GDF-8 are raised in the MCT model suggesting that other ligands acting through TAK1 contribute to muscle wasting *in vivo*. Finally I have been able to show that TAK1 inhibition with 5(Z)-7-oxozeaenol can prevent some of the muscle atrophy seen in the MCT rat model of PAH. Importantly GDF-15 is raised in a wide range of conditions (262, 265, 489-492), and muscle loss is a ubiquitous outcome in chronic disease (21), meaning my data has implications both in the management of PAH associated muscle loss and in the wider context of cachexia in chronic disease .

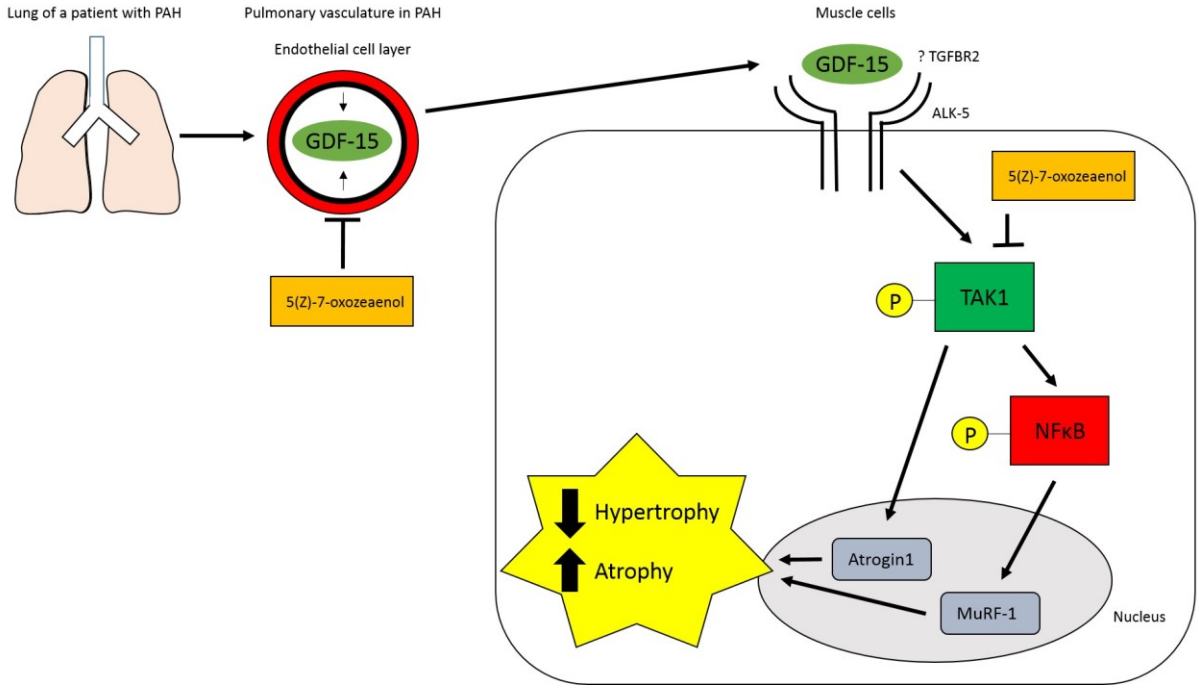

Figure 7.1 Diagram showing potential mechanism through which GDF-15 may cause direct muscle atrophy in patients with PAH and the potential sites of action of 5(Z)-7-oxozeaenol.

7.5 Future Work

A larger prospective study across a number of centres should be set up to corroborate the associations of muscle loss and low physical activity that I have found in this small study. A longer follow up of 5 years may allow stronger conclusions to be drawn. Interventional studies should focus on the optimal method by which rehabilitation could be delivered and transferred into gains in physical activity in this group. One such study that I am currently pursuing is the use of a personal trainer at home to augment general exercise advice in this group. A particularly important group to study identified by this thesis is those undergoing transplant assessment. Careful attention to physical performance and muscle wasting in this group may identify those at especially increased risk and be a modifiable risk factor for post-operative complications and increased mortality.

GDF-15 has been shown to be a biomarker of muscle wasting in PAH as well as in a number of other conditions (218, 263, 269, 453). My data suggests that it may be responsive to change but this has not

been confirmed outside my animal model (257). The next steps might be to track GDF-15's associations with muscle wasting longitudinally in a large cohort of unselected patients with chronic diseases to examine its validity, variability and responsiveness to change. This would allow me to fully map GDF-15's utility as a biomarker of muscle loss.

I have demonstrated that physical activity scores from QOL questionnaires are a reasonable surrogate of objectively measured physical activity in patients with PAH. Like GDF-15, more data is required to show that they have low enough variability and that they are responsive enough to be used instead of activity monitors in this population. Large trials with assessment using both questionnaire and activity monitors contemporaneously are required to inform these decisions.

I have shown that GDF-15 over-expression in the lung homogenates and particularly in the pulmonary vasculature is correlated with circulating levels of the protein in the MCT rat model of PAH. There was no increase in expression in the skeletal muscle of this animal. This suggests but does not confirm that the pulmonary vasculature is the major source of GDF-15 in this model. Tissue is available from other potential sources of GDF-15 including the liver and the heart, both of which are known to be damaged by exposure to MCT (474, 493). Examination of these other tissues may be useful in confirming the pulmonary vasculature as the main source of GDF-15 in the circulation of the MCT rat. Furthermore a conditional GDF-15 knockout in the pulmonary vascular endothelial cells of a transgenic mouse treated with Sugen/hypoxia which did not have raised circulating GDF-15 levels would support my hypothesis.

The discovery of the GFRAL receptor as the mediator of appetite driven GDF-15 induced weight loss (292, 293, 296) has shed new light on GDF-15's action in neural tissue. GDF-15's role and mechanism of action in other tissues including, but not limited to the pulmonary vasculature and skeletal muscle has yet to be defined in a similar way. Generation of conditional and conditional tissue specific knockout mice would shed further light on GDF-15's role in both the development of pulmonary hypertension and in skeletal muscle wasting. The experiments would have to include pair fed animals

as well as an insult to induce muscle wasting that was associated under normal circumstances with a significant rise in GDF-15 production.

I have confirmed the work of Bloch *et al*. (265) showing that GDF-15 can cause over-expression of the mRNA of ubiquitin ligases atrogin-1 and MuRF-1 *in vitro*. I have shown that GDF-15 levels correlate with TA atrogin-1 mRNA levels in the MCT rat. This is unlikely to be the complete story as the changes in atrogin-1 levels are small and are not likely to be explained by my other finding of raised NFκB p65 phosphorylation (467) in response to GDF-15. Important future steps would be to perform a time course of circulating levels of GDF-15 and TA ubiquitin ligase expression in the MCT rat model to give a better understanding of the dynamic shift in mRNA expression of ubiquitin ligases over time. Tissue is available for assessment of protein levels of both ubiquitin ligases in the TA of the MCT rat. This would add weight to my argument that these pro-atrophic factors are involved in the muscle wasting seen in this model. Importantly changes in atrogin-1 and MuRF-1 proteins have been described previously in MCT rat muscle (468).

The receptor through which GDF-15 acts in skeletal muscle is still not clear. I have produced some evidence that GDF-15 can interact through the TGFBR2. I have also shown that GDF-15 can interact with the ALK-5. The main body of evidence in the wider literature suggests that GDF-15's effects are mediated through the GFRAL (296) TGFBR2 and ALK-5 (288, 301). In the first instance I would attempt to use siRNA to inhibit each TGF-beta type 1 and each type 2 receptor in turn to identify those which is most likely to propagate GDF-15's downstream signal. I would also investigate the role of the GFRAL in propagating GDF-15's signals in skeletal muscle, despite previous authors showing that it wasn't present in this tissue (295).

My results suggest that inhibiting TAK1 with 5(Z)-7-oxozeaenol both in vitro an in vivo can prevent muscle loss and atrophy signalling. A prevention study in the MCT may yield more consistent results, proving the concept that TAK1 inhibition may be beneficial in preventing muscle atrophy. Alternatively it could be detrimental in downregulating the rats' population of pluripotent satellite stem cells from

the outset preventing regeneration. Pharmaco-dynamic and pharmaco-kinetic assessment of 5(Z)-7-oxozeaenol at number of doses and time points is required to assess in detail the drug's mechanism of actions and its downstream on and off target effects and is vital to continuing this research. A number of drug companies have compounds in development targeting TAK1. A commercial collaboration may yield very helpful results as some of these other compounds are potentially translatable to human studies (356). Careful assessment of muscle strength and size in any future human studies of a TAK1 inhibitor should be undertaken. This is most likely to be relevant, in the first instance, in studies using TAK1 inhibitors as adjuncts to chemotherapy in patients with cancer.

The complex interplay between GDF-15 and TAK1 deserves further attention. Hypoxia and sheer stress have both been identified as potentially important in stimulating GDF-15 production from human microvascular pulmonary endothelial cells (283). The exact mechanism and the physiological effects of this on the pulmonary vasculature has yet to be defined.

Through this thesis I have identified both GDF-15 and TAK1 as potential therapeutic targets for muscle wasting in PAH an unmet but important need in this population. Much work needs to be done to translate these preliminary findings from bench to bedside but this data could be the start of a process of drug development aimed at improving exercise tolerance, QOL and even mortality in patients with PAH as well as in other conditions.

Chapter 8 References

1. PHA. http://www.phauk.org/what-is-ph/the-heart-and-circulatory-system/. 2016.
2. Barst RJ. Pulmonary hypertension: past, present and future. Ann Thorac Med. 2008;3(1):1-4.
3. Romberg E. Ueber Sklerose der Lungen arterie. Dtsch Archiv Klin Med. 1891;48:197–206.
4. Hoeper MM, Bogaard HJ, Condliffe R, Frantz R, Khanna D, Kurzyna M, et al. Definitions and diagnosis of pulmonary hypertension. Journal of the American College of Cardiology. 2013;62(25 Suppl):D42-50.
5. Simonneau G, Gatzoulis MA, Adatia I, Celermajer D, Denton C, Ghofrani A, et al. Updated clinical classification of pulmonary hypertension. Journal of the American College of Cardiology. 2013;62(25 Suppl):D34-41.
6. Fishman AP. Clinical classification of pulmonary hypertension. Clin Chest Med. 2001;22(3):385-91, vii.
7. Galie N, Humbert M, Vachiery JL, Gibbs S, Lang I, Torbicki A, et al. 2015 ESC/ERS Guidelines for the diagnosis and treatment of pulmonary hypertension: The Joint Task Force for the Diagnosis and Treatment of Pulmonary Hypertension of the European Society of Cardiology (ESC) and the European Respiratory Society (ERS): Endorsed by: Association for European Paediatric and Congenital Cardiology (AEPC), International Society for Heart and Lung Transplantation (ISHLT). Eur Heart J. 2016;37(1):67-119.
8. Hoeper MM, Simon RGJ. The changing landscape of pulmonary arterial hypertension and implications for patient care. European respiratory review : an official journal of the European Respiratory Society. 2014;23(134):450-7.
9. McLaughlin VV, Archer SL, Badesch DB, Barst RJ, Farber HW, Lindner JR, et al. ACCF/AHA 2009 expert consensus document on pulmonary hypertension: a report of the American College of Cardiology Foundation Task Force on Expert Consensus Documents and the American Heart Association: developed in collaboration with the American College of Chest Physicians, American Thoracic Society, Inc., and the Pulmonary Hypertension Association. Circulation. 2009;119(16):2250-94.
10. Humbert M, Sitbon O, Chaouat A, Bertocchi M, Habib G, Gressin V, et al. Pulmonary arterial hypertension in France: results from a national registry. American journal of respiratory and critical care medicine. 2006;173(9):1023-30.
11. McGoon MD, Benza RL, Escribano-Subias P, Jiang X, Miller DP, Peacock AJ, et al. Pulmonary arterial hypertension: epidemiology and registries. Journal of the American College of Cardiology. 2013;62(25 Suppl):D51-9.
12. Peacock AJ, Murphy NF, McMurray JJ, Caballero L, Stewart S. An epidemiological study of pulmonary arterial hypertension. The European respiratory journal. 2007;30(1):104-9.
13. Humbert M, Sitbon O, Yaici A, Montani D, O'Callaghan DS, Jais X, et al. Survival in incident and prevalent cohorts of patients with pulmonary arterial hypertension. The European respiratory journal. 2010;36(3):549-55.
14. Lai YC, Potoka KC, Champion HC, Mora AL, Gladwin MT. Pulmonary arterial hypertension: the clinical syndrome. Circ Res. 2014;115(1):115-30.
15. Farber HW, Miller DP, Poms AD, Badesch DB, Frost AE, Muros-Le Rouzic E, et al. Five-Year outcomes of patients enrolled in the REVEAL Registry. Chest. 2015;148(4):1043-54.
16. Toshner M, Tajsic T, Morrell NW. Pulmonary hypertension: advances in pathogenesis and treatment. Br Med Bull. 2010;94:21-32.
17. Benza RL, Miller DP, Gomberg-Maitland M, Frantz RP, Foreman AJ, Coffey CS, et al. Predicting survival in pulmonary arterial hypertension: insights from the Registry to Evaluate Early and Long-Term Pulmonary Arterial Hypertension Disease Management (REVEAL). Circulation. 2010;122(2):164-72.
18. Zafrir B. Exercise training and rehabilitation in pulmonary arterial hypertension: rationale and current data evaluation. J Cardiopulm Rehabil Prev. 2013;33(5):263-73.

19. Rubin LJ. The 6-minute walk test in pulmonary arterial hypertension: how far is enough? American journal of respiratory and critical care medicine. 2012;186(5):396-7.
20. Impens AJ, Wangkaew S, Seibold JR. The 6-minute walk test in scleroderma--how measuring everything measures nothing. Rheumatology (Oxford). 2008;47 Suppl 5:v68-9.
21. Nathan J, Fuld J. Skeletal muscle dysfunction: a ubiquitous outcome in chronic disease? Thorax. 2010;65(2):97-8.
22. Galie N, Humbert M, Vachiery JL, Gibbs S, Lang I, Torbicki A, et al. 2015 ESC/ERS Guidelines for the diagnosis and treatment of pulmonary hypertension: The Joint Task Force for the Diagnosis and Treatment of Pulmonary Hypertension of the European Society of Cardiology (ESC) and the European Respiratory Society (ERS): Endorsed by: Association for European Paediatric and Congenital Cardiology (AEPC), International Society for Heart and Lung Transplantation (ISHLT). The European respiratory journal. 2015;46(4):903-75.
23. Polkey MI, Moxham J. Attacking the disease spiral in chronic obstructive pulmonary disease: an update. Clinical medicine. 2011;11(5):461-4.
24. Schols AM, Soeters PB, Dingemans AM, Mostert R, Frantzen PJ, Wouters EF. Prevalence and characteristics of nutritional depletion in patients with stable COPD eligible for pulmonary rehabilitation. Am Rev Respir Dis. 1993;147(5):1151-6.
25. McDonald ML, Diaz AA, Ross JC, San Jose Estepar R, Zhou L, Regan EA, et al. Quantitative computed tomography measures of pectoralis muscle area and disease severity in chronic obstructive pulmonary disease. A cross-sectional study. Annals of the American Thoracic Society. 2014;11(3):326-34.
26. Jones SE, Maddocks M, Kon SS, Canavan JL, Nolan CM, Clark AL, et al. Sarcopenia in COPD: prevalence, clinical correlates and response to pulmonary rehabilitation. Thorax. 2015;70(3):213-8.
27. Seymour JM, Spruit MA, Hopkinson NS, Natanek SA, Man WD, Jackson A, et al. The prevalence of quadriceps weakness in COPD and the relationship with disease severity. The European respiratory journal. 2010;36(1):81-8.
28. Seymour JM, Ward K, Sidhu PS, Puthucheary Z, Steier J, Jolley CJ, et al. Ultrasound measurement of rectus femoris cross-sectional area and the relationship with quadriceps strength in COPD. Thorax. 2009;64(5):418-23.
29. Bernard S, LeBlanc P, Whittom F, Carrier G, Jobin J, Belleau R, et al. Peripheral muscle weakness in patients with chronic obstructive pulmonary disease. American journal of respiratory and critical care medicine. 1998;158(2):629-34.
30. Maltais F, Decramer M, Casaburi R, Barreiro E, Burelle Y, Debigare R, et al. An official American Thoracic Society/European Respiratory Society statement: update on limb muscle dysfunction in chronic obstructive pulmonary disease. American journal of respiratory and critical care medicine. 2014;189(9):e15-62.
31. Gosselink R, Troosters T, Decramer M. Peripheral muscle weakness contributes to exercise limitation in COPD. American journal of respiratory and critical care medicine. 1996;153(3):976-80.
32. Mostert R, Goris A, Weling-Scheepers C, Wouters EF, Schols AM. Tissue depletion and health related quality of life in patients with chronic obstructive pulmonary disease. Respiratory medicine. 2000;94(9):859-67.
33. Decramer M, Gosselink R, Troosters T, Verschueren M, Evers G. Muscle weakness is related to utilization of health care resources in COPD patients. The European respiratory journal. 1997;10(2):417-23.
34. Swallow EB, Reyes D, Hopkinson NS, Man WD, Porcher R, Cetti EJ, et al. Quadriceps strength predicts mortality in patients with moderate to severe chronic obstructive pulmonary disease. Thorax. 2007;62(2):115-20.
35. Fulster S, Tacke M, Sandek A, Ebner N, Tschope C, Doehner W, et al. Muscle wasting in patients with chronic heart failure: results from the studies investigating co-morbidities aggravating heart failure (SICA-HF). Eur Heart J. 2013;34(7):512-9.

36. Harrington D, Anker SD, Chua TP, Webb-Peploe KM, Ponikowski PP, Poole-Wilson PA, et al. Skeletal muscle function and its relation to exercise tolerance in chronic heart failure. Journal of the American College of Cardiology. 1997;30(7):1758-64.
37. Seymour JM, Moore L, Jolley CJ, Ward K, Creasey J, Steier JS, et al. Outpatient pulmonary rehabilitation following acute exacerbations of COPD. Thorax. 2010;65(5):423-8.
38. Jankowska EA, Wegrzynowska K, Superlak M, Nowakowska K, Lazorczyk M, Biel B, et al. The 12-week progressive quadriceps resistance training improves muscle strength, exercise capacity and quality of life in patients with stable chronic heart failure. International journal of cardiology. 2008;130(1):36-43.
39. Hulsmann M, Quittan M, Berger R, Crevenna R, Springer C, Nuhr M, et al. Muscle strength as a predictor of long-term survival in severe congestive heart failure. Eur J Heart Fail. 2004;6(1):101-7.
40. Okita K, Kinugawa S, Tsutsui H. Exercise intolerance in chronic heart failure--skeletal muscle dysfunction and potential therapies. Circulation journal : official journal of the Japanese Circulation Society. 2013;77(2):293-300.
41. Pette D, Staron RS. Mammalian skeletal muscle fiber type transitions. International review of cytology. 1997;170:143-223.
42. Ciciliot S, Rossi AC, Dyar KA, Blaauw B, Schiaffino S. Muscle type and fiber type specificity in muscle wasting. The international journal of biochemistry & cell biology. 2013;45(10):2191-9.
43. Gosker HR, Zeegers MP, Wouters EF, Schols AM. Muscle fibre type shifting in the vastus lateralis of patients with COPD is associated with disease severity: a systematic review and meta-analysis. Thorax. 2007;62(11):944-9.
44. Natanek SA, Gosker HR, Slot IG, Marsh GS, Hopkinson NS, Moxham J, et al. Pathways associated with reduced quadriceps oxidative fibres and endurance in COPD. The European respiratory journal. 2013;41(6):1275-83.
45. Gosker HR, Kubat B, Schaart G, van der Vusse GJ, Wouters EF, Schols AM. Myopathological features in skeletal muscle of patients with chronic obstructive pulmonary disease. The European respiratory journal. 2003;22(2):280-5.
46. Maltais F, Simard AA, Simard C, Jobin J, Desgagnes P, LeBlanc P. Oxidative capacity of the skeletal muscle and lactic acid kinetics during exercise in normal subjects and in patients with COPD. American journal of respiratory and critical care medicine. 1996;153(1):288-93.
47. Drexler H, Riede U, Munzel T, Konig H, Funke E, Just H. Alterations of skeletal muscle in chronic heart failure. Circulation. 1992;85(5):1751-9.
48. Schaufelberger M, Andersson G, Eriksson BO, Grimby G, Held P, Swedberg K. Skeletal muscle changes in patients with chronic heart failure before and after treatment with enalapril. Eur Heart J. 1996;17(11):1678-85.
49. Levine S, Kaiser L, Leferovich J, Tikunov B. Cellular adaptations in the diaphragm in chronic obstructive pulmonary disease. N Engl J Med. 1997;337(25):1799-806.
50. Tikunov B, Levine S, Mancini D. Chronic congestive heart failure elicits adaptations of endurance exercise in diaphragmatic muscle. Circulation. 1997;95(4):910-6.
51. Schiaffino S, Dyar KA, Ciciliot S, Blaauw B, Sandri M. Mechanisms regulating skeletal muscle growth and atrophy. FEBS J. 2013;280(17):4294-314.
52. Donaldson AV, Maddocks M, Martolini D, Polkey MI, Man WD. Muscle function in COPD: a complex interplay. International journal of chronic obstructive pulmonary disease. 2012;7:523-35.
53. Sandri M. Signaling in muscle atrophy and hypertrophy. Physiology. 2008;23:160-70.
54. Bodine SC, Latres E, Baumhueter S, Lai VK, Nunez L, Clarke BA, et al. Identification of ubiquitin ligases required for skeletal muscle atrophy. Science. 2001;294(5547):1704-8.
55. Lemire BB, Debigare R, Dube A, Theriault ME, Cote CH, Maltais F. MAPK signaling in the quadriceps of patients with chronic obstructive pulmonary disease. Journal of applied physiology. 2012;113(1):159-66.

56. Vogiatzis I, Simoes DC, Stratakos G, Kourepini E, Terzis G, Manta P, et al. Effect of pulmonary rehabilitation on muscle remodelling in cachectic patients with COPD. The European respiratory journal. 2010;36(2):301-10.
57. Plant PJ, Brooks D, Faughnan M, Bayley T, Bain J, Singer L, et al. Cellular markers of muscle atrophy in chronic obstructive pulmonary disease. American journal of respiratory cell and molecular biology. 2010;42(4):461-71.
58. Doucet M, Russell AP, Leger B, Debigare R, Joanisse DR, Caron MA, et al. Muscle atrophy and hypertrophy signaling in patients with chronic obstructive pulmonary disease. American journal of respiratory and critical care medicine. 2007;176(3):261-9.
59. Gielen S, Sandri M, Kozarez I, Kratzsch J, Teupser D, Thiery J, et al. Exercise training attenuates MuRF-1 expression in the skeletal muscle of patients with chronic heart failure independent of age: the randomized Leipzig Exercise Intervention in Chronic Heart Failure and Aging catabolism study. Circulation. 2012;125(22):2716-27.
60. Carvalho RF, Castan EP, Coelho CA, Lopes FS, Almeida FL, Michelin A, et al. Heart failure increases atrogin-1 and MuRF1 gene expression in skeletal muscle with fiber type-specific atrophy. Journal of molecular histology. 2010;41(1):81-7.
61. Natanek SA, Riddoch-Contreras J, Marsh GS, Hopkinson NS, Moxham J, Man WD, et al. MuRF-1 and atrogin-1 protein expression and quadriceps fiber size and muscle mass in stable patients with COPD. Copd. 2013;10(5):618-24.
62. Debigare R, Maltais F, Cote CH, Michaud A, Caron MA, Mofarrahi M, et al. Profiling of mRNA expression in quadriceps of patients with COPD and muscle wasting. Copd. 2008;5(2):75-84.
63. Lewis A, Riddoch-Contreras J, Natanek SA, Donaldson A, Man WD, Moxham J, et al. Downregulation of the serum response factor/miR-1 axis in the quadriceps of patients with COPD. Thorax. 2012;67(1):26-34.
64. Godard MP, Whitman SA, Song YH, Delafontaine P. Skeletal muscle molecular alterations precede whole-muscle dysfunction in NYHA Class II heart failure patients. Clinical interventions in aging. 2012;7:489-97.
65. McPherron AC, Lawler AM, Lee SJ. Regulation of skeletal muscle mass in mice by a new TGF-beta superfamily member. Nature. 1997;387(6628):83-90.
66. #Langley B, Thomas M, Bishop A, Sharma M, Gilmour S, Kambadur R. Myostatin inhibits myoblast differentiation by down-regulating MyoD expression. The Journal of biological chemistry. 2002;277(51):49831-40.
67. Philip B, Lu Z, Gao Y. Regulation of GDF-8 signaling by the p38 MAPK. Cellular signalling. 2005;17(3):365-75.
68. Man WD, Natanek SA, Riddoch-Contreras J, Lewis A, Marsh GS, Kemp PR, et al. Quadriceps myostatin expression in COPD. The European respiratory journal. 2010;36(3):686-8.
69. Lenk K, Erbs S, Hollriegel R, Beck E, Linke A, Gielen S, et al. Exercise training leads to a reduction of elevated myostatin levels in patients with chronic heart failure. European journal of preventive cardiology. 2012;19(3):404-11.
70. Han HQ, Mitch WE. Targeting the myostatin signaling pathway to treat muscle wasting diseases. Curr Opin Support Palliat Care. 2011;5(4):334-41.
71. Elliott B, Renshaw D, Getting S, Mackenzie R. The central role of myostatin in skeletal muscle and whole body homeostasis. Acta physiologica. 2012;205(3):324-40.
72. Huang Z, Chen X, Chen D. Myostatin: a novel insight into its role in metabolism, signal pathways, and expression regulation. Cellular signalling. 2011;23(9):1441-6.
73. Elkina Y, von Haehling S, Anker SD, Springer J. The role of myostatin in muscle wasting: an overview. Journal of cachexia, sarcopenia and muscle. 2011;2(3):143-51.
74. He J, Ogden LG, Bazzano LA, Vupputuri S, Loria C, Whelton PK. Risk factors for congestive heart failure in US men and women: NHANES I epidemiologic follow-up study. Archives of internal medicine. 2001;161(7):996-1002.

75. Polkey MI, Rabe KF. Chicken or egg: physical activity in COPD revisited. The European respiratory journal. 2009;33(2):227-9.
76. Vogiatzis I, Zakynthinos S. Physical inactivity: common pathway to peripheral muscle weakness in chronic respiratory diseases? The European respiratory journal. 2009;34(6):1213-4.
77. Gratas-Delamarche A, Derbre F, Vincent S, Cillard J. Physical inactivity, insulin resistance, and the oxidative-inflammatory loop. Free radical research. 2014;48(1):93-108.
78. Chopard A, Hillock S, Jasmin BJ. Molecular events and signalling pathways involved in skeletal muscle disuse-induced atrophy and the impact of countermeasures. Journal of cellular and molecular medicine. 2009;13(9B):3032-50.
79. Wust RC, Degens H. Factors contributing to muscle wasting and dysfunction in COPD patients. International journal of chronic obstructive pulmonary disease. 2007;2(3):289-300.
80. Taegtmeyer H, Harinstein ME, Gheorghiade M. More than bricks and mortar: comments on protein and amino acid metabolism in the heart. The American journal of cardiology. 2008;101(11A):3E-7E.
81. Casperson SL, Sheffield-Moore M, Hewlings SJ, Paddon-Jones D. Leucine supplementation chronically improves muscle protein synthesis in older adults consuming the RDA for protein. Clin Nutr. 2012;31(4):512-9.
82. MacNee W. Is Chronic Obstructive Pulmonary Disease an Accelerated Aging Disease? Annals of the American Thoracic Society. 2016;13(Supplement_5):S429-S37.
83. Jankowska EA, Biel B, Majda J, Szklarska A, Lopuszanska M, Medras M, et al. Anabolic deficiency in men with chronic heart failure: prevalence and detrimental impact on survival. Circulation. 2006;114(17):1829-37.
84. Gan WQ, Man SF, Senthilselvan A, Sin DD. Association between chronic obstructive pulmonary disease and systemic inflammation: a systematic review and a meta-analysis. Thorax. 2004;59(7):574-80.
85. Yndestad A, Damas JK, Oie E, Ueland T, Gullestad L, Aukrust P. Systemic inflammation in heart failure--the whys and wherefores. Heart Fail Rev. 2006;11(1):83-92.
86. Man WD, Kemp P, Moxham J, Polkey MI. Skeletal muscle dysfunction in COPD: clinical and laboratory observations. Clinical science. 2009;117(7):251-64.
87. Taylor BJ, Mojica CR, Olson TP, Woods PR, Frantz RP, Johnson BD. A possible role for systemic hypoxia in the reactive component of pulmonary hypertension in heart failure. Journal of cardiac failure. 2013;19(1):50-9.
88. Hoppeler H, Howald H, Cerretelli P. Human muscle structure after exposure to extreme altitude. Experientia. 1990;46(11-12):1185-7.
89. Abdelmalki A, Fimbel S, Mayet-Sornay MH, Sempore B, Favier R. Aerobic capacity and skeletal muscle properties of normoxic and hypoxic rats in response to training. Pflugers Arch. 1996;431(5):671-9.
90. de Theije C, Costes F, Langen RC, Pison C, Gosker HR. Hypoxia and muscle maintenance regulation: implications for chronic respiratory disease. Current opinion in clinical nutrition and metabolic care. 2011;14(6):548-53.
91. Puente-Maestu L, Perez-Parra J, Godoy R, Moreno N, Tejedor A, Gonzalez-Aragoneses F, et al. Abnormal mitochondrial function in locomotor and respiratory muscles of COPD patients. The European respiratory journal. 2009;33(5):1045-52.
92. Tsutsui H, Kinugawa S, Matsushima S. Oxidative stress and heart failure. Am J Physiol Heart Circ Physiol. 2011;301(6):H2181-90.
93. Calvani R, Joseph AM, Adhihetty PJ, Miccheli A, Bossola M, Leeuwenburgh C, et al. Mitochondrial pathways in sarcopenia of aging and disuse muscle atrophy. Biological chemistry. 2013;394(3):393-414.
94. McCarthy B, Casey D, Devane D, Murphy K, Murphy E, Lacasse Y. Pulmonary rehabilitation for chronic obstructive pulmonary disease. Cochrane Database Syst Rev. 2015(2):CD003793.

95. Coventry PA, Hind D. Comprehensive pulmonary rehabilitation for anxiety and depression in adults with chronic obstructive pulmonary disease: Systematic review and meta-analysis. J Psychosom Res. 2007;63(5):551-65.
96. Ries AL, Kaplan RM, Limberg TM, Prewitt LM. Effects of pulmonary rehabilitation on physiologic and psychosocial outcomes in patients with chronic obstructive pulmonary disease. Ann Intern Med. 1995;122(11):823-32.
97. Puhan MA, Scharplatz M, Troosters T, Steurer J. Respiratory rehabilitation after acute exacerbation of COPD may reduce risk for readmission and mortality -- a systematic review. Respiratory research. 2005;6:54.
98. Puhan MA, Gimeno-Santos E, Cates CJ, Troosters T. Pulmonary rehabilitation following exacerbations of chronic obstructive pulmonary disease. Cochrane Database Syst Rev. 2016;12:CD005305.
99. Sagar VA, Davies EJ, Briscoe S, Coats AJ, Dalal HM, Lough F, et al. Exercise-based rehabilitation for heart failure: systematic review and meta-analysis. Open Heart. 2015;2(1):e000163.
100. Marchionni N, Fattirolli F, Fumagalli S, Oldridge N, Del Lungo F, Morosi L, et al. Improved exercise tolerance and quality of life with cardiac rehabilitation of older patients after myocardial infarction: results of a randomized, controlled trial. Circulation. 2003;107(17):2201-6.
101. Heran BS, Chen JM, Ebrahim S, Moxham T, Oldridge N, Rees K, et al. Exercise-based cardiac rehabilitation for coronary heart disease. Cochrane Database Syst Rev. 2011(7):CD001800.
102. Clark CJ, Cochrane LM, Mackay E, Paton B. Skeletal muscle strength and endurance in patients with mild COPD and the effects of weight training. The European respiratory journal. 2000;15(1):92-7.
103. O'Shea SD, Taylor NF, Paratz JD. A predominantly home-based progressive resistance exercise program increases knee extensor strength in the short-term in people with chronic obstructive pulmonary disease: a randomised controlled trial. Aust J Physiother. 2007;53(4):229-37.
104. Troosters T, Gosselink R, Decramer M. Short- and long-term effects of outpatient rehabilitation in patients with chronic obstructive pulmonary disease: a randomized trial. The American journal of medicine. 2000;109(3):207-12.
105. Gordon A, Tyni-Lenne R, Persson H, Kaijser L, Hultman E, Sylven C. Markedly improved skeletal muscle function with local muscle training in patients with chronic heart failure. Clinical cardiology. 1996;19(7):568-74.
106. Yang YJ, He XH, Guo HY, Wang XQ, Zhu Y. Efficiency of muscle strength training on motor function in patients with coronary artery disease: a meta-analysis. Int J Clin Exp Med. 2015;8(10):17536-50.
107. Constantin D, Menon MK, Houchen-Wolloff L, Morgan MD, Singh SJ, Greenhaff P, et al. Skeletal muscle molecular responses to resistance training and dietary supplementation in COPD. Thorax. 2013;68(7):625-33.
108. Schols AM. Nutrition as a metabolic modulator in COPD. Chest. 2013;144(4):1340-5.
109. Collins PF, Elia M, Stratton RJ. Nutritional support and functional capacity in chronic obstructive pulmonary disease: a systematic review and meta-analysis. Respirology. 2013;18(4):616-29.
110. Collins PF, Stratton RJ, Elia M. Nutritional support in chronic obstructive pulmonary disease: a systematic review and meta-analysis. The American journal of clinical nutrition. 2012;95(6):1385-95.
111. Weekes CE, Emery PW, Elia M. Dietary counselling and food fortification in stable COPD: a randomised trial. Thorax. 2009;64(4):326-31.
112. Lombardi C, Carubelli V, Lazzarini V, Vizzardi E, Quinzani F, Guidetti F, et al. Effects of oral amino Acid supplements on functional capacity in patients with chronic heart failure. Clinical Medicine Insights Cardiology. 2014;8:39-44.

113. Creutzberg EC, Wouters EF, Mostert R, Weling-Scheepers CA, Schols AM. Efficacy of nutritional supplementation therapy in depleted patients with chronic obstructive pulmonary disease. Nutrition. 2003;19(2):120-7.
114. Dal Negro RW, Aquilani R, Bertacco S, Boschi F, Micheletto C, Tognella S. Comprehensive effects of supplemented essential amino acids in patients with severe COPD and sarcopenia. Monaldi Arch Chest Dis. 2010;73(1):25-33.
115. Liu H, Liu R, Xiong Y, Li X, Wang X, Ma Y, et al. Leucine facilitates the insulin-stimulated glucose uptake and insulin signaling in skeletal muscle cells: involving mTORC1 and mTORC2. Amino Acids. 2014;46(8):1971-9.
116. Gullett NP, Hebbar G, Ziegler TR. Update on clinical trials of growth factors and anabolic steroids in cachexia and wasting. The American journal of clinical nutrition. 2010;91(4):1143S-7S.
117. Basaria S, Coviello AD, Travison TG, Storer TW, Farwell WR, Jette AM, et al. Adverse events associated with testosterone administration. N Engl J Med. 2010;363(2):109-22.
118. Schambelan M, Mulligan K, Grunfeld C, Daar ES, LaMarca A, Kotler DP, et al. Recombinant human growth hormone in patients with HIV-associated wasting. A randomized, placebo-controlled trial. Serostim Study Group. Ann Intern Med. 1996;125(11):873-82.
119. Pape GS, Friedman M, Underwood LE, Clemmons DR. The effect of growth hormone on weight gain and pulmonary function in patients with chronic obstructive lung disease. Chest. 1991;99(6):1495-500.
120. Burdet L, de Muralt B, Schutz Y, Pichard C, Fitting JW. Administration of growth hormone to underweight patients with chronic obstructive pulmonary disease. A prospective, randomized, controlled study. American journal of respiratory and critical care medicine. 1997;156(6):1800-6.
121. Isgaard J, Bergh CH, Caidahl K, Lomsky M, Hjalmarson A, Bengtsson BA. A placebo-controlled study of growth hormone in patients with congestive heart failure. Eur Heart J. 1998;19(11):1704-11.
122. Cittadini A, Saldamarco L, Marra AM, Arcopinto M, Carlomagno G, Imbriaco M, et al. Growth hormone deficiency in patients with chronic heart failure and beneficial effects of its correction. The Journal of clinical endocrinology and metabolism. 2009;94(9):3329-36.
123. Casaburi R, Bhasin S, Cosentino L, Porszasz J, Somfay A, Lewis MI, et al. Effects of testosterone and resistance training in men with chronic obstructive pulmonary disease. American journal of respiratory and critical care medicine. 2004;170(8):870-8.
124. Atlantis E, Fahey P, Cochrane B, Wittert G, Smith S. Endogenous testosterone level and testosterone supplementation therapy in chronic obstructive pulmonary disease (COPD): a systematic review and meta-analysis. BMJ open. 2013;3(8).
125. Yoshida T, Tabony AM, Galvez S, Mitch WE, Higashi Y, Sukhanov S, et al. Molecular mechanisms and signaling pathways of angiotensin II-induced muscle wasting: potential therapeutic targets for cardiac cachexia. The international journal of biochemistry & cell biology. 2013;45(10):2322-32.
126. Shrikrishna D, Tanner RJ, Lee JY, Natanek A, Lewis A, Murphy PB, et al. A randomized controlled trial of angiotensin-converting enzyme inhibition for skeletal muscle dysfunction in COPD. Chest. 2014;146(4):932-40.
127. Dobs AS, Boccia RV, Croot CC, Gabrail NY, Dalton JT, Hancock ML, et al. Effects of enobosarm on muscle wasting and physical function in patients with cancer: a double-blind, randomised controlled phase 2 trial. Lancet Oncol. 2013;14(4):335-45.
128. Zhang L, Rajan V, Lin E, Hu Z, Han HQ, Zhou X, et al. Pharmacological inhibition of myostatin suppresses systemic inflammation and muscle atrophy in mice with chronic kidney disease. FASEB J. 2011;25(5):1653-63.
129. Kamiji MM, Inui A. The role of ghrelin and ghrelin analogues in wasting disease. Current opinion in clinical nutrition and metabolic care. 2008;11(4):443-51.
130. Stewart Coats AJ, Srinivasan V, Surendran J, Chiramana H, Vangipuram SR, Bhatt NN, et al. The ACT-ONE trial, a multicentre, randomised, double-blind, placebo-controlled, dose-finding study of the anabolic/catabolic transforming agent, MT-102 in subjects with cachexia related to stage III

and IV non-small cell lung cancer and colorectal cancer: study design. Journal of cachexia, sarcopenia and muscle. 2011;2(4):201-7.
131. Meyrick B, Gamble W, Reid L. Development of Crotalaria pulmonary hypertension: hemodynamic and structural study. The American journal of physiology. 1980;239(5):H692-702.
132. Bernocchi P, Ceconi C, Pedersini P, Pasini E, Curello S, Ferrari R. Skeletal muscle metabolism in experimental heart failure. Journal of molecular and cellular cardiology. 1996;28(11):2263-73.
133. Vescovo G, Ceconi C, Bernocchi P, Ferrari R, Carraro U, Ambrosio GB, et al. Skeletal muscle myosin heavy chain expression in rats with monocrotaline-induced cardiac hypertrophy and failure. Relation to blood flow and degree of muscle atrophy. Cardiovascular research. 1998;39(1):233-41.
134. Dalla Libera L, Ravara B, Volterrani M, Gobbo V, Della Barbera M, Angelini A, et al. Beneficial effects of GH/IGF-1 on skeletal muscle atrophy and function in experimental heart failure. Am J Physiol Cell Physiol. 2004;286(1):C138-44.
135. Vescovo G, Ravara B, Gobbo V, Angelini A, Dalla Libera L. Skeletal muscle fibres synthesis in heart failure: role of PGC-1alpha, calcineurin and GH. International journal of cardiology. 2005;104(3):298-306.
136. Steffen BT, Lees SJ, Booth FW. Anti-TNF treatment reduces rat skeletal muscle wasting in monocrotaline-induced cardiac cachexia. Journal of applied physiology. 2008;105(6):1950-8.
137. Ahn B, Empinado HM, Al-Rajhi M, Judge AR, Ferreira LF. Diaphragm atrophy and contractile dysfunction in a murine model of pulmonary hypertension. PloS one. 2013;8(4):e62702.
138. Vescovo G, Zennaro R, Sandri M, Carraro U, Leprotti C, Ceconi C, et al. Apoptosis of skeletal muscle myofibers and interstitial cells in experimental heart failure. Journal of molecular and cellular cardiology. 1998;30(11):2449-59.
139. Carvalho RF, Cicogna AC, Campos GE, Lopes Fda S, Sugizaki MM, Nogueira CR, et al. Heart failure alters MyoD and MRF4 expressions in rat skeletal muscle. International journal of experimental pathology. 2006;87(3):219-25.
140. Dalla Libera L, Ravara B, Gobbo V, Betto DD, Germinario E, Angelini A, et al. Skeletal muscle proteins oxidation in chronic right heart failure in rats: can different beta-blockers prevent it to the same degree? International journal of cardiology. 2010;143(2):192-9.
141. Bertaglia RS, Reissler J, Lopes FS, Cavalcante WL, Carani FR, Padovani CR, et al. Differential morphofunctional characteristics and gene expression in fast and slow muscle of rats with monocrotaline-induced heart failure. Journal of molecular histology. 2011;42(3):205-15.
142. DeNardi C, Ausoni S, Moretti P, Gorza L, Velleca M, Buckingham M, et al. Type 2X-myosin heavy chain is coded by a muscle fiber type-specific and developmentally regulated gene. The Journal of cell biology. 1993;123(4):823-35.
143. Dalla Libera L, Ravara B, Gobbo V, Danieli Betto D, Germinario E, Angelini A, et al. Skeletal muscle myofibrillar protein oxidation in heart failure and the protective effect of Carvedilol. Journal of molecular and cellular cardiology. 2005;38(5):803-7.
144. Bernocchi P, Cargnoni A, Vescovo G, Dalla Libera L, Parrinello G, Boraso A, et al. Skeletal muscle abnormalities in rats with experimentally induced heart hypertrophy and failure. Basic research in cardiology. 2003;98(2):114-23.
145. Dalla Libera L, Sabbadini R, Renken C, Ravara B, Sandri M, Betto R, et al. Apoptosis in the skeletal muscle of rats with heart failure is associated with increased serum levels of TNF-alpha and sphingosine. Journal of molecular and cellular cardiology. 2001;33(10):1871-8.
146. Dalla Libera L, Ravara B, Angelini A, Rossini K, Sandri M, Thiene G, et al. Beneficial effects on skeletal muscle of the angiotensin II type 1 receptor blocker irbesartan in experimental heart failure. Circulation. 2001;103(17):2195-200.
147. Castellani C, Vescovo G, Ravara B, Franzin C, Pozzobon M, Tavano R, et al. The contribution of stem cell therapy to skeletal muscle remodeling in heart failure. International journal of cardiology. 2013;168(3):2014-21.

148. Libera LD, Zennaro R, Sandri M, Ambrosio GB, Vescovo G. Apoptosis and atrophy in rat slow skeletal muscles in chronic heart failure. The American journal of physiology. 1999;277(5 Pt 1):C982-6.
149. Enache AM, Nicolescu I, Georgescu CE. Mandibular second molar impaction treatment using skeletal anchorage. Romanian journal of morphology and embryology = Revue roumaine de morphologie et embryologie. 2012;53(4):1107-10.
150. Carvalho RF, Dariolli R, Justulin Junior LA, Sugizaki MM, Politi Okoshi M, Cicogna AC, et al. Heart failure alters matrix metalloproteinase gene expression and activity in rat skeletal muscle. International journal of experimental pathology. 2006;87(6):437-43.
151. Vescovo G, Ravara B, Angelini A, Sandri M, Carraro U, Ceconi C, et al. Effect of thalidomide on the skeletal muscle in experimental heart failure. Eur J Heart Fail. 2002;4(4):455-60.
152. Vescovo G, Ravara B, Gobbo V, Sandri M, Angelini A, Della Barbera M, et al. L-Carnitine: a potential treatment for blocking apoptosis and preventing skeletal muscle myopathy in heart failure. Am J Physiol Cell Physiol. 2002;283(3):C802-10.
153. Moreira-Goncalves D, Padrao AI, Ferreira R, Justino J, Nogueira-Ferreira R, Neuparth MJ, et al. Signaling pathways underlying skeletal muscle wasting in experimental pulmonary arterial hypertension. Biochimica et biophysica acta. 2015;1852(12):2722-31.
154. Meyer FJ, Lossnitzer D, Kristen AV, Schoene AM, Kubler W, Katus HA, et al. Respiratory muscle dysfunction in idiopathic pulmonary arterial hypertension. The European respiratory journal : official journal of the European Society for Clinical Respiratory Physiology. 2005;25(1):125-30.
155. Mancini DM, Henson D, La Manca J, Donchez L, Levine S. Benefit of selective respiratory muscle training on exercise capacity in patients with chronic congestive heart failure. Circulation. 1995;91(2):320-9.
156. Meyer FJ, Borst MM, Zugck C, Kirschke A, Schellberg D, Kubler W, et al. Respiratory muscle dysfunction in congestive heart failure: clinical correlation and prognostic significance. Circulation. 2001;103(17):2153-8.
157. Rochester DF, Braun NM. Determinants of maximal inspiratory pressure in chronic obstructive pulmonary disease. The American review of respiratory disease. 1985;132(1):42-7.
158. Naeije R. Breathing more with weaker respiratory muscles in pulmonary arterial hypertension. The European respiratory journal : official journal of the European Society for Clinical Respiratory Physiology. 2005;25(1):6-8.
159. Kabitz HJ, Walterspacher S, Walker D, Windisch W. Inspiratory muscle strength in chronic obstructive pulmonary disease depending on disease severity. Clinical science. 2007;113(5):243-9.
160. Bauer R, Dehnert C, Schoene P, Filusch A, Bartsch P, Borst MM, et al. Skeletal muscle dysfunction in patients with idiopathic pulmonary arterial hypertension. Respiratory medicine. 2007;101(11):2366-9.
161. Mainguy V, Maltais F, Saey D, Gagnon P, Martel S, Simon M, et al. Peripheral muscle dysfunction in idiopathic pulmonary arterial hypertension. Thorax. 2010;65(2):113-7.
162. de Man FS, van Hees HW, Handoko ML, Niessen HW, Schalij I, Humbert M, et al. Diaphragm muscle fiber weakness in pulmonary hypertension. American journal of respiratory and critical care medicine. 2011;183(10):1411-8.
163. Batt J, Ahmed SS, Correa J, Bain A, Granton J. Skeletal muscle dysfunction in idiopathic pulmonary arterial hypertension. American journal of respiratory cell and molecular biology. 2014;50(1):74-86.
164. Mainguy V, Maltais F, Saey D, Gagnon P, Martel S, Simon M, et al. Effects of a rehabilitation program on skeletal muscle function in idiopathic pulmonary arterial hypertension. J Cardiopulm Rehabil Prev. 2010;30(5):319-23.
165. Scott AC, Francis DP, Davies LC, Ponikowski P, Coats AJ, Piepoli MF. Contribution of skeletal muscle 'ergoreceptors' in the human leg to respiratory control in chronic heart failure. J Physiol. 2000;529 Pt 3:863-70.

166. Lang CC, Chomsky DB, Butler J, Kapoor S, Wilson JR. Prostaglandin production contributes to exercise-induced vasodilation in heart failure. J Appl Physiol. 1997;83(6):1933-40.
167. Guazzi M, Casali M, Berti F, Rossoni G, Colonna VD, Guazzi MD. Endothelium-mediated modulation of ergoreflex and improvement in exercise ventilation by acute sildenafil in heart failure patients. Clin Pharmacol Ther. 2008;83(2):336-41.
168. Wray DW, Nishiyama SK, Donato AJ, Sander M, Wagner PD, Richardson RS. Endothelin-1-mediated vasoconstriction at rest and during dynamic exercise in healthy humans. Am J Physiol Heart Circ Physiol. 2007;293(4):H2550-6.
169. Rich S. The effects of vasodilators in pulmonary hypertension: pulmonary vascular or peripheral vascular? Circ Heart Fail. 2009;2(2):145-50.
170. Filusch A, Ewert R, Altesellmeier M, Zugck C, Hetzer R, Borst MM, et al. Respiratory muscle dysfunction in congestive heart failure--the role of pulmonary hypertension. International journal of cardiology. 2011;150(2):182-5.
171. Mereles D, Ehlken N, Kreuscher S, Ghofrani S, Hoeper MM, Halank M, et al. Exercise and respiratory training improve exercise capacity and quality of life in patients with severe chronic pulmonary hypertension. Circulation. 2006;114(14):1482-9.
172. de Man FS, Handoko ML, Groepenhoff H, van 't Hul AJ, Abbink J, Koppers RJ, et al. Effects of exercise training in patients with idiopathic pulmonary arterial hypertension. The European respiratory journal. 2009;34(3):669-75.
173. Mainguy V, Provencher S, Maltais F, Malenfant S, Saey D. Assessment of daily life physical activities in pulmonary arterial hypertension. PloS one. 2011;6(11):e27993.
174. Pugh ME, Buchowski MS, Robbins IM, Newman JH, Hemnes AR. Physical activity limitation as measured by accelerometry in pulmonary arterial hypertension. Chest. 2012;142(6):1391-8.
175. Matura LA, McDonough A, Carroll DL. Symptom Interference Severity and Health-Related Quality of Life in Pulmonary Arterial Hypertension. J Pain Symptom Manage. 2016;51(1):25-32.
176. Saglam M, Vardar-Yagli N, Calik-Kutukcu E, Arikan H, Savci S, Inal-Ince D, et al. Functional exercise capacity, physical activity, and respiratory and peripheral muscle strength in pulmonary hypertension according to disease severity. J Phys Ther Sci. 2015;27(5):1309-12.
177. Tudor-Locke CE, Myers AM. Challenges and opportunities for measuring physical activity in sedentary adults. Sports Med. 2001;31(2):91-100.
178. Mueller TD, Nickel J. Promiscuity and specificity in BMP receptor activation. FEBS Lett. 2012;586(14):1846-59.
179. Massague J. TGFbeta signalling in context. Nature reviews Molecular cell biology. 2012;13(10):616-30.
180. Galat A. Common structural traits for cystine knot domain of the TGFbeta superfamily of proteins and three-fingered ectodomain of their cellular receptors. Cellular and molecular life sciences : CMLS. 2011;68(20):3437-51.
181. Wrighton KH, Lin X, Feng XH. Phospho-control of TGF-beta superfamily signaling. Cell Res. 2009;19(1):8-20.
182. Lee YS, Huynh TV, Lee SJ. Paracrine and endocrine modes of myostatin action. Journal of applied physiology. 2016;120(6):592-8.
183. Koli K, Saharinen J, Hyytiainen M, Penttinen C, Keski-Oja J. Latency, activation, and binding proteins of TGF-beta. Microscopy research and technique. 2001;52(4):354-62.
184. Wrana JL, Attisano L, Wieser R, Ventura F, Massague J. Mechanism of activation of the TGF-beta receptor. Nature. 1994;370(6488):341-7.
185. Huang T, David L, Mendoza V, Yang Y, Villarreal M, De K, et al. TGF-beta signalling is mediated by two autonomously functioning TbetaRI:TbetaRII pairs. EMBO J. 2011;30(7):1263-76.
186. Heldin CH, Miyazono K, ten Dijke P. TGF-beta signalling from cell membrane to nucleus through SMAD proteins. Nature. 1997;390(6659):465-71.
187. Upton PD, Morrell NW. TGF-beta and BMPR-II pharmacology--implications for pulmonary vascular diseases. Current opinion in pharmacology. 2009;9(3):274-80.

188. Derynck R, Zhang YE. Smad-dependent and Smad-independent pathways in TGF-beta family signalling. Nature. 2003;425(6958):577-84.
189. Hariharan R, Pillai MR. Structure-function relationship of inhibitory Smads: Structural flexibility contributes to functional divergence. Proteins. 2008;71(4):1853-62.
190. Mu Y, Gudey SK, Landstrom M. Non-Smad signaling pathways. Cell Tissue Res. 2012;347(1):11-20.
191. Yu L, Hebert MC, Zhang YE. TGF-beta receptor-activated p38 MAP kinase mediates Smad-independent TGF-beta responses. EMBO J. 2002;21(14):3749-59.
192. Hough C, Radu M, Dore JJ. Tgf-beta induced Erk phosphorylation of smad linker region regulates smad signaling. PloS one. 2012;7(8):e42513.
193. Engel ME, McDonnell MA, Law BK, Moses HL. Interdependent SMAD and JNK signaling in transforming growth factor-beta-mediated transcription. The Journal of biological chemistry. 1999;274(52):37413-20.
194. Lamouille S, Derynck R. Cell size and invasion in TGF-beta-induced epithelial to mesenchymal transition is regulated by activation of the mTOR pathway. The Journal of cell biology. 2007;178(3):437-51.
195. Guo X, Wang XF. Signaling cross-talk between TGF-beta/BMP and other pathways. Cell Res. 2009;19(1):71-88.
196. Machado RD, Aldred MA, James V, Harrison RE, Patel B, Schwalbe EC, et al. Mutations of the TGF-beta type II receptor BMPR2 in pulmonary arterial hypertension. Hum Mutat. 2006;27(2):121-32.
197. Atkinson C, Stewart S, Upton PD, Machado R, Thomson JR, Trembath RC, et al. Primary pulmonary hypertension is associated with reduced pulmonary vascular expression of type II bone morphogenetic protein receptor. Circulation. 2002;105(14):1672-8.
198. Harrison RE, Flanagan JA, Sankelo M, Abdalla SA, Rowell J, Machado RD, et al. Molecular and functional analysis identifies ALK-1 as the predominant cause of pulmonary hypertension related to hereditary haemorrhagic telangiectasia. Journal of medical genetics. 2003;40(12):865-71.
199. Gallione CJ, Richards JA, Letteboer TG, Rushlow D, Prigoda NL, Leedom TP, et al. SMAD4 mutations found in unselected HHT patients. Journal of medical genetics. 2006;43(10):793-7.
200. Yu PB, Beppu H, Kawai N, Li E, Bloch KD. Bone morphogenetic protein (BMP) type II receptor deletion reveals BMP ligand-specific gain of signaling in pulmonary artery smooth muscle cells. The Journal of biological chemistry. 2005;280(26):24443-50.
201. Yang X, Long L, Southwood M, Rudarakanchana N, Upton PD, Jeffery TK, et al. Dysfunctional Smad signaling contributes to abnormal smooth muscle cell proliferation in familial pulmonary arterial hypertension. Circ Res. 2005;96(10):1053-63.
202. Morrell NW, Adnot S, Archer SL, Dupuis J, Jones PL, MacLean MR, et al. Cellular and molecular basis of pulmonary arterial hypertension. Journal of the American College of Cardiology. 2009;54(1 Suppl):S20-31.
203. Zaiman AL, Podowski M, Medicherla S, Gordy K, Xu F, Zhen L, et al. Role of the TGF-beta/Alk5 signaling pathway in monocrotaline-induced pulmonary hypertension. American journal of respiratory and critical care medicine. 2008;177(8):896-905.
204. Morrell NW, Yang X, Upton PD, Jourdan KB, Morgan N, Sheares KK, et al. Altered growth responses of pulmonary artery smooth muscle cells from patients with primary pulmonary hypertension to transforming growth factor-beta(1) and bone morphogenetic proteins. Circulation. 2001;104(7):790-5.
205. Zakrzewicz A, Kouri FM, Nejman B, Kwapiszewska G, Hecker M, Sandu R, et al. The transforming growth factor-beta/Smad2,3 signalling axis is impaired in experimental pulmonary hypertension. The European respiratory journal. 2007;29(6):1094-104.
206. Yndestad A, Larsen KO, Oie E, Ueland T, Smith C, Halvorsen B, et al. Elevated levels of activin A in clinical and experimental pulmonary hypertension. Journal of applied physiology. 2009;106(4):1356-64.

207. Nickel N, Kempf T, Tapken H, Tongers J, Laenger F, Lehmann U, et al. Growth differentiation factor-15 in idiopathic pulmonary arterial hypertension. American journal of respiratory and critical care medicine. 2008;178(5):534-41.
208. McPherron AC, Lee SJ. Double muscling in cattle due to mutations in the myostatin gene. Proceedings of the National Academy of Sciences of the United States of America. 1997;94(23):12457-61.
209. Lee SJ. Quadrupling muscle mass in mice by targeting TGF-beta signaling pathways. PloS one. 2007;2(8):e789.
210. Amirouche A, Durieux AC, Banzet S, Koulmann N, Bonnefoy R, Mouret C, et al. Down-regulation of Akt/mammalian target of rapamycin signaling pathway in response to myostatin overexpression in skeletal muscle. Endocrinology. 2009;150(1):286-94.
211. Winbanks CE, Weeks KL, Thomson RE, Sepulveda PV, Beyer C, Qian H, et al. Follistatin-mediated skeletal muscle hypertrophy is regulated by Smad3 and mTOR independently of myostatin. The Journal of cell biology. 2012;197(7):997-1008.
212. Heineke J, Auger-Messier M, Xu J, Sargent M, York A, Welle S, et al. Genetic deletion of myostatin from the heart prevents skeletal muscle atrophy in heart failure. Circulation. 2010;121(3):419-25.
213. Mendias CL, Gumucio JP, Davis ME, Bromley CW, Davis CS, Brooks SV. Transforming growth factor-beta induces skeletal muscle atrophy and fibrosis through the induction of atrogin-1 and scleraxis. Muscle & nerve. 2012;45(1):55-9.
214. Kollias HD, McDermott JC. Transforming growth factor-beta and myostatin signaling in skeletal muscle. Journal of applied physiology. 2008;104(3):579-87.
215. Sartori R, Schirwis E, Blaauw B, Bortolanza S, Zhao J, Enzo E, et al. BMP signaling controls muscle mass. Nat Genet. 2013;45(11):1309-18.
216. Winbanks CE, Chen JL, Qian H, Liu Y, Bernardo BC, Beyer C, et al. The bone morphogenetic protein axis is a positive regulator of skeletal muscle mass. The Journal of cell biology. 2013;203(2):345-57.
217. Zhou X, Wang JL, Lu J, Song Y, Kwak KS, Jiao Q, et al. Reversal of cancer cachexia and muscle wasting by ActRIIB antagonism leads to prolonged survival. Cell. 2010;142(4):531-43.
218. Bloch SA, Lee JY, Wort SJ, Polkey MI, Kemp PR, Griffiths MJ. Sustained elevation of circulating growth and differentiation factor-15 and a dynamic imbalance in mediators of muscle homeostasis are associated with the development of acute muscle wasting following cardiac surgery. Critical care medicine. 2013;41(4):982-9.
219. Bootcov MR, Bauskin AR, Valenzuela SM, Moore AG, Bansal M, He XY, et al. MIC-1, a novel macrophage inhibitory cytokine, is a divergent member of the TGF-beta superfamily. Proceedings of the National Academy of Sciences of the United States of America. 1997;94(21):11514-9.
220. Hromas R, Hufford M, Sutton J, Xu D, Li Y, Lu L. PLAB, a novel placental bone morphogenetic protein. Biochimica et biophysica acta. 1997;1354(1):40-4.
221. Paralkar VM, Vail AL, Grasser WA, Brown TA, Xu H, Vukicevic S, et al. Cloning and characterization of a novel member of the transforming growth factor-beta/bone morphogenetic protein family. The Journal of biological chemistry. 1998;273(22):13760-7.
222. Lawton LN, Bonaldo MF, Jelenc PC, Qiu L, Baumes SA, Marcelino RA, et al. Identification of a novel member of the TGF-beta superfamily highly expressed in human placenta. Gene. 1997;203(1):17-26.
223. Baek SJ, Kim KS, Nixon JB, Wilson LC, Eling TE. Cyclooxygenase inhibitors regulate the expression of a TGF-beta superfamily member that has proapoptotic and antitumorigenic activities. Mol Pharmacol. 2001;59(4):901-8.
224. Bottner M, Suter-Crazzolara C, Schober A, Unsicker K. Expression of a novel member of the TGF-beta superfamily, growth/differentiation factor-15/macrophage-inhibiting cytokine-1 (GDF-15/MIC-1) in adult rat tissues. Cell Tissue Res. 1999;297(1):103-10.

225. Bottner M, Laaff M, Schechinger B, Rappold G, Unsicker K, Suter-Crazzolara C. Characterization of the rat, mouse, and human genes of growth/differentiation factor-15/macrophage inhibiting cytokine-1 (GDF-15/MIC-1). Gene. 1999;237(1):105-11.
226. Strelau J, Sullivan A, Bottner M, Lingor P, Falkenstein E, Suter-Crazzolara C, et al. Growth/differentiation factor-15/macrophage inhibitory cytokine-1 is a novel trophic factor for midbrain dopaminergic neurons in vivo. J Neurosci. 2000;20(23):8597-603.
227. Mimeault M, Batra SK. Divergent molecular mechanisms underlying the pleiotropic functions of macrophage inhibitory cytokine-1 in cancer. Journal of cellular physiology. 2010;224(3):626-35.
228. Moore AG, Brown DA, Fairlie WD, Bauskin AR, Brown PK, Munier ML, et al. The transforming growth factor-ss superfamily cytokine macrophage inhibitory cytokine-1 is present in high concentrations in the serum of pregnant women. The Journal of clinical endocrinology and metabolism. 2000;85(12):4781-8.
229. Marjono AB, Brown DA, Horton KE, Wallace EM, Breit SN, Manuelpillai U. Macrophage inhibitory cytokine-1 in gestational tissues and maternal serum in normal and pre-eclamptic pregnancy. Placenta. 2003;24(1):100-6.
230. Tong S, Marjono B, Brown DA, Mulvey S, Breit SN, Manuelpillai U, et al. Serum concentrations of macrophage inhibitory cytokine 1 (MIC 1) as a predictor of miscarriage. Lancet. 2004;363(9403):129-30.
231. Soucek K, Slabakova E, Ovesna P, Malenovska A, Kozubik A, Hampl A. Growth/differentiation factor-15 is an abundant cytokine in human seminal plasma. Hum Reprod. 2010;25(12):2962-71.
232. Hsiao EC, Koniaris LG, Zimmers-Koniaris T, Sebald SM, Huynh TV, Lee SJ. Characterization of growth-differentiation factor 15, a transforming growth factor beta superfamily member induced following liver injury. Mol Cell Biol. 2000;20(10):3742-51.
233. Wang X, Krebbers J, Charalambous P, Machado V, Schober A, Bosse F, et al. Growth/differentiation factor-15 and its role in peripheral nervous system lesion and regeneration. Cell Tissue Res. 2015;362(2):317-30.
234. Strelau J, Strzelczyk A, Rusu P, Bendner G, Wiese S, Diella F, et al. Progressive postnatal motoneuron loss in mice lacking GDF-15. J Neurosci. 2009;29(43):13640-8.
235. Xu J, Kimball TR, Lorenz JN, Brown DA, Bauskin AR, Klevitsky R, et al. GDF15/MIC-1 functions as a protective and antihypertrophic factor released from the myocardium in association with SMAD protein activation. Circ Res. 2006;98(3):342-50.
236. Kempf T, Eden M, Strelau J, Naguib M, Willenbockel C, Tongers J, et al. The transforming growth factor-beta superfamily member growth-differentiation factor-15 protects the heart from ischemia/reperfusion injury. Circ Res. 2006;98(3):351-60.
237. Kempf T, Zarbock A, Widera C, Butz S, Stadtmann A, Rossaint J, et al. GDF-15 is an inhibitor of leukocyte integrin activation required for survival after myocardial infarction in mice. Nature medicine. 2011;17(5):581-8.
238. Heger J, Schiegnitz E, von Waldthausen D, Anwar MM, Piper HM, Euler G. Growth differentiation factor 15 acts anti-apoptotic and pro-hypertrophic in adult cardiomyocytes. Journal of cellular physiology. 2010;224(1):120-6.
239. de Jager SC, Bermudez B, Bot I, Koenen RR, Bot M, Kavelaars A, et al. Growth differentiation factor 15 deficiency protects against atherosclerosis by attenuating CCR2-mediated macrophage chemotaxis. J Exp Med. 2011;208(2):217-25.
240. Bonaterra GA, Zugel S, Thogersen J, Walter SA, Haberkorn U, Strelau J, et al. Growth differentiation factor-15 deficiency inhibits atherosclerosis progression by regulating interleukin-6-dependent inflammatory response to vascular injury. J Am Heart Assoc. 2012;1(6):e002550.
241. Li PX, Wong J, Ayed A, Ngo D, Brade AM, Arrowsmith C, et al. Placental transforming growth factor-beta is a downstream mediator of the growth arrest and apoptotic response of tumor cells to DNA damage and p53 overexpression. The Journal of biological chemistry. 2000;275(26):20127-35.

242. Boyle GM, Pedley J, Martyn AC, Banducci KJ, Strutton GM, Brown DA, et al. Macrophage inhibitory cytokine-1 is overexpressed in malignant melanoma and is associated with tumorigenicity. J Invest Dermatol. 2009;129(2):383-91.
243. Lee DH, Yang Y, Lee SJ, Kim KY, Koo TH, Shin SM, et al. Macrophage inhibitory cytokine-1 induces the invasiveness of gastric cancer cells by up-regulating the urokinase-type plasminogen activator system. Cancer Res. 2003;63(15):4648-55.
244. Kim KK, Lee JJ, Yang Y, You KH, Lee JH. Macrophage inhibitory cytokine-1 activates AKT and ERK-1/2 via the transactivation of ErbB2 in human breast and gastric cancer cells. Carcinogenesis. 2008;29(4):704-12.
245. Wollmann W, Goodman ML, Bhat-Nakshatri P, Kishimoto H, Goulet RJ, Jr., Mehrotra S, et al. The macrophage inhibitory cytokine integrates AKT/PKB and MAP kinase signaling pathways in breast cancer cells. Carcinogenesis. 2005;26(5):900-7.
246. Zhang L, Yang X, Pan HY, Zhou XJ, Li J, Chen WT, et al. Expression of growth differentiation factor 15 is positively correlated with histopathological malignant grade and in vitro cell proliferation in oral squamous cell carcinoma. Oral Oncol. 2009;45(7):627-32.
247. Chen SJ, Karan D, Johansson SL, Lin FF, Zeckser J, Singh AP, et al. Prostate-derived factor as a paracrine and autocrine factor for the proliferation of androgen receptor-positive human prostate cancer cells. Prostate. 2007;67(5):557-71.
248. Campbell RA, Bhat-Nakshatri P, Patel NM, Constantinidou D, Ali S, Nakshatri H. Phosphatidylinositol 3-kinase/AKT-mediated activation of estrogen receptor alpha: a new model for anti-estrogen resistance. The Journal of biological chemistry. 2001;276(13):9817-24.
249. Huang CY, Beer TM, Higano CS, True LD, Vessella R, Lange PH, et al. Molecular alterations in prostate carcinomas that associate with in vivo exposure to chemotherapy: identification of a cytoprotective mechanism involving growth differentiation factor 15. Clin Cancer Res. 2007;13(19):5825-33.
250. Zhao L, Lee BY, Brown DA, Molloy MP, Marx GM, Pavlakis N, et al. Identification of candidate biomarkers of therapeutic response to docetaxel by proteomic profiling. Cancer Res. 2009;69(19):7696-703.
251. Xu X, Li Z, Gao W. Growth differentiation factor 15 in cardiovascular diseases: from bench to bedside. Biomarkers. 2011;16(6):466-75.
252. Groschel K, Schnaudigel S, Edelmann F, Niehaus CF, Weber-Kruger M, Haase B, et al. Growth-differentiation factor-15 and functional outcome after acute ischemic stroke. Journal of neurology. 2012;259(8):1574-9.
253. Clark BJ, Bull TM, Benson AB, Stream AR, Macht M, Gaydos J, et al. Growth differentiation factor-15 and prognosis in acute respiratory distress syndrome: a retrospective cohort study. Crit Care. 2013;17(3):R92.
254. Breit SN, Carrero JJ, Tsai VW, Yagoutifam N, Luo W, Kuffner T, et al. Macrophage inhibitory cytokine-1 (MIC-1/GDF15) and mortality in end-stage renal disease. Nephrol Dial Transplant. 2012;27(1):70-5.
255. Khaled YS, Elkord E, Ammori BJ. Macrophage inhibitory cytokine-1: a review of its pleiotropic actions in cancer. Cancer biomarkers : section A of Disease markers. 2012;11(5):183-90.
256. Eggers KM, Kempf T, Wallentin L, Wollert KC, Lind L. Change in growth differentiation factor 15 concentrations over time independently predicts mortality in community-dwelling elderly individuals. Clinical chemistry. 2013;59(7):1091-8.
257. Munk PS, Valborgland T, Butt N, Larsen AI. Response of growth differentiation factor-15 to percutaneous coronary intervention and regular exercise training. Scandinavian cardiovascular journal : SCJ. 2011;45(1):27-32.
258. Daniels LB, Clopton P, Laughlin GA, Maisel AS, Barrett-Connor E. Growth-differentiation factor-15 is a robust, independent predictor of 11-year mortality risk in community-dwelling older adults: the Rancho Bernardo Study. Circulation. 2011;123(19):2101-10.

259. Baek SJ, Okazaki R, Lee SH, Martinez J, Kim JS, Yamaguchi K, et al. Nonsteroidal anti-inflammatory drug-activated gene-1 over expression in transgenic mice suppresses intestinal neoplasia. Gastroenterology. 2006;131(5):1553-60.
260. Johnen H, Lin S, Kuffner T, Brown DA, Tsai VW, Bauskin AR, et al. Tumor-induced anorexia and weight loss are mediated by the TGF-beta superfamily cytokine MIC-1. Nature medicine. 2007;13(11):1333-40.
261. Kalko SG, Paco S, Jou C, Rodriguez MA, Meznaric M, Rogac M, et al. Transcriptomic profiling of TK2 deficient human skeletal muscle suggests a role for the p53 signalling pathway and identifies growth and differentiation factor-15 as a potential novel biomarker for mitochondrial myopathies. BMC Genomics. 2014;15:91.
262. Lerner L, Hayes TG, Tao N, Krieger B, Feng B, Wu Z, et al. Plasma growth differentiation factor 15 is associated with weight loss and mortality in cancer patients. Journal of cachexia, sarcopenia and muscle. 2015;6(4):317-24.
263. Hofmann M, Halper B, Oesen S, Franzke B, Stuparits P, Tschan H, et al. Serum concentrations of insulin-like growth factor-1, members of the TGF-beta superfamily and follistatin do not reflect different stages of dynapenia and sarcopenia in elderly women. Exp Gerontol. 2015;64:35-45.
264. Tsai VW, Husaini Y, Manandhar R, Lee-Ng KK, Zhang HP, Harriott K, et al. Anorexia/cachexia of chronic diseases: a role for the TGF-beta family cytokine MIC-1/GDF15. Journal of cachexia, sarcopenia and muscle. 2012;3(4):239-43.
265. Bloch SA, Lee JY, Syburra T, Rosendahl U, Griffiths MJ, Kemp PR, et al. Increased expression of GDF-15 may mediate ICU-acquired weakness by down-regulating muscle microRNAs. Thorax. 2015;70(3):219-28.
266. Patel MS, Lee J, Baz M, Wells CE, Bloch S, Lewis A, et al. Growth differentiation factor-15 is associated with muscle mass in chronic obstructive pulmonary disease and promotes muscle wasting in vivo. Journal of cachexia, sarcopenia and muscle. 2016;7(4):436-48.
267. Dostalova I, Roubicek T, Bartlova M, Mraz M, Lacinova Z, Haluzikova D, et al. Increased serum concentrations of macrophage inhibitory cytokine-1 in patients with obesity and type 2 diabetes mellitus: the influence of very low calorie diet. Eur J Endocrinol. 2009;161(3):397-404.
268. Skipworth RJ, Deans DA, Tan BH, Sangster K, Paterson-Brown S, Brown DA, et al. Plasma MIC-1 correlates with systemic inflammation but is not an independent determinant of nutritional status or survival in oesophago-gastric cancer. British journal of cancer. 2010;102(4):665-72.
269. Lerner L, Tao J, Liu Q, Nicoletti R, Feng B, Krieger B, et al. MAP3K11/GDF15 axis is a critical driver of cancer cachexia. Journal of cachexia, sarcopenia and muscle. 2015.
270. Macia L, Tsai VW, Nguyen AD, Johnen H, Kuffner T, Shi YC, et al. Macrophage inhibitory cytokine 1 (MIC-1/GDF15) decreases food intake, body weight and improves glucose tolerance in mice on normal & obesogenic diets. PloS one. 2012;7(4):e34868.
271. Tsai VW, Macia L, Johnen H, Kuffner T, Manadhar R, Jorgensen SB, et al. TGF-b superfamily cytokine MIC-1/GDF15 is a physiological appetite and body weight regulator. PloS one. 2013;8(2):e55174.
272. Tsai VW, Manandhar R, Jorgensen SB, Lee-Ng KK, Zhang HP, Marquis CP, et al. The anorectic actions of the TGFbeta cytokine MIC-1/GDF15 require an intact brainstem area postrema and nucleus of the solitary tract. PloS one. 2014;9(6):e100370.
273. Chrysovergis K, Wang X, Kosak J, Lee SH, Kim JS, Foley JF, et al. NAG-1/GDF-15 prevents obesity by increasing thermogenesis, lipolysis and oxidative metabolism. Int J Obes (Lond). 2014;38(12):1555-64.
274. Tsai VW, Macia L, Feinle-Bisset C, Manandhar R, Astrup A, Raben A, et al. Serum Levels of Human MIC-1/GDF15 Vary in a Diurnal Pattern, Do Not Display a Profile Suggestive of a Satiety Factor and Are Related to BMI. PloS one. 2015;10(7):e0133362.
275. Tchou I, Margeli A, Tsironi M, Skenderi K, Barnet M, Kanaka-Gantenbein C, et al. Growth-differentiation factor-15, endoglin and N-terminal pro-brain natriuretic peptide induction in athletes participating in an ultramarathon foot race. Biomarkers. 2009;14(6):418-22.

276. Sanchis-Gomar F, Bonaguri C, Aloe R, Pareja-Galeano H, Martinez-Bello V, Gomez-Cabrera MC, et al. Effects of acute exercise and xanthine oxidase inhibition on novel cardiovascular biomarkers. Transl Res. 2013;162(2):102-9.
277. Galliera E, Lombardi G, Marazzi MG, Grasso D, Vianello E, Pozzoni R, et al. Acute exercise in elite rugby players increases the circulating level of the cardiovascular biomarker GDF-15. Scand J Clin Lab Invest. 2014;74(6):492-9.
278. Eindhoven JA, van den Bosch AE, Oemrawsingh RM, Baggen VJ, Kardys I, Cuypers JA, et al. Release of growth-differentiation factor 15 and associations with cardiac function in adult patients with congenital heart disease. International journal of cardiology. 2016;202:246-51.
279. Meadows CA, Risbano MG, Zhang L, Geraci MW, Tuder RM, Collier DH, et al. Increased expression of growth differentiation factor-15 in systemic sclerosis-associated pulmonary arterial hypertension. Chest. 2011;139(5):994-1002.
280. Klok FA, Surie S, Kempf T, Eikenboom J, van Straalen JP, van Kralingen KW, et al. A simple non-invasive diagnostic algorithm for ruling out chronic thromboembolic pulmonary hypertension in patients after acute pulmonary embolism. Thrombosis research. 2011;128(1):21-6.
281. Tantawy AA, Adly AA, Ismail EA, Darwish YW, Ali Zedan M. Growth differentiation factor-15 in young sickle cell disease patients: relation to hemolysis, iron overload and vascular complications. Blood Cells Mol Dis. 2014;53(4):189-93.
282. Tantawy AA, Adly AA, Ismail EA, Youssef OI, Ali ME. Growth differentiation factor-15 in children and adolescents with thalassemia intermedia: Relation to subclinical atherosclerosis and pulmonary vasculopathy. Blood Cells Mol Dis. 2015;55(2):144-50.
283. Nickel N, Jonigk D, Kempf T, Bockmeyer CL, Maegel L, Rische J, et al. GDF-15 is abundantly expressed in plexiform lesions in patients with pulmonary arterial hypertension and affects proliferation and apoptosis of pulmonary endothelial cells. Respiratory research. 2011;12:62.
284. Song H, Yin D, Liu Z. GDF-15 promotes angiogenesis through modulating p53/HIF-1alpha signaling pathway in hypoxic human umbilical vein endothelial cells. Mol Biol Rep. 2012;39(4):4017-22.
285. Eggers KM, Kempf T, Lind L, Sundstrom J, Wallentin L, Wollert KC, et al. Relations of growth-differentiation factor-15 to biomarkers reflecting vascular pathologies in a population-based sample of elderly subjects. Scand J Clin Lab Invest. 2012;72(1):45-51.
286. Rossaint J, Vestweber D, Zarbock A. GDF-15 prevents platelet integrin activation and thrombus formation. J Thromb Haemost. 2013;11(2):335-44.
287. Mazagova M, Buikema H, Landheer SW, Vavrinec P, Buiten A, Henning RH, et al. Growth differentiation factor 15 impairs aortic contractile and relaxing function through altered caveolar signaling of the endothelium. Am J Physiol Heart Circ Physiol. 2013;304(5):H709-18.
288. Tan M, Wang Y, Guan K, Sun Y. PTGF-beta, a type beta transforming growth factor (TGF-beta) superfamily member, is a p53 target gene that inhibits tumor cell growth via TGF-beta signaling pathway. Proceedings of the National Academy of Sciences of the United States of America. 2000;97(1):109-14.
289. Lu JM, Wang CY, Hu C, Fang YJ, Mei YA. GDF-15 enhances intracellular Ca2+ by increasing Cav1.3 expression in rat cerebellar granule neurons. The Biochemical journal. 2016;473(13):1895-904.
290. Li C, Wang J, Kong J, Tang J, Wu Y, Xu E, et al. GDF15 promotes EMT and metastasis in colorectal cancer. Oncotarget. 2016;7(1):860-72.
291. Wu Q, Jiang D, Matsuda JL, Ternyak K, Zhang B, Chu HW. Cigarette Smoke Induces Human Airway Epithelial Senescence via Growth Differentiation Factor 15 Production. American journal of respiratory cell and molecular biology. 2016;55(3):429-38.
292. Emmerson PJ, Wang F, Du Y, Liu Q, Pickard RT, Gonciarz MD, et al. The metabolic effects of GDF15 are mediated by the orphan receptor GFRAL. Nature medicine. 2017;23(10):1215-9.

293. Hsu JY, Crawley S, Chen M, Ayupova DA, Lindhout DA, Higbee J, et al. Non-homeostatic body weight regulation through a brainstem-restricted receptor for GDF15. Nature. 2017;550(7675):255-9.
294. Yang L, Chang CC, Sun Z, Madsen D, Zhu H, Padkjaer SB, et al. GFRAL is the receptor for GDF15 and is required for the anti-obesity effects of the ligand. Nature medicine. 2017;23(10):1158-66.
295. Li Z, Wang B, Wu X, Cheng SY, Paraoan L, Zhou J. Identification, expression and functional characterization of the GRAL gene. J Neurochem. 2005;95(2):361-76.
296. Mullican SE, Lin-Schmidt X, Chin CN, Chavez JA, Furman JL, Armstrong AA, et al. GFRAL is the receptor for GDF15 and the ligand promotes weight loss in mice and nonhuman primates. Nature medicine. 2017;23(10):1150-7.
297. Zhang Z, Wu L, Wang J, Li G, Feng D, Zhang B, et al. Opposing effects of PI3K/Akt and Smad-dependent signaling pathways in NAG-1-induced glioblastoma cell apoptosis. PloS one. 2014;9(4):e96283.
298. Min KW, Liggett JL, Silva G, Wu WW, Wang R, Shen RF, et al. NAG-1/GDF15 accumulates in the nucleus and modulates transcriptional regulation of the Smad pathway. Oncogene. 2016;35(3):377-88.
299. Codo P, Weller M, Kaulich K, Schraivogel D, Silginer M, Reifenberger G, et al. Control of glioma cell migration and invasiveness by GDF-15. Oncotarget. 2016;7(7):7732-46.
300. Vanhara P, Lincova E, Kozubik A, Jurdic P, Soucek K, Smarda J. Growth/differentiation factor-15 inhibits differentiation into osteoclasts--a novel factor involved in control of osteoclast differentiation. Differentiation. 2009;78(4):213-22.
301. Artz A, Butz S, Vestweber D. GDF-15 inhibits integrin activation and mouse neutrophil recruitment through the ALK-5/TGF-betaRII heterodimer. Blood. 2016;128(4):529-41.
302. Proutski I, Stevenson L, Allen WL, McCulla A, Boyer J, McLean EG, et al. Prostate-derived factor--a novel inhibitor of drug-induced cell death in colon cancer cells. Mol Cancer Ther. 2009;8(9):2566-74.
303. Park YJ, Lee H, Lee JH. Macrophage inhibitory cytokine-1 transactivates ErbB family receptors via the activation of Src in SK-BR-3 human breast cancer cells. BMB Rep. 2010;43(2):91-6.
304. Griner SE, Joshi JP, Nahta R. Growth differentiation factor 15 stimulates rapamycin-sensitive ovarian cancer cell growth and invasion. Biochem Pharmacol. 2013;85(1):46-58.
305. Urakawa N, Utsunomiya S, Nishio M, Shigeoka M, Takase N, Arai N, et al. GDF15 derived from both tumor-associated macrophages and esophageal squamous cell carcinomas contributes to tumor progression via Akt and Erk pathways. Lab Invest. 2015;95(5):491-503.
306. Si Y, Liu X, Cheng M, Wang M, Gong Q, Yang Y, et al. Growth differentiation factor 15 is induced by hepatitis C virus infection and regulates hepatocellular carcinoma-related genes. PloS one. 2011;6(5):e19967.
307. Tanno T, Lim Y, Wang Q, Chesi M, Bergsagel PL, Matthews G, et al. Growth differentiating factor 15 enhances the tumor-initiating and self-renewal potential of multiple myeloma cells. Blood. 2014;123(5):725-33.
308. Wu Q, Jiang D, Chu HW. Cigarette smoke induces growth differentiation factor 15 production in human lung epithelial cells: implication in mucin over-expression. Innate Immun. 2012;18(4):617-26.
309. Uchiyama T, Kawabata H, Miura Y, Yoshioka S, Iwasa M, Yao H, et al. The role of growth differentiation factor 15 in the pathogenesis of primary myelofibrosis. Cancer Med. 2015;4(10):1558-72.
310. Subramaniam S, Strelau J, Unsicker K. Growth differentiation factor-15 prevents low potassium-induced cell death of cerebellar granule neurons by differential regulation of Akt and ERK pathways. The Journal of biological chemistry. 2003;278(11):8904-12.

311. Yang H, Choi HJ, Park SH, Kim JS, Moon Y. Macrophage inhibitory cytokine-1 (MIC-1) and subsequent urokinase-type plasminogen activator mediate cell death responses by ribotoxic anisomycin in HCT-116 colon cancer cells. Biochem Pharmacol. 2009;78(9):1205-13.
312. Cekanova M, Lee SH, Donnell RL, Sukhthankar M, Eling TE, Fischer SM, et al. Nonsteroidal anti-inflammatory drug-activated gene-1 expression inhibits urethane-induced pulmonary tumorigenesis in transgenic mice. Cancer Prev Res (Phila). 2009;2(5):450-8.
313. Xu XY, Nie Y, Wang FF, Bai Y, Lv ZZ, Zhang YY, et al. Growth differentiation factor (GDF)-15 blocks norepinephrine-induced myocardial hypertrophy via a novel pathway involving inhibition of epidermal growth factor receptor transactivation. The Journal of biological chemistry. 2014;289(14):10084-94.
314. Donnelly SM, Paplomata E, Peake BM, Sanabria E, Chen Z, Nahta R. P38 MAPK contributes to resistance and invasiveness of HER2- overexpressing breast cancer. Curr Med Chem. 2014;21(4):501-10.
315. Jin YJ, Lee JH, Kim YM, Oh GT, Lee H. Macrophage inhibitory cytokine-1 stimulates proliferation of human umbilical vein endothelial cells by up-regulating cyclins D1 and E through the PI3K/Akt-, ERK-, and JNK-dependent AP-1 and E2F activation signaling pathways. Cellular signalling. 2012;24(8):1485-95.
316. Li J, Yang L, Qin W, Zhang G, Yuan J, Wang F. Adaptive induction of growth differentiation factor 15 attenuates endothelial cell apoptosis in response to high glucose stimulus. PloS one. 2013;8(6):e65549.
317. Hinoi E, Ochi H, Takarada T, Nakatani E, Iezaki T, Nakajima H, et al. Positive regulation of osteoclastic differentiation by growth differentiation factor 15 upregulated in osteocytic cells under hypoxia. J Bone Miner Res. 2012;27(4):938-49.
318. Choi HJ, Kim J, Do KH, Park SH, Moon Y. Prolonged NF-kappaB activation by a macrophage inhibitory cytokine 1-linked signal in enteropathogenic Escherichia coli-infected epithelial cells. Infection and immunity. 2013;81(6):1860-9.
319. Choi HJ, Kim J, Do KH, Park SH, Moon Y. Enteropathogenic Escherichia coli-induced macrophage inhibitory cytokine 1 mediates cancer cell survival: an in vitro implication of infection-linked tumor dissemination. Oncogene. 2013;32(41):4960-9.
320. Yamaguchi K, Shirakabe K, Shibuya H, Irie K, Oishi I, Ueno N, et al. Identification of a member of the MAPKKK family as a potential mediator of TGF-beta signal transduction. Science. 1995;270(5244):2008-11.
321. Shibuya H, Yamaguchi K, Shirakabe K, Tonegawa A, Gotoh Y, Ueno N, et al. TAB1: an activator of the TAK1 MAPKKK in TGF-beta signal transduction. Science. 1996;272(5265):1179-82.
322. Takaesu G, Kishida S, Hiyama A, Yamaguchi K, Shibuya H, Irie K, et al. TAB2, a novel adaptor protein, mediates activation of TAK1 MAPKKK by linking TAK1 to TRAF6 in the IL-1 signal transduction pathway. Mol Cell. 2000;5(4):649-58.
323. Cheung PC, Nebreda AR, Cohen P. TAB3, a new binding partner of the protein kinase TAK1. The Biochemical journal. 2004;378(Pt 1):27-34.
324. Watkins SJ, Jonker L, Arthur HM. A direct interaction between TGFbeta activated kinase 1 and the TGFbeta type II receptor: implications for TGFbeta signalling and cardiac hypertrophy. Cardiovascular research. 2006;69(2):432-9.
325. Kim SI, Kwak JH, Na HJ, Kim JK, Ding Y, Choi ME. Transforming growth factor-beta (TGF-beta1) activates TAK1 via TAB1-mediated autophosphorylation, independent of TGF-beta receptor kinase activity in mesangial cells. The Journal of biological chemistry. 2009;284(33):22285-96.
326. Mao R, Fan Y, Mou Y, Zhang H, Fu S, Yang J. TAK1 lysine 158 is required for TGF-beta-induced TRAF6-mediated Smad-independent IKK/NF-kappaB and JNK/AP-1 activation. Cellular signalling. 2011;23(1):222-7.
327. Biesemann N, Mendler L, Kostin S, Wietelmann A, Borchardt T, Braun T. Myostatin induces interstitial fibrosis in the heart via TAK1 and p38. Cell Tissue Res. 2015;361(3):779-87.

328. Ninomiya-Tsuji J, Kishimoto K, Hiyama A, Inoue J, Cao Z, Matsumoto K. The kinase TAK1 can activate the NIK-I kappaB as well as the MAP kinase cascade in the IL-1 signalling pathway. Nature. 1999;398(6724):252-6.
329. Wald D, Commane M, Stark GR, Li X. IRAK and TAK1 are required for IL-18-mediated signaling. Eur J Immunol. 2001;31(12):3747-54.
330. Sakurai H, Miyoshi H, Toriumi W, Sugita T. Functional interactions of transforming growth factor beta-activated kinase 1 with IkappaB kinases to stimulate NF-kappaB activation. The Journal of biological chemistry. 1999;274(15):10641-8.
331. Irie T, Muta T, Takeshige K. TAK1 mediates an activation signal from toll-like receptor(s) to nuclear factor-kappaB in lipopolysaccharide-stimulated macrophages. FEBS Lett. 2000;467(2-3):160-4.
332. Kishimoto K, Matsumoto K, Ninomiya-Tsuji J. TAK1 mitogen-activated protein kinase kinase kinase is activated by autophosphorylation within its activation loop. The Journal of biological chemistry. 2000;275(10):7359-64.
333. Scholz R, Sidler CL, Thali RF, Winssinger N, Cheung PC, Neumann D. Autoactivation of transforming growth factor beta-activated kinase 1 is a sequential bimolecular process. The Journal of biological chemistry. 2010;285(33):25753-66.
334. Singhirunnusorn P, Suzuki S, Kawasaki N, Saiki I, Sakurai H. Critical roles of threonine 187 phosphorylation in cellular stress-induced rapid and transient activation of transforming growth factor-beta-activated kinase 1 (TAK1) in a signaling complex containing TAK1-binding protein TAB1 and TAB2. The Journal of biological chemistry. 2005;280(8):7359-68.
335. Ouyang C, Nie L, Gu M, Wu A, Han X, Wang X, et al. Transforming growth factor (TGF)-beta-activated kinase 1 (TAK1) activation requires phosphorylation of serine 412 by protein kinase A catalytic subunit alpha (PKACalpha) and X-linked protein kinase (PRKX). The Journal of biological chemistry. 2014;289(35):24226-37.
336. Sakurai H, Shigemori N, Hasegawa K, Sugita T. TGF-beta-activated kinase 1 stimulates NF-kappa B activation by an NF-kappa B-inducing kinase-independent mechanism. Biochem Biophys Res Commun. 1998;243(2):545-9.
337. Moriguchi T, Kuroyanagi N, Yamaguchi K, Gotoh Y, Irie K, Kano T, et al. A novel kinase cascade mediated by mitogen-activated protein kinase kinase 6 and MKK3. The Journal of biological chemistry. 1996;271(23):13675-9.
338. Shirakabe K, Yamaguchi K, Shibuya H, Irie K, Matsuda S, Moriguchi T, et al. TAK1 mediates the ceramide signaling to stress-activated protein kinase/c-Jun N-terminal kinase. The Journal of biological chemistry. 1997;272(13):8141-4.
339. Behrens J. Cross-regulation of the Wnt signalling pathway: a role of MAP kinases. J Cell Sci. 2000;113 (Pt 6):911-9.
340. Suzawa M, Takada I, Yanagisawa J, Ohtake F, Ogawa S, Yamauchi T, et al. Cytokines suppress adipogenesis and PPAR-gamma function through the TAK1/TAB1/NIK cascade. Nat Cell Biol. 2003;5(3):224-30.
341. Yanagisawa M, Nakashima K, Takeda K, Ochiai W, Takizawa T, Ueno M, et al. Inhibition of BMP2-induced, TAK1 kinase-mediated neurite outgrowth by Smad6 and Smad7. Genes Cells. 2001;6(12):1091-9.
342. Hong S, Lim S, Li AG, Lee C, Lee YS, Lee EK, et al. Smad7 binds to the adaptors TAB2 and TAB3 to block recruitment of the kinase TAK1 to the adaptor TRAF2. Nat Immunol. 2007;8(5):504-13.
343. Yumoto K, Thomas PS, Lane J, Matsuzaki K, Inagaki M, Ninomiya-Tsuji J, et al. TGF-beta-activated kinase 1 (Tak1) mediates agonist-induced Smad activation and linker region phosphorylation in embryonic craniofacial neural crest-derived cells. The Journal of biological chemistry. 2013;288(19):13467-80.
344. Ajibade AA, Wang HY, Wang RF. Cell type-specific function of TAK1 in innate immune signaling. Trends Immunol. 2013;34(7):307-16.

345. Dai L, Aye Thu C, Liu XY, Xi J, Cheung PC. TAK1, more than just innate immunity. IUBMB life. 2012;64(10):825-34.
346. Li L, Chen Y, Doan J, Murray J, Molkentin JD, Liu Q. Transforming growth factor beta-activated kinase 1 signaling pathway critically regulates myocardial survival and remodeling. Circulation. 2014;130(24):2162-72.
347. Sakurai H. Targeting of TAK1 in inflammatory disorders and cancer. Trends Pharmacol Sci. 2012;33(10):522-30.
348. Zhang D, Gaussin V, Taffet GE, Belaguli NS, Yamada M, Schwartz RJ, et al. TAK1 is activated in the myocardium after pressure overload and is sufficient to provoke heart failure in transgenic mice. Nature medicine. 2000;6(5):556-63.
349. Choi ME, Ding Y, Kim SI. TGF-beta signaling via TAK1 pathway: role in kidney fibrosis. Semin Nephrol. 2012;32(3):244-52.
350. Shi-Wen X, Rodriguez-Pascual F, Lamas S, Holmes A, Howat S, Pearson JD, et al. Constitutive ALK5-independent c-Jun N-terminal kinase activation contributes to endothelin-1 overexpression in pulmonary fibrosis: evidence of an autocrine endothelin loop operating through the endothelin A and B receptors. Mol Cell Biol. 2006;26(14):5518-27.
351. Kilty I, Jones LH. TAK1 selective inhibition: state of the art and future opportunities. Future Med Chem. 2015;7(1):23-33.
352. Ninomiya-Tsuji J, Kajino T, Ono K, Ohtomo T, Matsumoto M, Shiina M, et al. A resorcylic acid lactone, 5Z-7-oxozeaenol, prevents inflammation by inhibiting the catalytic activity of TAK1 MAPK kinase kinase. The Journal of biological chemistry. 2003;278(20):18485-90.
353. Wu J, Powell F, Larsen NA, Lai Z, Byth KF, Read J, et al. Mechanism and in vitro pharmacology of TAK1 inhibition by (5Z)-7-Oxozeaenol. ACS Chem Biol. 2013;8(3):643-50.
354. Fan Y, Cheng J, Vasudevan SA, Patel RH, Liang L, Xu X, et al. TAK1 inhibitor 5Z-7-oxozeaenol sensitizes neuroblastoma to chemotherapy. Apoptosis. 2013;18(10):1224-34.
355. Cao H, Lu J, Du J, Xia F, Wei S, Liu X, et al. TAK1 inhibition prevents the development of autoimmune diabetes in NOD mice. Scientific reports. 2015;5:14593.
356. Xu X, Fan Z, Qi X, Shao Y, Wu Y. The role of TGF-beta-activated kinase 1 in db/db mice and high glucose-induced macrophage. Int Immunopharmacol. 2016;38:120-31.
357. Tian Q, Xiao Q, Yu W, Gu M, Zhao N, Lu Y. The inhibition of transforming growth factor beta-activated kinase 1 contributed to neuroprotection via inflammatory reaction in pilocarpine-induced rats with epilepsy. Neuroscience. 2016;325:111-23.
358. White BJ, Tarabishy S, Venna VR, Manwani B, Benashski S, McCullough LD, et al. Protection from cerebral ischemia by inhibition of TGFbeta-activated kinase. Experimental neurology. 2012;237(1):238-45.
359. Song Z, Zhu X, Jin R, Wang C, Yan J, Zheng Q, et al. Roles of the kinase TAK1 in CD40-mediated effects on vascular oxidative stress and neointima formation after vascular injury. PloS one. 2014;9(7):e101671.
360. Nasim MT, Ogo T, Chowdhury HM, Zhao L, Chen CN, Rhodes C, et al. BMPR-II deficiency elicits pro-proliferative and anti-apoptotic responses through the activation of TGFbeta-TAK1-MAPK pathways in PAH. Hum Mol Genet. 2012;21(11):2548-58.
361. Bhatnagar S, Kumar A, Makonchuk DY, Li H, Kumar A. Transforming growth factor-beta-activated kinase 1 is an essential regulator of myogenic differentiation. The Journal of biological chemistry. 2010;285(9):6401-11.
362. Xiao F, Wang H, Fu X, Li Y, Wu Z. TRAF6 promotes myogenic differentiation via the TAK1/p38 mitogen-activated protein kinase and Akt pathways. PloS one. 2012;7(4):e34081.
363. Ogura Y, Hindi SM, Sato S, Xiong G, Akira S, Kumar A. TAK1 modulates satellite stem cell homeostasis and skeletal muscle repair. Nat Commun. 2015;6:10123.
364. Sato S, Hindi SM, Tajrishi MM, Xiong G, Kumar A. TAK1 Is a Key Regulator of Skeletal Muscle Maintenance in Mice: 122 June 1, 9: 45 AM - 10: 00 AM. Med Sci Sports Exerc. 2016;48(5 Suppl 1):15.

365. Xie M, Zhang D, Dyck JR, Li Y, Zhang H, Morishima M, et al. A pivotal role for endogenous TGF-beta-activated kinase-1 in the LKB1/AMP-activated protein kinase energy-sensor pathway. Proceedings of the National Academy of Sciences of the United States of America. 2006;103(46):17378-83.
366. Huang Z, Chen D, Zhang K, Yu B, Chen X, Meng J. Regulation of myostatin signaling by c-Jun N-terminal kinase in C2C12 cells. Cellular signalling. 2007;19(11):2286-95.
367. Srivastava AK, Qin X, Wedhas N, Arnush M, Linkhart TA, Chadwick RB, et al. Tumor necrosis factor-alpha augments matrix metalloproteinase-9 production in skeletal muscle cells through the activation of transforming growth factor-beta-activated kinase 1 (TAK1)-dependent signaling pathway. The Journal of biological chemistry. 2007;282(48):35113-24.
368. Sente T, Van Berendoncks AM, Hoymans VY, Vrints CJ. Adiponectin resistance in skeletal muscle: pathophysiological implications in chronic heart failure. Journal of cachexia, sarcopenia and muscle. 2016;7(3):261-74.
369. Xin X, Zhou L, Reyes CM, Liu F, Dong LQ. APPL1 mediates adiponectin-stimulated p38 MAPK activation by scaffolding the TAK1-MKK3-p38 MAPK pathway. Am J Physiol Endocrinol Metab. 2011;300(1):E103-10.
370. Schutz Y, Kyle UU, Pichard C. Fat-free mass index and fat mass index percentiles in Caucasians aged 18-98 y. Int J Obes Relat Metab Disord. 2002;26(7):953-60.
371. Puthucheary ZA, Rawal J, McPhail M, Connolly B, Ratnayake G, Chan P, et al. Acute skeletal muscle wasting in critical illness. Jama. 2013;310(15):1591-600.
372. Shrikrishna D, Patel M, Tanner RJ, Seymour JM, Connolly BA, Puthucheary ZA, et al. Quadriceps wasting and physical inactivity in patients with COPD. The European respiratory journal. 2012;40(5):1115-22.
373. Maddocks M, Nolan C, Man WD, Polkey M, Hart N, Gao W, et al. Neuromuscular electrical stimulation to improve exercise capacity in patients with severe COPD - Authors' reply. Lancet Respir Med. 2016;4(4):e16.
374. Edwards RH, Young A, Hosking GP, Jones DA. Human skeletal muscle function: description of tests and normal values. Clinical science and molecular medicine. 1977;52(3):283-90.
375. Canavan JL, Maddocks M, Nolan CM, Jones SE, Kon SS, Clark AL, et al. Functionally Relevant Cut Point for Isometric Quadriceps Muscle Strength in Chronic Respiratory Disease. American journal of respiratory and critical care medicine. 2015;192(3):395-7.
376. Fruin ML, Rankin JW. Validity of a multi-sensor armband in estimating rest and exercise energy expenditure. Med Sci Sports Exerc. 2004;36(6):1063-9.
377. Van Remoortel H, Raste Y, Louvaris Z, Giavedoni S, Burtin C, Langer D, et al. Validity of six activity monitors in chronic obstructive pulmonary disease: a comparison with indirect calorimetry. PloS one. 2012;7(6):e39198.
378. Watz H, Waschki B, Meyer T, Magnussen H. Physical activity in patients with COPD. The European respiratory journal. 2009;33(2):262-72.
379. Watz H, Waschki B, Boehme C, Claussen M, Meyer T, Magnussen H. Extrapulmonary effects of chronic obstructive pulmonary disease on physical activity: a cross-sectional study. American journal of respiratory and critical care medicine. 2008;177(7):743-51.
380. Demeyer H, Burtin C, Van Remoortel H, Hornikx M, Langer D, Decramer M, et al. Standardizing the analysis of physical activity in patients with COPD following a pulmonary rehabilitation program. Chest. 2014;146(2):318-27.
381. Tudor-Locke C, Craig CL, Brown WJ, Clemes SA, De Cocker K, Giles-Corti B, et al. How many steps/day are enough? For adults. Int J Behav Nutr Phys Act. 2011;8:79.
382. Manini TM, Everhart JE, Patel KV, Schoeller DA, Colbert LH, Visser M, et al. Daily activity energy expenditure and mortality among older adults. Jama. 2006;296(2):171-9.
383. Garfield BE, Canavan JL, Smith CJ, Ingram KA, Fowler RP, Clark AL, et al. Stanford Seven-Day Physical Activity Recall questionnaire in COPD. The European respiratory journal. 2012;40(2):356-62.

384. Haskell WL, Lee IM, Pate RR, Powell KE, Blair SN, Franklin BA, et al. Physical activity and public health: updated recommendation for adults from the American College of Sports Medicine and the American Heart Association. Circulation. 2007;116(9):1081-93.
385. Jones PW, Quirk FH, Baveystock CM, Littlejohns P. A self-complete measure of health status for chronic airflow limitation. The St. George's Respiratory Questionnaire. Am Rev Respir Dis. 1992;145(6):1321-7.
386. P. J. SGRQ Manual - St George's Respiratory Questionnaire. wwwhealthstatussgulacuk/SGRQ/SGRQ%20Manual%20June%202009pdf. 2012.
387. Taichman DB, Shin J, Hud L, Archer-Chicko C, Kaplan S, Sager JS, et al. Health-related quality of life in patients with pulmonary arterial hypertension. Respiratory research. 2005;6:92.
388. Jones PW, Quirk FH, Baveystock CM. The St George's Respiratory Questionnaire. Respiratory medicine. 1991;85 Suppl B:25-31; discussion 3-7.
389. McKenna SP, Doughty N, Meads DM, Doward LC, Pepke-Zaba J. The Cambridge Pulmonary Hypertension Outcome Review (CAMPHOR): a measure of health-related quality of life and quality of life for patients with pulmonary hypertension. Qual Life Res. 2006;15(1):103-15.
390. McCabe C, Bennett M, Doughty N, MacKenzie Ross R, Sharples L, Pepke-Zaba J. Patient-reported outcomes assessed by the CAMPHOR questionnaire predict clinical deterioration in idiopathic pulmonary arterial hypertension and chronic thromboembolic pulmonary hypertension. Chest. 2013;144(2):522-30.
391. Yorke J, Corris P, Gaine S, Gibbs JS, Kiely DG, Harries C, et al. emPHasis-10: development of a health-related quality of life measure in pulmonary hypertension. The European respiratory journal. 2014;43(4):1106-13.
392. Rudski LG, Lai WW, Afilalo J, Hua L, Handschumacher MD, Chandrasekaran K, et al. Guidelines for the echocardiographic assessment of the right heart in adults: a report from the American Society of Echocardiography endorsed by the European Association of Echocardiography, a registered branch of the European Society of Cardiology, and the Canadian Society of Echocardiography. Journal of the American Society of Echocardiography : official publication of the American Society of Echocardiography. 2010;23(7):685-713; quiz 86-8.
393. Howard LS, Grapsa J, Dawson D, Bellamy M, Chambers JB, Masani ND, et al. Echocardiographic assessment of pulmonary hypertension: standard operating procedure. European respiratory review : an official journal of the European Respiratory Society. 2012;21(125):239-48.
394. Yared K, Noseworthy P, Weyman AE, McCabe E, Picard MH, Baggish AL. Pulmonary artery acceleration time provides an accurate estimate of systolic pulmonary arterial pressure during transthoracic echocardiography. Journal of the American Society of Echocardiography : official publication of the American Society of Echocardiography. 2011;24(6):687-92.
395. Miyamoto S, Nagaya N, Satoh T, Kyotani S, Sakamaki F, Fujita M, et al. Clinical correlates and prognostic significance of six-minute walk test in patients with primary pulmonary hypertension. Comparison with cardiopulmonary exercise testing. American journal of respiratory and critical care medicine. 2000;161(2 Pt 1):487-92.
396. Gaine S, Simonneau G. The need to move from 6-minute walk distance to outcome trials in pulmonary arterial hypertension. European respiratory review : an official journal of the European Respiratory Society. 2013;22(130):487-94.
397. Laboratories ATSCoPSfCPF. ATS statement: guidelines for the six-minute walk test. American journal of respiratory and critical care medicine. 2002;166(1):111-7.
398. Nagaya N, Nishikimi T, Uematsu M, Satoh T, Kyotani S, Sakamaki F, et al. Plasma brain natriuretic peptide as a prognostic indicator in patients with primary pulmonary hypertension. Circulation. 2000;102(8):865-70.
399. Bergstrom J. Percutaneous needle biopsy of skeletal muscle in physiological and clinical research. Scand J Clin Lab Invest. 1975;35(7):609-16.
400. Tarnopolsky MA, Pearce E, Smith K, Lach B. Suction-modified Bergstrom muscle biopsy technique: experience with 13,500 procedures. Muscle & nerve. 2011;43(5):717-25.

401. Handoko ML, de Man FS, Happe CM, Schalij I, Musters RJ, Westerhof N, et al. Opposite effects of training in rats with stable and progressive pulmonary hypertension. Circulation. 2009;120(1):42-9.
402. Long L, Crosby A, Yang X, Southwood M, Upton PD, Kim DK, et al. Altered bone morphogenetic protein and transforming growth factor-beta signaling in rat models of pulmonary hypertension: potential for activin receptor-like kinase-5 inhibition in prevention and progression of disease. Circulation. 2009;119(4):566-76.
403. Ciuclan L, Bonneau O, Hussey M, Duggan N, Holmes AM, Good R, et al. A novel murine model of severe pulmonary arterial hypertension. American journal of respiratory and critical care medicine. 2011;184(10):1171-82.
404. Reeder SB, Pineda AR, Wen Z, Shimakawa A, Yu H, Brittain JH, et al. Iterative decomposition of water and fat with echo asymmetry and least-squares estimation (IDEAL): application with fast spin-echo imaging. Magn Reson Med. 2005;54(3):636-44.
405. Yang P, Read C, Kuc RE, Buonincontri G, Southwood M, Torella R, et al. Elabela/Toddler Is an Endogenous Agonist of the Apelin APJ Receptor in the Adult Cardiovascular System, and Exogenous Administration of the Peptide Compensates for the Downregulation of Its Expression in Pulmonary Arterial Hypertension. Circulation. 2017;135(12):1160-73.
406. Phillips PG, Long L, Wilkins MR, Morrell NW. cAMP phosphodiesterase inhibitors potentiate effects of prostacyclin analogs in hypoxic pulmonary vascular remodeling. American journal of physiology Lung cellular and molecular physiology. 2005;288(1):L103-15.
407. Clark AD, Youd JM, Rattigan S, Barrett EJ, Clark MG. Heterogeneity of laser Doppler flowmetry in perfused muscle indicative of nutritive and nonnutritive flow. Am J Physiol Heart Circ Physiol. 2001;280(3):H1324-33.
408. Halder SK, Beauchamp RD, Datta PK. A specific inhibitor of TGF-beta receptor kinase, SB-431542, as a potent antitumor agent for human cancers. Neoplasia. 2005;7(5):509-21.
409. Korchynskyi O, ten Dijke P. Identification and functional characterization of distinct critically important bone morphogenetic protein-specific response elements in the Id1 promoter. The Journal of biological chemistry. 2002;277(7):4883-91.
410. Lee JY, Lori D, Wells DJ, Kemp PR. FHL1 activates myostatin signalling in skeletal muscle and promotes atrophy. FEBS Open Bio. 2015;5:753-62.
411. Noursadeghi M, Tsang J, Haustein T, Miller RF, Chain BM, Katz DR. Quantitative imaging assay for NF-kappaB nuclear translocation in primary human macrophages. J Immunol Methods. 2008;329(1-2):194-200.
412. Felsheim RF, Chavez AS, Palmer GH, Crosby L, Barbet AF, Kurtti TJ, et al. Transformation of Anaplasma marginale. Veterinary parasitology. 2010;167(2-4):167-74.
413. Matura LA, Shou H, Fritz JS, Smith KA, Vaidya A, Pinder D, et al. Physical Activity and Symptoms in Pulmonary Arterial Hypertension. Chest. 2016.
414. Lee WT, Ling Y, Sheares KK, Pepke-Zaba J, Peacock AJ, Johnson MK. Predicting survival in pulmonary arterial hypertension in the UK. The European respiratory journal. 2012;40(3):604-11.
415. Thenappan T, Shah SJ, Rich S, Tian L, Archer SL, Gomberg-Maitland M. Survival in pulmonary arterial hypertension: a reappraisal of the NIH risk stratification equation. The European respiratory journal. 2010;35(5):1079-87.
416. Westerterp KR. Assessment of physical activity: a critical appraisal. Eur J Appl Physiol. 2009;105(6):823-8.
417. Pitta F, Troosters T, Probst VS, Spruit MA, Decramer M, Gosselink R. Quantifying physical activity in daily life with questionnaires and motion sensors in COPD. The European respiratory journal. 2006;27(5):1040-55.
418. Tierney M, Fraser A, Purtill H, Kennedy N. Study to determine the criterion validity of the SenseWear Armband as a measure of physical activity in people with rheumatoid arthritis. Arthritis Care Res (Hoboken). 2013;65(6):888-95.

419. Farooqi N, Slinde F, Haglin L, Sandstrom T. Validation of SenseWear Armband and ActiHeart monitors for assessments of daily energy expenditure in free-living women with chronic obstructive pulmonary disease. Physiol Rep. 2013;1(6):e00150.
420. Strath SJ, Kaminsky LA, Ainsworth BE, Ekelund U, Freedson PS, Gary RA, et al. Guide to the assessment of physical activity: Clinical and research applications: a scientific statement from the American Heart Association. Circulation. 2013;128(20):2259-79.
421. Batal O, Khatib OF, Dweik RA, Hammel JP, McCarthy K, Minai OA. Comparison of baseline predictors of prognosis in pulmonary arterial hypertension in patients surviving </=2 years and those surviving >/=5 years after baseline right-sided cardiac catheterization. The American journal of cardiology. 2012;109(10):1514-20.
422. Matura LA, McDonough A, Carroll DL. Health-related quality of life and psychological states in patients with pulmonary arterial hypertension. J Cardiovasc Nurs. 2014;29(2):178-84.
423. Waschki B, Kirsten A, Holz O, Muller KC, Meyer T, Watz H, et al. Physical activity is the strongest predictor of all-cause mortality in patients with COPD: a prospective cohort study. Chest. 2011;140(2):331-42.
424. Schols AM, Broekhuizen R, Weling-Scheepers CA, Wouters EF. Body composition and mortality in chronic obstructive pulmonary disease. The American journal of clinical nutrition. 2005;82(1):53-9.
425. Narumi T, Watanabe T, Kadowaki S, Takahashi T, Yokoyama M, Kinoshita D, et al. Sarcopenia evaluated by fat-free mass index is an important prognostic factor in patients with chronic heart failure. Eur J Intern Med. 2015;26(2):118-22.
426. Anker SD, Ponikowski P, Varney S, Chua TP, Clark AL, Webb-Peploe KM, et al. Wasting as independent risk factor for mortality in chronic heart failure. Lancet. 1997;349(9058):1050-3.
427. Wannamethee SG, Shaper AG, Walker M. Physical activity and mortality in older men with diagnosed coronary heart disease. Circulation. 2000;102(12):1358-63.
428. Tudor-Locke C, Johnson WD, Katzmarzyk PT. Accelerometer-determined steps per day in US adults. Med Sci Sports Exerc. 2009;41(7):1384-91.
429. Wickerson L, Rozenberg D, Janaudis-Ferreira T, Deliva R, Lo V, Beauchamp G, et al. Physical rehabilitation for lung transplant candidates and recipients: An evidence-informed clinical approach. World J Transplant. 2016;6(3):517-31.
430. Hoeper MM, Oudiz RJ, Peacock A, Tapson VF, Haworth SG, Frost AE, et al. End points and clinical trial designs in pulmonary arterial hypertension: clinical and regulatory perspectives. Journal of the American College of Cardiology. 2004;43(12 Suppl S):48S-55S.
431. Maron BA, Hess E, Maddox TM, Opotowsky AR, Tedford RJ, Lahm T, et al. Association of Borderline Pulmonary Hypertension With Mortality and Hospitalization in a Large Patient Cohort: Insights From the Veterans Affairs Clinical Assessment, Reporting, and Tracking Program. Circulation. 2016;133(13):1240-8.
432. Health Do. https://data.gov.uk/data-request/nhs-hospital-stay. 2015.
433. Burke JP, Hunsche E, Regulier E, Nagao M, Buzinec P, Drake Iii W. Characterizing pulmonary hypertension-related hospitalization costs among Medicare Advantage or commercially insured patients with pulmonary arterial hypertension: a retrospective database study. Am J Manag Care. 2015;21(3 Suppl):s47-58.
434. Feemster LC, Cooke CR, Rubenfeld GD, Hough CL, Ehlenbach WJ, Au DH, et al. The influence of hospitalization or intensive care unit admission on declines in health-related quality of life. Annals of the American Thoracic Society. 2015;12(1):35-45.
435. Hou WH, Ni CH, Li CY, Tsai PS, Lin LF, Shen HN. Stroke rehabilitation and risk of mortality: a population-based cohort study stratified by age and gender. J Stroke Cerebrovasc Dis. 2015;24(6):1414-22.
436. Lahtinen A, Leppilahti J, Harmainen S, Sipila J, Antikainen R, Seppanen ML, et al. Geriatric and physically oriented rehabilitation improves the ability of independent living and physical

rehabilitation reduces mortality: a randomised comparison of 538 patients. Clin Rehabil. 2015;29(9):892-906.
437. Goel K, Pack QR, Lahr B, Greason KL, Lopez-Jimenez F, Squires RW, et al. Cardiac rehabilitation is associated with reduced long-term mortality in patients undergoing combined heart valve and CABG surgery. European journal of preventive cardiology. 2015;22(2):159-68.
438. Armstrong MJ, Sigal RJ, Arena R, Hauer TL, Austford LD, Aggarwal S, et al. Cardiac rehabilitation completion is associated with reduced mortality in patients with diabetes and coronary artery disease. Diabetologia. 2015;58(4):691-8.
439. Spruit MA, Singh SJ, Garvey C, ZuWallack R, Nici L, Rochester C, et al. An official American Thoracic Society/European Respiratory Society statement: key concepts and advances in pulmonary rehabilitation. American journal of respiratory and critical care medicine. 2013;188(8):e13-64.
440. Jack K, McLean SM, Moffett JK, Gardiner E. Barriers to treatment adherence in physiotherapy outpatient clinics: a systematic review. Man Ther. 2010;15(3):220-8.
441. Ribeiro F, Theriault ME, Debigare R, Maltais F. Should all patients with COPD be exercise trained? Journal of applied physiology. 2013;114(9):1300-8.
442. Cohen S, Nathan JA, Goldberg AL. Muscle wasting in disease: molecular mechanisms and promising therapies. Nat Rev Drug Discov. 2015;14(1):58-74.
443. Drescher C, Konishi M, Ebner N, Springer J. Loss of muscle mass: current developments in cachexia and sarcopenia focused on biomarkers and treatment. Journal of cachexia, sarcopenia and muscle. 2015;6(4):303-11.
444. Shephard RJ. Limits to the measurement of habitual physical activity by questionnaires. Br J Sports Med. 2003;37(3):197-206; discussion
445. Arpinelli F, Carone M, Riccardo G, Bertolotti G. Health-related quality of life measurement in asthma and chronic obstructive pulmonary disease: review of the 2009-2014 literature. Multidiscip Respir Med. 2015;11:5.
446. Garrod R, Bestall JC, Paul EA, Wedzicha JA, Jones PW. Development and validation of a standardized measure of activity of daily living in patients with severe COPD: the London Chest Activity of Daily Living scale (LCADL). Respiratory medicine. 2000;94(6):589-96.
447. Moy ML, Teylan M, Weston NA, Gagnon DR, Garshick E. Daily step count predicts acute exacerbations in a US cohort with COPD. PLoS One. 2013;8(4):e60400.
448. Sylvia LG, Bernstein EE, Hubbard JL, Keating L, Anderson EJ. Practical guide to measuring physical activity. J Acad Nutr Diet. 2014;114(2):199-208.
449. Nakagawa S. A farewell to Bonferroni: the problems of low statistical power and publication bias. Behavioral Ecology. 2004;15(6):1044-5.
450. Austin PC, Steyerberg EW. The number of subjects per variable required in linear regression analyses. Journal of clinical epidemiology. 2015;68(6):627-36.
451. Dziura JD, Post LA, Zhao Q, Fu Z, Peduzzi P. Strategies for dealing with missing data in clinical trials: from design to analysis. Yale J Biol Med. 2013;86(3):343-58.
452. Vitali SH, Hansmann G, Rose C, Fernandez-Gonzalez A, Scheid A, Mitsialis SA, et al. The Sugen 5416/hypoxia mouse model of pulmonary hypertension revisited: long-term follow-up. Pulmonary circulation. 2014;4(4):619-29.
453. Mehul S. Patel JL, Manuel Baz, Claire E. Wells, Susannah Bloch, Amy Lewis, Anna V. Donaldson, Benjamin E. Garfield, Nicholas S Hopkinson, Amanda Natanek, William D-C Man, Dominic J. Wells, Emma H. Bake3, Michael I. Polkey, Paul R. Kemp. GDF-15 is associated with muscle mass in COPD and promotes muscle wasting in vivo. Journal of Cachexia and Sarcopaenia (Manuscript accepted for publication). 2016.
454. Wiklund FE, Bennet AM, Magnusson PK, Eriksson UK, Lindmark F, Wu L, et al. Macrophage inhibitory cytokine-1 (MIC-1/GDF15): a new marker of all-cause mortality. Aging Cell. 2010;9(6):1057-64.
455. Muscaritoli M, Anker SD, Argiles J, Aversa Z, Bauer JM, Biolo G, et al. Consensus definition of sarcopenia, cachexia and pre-cachexia: joint document elaborated by Special Interest Groups (SIG)

"cachexia-anorexia in chronic wasting diseases" and "nutrition in geriatrics". Clin Nutr. 2010;29(2):154-9.
456. Huh SJ, Chung CY, Sharma A, Robertson GP. Macrophage inhibitory cytokine-1 regulates melanoma vascular development. Am J Pathol. 2010;176(6):2948-57.
457. Taraseviciene-Stewart L, Kasahara Y, Alger L, Hirth P, Mc Mahon G, Waltenberger J, et al. Inhibition of the VEGF receptor 2 combined with chronic hypoxia causes cell death-dependent pulmonary endothelial cell proliferation and severe pulmonary hypertension. FASEB J. 2001;15(2):427-38.
458. Sharma M, McFarlane C, Kambadur R, Kukreti H, Bonala S, Srinivasan S. Myostatin: expanding horizons. IUBMB life. 2015;67(8):589-600.
459. Wagner KR, Fleckenstein JL, Amato AA, Barohn RJ, Bushby K, Escolar DM, et al. A phase I/IItrial of MYO-029 in adult subjects with muscular dystrophy. Annals of neurology. 2008;63(5):561-71.
460. Patel MS, Lee J, Baz M, Wells CE, Bloch S, Lewis A, et al. Growth differentiation factor-15 is associated with muscle mass in chronic obstructive pulmonary disease and promotes muscle wasting. Journal of cachexia, sarcopenia and muscle. 2015.
461. Laping NJ, Grygielko E, Mathur A, Butter S, Bomberger J, Tweed C, et al. Inhibition of transforming growth factor (TGF)-beta1-induced extracellular matrix with a novel inhibitor of the TGF-beta type I receptor kinase activity: SB-431542. Mol Pharmacol. 2002;62(1):58-64.
462. Inman GJ, Nicolas FJ, Callahan JF, Harling JD, Gaster LM, Reith AD, et al. SB-431542 is a potent and specific inhibitor of transforming growth factor-beta superfamily type I activin receptor-like kinase (ALK) receptors ALK4, ALK5, and ALK7. Mol Pharmacol. 2002;62(1):65-74.
463. Accornero F, Kanisicak O, Tjondrokoesoemo A, Attia AC, McNally EM, Molkentin JD. Myofiber-specific inhibition of TGFbeta signaling protects skeletal muscle from injury and dystrophic disease in mice. Hum Mol Genet. 2014;23(25):6903-15.
464. Guttridge DC, Albanese C, Reuther JY, Pestell RG, Baldwin AS, Jr. NF-kappaB controls cell growth and differentiation through transcriptional regulation of cyclin D1. Mol Cell Biol. 1999;19(8):5785-99.
465. Li YP, Chen Y, John J, Moylan J, Jin B, Mann DL, et al. TNF-alpha acts via p38 MAPK to stimulate expression of the ubiquitin ligase atrogin1/MAFbx in skeletal muscle. FASEB J. 2005;19(3):362-70.
466. Li H, Malhotra S, Kumar A. Nuclear factor-kappa B signaling in skeletal muscle atrophy. J Mol Med (Berl). 2008;86(10):1113-26.
467. Gumucio JP, Mendias CL. Atrogin-1, MuRF-1, and sarcopenia. Endocrine. 2013;43(1):12-21.
468. Fujita N, Fujino H, Sakamoto H, Takegaki J, Deie M. Time course of ubiquitin-proteasome and macroautophagy-lysosome pathways in skeletal muscle in rats with heart failure. Biomed Res. 2015;36(6):383-92.
469. de Boer MD, Selby A, Atherton P, Smith K, Seynnes OR, Maganaris CN, et al. The temporal responses of protein synthesis, gene expression and cell signalling in human quadriceps muscle and patellar tendon to disuse. J Physiol. 2007;585(Pt 1):241-51.
470. Lang CH, Huber D, Frost RA. Burn-induced increase in atrogin-1 and MuRF-1 in skeletal muscle is glucocorticoid independent but downregulated by IGF-I. Am J Physiol Regul Integr Comp Physiol. 2007;292(1):R328-36.
471. Cai PC, Shi L, Liu VW, Tang HW, Liu IJ, Leung TH, et al. Elevated TAK1 augments tumor growth and metastatic capacities of ovarian cancer cells through activation of NF-kappaB signaling. Oncotarget. 2014;5(17):7549-62.
472. Treiber DK, Shah NP. Ins and outs of kinase DFG motifs. Chem Biol. 2013;20(6):745-6.
473. McKenzie AI, Briggs RA, Barrows KM, Nelson DS, Kwon OS, Hopkins PN, et al. A pilot study examining the impact of exercise training on skeletal muscle genes related to the TLR signaling pathway in older adults following hip fracture recovery. Journal of applied physiology. 2017;122(1):68-75.

474. Hessel MH, Steendijk P, den Adel B, Schutte CI, van der Laarse A. Characterization of right ventricular function after monocrotaline-induced pulmonary hypertension in the intact rat. Am J Physiol Heart Circ Physiol. 2006;291(5):H2424-30.
475. Buermans HP, Redout EM, Schiel AE, Musters RJ, Zuidwijk M, Eijk PP, et al. Microarray analysis reveals pivotal divergent mRNA expression profiles early in the development of either compensated ventricular hypertrophy or heart failure. Physiol Genomics. 2005;21(3):314-23.
476. Takaesu G, Surabhi RM, Park KJ, Ninomiya-Tsuji J, Matsumoto K, Gaynor RB. TAK1 is critical for IkappaB kinase-mediated activation of the NF-kappaB pathway. J Mol Biol. 2003;326(1):105-15.
477. Smith RC, Cramer MS, Mitchell PJ, Capen A, Huber L, Wang R, et al. Myostatin Neutralization Results in Preservation of Muscle Mass and Strength in Preclinical Models of Tumor-Induced Muscle Wasting. Mol Cancer Ther. 2015;14(7):1661-70.
478. Trendelenburg AU, Meyer A, Jacobi C, Feige JN, Glass DJ. TAK-1/p38/nNFkappaB signaling inhibits myoblast differentiation by increasing levels of Activin A. Skelet Muscle. 2012;2(1):3.
479. Wang X, Baek SJ, Eling TE. The diverse roles of nonsteroidal anti-inflammatory drug activated gene (NAG-1/GDF15) in cancer. Biochem Pharmacol. 2013;85(5):597-606.
480. Shin JH, Min SH. Novel functional roles of caspase-related genes in the regulation of apoptosis and autophagy. Korean J Physiol Pharmacol. 2016;20(6):573-80.
481. Mayeux R. Biomarkers: potential uses and limitations. NeuroRx. 2004;1(2):182-8.
482. Fleming TR, Powers JH. Biomarkers and surrogate endpoints in clinical trials. Stat Med. 2012;31(25):2973-84.
483. Matura LA, Shou H, Fritz JS, Smith KA, Vaidya A, Pinder D, et al. Physical Activity and Symptoms in Pulmonary Arterial Hypertension. Chest. 2016;150(1):46-56.
484. Serres I, Gautier V, Varray A, Prefaut C. Impaired skeletal muscle endurance related to physical inactivity and altered lung function in COPD patients. Chest. 1998;113(4):900-5.
485. Hayton C, Clark A, Olive S, Browne P, Galey P, Knights E, et al. Barriers to pulmonary rehabilitation: characteristics that predict patient attendance and adherence. Respiratory medicine. 2013;107(3):401-7.
486. Lyons RM, Moses HL. Transforming growth factors and the regulation of cell proliferation. Eur J Biochem. 1990;187(3):467-73.
487. Thomas M, Langley B, Berry C, Sharma M, Kirk S, Bass J, et al. Myostatin, a negative regulator of muscle growth, functions by inhibiting myoblast proliferation. The Journal of biological chemistry. 2000;275(51):40235-43.
488. Weiss WA, Taylor SS, Shokat KM. Recognizing and exploiting differences between RNAi and small-molecule inhibitors. Nat Chem Biol. 2007;3(12):739-44.
489. Zhou YM, Li MJ, Zhou YL, Ma LL, Yi X. Growth differentiation factor-15 (GDF-15), novel biomarker for assessing atrial fibrosis in patients with atrial fibrillation and rheumatic heart disease. Int J Clin Exp Med. 2015;8(11):21201-7.
490. Freeman CM, Martinez CH, Todt JC, Martinez FJ, Han MK, Thompson DL, et al. Acute exacerbations of chronic obstructive pulmonary disease are associated with decreased CD4+ & CD8+ T cells and increased growth & differentiation factor-15 (GDF-15) in peripheral blood. Respiratory research. 2015;16:94.
491. Cotter G, Voors AA, Prescott MF, Felker GM, Filippatos G, Greenberg BH, et al. Growth differentiation factor 15 (GDF-15) in patients admitted for acute heart failure: results from the RELAX-AHF study. Eur J Heart Fail. 2015;17(11):1133-43.
492. Lajer M, Jorsal A, Tarnow L, Parving HH, Rossing P. Plasma growth differentiation factor-15 independently predicts all-cause and cardiovascular mortality as well as deterioration of kidney function in type 1 diabetic patients with nephropathy. Diabetes Care. 2010;33(7):1567-72.
493. Copple BL, Banes A, Ganey PE, Roth RA. Endothelial cell injury and fibrin deposition in rat liver after monocrotaline exposure. Toxicol Sci. 2002;65(2):309-18.

Appendix 2.1

Medicine, Biomedical Sciences, Health and Social Care Sciences

24 July 2014

To Whom It May Concern:

This is to confirm that St George's, University of London (St George's

Hospital Medical School) has given permission for Dr Ben Garfield, Research Registrar Royal Brompton Hospital and Imperial College to use the SGRQ for investigating quality of life in pulmonary hypertension.

Cranmer Terrace
London SW17 0RE
Switchboard
+44 (0)20 8672 9944
www.sgul.ac.uk

Professor Paul Jones, PhD FRCP
Professor of Respiratory Medicine

P.W. Jones, PhD FRCP
Professor of Respiratory Medicine
Tel. ++44 (0)20 8725 5371 Fax. ++44 (0)20 8725 5955 email pjones@sgul.ac.uk

Appendix 2.2

GALEN RESEARCH LIMITED

Enterprise House, Manchester Science Park,

Lloyd Street North, Manchester, M15 6SE.

Phone: +44 (0)161 226 4446 Fax: +44 (0)161 226 4478

E-mail: jwilburn@galen-research.com

INVOICE

13th August 2014

Invoice number: I14/020

For the attention of:

Dr. Benjamin Garfield

Royal Brompton & Harefield NHS Foundation Trust

Harefield Hospital

Accounts Payable Department

Hill End Road

Harefield, Middlesex

UB9 6TH

To:	GBP £
Administration and supply of CAMPHOR UK English for use in the	100.00

study **'Transforming growth factor beta signalling in the development of muscle weakness in pulmonary arterial hypertension'**

VAT @ 20%	20.00
Total amount due and payable:	**£120.00**

Payment terms: **Immediate**

Bank Details

Account: Galen Research Limited

Sort code: 09-07-20

Account number: 01932020

Bank: Santander Corporate Bank

Bank Address: Bridle Road, Bootle, Merseyside. L30 4GB

Vat Reg No.: GB 519 5394 21

Company Registration Number 6282937

Appendix 2.3

pCDNA3 hum TTGFBR2 100% homology

Truncated TGFBR2 in PCDNA 3.1 3 (100% homolog)

NNNNNNCNNNCTCGGNNNNCTAGTACGGCCGCCAGTGTGCTGGAATTCGATTGC
GCTGGGGGCTCGGTCTATGAC

GAGCAGCGGGGTCTGCCATGGGTCGGGGGCTGCTCAGGGGCCTGTGGCCGCTGC
ACATCGTCCTGTGGACGCGTATCGCCAGCACGATCCCACCGCACGTTCAGAAGTC
GGTTAATAACGACATGATAGTCACTGACAACAACGGTGCAGTCAAGTTTCCACA
ACTGTGTAAATTTTGTGATGTGAGATTTTCCACCTGTGACAACCAGAAATCCTGC
ATGAGCAACTGCAGCATCACCTCCATCTGTGAGAAGCCACAGGAAGTCTGTGTG
GCTGTATGGAGAAAGAATGACGAGAACATAACACTAGAGACAGTTTGCCATGAC
CCCAAGCTCCCCTACCATGACTTTATTCTGGAAGATGCTGCTTCTCCAAAGTGCA
TTATGAAGGAAAAAAAAAAAGCCTGGTGAGACTTTCTTCATGTGTTCCTGTAGCTC
TGATGAGTGCAATGACAACATCATCTTCTCAGAAGAATATAACACCAGCAATCCT
GACTTGTTGCTAGTCATATTTCAAGTGACAGGCATCAGCCTCCTGCCACCACTGG
GAGTTGCCATATCTGTCATCATCATCTTCTACTGCTACCGCGTTAACCGGCAGCA
GAAGCT
GAGTTCAACCTGGGAAACCGGCAATCACTAGTGAATTCTGCAGATATCCATCAC
ACTGGCGGCCGCTCGAGCATGCATCTAGAGGGCCCTATTCTATAGTGTCACCTAA
ATGCTAGAGCTCGCTGATCAGCCTCGACTGTGCCTTCTAGTTGCCAGCCATCTGT
TGTTTGCCCCTCCCCCGTGCCTTCCTTGACCCTGGAAGGTGCCACTCCCACTGTCC
TTTCCTAATAAAATGAGGAAATTGCATCGCATTGTCTGAGTAGGTGTCATTCTAT
TCTGGGGGGGTGGGGNNGGGGGCAGGACAGCAAGGGGGAGGATTGGGAAGACA
ATAGCAGGCA
TGCTGGGGATGCGGTGGGCTCTATGGCTTCTGAGGCGGAAGAACCAGCTGGGGC
TCTAGG
GGGTATCCCCACGCGCCCTGTAGCGNCGCATTAAGCNCGNGGGNGTGGNNNNNC
GCGCAG
CGNGACCGCTACANNNNNGCGCCNTANNNCNNNNNCTTCGCTTNTNCCTCNTCT
CNCNCN
TNNNNNTTCCCGTNAGCNNTAATCGGGGNTCCCTTNNNNNNANNNNNGNTTNNN
NACCTC
NACCCNAAACTGNNAGNNNNANGNNNNACNNNNNGNNNNNCNCCNNNANNNA
NNNNNNNN
NNNNACNNNNNTNNNNNNNNTNAANGNNNNNNTNNNNNNNNANCNNNN

Appendix 2.4

PRLTK has a BMP response element in the HSV promoter region 240-247

AGATCTAAATGAGTCTTCGGACCTCGCGGGGGCCGCTTAAGCGGTGGTTA
GGGTTTGTCTGACGCGGGGGGAGGGGGAAGGAACGAAACACTCTCATTCG
GAGGCGGCTCGGGGTTTGGTCTTGGTGGCCACGGGCACGCAGAAGAGCGC
CGCGATCCTCTTAAGCACCCCCCCGCCCTCCGTGGAGGCGGGGGTTTGGT
CGGCGGGTGGTAACTGGCGGGCCGCTGACTCGGGCGGGTCGCGCGCCCCA
GAGTGTGACCTTTTCGGTCTGCTCGCAGACCCCCGGGCGGCGCCGCCGCG
GCGGCGACGGGCTCGCTGGGTCCTAGGCTCCATGGGGACCGTATACGTGG
ACAGGCTCTGGAGCATCCGCACGACTGCGGTGATATTACCGGAGACCTTC
TGCGGGACGAGCCGGGTCACGCGGCTGACGCGGAGCGTCCGTTGGGCGAC
AAACACCAGGACGGGGCACAGGTACACTATCTTGTCACCCGGAGGCGCGA
GGGACTGCAGGAGCTTCAGGGAGTGGCGCAGCTGCTTCATCCCCGTGGCC
CGTTGCTCGCGTTTGCTGGCGGTGTCCCCGGAAGAAATATATTTGCATGT
CTTTAGTTCTATGATGACACAAACCCCGCCCAGCGTCTTGTCATTGGCGA
ATTCGAACACGCAGATGCAGTCGGGGCGGCGCGGTCCCAGGTCCACTTCG
CATATTAAGGTGACGCGTGTGGCCTCGAACACCGAGCGACCCTGCAGCGA
CCCGCTTAAAAGCTTGATTCTTCTGACACAACAGTCTCGAACTTAAGCTG
CAGAAGTTGGTCGTGAGGCACTGGGCAGGTAAGTATCAAGGTTACAAGAC
AGGTTTAAGGAGACCAATAGAAACTGGGCTTGTCGAGACAGAGAAGACTC
TTGCGTTTCTGATAGGCACCTATTGGTCTTACTGACATCCACTTTGCCTT
TCTCTCCACAGGTGTCCACTCCCAGTTCAATTACAGCTCTTAAGGCTAGA
GTACTTAATACGACTCACTATAGGCTAGCCACCATGACTTCGAAAGTTTA
TGATCCAGAACAAAGGAAACGGATGATAACTGGTCCGCAGTGGTGGGCCA
GATGTAAACAAATGAATGTTCTTGATTCATTTATTAATTATTATGATTCA
GAAAAACATGCAGAAAATGCTGTTATTTTTTTACATGGTAACGCGGCCTC
TTCTTATTTATGGCGACATGTTGTGCCACATATTGAGCCAGTAGCGCGGT
GTATTATACCAGACCTTATTGGTATGGGCAAATCAGGCAAATCTGGTAAT
GGTTCTTATAGGTTACTTGATCATTACAAATATCTTACTGCATGGTTTGA
ACTTCTTAATTTACCAAAGAAGATCATTTTTGTCGGCCATGATTGGGGTG
CTTGTTTGGCATTTCATTATAGCTATGAGCATCAAGATAAGATCAAAGCA
ATAGTTCACGCTGAAAGTGTAGTAGATGTGATTGAATCATGGGATGAATG
GCCTGATATTGAAGAAGATATTGCGTTGATCAAATCTGAAGAAGGAGAAA
AAATGGTTTTGGAGAATAACTTCTTCGTGGAAACCATGTTGCCATCAAAA
ATCATGAGAAAGTTAGAACCAGAAGAATTTGCAGCATATCTTGAACCATT
CAAAGAGAAAGGTGAAGTTCGTCGTCCAACATTATCATGGCCTCGTGAAA
TCCCGTTAGTAAAAGGTGGTAAACCTGACGTTGTACAAATTGTTAGGAAT
TATAATGCTTATCTACGTGCAAGTGATGATTTACCAAAAATGTTTATTGA
ATCGGACCCAGGATTCTTTTCCAATGCTATTGTTGAAGGTGCCAAGAAGT
TTCCTAATACTGAATTTGTCAAAGTAAAAGGTCTTCATTTTTCGCAAGAA
GATGCACCTGATGAAATGGGAAAATATATCAAATCGTTCGTTGAGCGAGT
TCTCAAAAATGAACAATAATTCTAGAGCGGCCGCTTCGAGCAGACATGAT
AAGATACATTGATGAGTTTGGACAAACCACAACTAGAATGCAGTGAAAAA
AATGCTTTATTTGTGAAATTTGTGATGCTATTGCTTTATTTGTAACCATT
ATAAGCTGCAATAAACAAGTTAACAACAACAATTGCATTCATTTTATGTT

TCAGGTTCAGGGGGAGGTGTGGGAGGTTTTTTAAAGCAAGTAAAACCTCT
ACAAATGTGGTAAAATCGATAAGGATCCAGGTGGCACTTTTCGGGGAAAT
GTGCGCGGAACCCCTATTTGTTTATTTTTCTAAATACATTCAAATATGTA
TCCGCTCATGAGACAATAACCCTGATAAATGCTTCAATAATATTGAAAAA
GGAAGAGTATGAGTATTCAACATTTCCGTGTCGCCCTTATTCCCTTTTTT
GCGGCATTTTGCCTTCCTGTTTTTGCTCACCCAGAAACGCTGGTGAAAGT
AAAAGATGCTGAAGATCAGTTGGGTGCACGAGTGGGTTACATCGAACTGG
ATCTCAACAGCGGTAAGATCCTTGAGAGTTTTCGCCCCGAAGAACGTTTT
CCAATGATGAGCACTTTTAAAGTTCTGCTATGTGGCGCGGTATTATCCCG
TATTGACGCCGGGCAAGAGCAACTCGGTCGCCGCATACACTATTCTCAGA
ATGACTTGGTTGAGTACTCACCAGTCACAGAAAAGCATCTTACGGATGGC
ATGACAGTAAGAGAATTATGCAGTGCTGCCATAACCATGAGTGATAACAC
TGCGGCCAACTTACTTCTGACAACGATCGGAGGACCGAAGGAGCTAACCG
CTTTTTTGCACAACATGGGGGATCATGTAACTCGCCTTGATCGTTGGGAA
CCGGAGCTGAATGAAGCCATACCAAACGACGAGCGTGACACCACGATGCC
TGTAGCAATGGCAACAACGTTGCGCAAACTATTAACTGGCGAACTACTTA
CTCTAGCTTCCCGGCAACAATTAATAGACTGGATGGAGGCGGATAAAGTT
GCAGGACCACTTCTGCGCTCGGCCCTTCCGGCTGGCTGGTTTATTGCTGA
TAAATCTGGAGCCGGTGAGCGTGGGTCTCGCGGTATCATTGCAGCACTGG
GGCCAGATGGTAAGCCCTCCCGTATCGTAGTTATCTACACGACGGGGAGT
CAGGCAACTATGGATGAACGAAATAGACAGATCGCTGAGATAGGTGCCTC
ACTGATTAAGCATTGGTAACTGTCAGACCAAGTTTACTCATATATACTTT
AGATTGATTTAAAACTTCATTTTTAATTTAAAAGGATCTAGGTGAAGATC
CTTTTTGATAATCTCATGACCAAAATCCCTTAACGTGAGTTTTCGTTCCA
CTGAGCGTCAGACCCCGTAGAAAAGATCAAAGGATCTTCTTGAGATCCTT
TTTTTCTGCGCGTAATCTGCTGCTTGCAAACAAAAAAACCACCGCTACCA
GCGGTGGTTTGTTTGCCGGATCAAGAGCTACCAACTCTTTTTCCGAAGGT
AACTGGCTTCAGCAGAGCGCAGATACCAAATACTGTTCTTCTAGTGTAGC
CGTAGTTAGGCCACCACTTCAAGAACTCTGTAGCACCGCCTACATACCTC
GCTCTGCTAATCCTGTTACCAGTGGCTGCTGCCAGTGGCGATAAGTCGTG
TCTTACCGGGTTGGACTCAAGACGATAGTTACCGGATAAGGCGCAGCGGT
CGGGCTGAACGGGGGGTTCGTGCACACAGCCCAGCTTGGAGCGAACGACC
TACACCGAACTGAGATACCTACAGCGTGAGCTATGAGAAAGCGCCACGCT
TCCCGAAGGGAGAAAGGCGGACAGGTATCCGGTAAGCGGCAGGGTCGGAA
CAGGAGAGCGCACGAGGGAGCTTCCAGGGGGAAACGCCTGGTATCTTTAT
AGTCCTGTCGGGTTTCGCCACCTCTGACTTGAGCGTCGATTTTTGTGATG
CTCGTCAGGGGGGCGGAGCCTATGGAAAAACGCCAGCAACGCGGCCTTTT
TACGGTTCCTGGCCTTTTGCTGGCCTTTTGCTCACATGGCTCGACCGG CGCC

GC G CGCC

CG A CGCC

GC A CGCC

Appendix 4.1

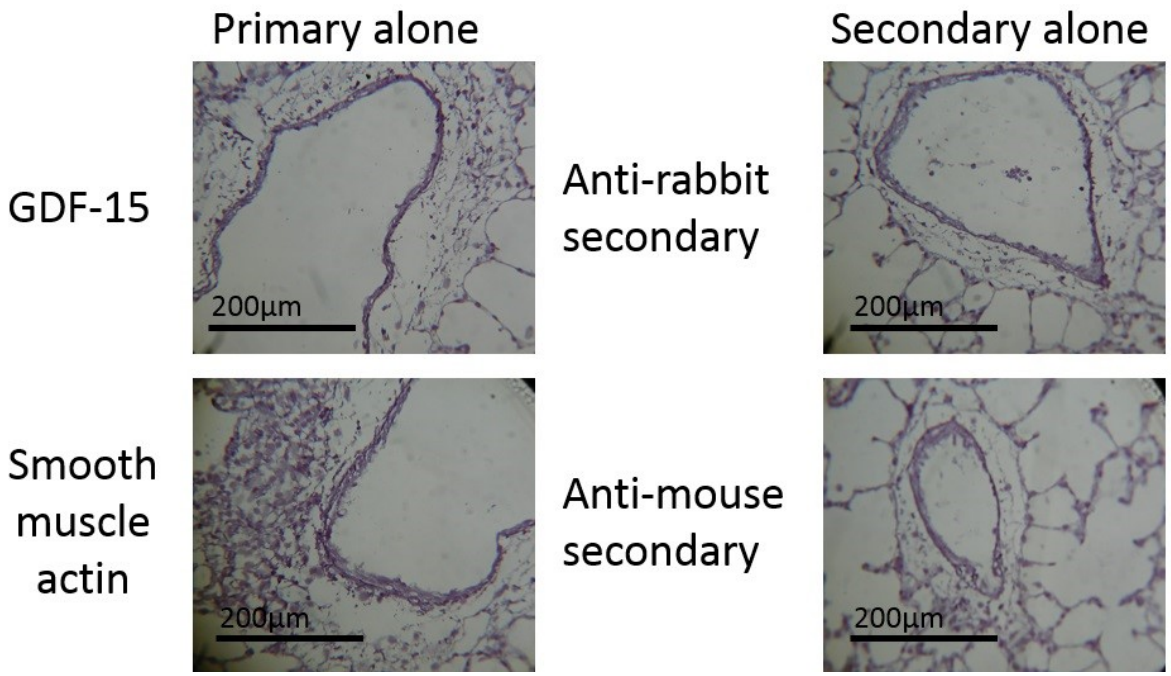

Negative controls for immunohistochemitry. Figure showing negative controls for immunohistochemistry for GDF-15, Smooth muscle actin and secondaries anti-rabbit and anti-mouse.

Appendix 5.1

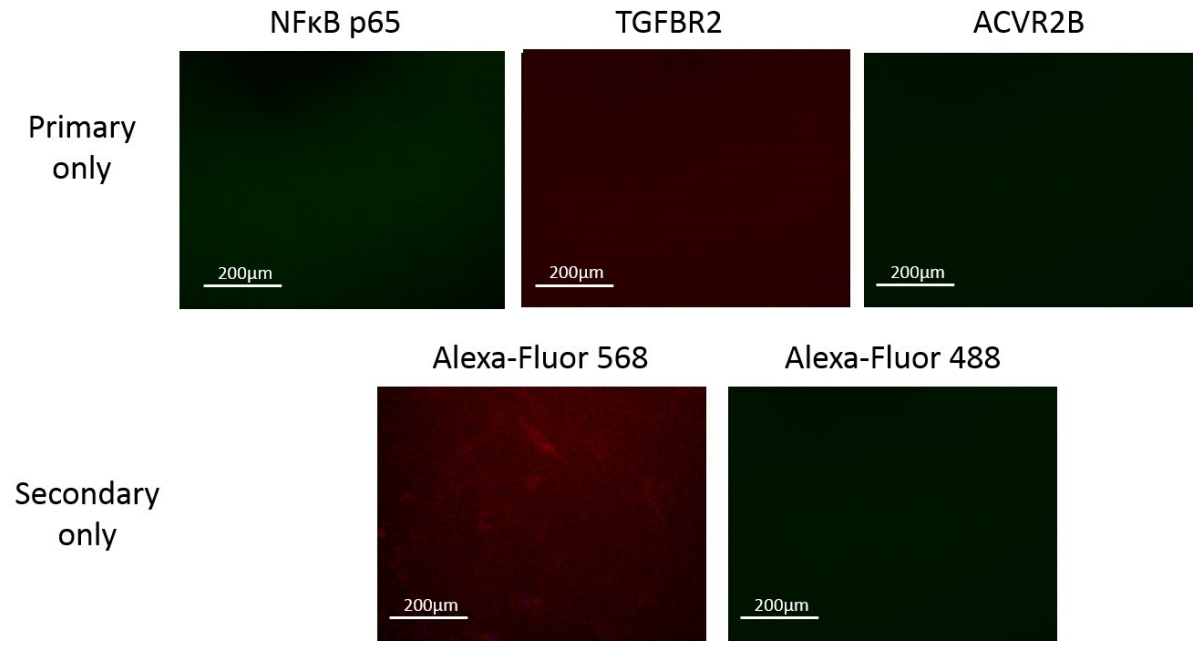

Negative controls for immunofluorescence. Figure showing negative controls for immunofluorescence for NFκB p65, TGFBR2, ACVR2B and Alexa-Fluor 488 and 568 secondary.

Appendix 5.2

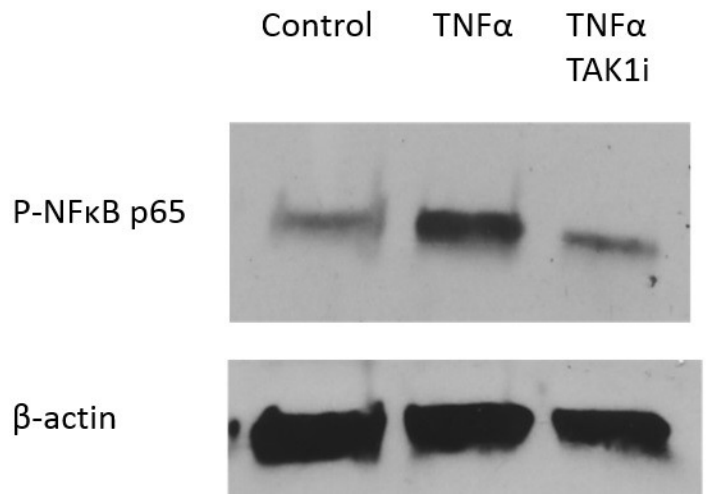

Positive control showing activity of 5(Z)-7-oxozeaenol in C2C12 myotubes. Western blot of Phospho NFκB p65 activity and β-actin levels in control, TNF-α (10 ng/ml) and TNF-α and 5(Z)-7-oxozeanol (TAK1i) (1000 nM) cells

Appendix 5.3

'lastly, it is opportune for me to warn you about issues associated with commercially available MIC-1/GDF15, available from R&D, but which is quite likely to effect other commercial suppliers of this protein

One of my pharamaceutical industry colleagues has been comparing MIC-1/GDF15 from R&D and their own in house material. They found that MIC-1/GDF15 from R&D induces smad phosphorylation but their in house material does not. They have traced the source of this disparity to a 2-3% contamination of MIC-1/GDF15 with TGF-b. They can block the smad phosphorylation of MIC-1/GDF15 with antibodies to TGF-b but not by antibodies to MIC-1/GDF15. The bioassay that R&D have on their web site seems to be based on TGF-b contamination of their purified MIC-1/GDF15.

The data seems very solid and there is not much doubt that this is why at least some people using cytokine from R&D (and perhaps from other suppliers) report smad phosphorylation and other changes that we cannot reproduce… Its pretty clear that it has created enormous confusion in the literature and that any data using R&D MIC-1/GDF15 (and perhaps from other suppliers) must be suspect.

They have approached R&D about this issue but the outcome is not clear at present.

I believe this issue has arisen because most cell lines make lots of endogenous TGF-b. The physico-chemical properties of MIC-1/GDF15 and TGF-b are very similar and hence they tend to co-purify and probably run together on a gel. It might also be that commercial sources, where MIC-1/GDF15 has been expressed in mammalian cells, may be contaminated with other TGF-b superfamily cytokines. Fortunately the MIC-1/GDF15 we make and purify in house is expressed in yeast where this type of contamination cannot occur.If relevant, you need to consider the possibility that some of your findings may be due to this problem'